The flexible brain:

Causes of individual variation in cognitive flexibility

Krista van den Heuvel

Propositions

1. Cognitive flexibility results from past experiences and how well they are memorized.
   (this thesis)

2. The contributions of epigenetic mechanisms to tissue specificity and behavioural variation are dissociable.
   (this thesis)

3. Given that individuals differ in cognition and behaviour, keeping animals in captivity is only justifiable when those animals can make autonomous choices.

4. Contrary to popular belief, food provisioning with bird feeders is not beneficial for wildlife and has ecosystem-wide negative consequences.

5. It is a waste to spend time and resources on space research as long as we fail to preserve life on earth.

6. A major mistake in science communication is reasoning with facts where emotions rule.

Propositions belonging to the thesis, entitled

'The flexible brain: Causes of individual variation in cognitive flexibility'

Krista van den Heuvel
Wageningen, 27th June 2023

The flexible brain:
Causes of individual variation in cognitive flexibility

Krista van den Heuvel

Thesis Committee

Promotor
Prof. Dr K. van Oers
Special Professor, Animal Personality
Wageningen University & Research
Senior scientist, Department of Animal Ecology
Netherlands Institute of Ecology (NIOO-KNAW), Wageningen

Co-promotor
Dr A. Kotrschal
Associate Professor, Behavioural Ecology Group
Wageningen University & Research

Other members
Prof. Dr M. Groenen, Wageningen University & Research
Prof. Dr D. Wright, Linköping University, Sweden
Prof. Dr R. van Damme, University of Antwerp, Belgium
Prof. Dr H.L. Dugdale, University of Groningen

This research was conducted under the auspices of the Graduate School
Wageningen Institute of Animal Sciences (WIAS).

The flexible brain:
Causes of individual variation in cognitive flexibility

Krista van den Heuvel

Thesis
submitted in fulfilment of the requirements for the degree of doctor
at Wageningen University
by the authority of the Rector Magnificus,
Prof. Dr A.P.J. Mol,
in the presence of the
Thesis Committee appointed by the Academic Board
to be defended in public
on Tuesday 27 June 2023
at 11 a.m. in the Omnia Auditorium.

Krista van den Heuvel
The flexible brain: Causes of individual variation in cognitive flexibility
236 pages

PhD thesis, Wageningen University, Wageningen, the Netherlands (2023)
With references, with summaries in English and in Dutch

ISBN: 978-94-6447-649-1
DOI: https://doi.org/10.18174/590711

"Sweet is the lore which Nature brings;
Our meddling intellect
Mis-shapes the beauteous forms of things;
—We murder to dissect."
William Wordsworth, "The Tables Turned", 1798

Table of Contents

Chapter 1.

General Introduction

The conditions in which an organism finds itself can change over different time intervals, both within a lifetime and across generations. When changes occur across generations, organisms have the potential to adapt to these changes via evolution, the change of species over time. Evolution can result from natural selection acting on phenotypic variation that arises from genetic mutations as well as standing genetic variation. However, the success of a phenotype in a current environment is only weakly predictable of success in future environments, and changes can occur rapidly within a single generation. Behavioural changes are an important mechanism allowing species to deal with changing environmental conditions. Learning allows for such behavioural changes as result of experience (Shettleworth, 2010). Organisms can obtain and memorize information from experiences and encounters, and use this knowledge to predict which behaviours are most likely leading to fruitful outcomes, ultimately enhancing fitness (McNamara and Dall, 2010; Laland et al., 2013). Rapid and extensive environmental changes induced by human activities are expected to occur more frequently, and a standing question is to what extent behavioural changes, guided by learning, might allow species to deal with these changes (Wong and Candolin, 2015; Greggor et al., 2019).

The pathways and mechanisms by which animals acquire, process and store information from the environment and respond appropriately to that information is referred to as *cognition* (Shettleworth, 2010). Learning and memory are cognitive processes that have evolved to obtain and store information, and these memories can be called upon when the environmental situation asks for it to facilitate experience-dependent flexibility in behaviour (Wright et al., 2022). Yet, when memories of past experiences do not adequately predict future situations, they can become disadvantageous. Therefore, it is equally important to flexibly use stored information and to ignore, or forget, memories that have become outdated or inappropriate. The ability to adaptively change a learned behaviour in response to changed contingencies in the environment, and the brain processes underlying that ability, is described as *cognitive flexibility* (Bond et al., 2007; Shettleworth, 2010; Tello-Ramos et al., 2019). Cognitive flexibility can be particularly useful when dealing with dynamic environments, but in highly stable environments the costs of investing in cognitive processes may overshadow the benefits (Mery and Burns, 2010; Niemelä et al., 2013). As a result, all species have evolved a unique set of cognitive abilities, tuned to their relevant ecological context. Nevertheless, exactly what drives the evolution of cognitive flexibility is largely unknown.

Cognitive flexibility has been postulated to be of high importance for individuals living in rapidly fluctuating environments, and might allow species to escape the evolutionary traps that come with human-induced rapid environmental change (Greggor et al., 2019). Indeed, evidence from several studies suggest that cognitive flexibility varies with environmental heterogeneity, for example across seasons (Rochais et al., 2021), along elevation gradients Hermer et al., 2018) and urbanization gradients (Batabyal and Thaker, 2019; Vardi and Berger-Tal, 2022; but see De Meester, Van Linden, et al., 2022). To better understand whether and

how these selective pressures will drive the evolution of cognitive flexibility, we should study what causes individual differences within a population, because natural selection ultimately acts on intraspecific variation (Thornton and Lukas, 2012; Boogert et al., 2018). Individual variation in cognitive flexibility may be shaped by genetic, developmental as well as environmental factors, leading to differences in functioning of the neurobiological systems that support cognitive flexibility. The relative contribution of each of these sources will determine how this trait will respond to selection (Boogert et al., 2018). However, despite the ecological relevance of cognitive flexibility, how individuals vary in this ability and which factors shape the expression of cognitive flexibility, has seldom been investigated in an ecologically relevant system. This is important, because these are the systems where an evolutionary hypothesis can be tested by manipulating genetic and environmental affects and where variation in cognitive abilities can be related to fitness. The aim of this thesis is therefore to explore the causes of individual differences in cognitive flexibility using the great tit (*Parus major),* as a model system.

Understanding cognitive flexibility

Cognitive, or behavioural flexibility?

Cognitive flexibility is among the cognitive processes that are classified as executive functions: control processes that decide what information should be acquired, selected, and subsequently acted upon (Bobrowicz and Greiff, 2022). The two other executive functions are response inhibition (the ability to inhibit dominant, automatic, or habitual responses) and working memory (the ability to temporarily store and act on information). In behavioural ecology, the ability to adaptively change a learned behaviour in response to changed environmental contingencies has been addressed interchangeably as 'cognitive flexibility' and 'behavioural flexibility' in the literature, causing confusion about the correct term to address this cognitive process (Audet and Lefebvre, 2017). In (medical) neuroscience the term 'cognitive flexibility' is used exclusively for human subjects, while 'behavioural flexibility' is used for non-human subjects (Highgate and Schenk, 2021; Uddin, 2021). However, in behavioural ecology, the term 'behavioural flexibility' has traditionally been used more broadly, describing a wide range of behavioural traits including innovation and problem-solving ability (Audet and Lefebvre, 2017) and even more generally as the reversible flexibility of behavioural phenotypes across contexts (Duckworth, 2010; Niemelä et al., 2013). In this thesis, I therefore use the more restricted term 'cognitive flexibility' to describe the ability to adaptively change behaviour in response to changed environmental contingencies.

Towards an understanding of the evolution of cognitive flexibility

To understand the role of natural selection in driving the evolution of any trait, we must understand

1) what causes trait variation among individuals (*phenotypic variation*),

2) whether there is a consistent relationship between the phenotype of parents and their offspring (*heritability*), and

3) whether heritable variation of the trait is associated with fitness consequences (*fitness variation*) (Charles Darwin, 1859).
The focus of this thesis is on points 1) and 2). While point 3), the fitness consequences of cognitive flexibility, is beyond the scope of this thesis, I provide suggestions how this may be addressed in the future in the general discussion. Below, I will discuss how research into cognitive flexibility has gained the current understanding of underlying causes of individual variation and which knowledge gaps have led to the formulation of the research questions that are addressed in this thesis.

Phenotypic variation
Understanding the ability of a trait to respond to selection starts with measuring the extent of phenotypic variation in a population. This can then be followed by partitioning the phenotypic variance into different sources, such as genetic variance and environmental variance (Falconer, 1989). A widely used method to characterize phenotypic variation in cognitive flexibility, is the reversal learning task (Izquierdo and Jentsch, 2012). In this task, an animal first learns that a certain action (e.g., pressing a lever, displacing an object, landing on a perch) will lead to a certain outcome (e.g. obtaining a food reward), but only for a certain sensory property of a cue (e.g., colour, location) and not another. For example, an animal will receive a food reward if it presses a lever with a red sign, but not if it presses a lever with a green sign. During this association task, the animal will become increasingly proficient at choosing the correct cue. Then, upon reaching a pre-defined learning criterion, the contingency of the rewarding cue is reversed to start the reversal phase. During this phase, responding to the previously correct cue will no longer be rewarded and instead the previously incorrect cue will provide a reward. Animals are expected to initially respond to the previously correct cue, but over time will learn from the lack of rewards and gradually start exploring the other option until they consistently choose the new contingency.

Performance on the reversal learning task depends on the ability to extinguish responses to the previously rewarded cue (perseverance) and to learn the new cue-reward association, which requires associative learning ability as well as the ability to unlearn a non-reward association which may have been made during the first phase of the task. Because previously learned information can hinder the acquisition of comparable new associations (proactive interference), proactive interference can affect reversal learning performance (Tello-Ramos et al., 2019; Morand-Ferron et al., 2022; Tsakanikos and Reed, 2022; Benedict et al., 2023). To quantify performance, studies have used the number of trials that individuals need to reach a predefined learning criterion as well as the number of errors, sometimes subcategorized in different error types, such as perseverative errors (incorrectly choosing the previously rewarded cue before a correct choice has been made) and regressive errors (incorrectly choosing the previously rewarded cue after a correct choice has been made). If more than two choice options are being presented (e.g., using three colours or four locations), also sampling errors can be scored (incorrectly choosing the neutral cue after a correct choice has been made).

Because of the relatively simple requirements for the reversal learning task, it is easy to adapt this paradigm to different species. As a result it has become an important measure of cognitive flexibility in laboratory as well as field settings (Dhawan et al., 2019). Different variants of the test have been implemented in many different species, including insects (Strang and Sherry, 2014; Biergans et al., 2016; Mancini et al., 2019; McCurdy et al., 2021), fish (Buechel et al., 2018; Bensky and Bell, 2020), lizards (Batabyal and Thaker, 2019; De Meester et al., 2022b, 2022c), birds (Bond et al., 2007; Boogert et al., 2010; Cole et al., 2012; Rayburn-Reeves et al., 2013; Cauchoix et al., 2017; Croston et al., 2017; Ashton et al., 2018, 2022; Hermer et al., 2018; van Horik and Emery, 2018; Reichert et al., 2020; Aljadeff and Lotem, 2021; Morand-Ferron et al., 2022; Soravia et al., 2022, 2022; Vardi and Berger-Tal, 2022) and mammals (Mackintosh et al., 1968; Izquierdo et al., 2006; Laughlin et al., 2011; Brust and Guenther, 2015; Klanker et al., 2015; Remmelink et al., 2016; Hassett and Hampton, 2017; Kumpan, 2020; Rochais et al., 2021; Bagley et al., 2022; Stanton et al., 2022)

Partitioning the variance

Repeatability

To ensure that robust measurements of individual cognitive flexibility are obtained, animals can be tested repeatedly to determine the consistency and plasticity of performance. When more than one measurement is taken per individual, the phenotypic variance can be partitioned into variance within individuals and variance between individuals. The ratio of the within-individual variance over the total phenotypic variance is called *repeatability* (Falconer, 1989). Repeatability is useful in order to quantify and validate the extent of consistent individual differences in cognitive flexibility over time, and to obtain the proportion of the variance that is expected to be heritable (Cauchoix et al., 2018; but see Dohm, 2002). A trait that has a repeatability that is larger than zero is considered to show some degree of consistency, and larger values increases the possibility that a large amount of the variance is of genetic, rather than environmental origin (Lynch and Walsh, 1998). Generally, morphological measures have a large repeatability, whereas the repeatability of behavioural measures is much smaller, around 0.35 (Bell et al., 2009), which is especially true for cognitive traits where repeatabilities below 0.30 are most common owing to the relatively large effect of internal and external influences on task performance (Cauchoix et al., 2018).

Measuring repeatability of cognitive flexibility in wild animals is a difficult and time-consuming undertaking, because it requires testing individuals at least twice, but preferably more often, on a task that generally can take up to a day or more to learn. This historically required keeping wild individuals in captivity or recapturing the same individuals for repeated measures, but technological advancements such as radio-frequency identification (RFID)-based conditioning devices have now made it possible to test free-ranging wild individuals repeatedly. Thanks to these systems, there is now (mixed) evidence that reversal learning performance is repeatable: some studies report significant repeatability such as in great tits (*Parus major*) (Reichert et al., 2020; Morand-Ferron et al., 2022) and Australian magpies

(*Cracticus tibicen dorsalis*) (Ashton et al., 2018, 2022), but in blue tits (*Cyanistes caeruleus*) (Reichert et al., 2020) and song sparrows (*Melospiza melodia*) reversal learning was not significantly repeatable (Soha et al., 2019).

Heritability
The repeatability expresses the proportion of the variance that is due to both genetic and environmental differences between individuals. Conceptually, repeatability estimates therefore provide a fundamental upper limit for heritability (Falconer, 1989). In practice, in the case of cognitive assays where animals can learn from experience, repeatability could actually be lower than heritability (Dohm, 2002). In the case of a reversal learning task, familiarity with the structure of the task may affect performance or the trait that is measured (e.g., long-term memory or rule-learning rather than cognitive flexibility). Quantitative genetic approaches such as experimental breeding can be used to directly estimate the proportion of phenotypic variance that is attributed to additive genetic variance, the narrow-sense *heritability*, while excluding environmental causes (Falconer, 1989; Boake et al., 2002). Current evidence using genetic relatedness matrices, such as in mice (Laughlin et al., 2011; Bagley et al., 2022) and red junglefowl (Sorato et al., 2018), suggests low to moderate heritability of reversal learning performance.

Adaptive variation–cognitive styles
An interesting theory is that repeatable and heritable variation in cognitive flexibility might be associated with differences in individual personality traits (Coppens et al., 2010; Sih and Del Giudice, 2012). For example, fast exploring, "proactive" personality types are associated with faster decision making, whereas slow exploring, "reactive" individuals pay more attention to task switches as required in a reversal learning task (Titulaer et al., 2012; Mazza et al., 2018). This hypothesis is ecologically and evolutionary very interesting, because it can explain how different cognitive phenotypes can coexist: fast explorers may have adopted a 'life fast, die young' strategy, whereas shy individuals may benefit more from the costs of higher cognitive flexibility as a longer life will lead to the experiences of more environmental changes. However, this idea is currently still controversial, with different studies pointing at converse directions between cognitive flexibility and personality (Griffin et al., 2015), perhaps because such relationships are often context (e.g. habitat) dependent (De Meester et al., 2022a).

Causes of individual variation in cognitive flexibility

The neurobiological basis of cognitive flexibility
Individual differences in cognitive flexibility are likely to reflect, and be explained by, individual variation in functioning of underlying neurobiological mechanisms. Cognitive flexibility has a high relevance to neuropsychology because it is compromised in many clinical conditions including autism spectral disorder, attention-deficit/hyperactivity disorder, obsessive compulsive disorder, schizophrenia, substance abuse, and dementias (Izquierdo et al., 2017; Uddin, 2021). As a result, the reversal learning task is a commonly used paradigm in this

field, and the brain regions and neurochemical substrates that support cognitive flexibility are relatively well understood (Izquierdo et al., 2017; Uddin, 2021). However, not all of these findings are readily translatable to birds, because of the differential structuring of the brains (Box 1.1, Figure 1.1).

Neuroanatomy of cognitive flexibility

In mammals, it is known that different aspects of reversal learning require differential involvement of brain regions. There is a large role of the frontal cortex, especially of the orbitofrontal cortex (OFC), which signals reward probability (Uddin, 2021; Rudebeck and Izquierdo, 2022). In the mouse, neurons of the OFC respond to the cue switches during reversal learning (Banerjee et al., 2020) and inactivation of the OFC causes perseverance of previously learned choices in rats (Klanker et al., 2013). There is also evidence for the involvement of the medial prefontal cortex (mPFC). The role of the mPFC is less clearly defined but lies in error detection and performance monitoring (Stolyarova et al., 2019; Avigan et al., 2020; Keefer and Petrovich, 2020; Rudebeck and Izquierdo, 2022). Intact communication between the OFC and other brain structures is crucial for reversal learning ability (Klanker et al., 2013). The OFC projects to the striatum, lesions of which impair reversal learning performance by affecting the generation of a new behavioural strategy (Ragozzino, 2007; Izquierdo et al., 2017). In addition, the OFC projects to the hippocampus, and hippocampal lesioning causes impaired reversal learning performance (Kosaki and Watanabe, 2012), especially when combined with lesioning of the OFC (Thonnard et al., 2021). The current view is that the hippocampus plays a role in the learning of the task structure during the reversal task (Vilà-Balló et al., 2017). However, (Seib et al., 2020) argue that the role for the hippocampus in a reversal learning task is limited to learning probabilistic nature of uncertain rewards, not necessary contingency reversals. Finally, there is also evidence for a brain region outside the telencephalon to be involved in reversal learning ability: the cerebellum. The cerebellum plays a role in error processing and performance monitoring, consistent with a functional link between the cerebellum and the prefrontal cortex (Thoma et al., 2008; Dickson et al., 2017; Badura et al., 2018; Peterburs et al., 2018).

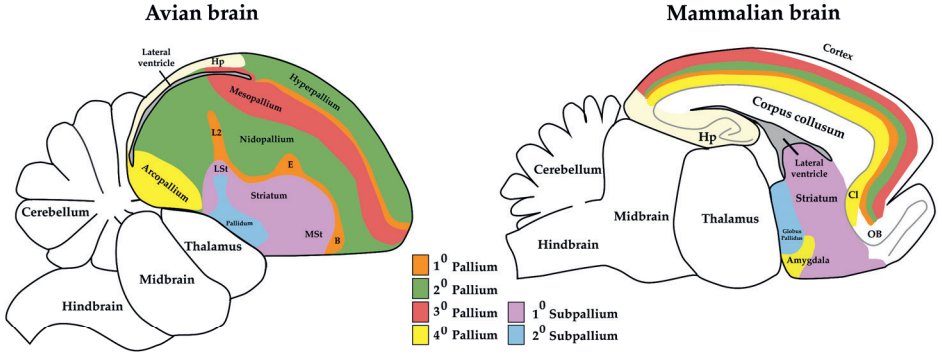

Figure 1.1 *Current view of avian brain evolution and the homologies between mammalian and avian brains according to Jarvis et al., (2013). B = Basorostralis, E= Entopallium, Hp = hippocampus, L2 = Field L2, LSt = Lateral striatum, MSt = medial striatum.*

Box 1.1 The avian brain
The main anatomical divisions of the vertebrate brain include: the hindbrain, cerebellum, midbrain, diencephalon (including thalamus and hypothalamus), and telencephalon (Karten, 2015). The telencephalic subdivisions can be further classified into pallial and subpallial (striatal and pallidal). The function and structural organization of the subpallium is highly similar in mammals and birds (Belgard et al., 2013; Kuenzel et al., 2011). However, to what extent the different subdivisions of the avian pallium relate to the subdivisions of the mammalian pallium are still a topic of debate (Gedman et al., 2021). Only the hippocampus is a pallial region with undisputed homology between birds and mammals (Belgard et al., 2013; Mayer et al., 2013), but even so, its structural organization is completely different (Herold et al., 2014). The mammalian pallium is structured into cortical layers and is subdivided into the neocortex (consisting of four lobes: frontal, parietal, temporal, and occipital) and the allocortex (including the hippocampal formation and the olfactory cortex) (Medina et al., 2022). The avian pallium lacks this cortical lamination and can be subdivided in to the hippocampus, hyperpallium, mesopallium, nidopallium, and arcopallium (Jarvis et al., 2013). Although not homologous, the nidopallium caudolaterale (NCL) is functionally equivalent to the prefrontal cortex (PFC): both are associative areas involved in executive functions with a close connection to many secondary and motor regions (Güntürkün & Bugnyar, 2016).

In birds, the involvement of specific brain regions in reversal learning performance is less clearly defined. Consistent with the involvement of mammalian pallial regions like the OFC and mPFC, lesions of two avian pallial structures, the hyperpallium (wulst) and the NCL result in reversal learning deficits (Hartmann and Güntürkün, 1998; Bingman et al., 2008). Furthermore, lesions of the striatum affect reversal learning ability in pigeons, increasing the number of errors after a contingency switch (Watanabe, 2005). Also lesioning of the hippocampus impaired reversal learning in pigeons, although the effect was mostly apparent on a spatial learning task rather than on a visual learning task (Good, 1987; Watanabe, 2005). Suppression of neurogenesis in the hippocampus resulted in an increase in reversal errors in chickadees (Guitar and Sherry, 2018), and hippocampal neurogenesis has been suggested to prevent proactive interference (Tello-Ramos et al., 2019).

Neurochemistry of cognitive flexibility
A further understanding of how these brain regions are critically involved in the modulation of cognitive flexibility can be achieved by understanding the neurotransmitter circuitry in these regions, especially because these circuits are often the basis of individual variation. The main neurotransmitter of the OFC is serotonin, and accordingly, individual variation in reversal learning performance can be predicted by serotonin availability in mammals. Reduced serotonin signalling in the cortex increases perseveration and impairs reversal learning, likely because it is involved in among others absence-of-reward processing (Izquierdo et al., 2017). For example, highly perseverative rats showed reduced

levels of serotonin metabolites, reduced serotonin receptor binding in the OFC and increased expression of enzymes that break down serotonin (Barlow et al., 2015). Despite the clear evidence for a role of serotonergic transmission in mammals, there are only a few studies on its involvement in reversal learning performance in birds, even though serotonin receptors are enriched in the NCL (Herold et al., 2012), making involvement of this neurotransmitter highly likely. Higher serotonin receptor gene expression in the telencephalon of chickens was associated with lower reversal learning performance (Boddington et al., 2020).

The OFC receives modulatory dopaminergic input from the striatum (Kahnt and Tobler, 2017) and consistently, the interaction between striatal dopamine levels and cortical serotonin levels explains more than half of the variance of reversal learning performance in vervet monkeys (*Chlorocebus aethiops sabaeus*) (Groman et al., 2013). Dopamine release in the striatum conveys unexpected reward (Klanker et al., 2015, 2017) and individual differences in the use of positive feedback during reversal learning can be predicted by striatal dopamine transporter binding (Stolyarova et al., 2014). Experimental blocking, or low availability, of dopamine receptors can disrupt reversal learning performance (Izquierdo et al., 2006; Groman et al., 2011; Laughlin et al., 2011; Linden et al., 2018; Alsiö et al., 2019), with distinct roles for the two major dopamine receptor subtypes (D1 and D2 receptors) in different striatal subregions (Sala-Bayo et al., 2020). Evidence of the involvement of dopamine signalling in birds is restricted to two studies, one showing that the blockade of dopamine D1 receptors in the NCL negatively affected reversal learning performance (Diekamp et al., 2000) and another showing a negative effect of dopamine D2 receptor blocking (Herold, 2010).

Lastly, there is also a role for another key regulatory neurotransmitter, glutamate, although its specific requirement for reversal learning ability is still under debate, as this neurotransmitter is broadly required for synaptic plasticity (Izquierdo et al., 2017). Yet, malfunctioning glutamatergic NMDA receptors can induce defective reversal learning performance through increased perseverative errors (Thonnard et al., 2019; Liu et al., 2020). Again, evidence in birds is restricted to two studies, both showing that NMDA receptor antagonists negatively affected reversal learning performance (Lissek et al., 2002; Herold, 2010).

In conclusion, despite some important dissimilarities in the organization of the avian and mammalian brain, the available evidence largely points to an involvement of similar brain regions and neurotransmitter systems. However, evidence in birds is largely restricted to lesions and receptor blockages, whereas studies on natural variability in neurotransmitter functioning (e.g., individual variation in neurotransmitter release and receptor abundance or expression), and the mechanisms that lead to these differences are lacking.

The (epi)genetic basis of cognitive flexibility

Genetic origins of individual variation in cognitive flexibility

The necessary information to develop and maintain the function of neural systems is encoded in the genetic material. Heritable differences in DNA sequence that lead to differential expression of genes like those required for neural development or receptor abundance can, therefore, lead to differences in cognitive abilities by affecting the ability of the neural system to acquire, store or act on environmental information (Friedman et al., 2008). To identify such heritable differences, genome-wide quantitative trait locus (QTL) mapping has been a useful means to localize polymorphisms and identify candidate genes for complex traits (Slate, 2005; van Oers and Mueller, 2010). Using QTL mapping combined with gene expression data for reversal learning, several candidate genes have been proposed in mice, among which *Wdr73*, a gene that is associated with heritable variation in striatal dopamine receptor expression (Bagley et al., 2022) and *Syn3*, which negatively regulates dopamine release and expression of which in the hippocampus, striatum, and neocortex is negatively correlated with reversal learning performance (Laughlin et al., 2011). Knockout of *Syn3* induced less flexible responding to the contingency reversal (Moore et al., 2021). Alternatively, if candidate genes are already known, polymorphisms can be studied on a single gene basis. A polymorphism in the *DRD2* gene was related to altered striatal and OFC activity and negatively affected performance on a reversal learning task in humans (Jocham et al., 2009). Polymorphisms in the serotonin transporter (*SLC6A4, SERT*) were associated with reversal learning ability in rhesus macaques (Vallender et al., 2009). However, a recent study in chickens showed that individuals with different *SLC6A4* polymorphisms did not differ in reversal learning ability (Dudde et al., 2022). Nonetheless, these findings suggest that reversal learning performance can vary as a function of the genotype, though yet again, evidence in birds is limited.

Epigenetic origins of individual variation in cognitive flexibility

Crucial here is to point out that not necessary the DNA sequence, but rather when, where and to what degree genes are expressed is what matters for phenotypic variation, especially in the context of behavioural traits (Fischer et al., 2021). That gene expression variation not only arises through the DNA sequence already becomes clear at a cellular level. Although each cell in an organism contains the same DNA, the sets of genes that are expressed are specific to each cell type. The developmental processes that define which genes are transcribed and where, involves local presence of transcription factors and the structure and organization of chromatin – the complex that the DNA forms with histones and other proteins (McGinty and Tan, 2015). The mechanisms that regulate this structuring without altering the DNA sequence are referred to as epigenetic mechanisms (Box 1.2). Because the expression of many locally essential genes simply must be precisely controlled in most cellular processes (Fraser et al., 2004), epigenetic mechanisms regulate developmental stability in cell differentiation.

For other genes however, there can be substantial variation in gene expression among individuals. Gene expression variation that arises from genetic factors can

be induced via alternative epigenetic states. For example, genetic variation can influence epigenetic gene regulation during neurogenesis (Liang et al., 2021). However, epigenetic induction of (among individual) gene expression variation can also have stochastic (Eling et al., 2019) and environmental origins such as the social environment (Bell, 2020). Moreover, the dynamic induction of transcription variation in response to the environment is a crucial mechanism underlying cognitive processes such as learning and memory formation. Dynamic gene expression of neural cells is essential for trans-synaptic plasticity: the structural changes at the synapse that follow experience and are necessary to encode memories (Sheng and Greenberg, 1990). Quite strikingly, activity-dependent neuronal gene expression is regulated via the same epigenetic mechanisms that regulate developmental gene expression (Boyce and Kobor, 2015). Mechanisms like histone deacetylation and DNA methylation regulate the changes in access to gene regulatory elements required for activity-dependent transcription that is necessary for learning and memory formation (Miller et al., 2008; Day et al., 2013; Schmauss, 2017). Evidence is now accumulating that epigenetic mechanisms are involved in associative learning. DNA methylation affects associative memory strength in mammals (Day et al., 2013) and in honeybees, inhibition of DNA methyltransferases, which induce DNA methylation, negatively affected reversal learning (Biergans et al., 2016). De novo DNA methylation in the hippocampus is required for neurogenesis and is critical for spatial reversal learning in mice (Zocher et al., 2021). Histone deacetylase inhibitors can enhance long-term memory formation (McQuown and Wood, 2011), whereas overexpression of histone deacetylase in the rat striatum prevented habit formation following associative learning (Malvaez et al., 2018) and induced fast, inflexible behaviour during reward-guided decision making (Pribut et al., 2021).

Together, these findings indicate the role of epigenetic mechanisms in experience-dependent behavioural change in adults, and how they are likely to contribute to the reversal learning process. Additionally, epigenetic processes are known to be involved in environmental influences on individuation during development. For example, early-life exercise induces histone modifications that promote the expression of genes involved in hippocampal memory formation (Raus et al., 2023), and social adolescence impaired reversal learning via increased expression of the *BDNF* gene in the mPFC and decreased expression in the hippocampus induced by altered histone acetylation (Li et al., 2016). There are many other studies indicating how early life experiences can affect reversal learning ability, for example food insecurity (Lin et al., 2022), environmental enrichment (Zeleznikow-Johnston et al., 2017), maternal separation (Noschang et al., 2012) and corticosterone exposure (Bebus et al., 2016). Although these studies did not directly study the contributions of epigenetic alterations to these phenotypic effects, many of these manipulations are known to induce epigenetic modifications (Moody et al., 2017; Zhang et al., 2018; Rahman and McGowan, 2022), providing a likely regulatory mechanism for the effect of these early life manipulations on reversal learning ability.

Box 1.2 A brief summary of epigenetic modifications
Histone modifications are chemical modifications to the tails of histone proteins that change the transcriptional state by influencing the accessibility of the underlying DNA to transcription factors or enzymes that regulate DNA methylation (Wilson & Merkenschlager, 2006). These modifications include acylation, methylation, phosphorylation, and ubiquitination (Huang et al., 2014). Enzymes that regulate these modifications, such as histone deacetylases (HDACs) which remove acetyl groups from histone tails, can modify gene transcription (Kouzarides, 2007). **DNA methylation** is the addition of a methyl group to cytosines. This usually occurs in CpG dinucleotides, but in neural cells, non-CpG methylation is also common (Kozlenkov et al., 2014). DNA methylation can result from the vacation of transcription factors at open chromatin regions, and is generally followed by tightening of the chromatin and suppression of gene expression (Thurman et al., 2012). DNA methylation and histone modifications often coexist at silenced genes and both can be the initial epigenetic event that initiates silencing (Vaissière et al., 2008). DNA methylation readers interact with histone modification erasers to suppress transcription. Vice-versa, DNA methyltransferases contain chromatin recognition domains and may induce DNA methylation upon recognition of certain histone modifications (Bohnsack & Pandey, 2021). Eventually, epigenetic modifications such as histone modifications and DNA methylation will alter accessibility of the underlying DNA sequence is to transcription factors; a phenomenon that is described as **chromatin accessibility**.

Aims and outline of this thesis

What are the regulatory mechanisms underlying possibly repeatable and heritable individual differences in cognitive flexibility in a wild avian species? Despite the likely importance of cognitive flexibility in dealing with unpredictable environments we currently lack such data. This knowledge would get us closer to understanding how this behaviour develops, how variation is maintained, and ultimately its fitness consequences, information that is altogether needed in order to understand what drives the evolution of cognitive flexibility. The overall aim of this thesis is therefore to study the causal mechanisms underlying individual differences in cognitive flexibility.

In this thesis, I will explore the extent to which both genetic and epigenetic variation underly individual variation in cognitive flexibility. As is the case for many cognitive traits, I expect the contribution of heritable genetic variation for cognitive flexibility to be relatively low. Because the currently available literature suggests that epigenetic mechanisms are not only essential for carrying out cognitive tasks but also for regulating the effects of early life experiences on neural development and cognitive performance, I will study their involvement in individual variation in cognitive flexibility. In addition, I want to contribute to a better understanding of the relationship between chromatin accessibility and gene expression in regulating

cell fates during brain development, because understanding the molecular profiles of specific brain regions will provide an important baseline for the comparison of cognitive and behavioural phenotypes of which the regulation is situated in these regions.

With this thesis, I aim to answer the following research questions:

1. How repeatable and heritable is cognitive flexibility in the great tit? (**Chapter 2**)
2. Can chromatin accessibility explain gene expression variation between cells from anatomically distinct origins in the brain in the great tit? (**Chapter 3**)
3. Can individual differences in cognitive flexibility be explained by variation in chromatin accessibility and gene expression from relevant brain regions in birds and mammals? (**Chapter 4 and 5**)

In **Chapter 2**, I set up a two-generation artificial selection experiment to assess narrow-sense heritability of reversal learning performance in great tits, which I complement with an animal model approach to additionally estimate heritability of associative learning and exploratory behaviour. Furthermore, I assess the repeatability of associative and reversal learning performance as well as correlations between the cognitive and personality traits. In **Chapter 3**, I use Assay for Transposase-Accessible Chromatin using sequencing (ATAC-seq) and RNA sequencing (RNA-seq)to study the relationship between chromatin accessibility and gene expression to determine functional divisions among neuronal and non-neuronal cells collected from the striatum, hippocampus and cerebellum, validating these findings with data collected from mice and rats. Then, in **Chapter 4,** I explore the role of gene expression variation in individual differences underlying reversal learning performance in great tits and mice, using RNA-seq to assess gene expression in the striatum and cerebellum; homologous brain regions between birds and mammals. In **Chapter 5,** I focus further on the great tit, asking whether individual differences in gene expression variation that underlie reversal learning performance are explained by chromatin accessibility and DNA methylation by combining data collected with RNA-seq (striatum, hippocampus and cerebellum), ATAC-seq (striatum and hippocampus), and Enzymatic methyl sequencing (EM-seq) (striatum). In the general discussion, **Chapter 6**, I integrate the findings of my thesis, place them into a wider context and discuss how this thesis has contributed to understanding the causes of individual variation in cognitive flexibility. I end the general discussion with several suggestions for future research.

General study methods

Study species – the great tit

In this thesis, I use the great tit (*Parus major*) as a model species to study the causes of individual variation in cognitive flexibility in birds (Figure 1.2). This passerine bird occurs in a wide geographical range throughout Eurasia and North Africa, where it lives in deciduous and mixed forests, although it is also commonly found in urban parks and gardens (Gosler, 1993). Although great tits are omnivorous, they are largely insectivorous in spring and summer, but switch their preference in autumn and winter towards nuts and seeds, also readily eating those offered in bird feeders when natural food is scarce. Its generalist nature combined with a strong learning ability (e.g., recognizing and abandoning food patches depending on their productivity), allows the great tit to exploit a wide range of ecological situations and resources (Gosler, 1993). The role of cognitive processes in individual foraging of great tits has for years been the interest of many behavioural ecologists (Krebs et al., 1978; Morand-Ferron et al., 2022).

Although great tits naturally breed in wood-cavities, they will nest almost exclusively in artificial nest boxes when sufficiently provided, which makes them very suitable for evolutionary, ecological, and behavioural studies. In addition, great tits are relatively easy to keep and breed under captive conditions, allowing researchers to study their behaviour in detail and to perform experimental breeding, including the creation of artificial selection lines (see below). The great tit also has become the focus point of detailed genomic analysis of behavioural and life-history traits, especially since its genome has been mapped (Laine et al., 2016). This makes this species one of the few in which behavioural traits can be extensively studied under laboratory conditions as well as tested in wild populations.

Figure 1.2 *The study species of this thesis, the great tit (Parus major).*

Measuring cognitive flexibility

To assess cognitive flexibility in great tits, I developed a reversal learning task using automated "smart" feeders designed by NatureCounters (Maidstone, UK). These feeders are equipped with an RFID antenna, which registers the unique code of a passive integrated transponder (PIT) Tag that can be attached to a bird's leg. Upon

registration of the PIT Tag, the door can open for a set duration of two seconds; opening and closure of a transparent plastic door is controlled with a micro-servomotor. After individuals are trained to use the feeders, individuals are tested individually in a testing aviary with three feeders positioned in a triangular array (Figure 1.3). These three feeders are connected through a network cable, allowing for integrated responses between the feeders and for the learning experiments to take place without human intervention. In the associative learning phase, one feeder provides a reward for an individual, the door of which opens upon tag registration, whereas the other two feeders stay closed when visited. This assigned feeder is reinforced until individuals reach a criterion level of six correct trials out of seven. After completing the associative learning phase, the reversal learning task is initiated and the reward contingency is reversed to one of the other two feeders. Again, birds have to reach the learning criterion of six correct visits over seven trials to the new feeder. Associative and reversal learning performance are scored as the total number of trials required to reach the learning criterion of six correct visits out of seven subsequent trials.

Artificial selection

To investigate the genetic basis of individual differences in cognitive flexibility, I used artificial selection, a technique widely used in domestic animal breeding. Artificial selections experiments are an excellent way of providing evidence for the genetic basis of naturally occurring based individual variation in learning and memory and the neural structures that support them (Dukas, 2004; Kotrschal et al., 2013; Dunlap and Stephens, 2014), and such experiments have been used before to estimate the heritability of behavioural traits in great tits (Drent et al., 2003; van Oers et al., 2004).

In this thesis, I performed a two-way selection for 'fast' and 'slow' reversal learning performance, scored as the number of trials to reach criterion in the reversal learning phase. Using 10-day old great tit nestlings collected from a wild population and hand-reared at the NIOO aviary facilities as a starting population for our selection experiment, we ensure a similar rearing environment to reduce the impact of early life effects on phenotypic variation. After measuring their reversal learning performance, I selected individuals with the highest scores for the 'fast' and lowest scores for the 'slow' reversal learning line to breed in aviaries at the NIOO. I transported their egg clutches to a field site, to be incubated by wild foster parents. These F1 chicks are again hand-reared, tested and selected for breeding, forming pairs from the offspring by selecting 'fast' individuals from the 'fast' reversal learning line, and 'slow' individuals from the 'slow' reversal learning line to produce the F2 generation. By measuring the response to selection as a change in mean phenotype (reversal learning performance) of the offspring compared the parental generation, and dividing that by the strength of selection, I could use this experiment to estimate the realized heritability (Falconer, 1989).

Figure 1.3 *Experimental setup for the reversal learning task.*

(Epi)genomic tools

FANS sorting

To selectively study gene expression and chromatin accessibility in nuclei from neuronal cells and non-neuronal cells, the nuclear neuronal marker (NeuN) can be used to distinguish neurons from non-neurons. After staining nuclei with an anti-NeuN antibody conjugated with the fluorescent Alexa488, labelled (NeuN+) neurons can be isolated from non-labelled (NeuN-) nuclei using fluorescence-activated nuclear sorting (FANS), allowing for separate sequencing of these cell populations separately.

Gene expression

The translation of DNA sequence into proteins first involves the transcription of the DNA sequence into an RNA sequence. The majority of the RNA sequence does not encode proteins and is named non-coding (ncRNA). RNA that is translated into proteins is named messenger RNA (mRNA). This mRNA is stabilized with a poly-A tail, a long chain of adenine nucleotides, before it is exported from the nucleus and transported to the cytoplasm, where it is translated into a protein by ribosomes. In this thesis, I use RNA-sequencing (RNA-seq) on total RNA that has been enriched for mRNA by removing polyadenylated negative transcripts, to explore gene expression differences between anatomically distinct groups (nuclei originating from different cell types or brain regions) and between phenotypically distinct individuals.

Chromatin accessibility

The assay for transposase accessible chromatin followed by sequencing (ATAC-seq) can be used to assess chromatin accessibility (Buenrostro et al., 2015; Corces et al., 2017). In this assay, the hyperactive enzyme Tn5 transposase recognizes and cuts DNA at open chromatin regions, and inserts sequencing adapters. These open chromatin regions are then amplified and sequenced, and identified genome-wide using bioinformatic analysis. This method allows identification of differential chromatin accessibility across samples.

DNA methylation

Enzymatic methyl sequencing (EM-seq) is a novel method to detect DNA methylation. This method uses an enzymatic conversion of unmethylated cytosines to uracils, which are replaced by thymine during PCR. Unmethylated cytosines are therefore read as thymine during Illumina sequencing, whereas methylated cytosines are read as cytosines (Vaisvila et al., 2021). This method circumvents issues (e.g., DNA degradation) often associated with bisulfite sequencing, the current gold standard for methylome mapping which uses sodium bisulfite to distinguish methylated from unmethylated cytosines.

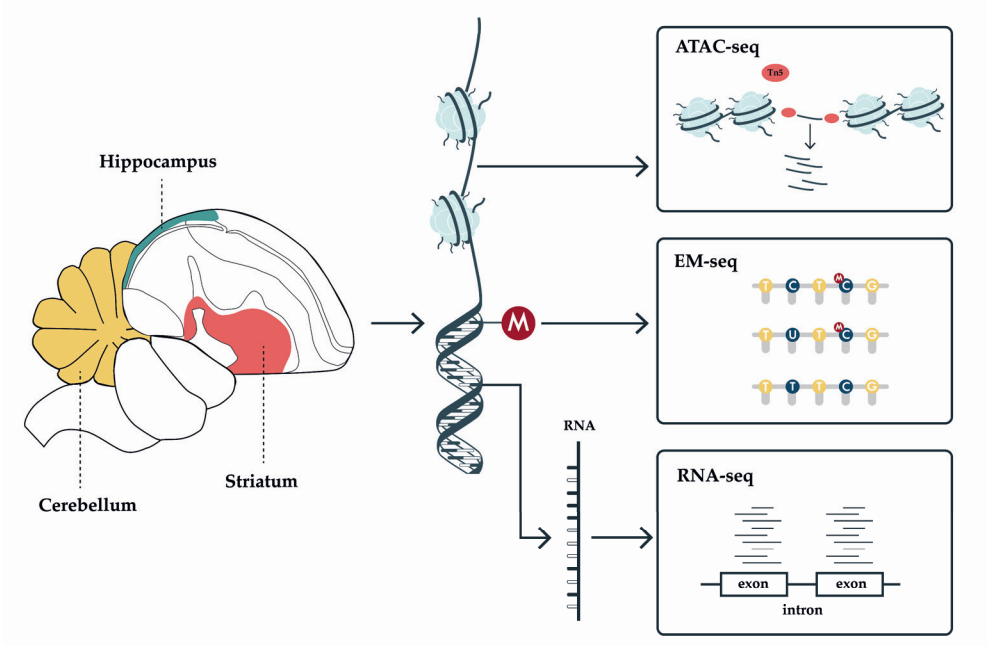

Figure 1.4 *Overview of studied brain regions and applied (epi)genomic tools.*

Chapter 2.

Artificial selection for reversal learning reveals limited repeatability and no heritability of cognitive flexibility in great tits (*Parus major*)

Krista van den Heuvel, John L. Quinn, Alexander Kotrschal, Kees van Oers

Abstract

Cognitive flexibility controls how animals respond to changing environmental conditions. Individuals within species often vary considerably in cognitive flexibility but the micro-evolutionary potential in animal populations remains enigmatic. One prerequisite for cognitive flexibility to be able to evolve is consistent among-individual variation with a heritable basis. Here we determine the repeatability and realized heritability of cognitive flexibility among great tits (*Parus major*) by performing an artificial selection experiment on reversal learning performance over three generations. We assessed associative and reversal learning repeatedly in 385 individuals. We found low, yet significant, repeatability ($R = 0.14$) of reversal learning performance. Our artificial selection showed no evidence for narrow-sense heritability of either associative or reversal learning, while we confirmed the heritability of exploratory behaviour. We did observe correlations between boldness and associative learning and between associative and reversal learning. Our findings suggests that while it seems possible to adequately measure individual performance in cognitive flexibility, its heritable component is absent or too small to detect. Although cognitive flexibility itself is not generally heritable, the underlying cognitive mechanisms may well be. Nonetheless, unidentified sources of presumably environmental variation may explain are large part of the variation in cognitive flexibility, which has important consequences for its evolvability and potentially for how effectively great tits respond to environmental change generally.

Under review at Proceedings of the Royal Society B: Biological Sciences

Introduction

The need for animals to flexibly adjust their behaviour to environmental changes has selected for the evolution of cognitive abilities, that is, the abilities to acquire, process, store and act on information from the environment (Shettleworth, 2010). Animals show consistency during foraging (Chittka et al., 1999; Naef-Daenzer and Keller, 1999) and are capable of memorizing various features of a food source (location, colour, shape) (Bitterman, 1965; Shettleworth, 2010). However, the ability to re-evaluate this behaviour can be equally essential if, for example, a source no longer provides food. One particularly relevant trait, therefore, is cognitive flexibility, the executive cognitive function that allows animals to update goal-directed behaviour in response to changing environmental conditions (Klanker et al., 2013). Frequent fluctuations in ecological resources, such as in spatially complex and heterogeneous environments, should select for greater cognitive flexibility, allowing individuals to respond more rapidly to changes in their environment (Bond et al., 2007; Shettleworth, 2010). However, whether cognitive flexibility can respond to selection is currently unknown. To understand this evolutionary potential of cognitive flexibility, we need to quantify the extent of stable individual differences in cognitive flexibility and whether that individual variation has a genetic basis (Houle, 1992; Dukas, 2004; Thornton and Lukas, 2012).

Determining stable individual differences in cognitive traits is crucial when investigating the adaptive nature of such traits, nevertheless, this has received relatively little attention in non-human animals (Griffin et al., 2015), although the literature is expanding (Cauchoix et al., 2018). To test whether individual differences in performance are consistent over time, studies so far have focused on the existence of consistent among-individual variation, or *repeatability* of cognitive traits (Dohm, 2002), finding that repeatability is usually below 0.28, with a significant publication bias in favour of reporting higher repeatabilities (Cauchoix et al., 2018). Cognitive flexibility is generally assessed with a reversal learning task (Klanker et al., 2013). In this assay, a previously rewarded option becomes non-rewarding and vice versa, in order to assess how flexible an animal can adapt its learned response by measuring the ability of animals to correctly respond to this change (Izquierdo et al., 2017). There is mixed evidence that reversal learning performance is repeatable: some studies report significant repeatability such as in great tits (*Parus major*) (Reichert et al., 2020; Morand-Ferron et al., 2022) and Australian magpies (*Cracticus tibicen dorsalis*) (Ashton et al., 2018, 2022), but in blue tits (*Cyanistes caeruleus*) (Reichert et al., 2020) and song sparrows (*Melospiza melodia*) reversal learning was not significantly repeatable (Soha et al., 2019). In the latter case, the authors suggest it is due to a change in the nature of a task, when it is measured repeatedly, because familiarity with the structure of the task may affect performance or even the trait that is measured. Nonetheless, repeated measures are needed to estimate consistent among-individual variation, in order to support the idea that there are intrinsic individual differences in performance.

Repeatability estimates provide a fundamental upper limit for heritability, but consistency can also arise from early environmental or maternal effects (Falconer, 1989; but see Dohm, 2002). Therefore, once intrinsic differences have been established, demonstrating that any phenotypic trait is heritable is a fundamental next step in understanding the trait's evolutionary potential (Boogert et al., 2018). Since reversal performance is always tested following an associative learning task, they are generally considered in concert. Assessing the extent of among-individual covariance between the two learning phases will be crucial to understand what drives, possibly heritable, among-individual differences in reversal learning performance. Following the hypothesized trade-off between learning and cognitive flexibility, animals that are quick at forming initial associations learn subsequent similar information less well (Amy et al., 2012; Del Giudice and Crespi, 2018; Tello-Ramos et al., 2019). Several studies have investigated both the phenotypic correlations between and the heritability of associative and reversal learning performance (Laughlin et al., 2011; Raine and Chittka, 2012; Nettle et al., 2015; Sorato et al., 2018; Vardi et al., 2020; Bailey et al., 2021; Prentice et al., 2021; De Meester et al., 2022b). Current evidence suggests low to moderate heritability of reversal learning performance across species, but how it relates to associative learning appears to vary between species. Identifying the existence of a trade of between learning and cognitive flexibility is important, because this has been hypothesised to maintain cognitive variation (Del Giudice and Crespi, 2018).

In line with this, personality traits and cognitive performance have been hypothesized to be correlated at the among-individual level (Griffin et al., 2015). Fast explorers would learn faster but inflexibly, meaning that they have more difficulty learning a new cue-reward association (Sih and Del Giudice, 2012; Dougherty and Guillette, 2018). However, even though correlations have been found between personality traits and (reversal) learning performance, the direction of this relationship varies widely across species or studies (Titulaer et al., 2012; Dougherty and Guillette, 2018), and these are generally raw phenotypic correlations with no partitioning of among- and between-individual components. Knowing to what extent variation in personality traits relates to reversal learning performance in great tits, will help us understand whether cognitive flexibility and personality variation are controlled by the same underlying factors in great tits (Morand-Ferron et al., 2016).

Experimental evidence for heritable variation in cognitive flexibility, or in any cognitive trait, is lacking in non-human animals (Croston et al., 2015b). Artificial selection experiments provide a powerful method for obtaining strong, direct evidence for naturally occurring, heritable individual variation in cognitive performance (Dukas, 2004). Therefore, we performed bi-directional artificial selection on natural variation in reversal learning ability under controlled laboratory conditions in hand-reared great tits (*Parus major*) collected from a natural population, while including repeated measures to estimate consistent among-individual differences. Previous artificial selection experiments in great tits have successfully demonstrated heritability of exploratory behaviour, risk-taking

behaviour and timing of reproduction (Drent et al., 2003; van Oers et al., 2004; Verhagen et al., 2019). Here we estimated (i) individual consistency and repeatability of performance on associative and reversal learning tasks, (ii) the covariation between performance on the associative and reversal learning task and two personality traits, and (iii) the narrow-sense heritabilities of these cognitive traits. We predicted significant, but low to moderate, individual consistency and heritability, since within-individual variation in cognitive performance is likely influenced by environmental effects, experience, and intrinsic motivation. We expected to find associations between associative learning, reversal learning, and personality traits; negative associations would support the above suggested trade-offs, while positive correlations could indicate they are determined by similar underlying mechanisms.

Methods

Study subjects

We conducted this study at the Netherlands Institute of Ecology (NIOO-KNAW) from May 2018 to April 2021 spanning 3 years. Each year in May, we hand-reared great tit (Parus major) nestlings until independence. As a starting population, we collected 322 10-day old nestlings from 42 broods originating from a nest box population at Boslust (Groot Warnsborn) near Arnhem, the Netherlands (5°850 E, 52°010 N), a 70 ha field site consisting of mixed pine-deciduous forest, and brought them to the aviary facilities at the NIOO-KNAW. We hand-reared the nestlings until independence according to the methods described by (Drent et al., 2003). Briefly, we transferred nestlings in sibling groups of three to four birds to a compartment within a wooden box, each box containing three compartments and each compartment containing a natural parasite-free nest. Upon fledging, around 17-20 days after hatching, birds were transferred to small wire-mesh cages in groups of three. Around day 35 after hatching**,** they were completely independent and we transferred them to standard individual cages of 0.9 m × 0.4 m × 0.5 m with solid bottom, top, side, and rear walls, a wire-mesh front and three perches. Birds were kept under natural light conditions in acoustic and visual contact with each other.

After two days of individual housing, in June/July, we performed a novel environment test and a novel object test on all hand-reared juveniles to test for early exploratory behaviour ((Drent et al., 2003); further details below). In July, we took a blood sample for sex determination. In September, after their first moult, we transferred individuals to single-sex groups (maximum 7 males or 8 females) in semi-open outdoor aviaries (2 m x 4 m x 2.5 m), which was there standard housing outside the breeding season. Food consisted of a homemade mixture of ground beef heart, egg, calcium and a multivitamin solution, supplemented with mealworms, apple, and sunflower seeds and fat balls in winter, and was available ad libitum. In October, when birds were full-grown, we measured tarsus with sliding callipers to the nearest 0.1 mm. From October-February, birds were tested for associative and reversal learning performance to assess their cognitive flexibility. Based on their performance in the reversal learning task, we selected individuals for the 'reversal

learning line' breeding pairs in the same semi-open aviaries to produce the next generation in captivity (for details see heading "*Selection procedure and breeding" below*).

Eggs produced by this parental (P) generation and the subsequent, first (F1) generation were placed in a natural nest at our field site to be incubated by wild foster females. Ten days after hatching, nestlings were collected, brought to our indoor facilities and hand-reared as described above (224 F1 chicks from 29 P pairs and 181 F2 chicks from 27 F1 pairs). These chicks were tested for exploratory behaviour for associative and reversal learning performance.

Reversal learning task

In total, we successfully tested 105 animals from 33 pairs (P), 149 (F1) and 131 (F2) individuals for reversal learning performance. From these birds, we tested 52 P, 55 F1 and 15 F2 individuals a second and 52 P individuals a third time to obtain repeated measures, from here on we refer to these repeated measures as 'testing rounds'. Supplementary Figure 2.1 and Supplementary Table 2.1 provide an overview of the sample sizes and timeline for the selection procedures as well as repeated measures.

Experimental apparatus

We used automated feeders to assess learning performance, using a three-choice spatial learning procedure. During each experiment, one feeder would provide a reward (freeze-dried mealworm) in a triangular array with two other unrewarding feeders, requiring individuals to learn the location of the rewarded feeder. A triangular array with three feeders is different from most laboratory setups, where there are typically two choices. However, spatial reversal learning paradigms can involve additional choice options (Kosaki and Watanabe, 2012; Remmelink et al., 2016; Tello-Ramos et al., 2019; Reichert et al., 2020; Morand-Ferron et al., 2022), making it possible to distinguish between error types and foraging strategies (Izquierdo et al., 2017). We used two feeder types for these experiments, the second type being a refined version that allowed for automated reversal switching.

Feeder type one (Supplementary Figure 2.2a): For the first testing round of the P generation, we used radio-frequency identification (RFID) controlled automated feeders (Reichert et al., 2020). Access to food (freeze-dried mealworms) was controlled by a transparent plastic door at the feeder opening, held in place by a solenoid. The solenoid would release for two seconds upon detection of a specific Passive Integrated Transponder (PIT) tag, allowing an individual access to one food item by pushing open the door. RFID readings and solenoid activation were controlled by a custom program loaded onto a printed circuit board ('Darwin Board', Stickman Technologies Inc., UK). All visits and their timestamps were monitored with the RFID antenna throughout the experiment.

Feeder type two (Supplementary Figure 2.2b): In subsequent experiments (P generation testing rounds two and three, F1 and F2 all testing rounds), we substituted the above-described feeding stations for automated "smart" feeders, designed by NatureCounters (Maidstone, UK). These feeders functioned similarly to the Type one devices, and were also equipped with an RFID antenna. Opening and closure of a transparent plastic door was controlled with a micro-servomotor. Upon registration of a PIT-tag, the door opened for a set duration of two seconds. The three feeders were connected through a network cable, allowing for integrated responses between the feeders.

Training

Eight days prior to testing, individuals were trained to use the feeders under standard housing conditions in semi-open outdoor aviaries. Before training, birds were weighed and provided with a PIT-tag. During this training period, food and water were available ad libitum, but live mealworms were excluded from the diet. On day one of the training period, we placed one or two feeders in the aviary, with the doors permanently open so that birds could learn to eat from the open door. On days two to seven, the door of the feeders was closed and set to a mode where it could only be opened when triggered by a landing and successful transponder reading of any of the birds. On day eight, birds were selected for testing if during that week, they had > 80 visits per day at least once, > 30 visits per day at least twice (mean of maximum visits per bird on the day it had the most visits = 268 visits, see Supplementary Figure 2.3a for distribution) or >30 visits per hour at least once (mean of maximum visits per bird in the hour it had the most visits = 60 visits, Supplementary Figure 2.3b). This selection criterion was chosen because the median number of visits that was needed to complete both the associative and reversal task was 31 visits, the criterion ensured that most individuals would be apt enough at using the devices to finalize the task within one day.

Learning experiment

We tested all birds between 9:00h and 15:00h. We caught individuals from the group, weighed them, and released them individually in a testing aviary. In this testing aviary, water was available ad libitum and food was not available during the test to maintain the motivation to take part in the learning test. Testing took place with three feeders positioned in a triangular array, doors facing inwards.

In the associative learning phase, we randomly chose a priori which feeder would provide a reward for that individual. The feeder door of the assigned feeder opened upon tag registration, whereas the other two feeders stayed closed when visited. This assigned feeder was reinforced until individuals reached a criterion level of six correct trials out of seven. This success rate is significantly different from the expectation if birds selected feeders at random (binomial test, $p < 0.01$). A trial was defined as a landing on the perch.

After completing the associative learning phase, the reversal learning task began and the reward contingencies were reversed to one of the other two feeders, which

was randomly chosen a priori. All experimental tests were observed live through a one-way observation screen and upon reaching criterion, the observer initiated the reversal manually. Again, birds had to reach the learning criterion of six correct visits over seven trials to the new feeder. Individuals had from 09:00 until 15:00 to complete both phases of the test. Both phases were filmed using a GoPro Hero5 (GoPro inc.) placed inside the aviary in case rewatching was necessary. After the test, birds were caught, weighed and released back in their home aviary or housed temporarily in a standard individual cage until release in their home aviary. Associative and reversal learning performance were scored as the total number of trials required to reach the learning criterion of six correct visits out of seven subsequent trials, including those last seven visits.

After testing the parental generation with the first feeder type, we refined our testing feeder to allow for automated high-throughput phenotyping. In summary, the following changes were implemented when using feeder type two: (i) For the associative learning phase, the first feeder that a bird chose to visit was rewarded, instead of a random feeder. This ensured faster completion of the associative learning phase and that any variations in reversal learning performance would not be due to differences in preferences. (ii) The devices were programmed such that the rewarded feeder switched automatically to initiate the reversal phase when the learning criterion was reached. This allowed for the learning experiments to take place without human intervention. Birds continued serial reversals until caught from the aviary at 15:00, but for all analysis in this paper we only included the first reversal of each testing round. (iii) Due to a difference in design and the cable that was needed to connect the three devices, the doors faced away from the centre of the three devices, instead of inwards. (iv) Energetic state and satiation can affect evaluation of the food reward as well as learning speed (Rowe and Healy, 2014). Therefore, we offered dry egg food ad libitum in the test aviary during the experiment, so birds could reach their desired satiation level, to reduce motivational differences between individuals. This was possible because great tits strongly prefer the dried mealworm rewards in the feeders over dried egg food. Despite these differences, the basic principles of the test remained the same: individuals were trained to visit one out of three feeders, and once learning was established (learning criterion was reached), one of the other two feeders would become rewarded. In all analyses, we controlled for the type of feeder used to measure learning performance.

Exploratory behaviour and boldness

To test birds for exploratory behaviour, we conducted a novel environment test in the observation room after two days of individual housing, when the birds were approximately 35 days old (for more details, see (Verbeek et al., 1994; Drent et al., 2003)) We used the total number of flights (movements between trees) and hops (movements within trees) within the first two minutes as an index of exploratory behaviour ('exploratory score') as in (Dingemanse et al., 2002). All birds were tested at the same age and around the same dates each year. We estimated a second personality measure, 'boldness', by executing a novel object test on day one and day

two after the novel environment test ($R = 0.54$, CI = [0.4,0.6], $p < 0.001$), for details see (Drent et al., 2003). Birds were characterized for shyness and boldness assessing their latency to approach the object and the shortest distance to it within 120 s, and the results for each test were converted linearly to a 0 – 5 scale. A score of five was given when the bird pecked the object, a score of zero when the bird did not land on the perch on which the object was situated. We summed scores from both novel object tests as an index of boldness (0 – 10, 'boldness score').

Selection procedure and breeding

From the parental generation, individuals were selected to breed based on their reversal learning performance (trials to criterion) in the first testing round. Individuals were ranked on the number of trials they required to reach learning criterion. For both the 'fast' and 'slow' learning lines we selected 18 males and 18 females and created 'fast' and 'slow' pairs. For each sex, we included a maximum of three siblings per line. Within each line, we ranked the selected birds for reversal learning performance for the two sexes separately. We then paired males and females that had contrasting reversal learning performances (e.g. a relatively high performing male with a relatively low performing female), avoiding full-sib mating. From February onwards, these 36 breeding pairs were housed in semi-open outdoor aviaries (approximately 2.0 m x 4.0 m x 2.5 m) under natural photoperiod length and temperatures. Each aviary contained four nest boxes. From March onwards, daily additional light was supplied from a single full-spectrum daylight fluorescent lamp (58W, 5500K, Truelight, the Netherlands) per aviary. Lights were on from 2.5 hr before sunrise (but never earlier than 02:00) until 24:00 to synchronize their breeding with the wild population. Moss as nesting material was supplied from mid-March onwards, and once nest building had started, dog hair was also supplied.

Nest boxes in the aviaries were checked twice a week for nest building. When nests were complete, next boxes were checked daily for egg laying. Freshly laid eggs were collected, replaced with dummy eggs, and stored for a maximum of 14 days in an egg-turner. For incubation by foster females, eggs were placed in a wild nest at the nest box population in Boslust. After five days of incubating the artificial dummy clutch, the nests in the aviaries were removed and females were allowed to relay. Alternatively, eggs were incubated by the female for five days and transported to the field using heat packs to keep eggs warm, after which they were placed in a wild nest to be further incubated by foster females.

To produce the F2 generation, we formed 18 pairs for each line from the F1 generation as described above for the P generation, selecting individuals with the lowest trials to criterion for the 'fast' line and highest trials to criterion for the 'slow' line, avoiding full-sib and first-cousin mating. Not all pairings bred successfully. We obtained 86 chicks from 16 'fast' broods and 63 chicks from 12 'slow' broods from the P generation, and 37 chicks from 10 'fast' broods and 94 chicks from 16 'slow' broods from the F1 generation (Supplementary Figure 2.1).

Statistical analysis

For both associative and reversal learning performance, we used the number of trials to reach learning criterion as performance measure. Across all reversal learning tests, 56 out of 573 times, the criterion was not reached before 15:00 hr, meaning trials to criterion was censored. To investigate if performance differed between associative and reversal learning performance while including censored individuals, we therefore compared survival curves between the associative and reversal learning task. We used the functions *Surv* and *Survfit* from the 'survival' package (Therneau et al., 2022) to compute Kaplan-Meier survival curves. The Kaplan-Meier method is normally used to estimate survival probability from observed survival times. We employ it to estimate number of trials to criterion for censored individuals. We used an individuals' maximum number of trials for "follow up time", and success (0 = criterion not reached, 1 = criterion reached) for "event". We used the function *survdiff* (Therneau et al., 2022) to compare the two survival curves of the associative and reversal learning task, by computing a log-rank test employing a chi-square test statistic. As expected, individuals needed more trials to finish the reversal learning task compared to the associative learning task (log-rank: χ_1^2 =136, $p < 0.01$, Supplementary Figure 2.4).

To include censored individuals in the linear regression models that we used to calculate heritability and repeatability, we computed so-called pseudo-values of the restricted mean survival time (which here reflects restricted mean trials to criterion) from the Kaplan-Meier survival curves (Andersen and Pohar Perme, 2010). As a measure of trials to criterion, pseudo-values were computed for all observed trials, both censored and uncensored, using the function *pseudo* (Therneau et al., 2022). Pseudo-values were evaluated at the maximum trial number reached by the individual with the highest trials to criterion. To prevent confusion, the pseudo-values will hereafter be referred to as 'trials to criterion (TTC)'.

To test whether variation in associative and reversal learning performance can be explained by feeder type, test round, start time, body condition (residuals of the regression of body weight at start of the experiment against tarsus) or sex, we constructed linear mixed models with the function *lmer* in the 'lme4' package (Bates et al., 2015) with these explanatory variables and trials to criterion (ln-transformed) as the dependent variable. To account for multiple observations, animal ID was included as random intercept. We created separate models for associative and for reversal learning performance. Significance of fixed-effects was tested using Type II ANOVAs Kenward-Roger degrees of freedom with the function *Anova* in the 'car' package (Fox and Weisberg, 2019). We evaluated terms using F-tests.

Heritability and repeatability of associative and reversal learning performance

We used two approaches to assess narrow-sense heritability of associative and reversal learning. Narrow-sense heritability (h^2) is the proportion of total

phenotypic variance (V_P) that is attributed to the additive effect of genes, i.e., additive genetic variance (V_A) (Falconer, 1989):

$$h^2 = \frac{V_A}{V_P} \quad (1)$$

First, we estimated narrow-sense heritability of reversal learning performance using the response to artificial selection on performance on the first testing round. Because we only tested the parental generation with the first feeder type, we could not control for this using only data from the first testing round. Therefore, we used reversal learning performance corrected for feeder type, by taking the residuals from a linear model of the complete dataset including all testing rounds (in later testing rounds, the parental generation was tested with feeder type two), with trials to criterion (ln-transformed) as the dependent variable, and feeder type as the fixed effect. Estimates of heritability based on the response to selection are referred to as realized heritabilities (Falconer, 1989), and can be estimated from the breeder's equation,

$$R = h^2 S \quad (2)$$

By calculating the ratio of observed response to selection (R), the difference between mean offspring value and mean parent value, to observed selection differential (S), the difference between mean value of selected parents (weighted for number of tested offspring) and mean parent value, we estimated the realized heritability:

$$\hat{h}_r^2 = \frac{R}{S} \quad (3)$$

To estimate realized heritability over several generations of selection, we summed R and S over successive generations respectively, to acquire the cumulative selection response $R_C(t)$ and cumulative selection differential $S_C(t)$. Then, by regressing $R_C(t)$ on $S_C(t)$, we estimated realized heritability as the slope of this regression (Falconer, 1989).

Secondly, we used the ASReml-R package (Butler et al., 2017) to compare univariate mixed models differing in random effect structure with likelihood ratio tests (LRT) to test for the presence of among-individual variance and additive genetic variance. Using measures from all individuals across each testing round, we calculated repeatability as the proportion of phenotypic variance explained by the individual (Falconer, 1989), using ASReml-R. For both associative and reversal learning performance, the response variable was trials to criterion (ln-transformed). Feeder type was included as a fixed effect in all models. The presence of among-individual variance was estimated by including a random effect of individual identity and comparing this model with the null model using a likelihood ratio test. Repeatability was then estimated as:

$$R = \frac{V_I}{V_P} = \frac{V_I}{V_I + V_R} \quad (4)$$

with V_I representing among-individual variance, V_P representing total phenotypic variance, and V_R representing within-individual variance originating from plasticity and/or measurement error.

We created a 'full' animal model to estimate the genetic parameters of both associative and reversal learning performance (Wilson et al., 2010). An animal model is a mixed-effects model that combines the information on phenotypes and the relationship between animals (pedigree) to partition total phenotypic variance (V_P) between various sources, including additive genetic variance (V_A). We included the following random effects: individual identity to account for repeated measures and estimate permanent environment effect (V_{PE}), individual identity linked to the pedigree to estimate additive genetic variance (V_A) and maternal identity to estimate maternal variance (V_M). To statistically test for the presence of each of the variances, we compared the fit of this model to intermediate models using LRT, removing each respective random effect that we aimed to test for. Estimates of genetic variance (V_A), permanent environmental variance (V_{PE}) and maternal variance (V_M) were extracted from the full animal model and scaled by the phenotypic variance (V_P, calculated as the sum of the estimated variance components). This yielded estimations of maternal effect (m), permanent environment effect (pe) and heritability (h^2), the latter being estimated as.

$$h^2 = \frac{V_A}{V_P} = \frac{V_A}{V_A + V_M + V_{PE}} \quad (5)$$

For early exploratory behaviour, response variables were either 'exploratory score' or 'boldness score'. We had no repeated measures, so tested only for the presence of additive genetic variance and maternal variance, by comparing a model containing either a random effect of individual identity linked to the pedigree or containing a random effect of maternal identity, with a 'null' model, containing no random effects. The estimate of genetic variance was then extracted from the animal model and scaled by the phenotypic variance to yield estimated heritability (h^2).

Relationship between associative and reversal learning performance

To explore the relationship between associative and reversal learning performance in the first testing round, we employed a linear model using function *lm* from the 'stats' package (R Core Team, 2022), with trials to criterion of reversal learning performance (ln-transformed) as the dependent variable and trials to criterion of associative learning performance (ln-transformed), feeder type and their interaction as fixed effects.

For feeder type one, where we had randomly assigned the rewarded feeder a priori, we also explored how the relationship between reversal learning performance and associative learning performance depended on the number of trials it took a bird

until the first correct visit was made, which we called 'correct visit lag number'. If the correct visit lag number equalled 1, the first feeder that an individual chose to land was also the rewarded feeder. If the correct lag visit number equalled 2 or higher, the individual first visited other unrewarded feeders. A higher correct visit lag number might indicate slow learning or a strong tendency to visit the other unrewarded feeder(s). For this, we used a linear model using function *lm* with trials to criterion (ln-transformed) of the reversal learning phase as the dependent variable, and trials to criterion (ln-transformed) of the associative phase, 'correct visit lag number' and their interaction as fixed effects.

Significance of fixed- effects was tested using Type III ANOVAs and Kenward-Roger degrees of freedom. We evaluated terms using F-tests. Post hoc comparisons were performed with the function *emtrends* command in 'emmeans' package (Lenth et al., 2022) to compare estimates of slopes of the trials to criterion trend for each level of feeder type and mean ± SE of 'correct visit lag number', using the Tukey test to correct for multiple comparisons.

Relationship between learning performance and exploratory behaviour and boldness

To explore the relationship between either associative or reversal learning performance and 'exploratory score' or 'boldness score' we used a linear model using function *lm* (for only the first test round) and a linear mixed model using function lmer (across all test rounds, including individual ID as random effect) with trials to criterion (ln-transformed) of either associative or reversal learning as the dependent variable, and boldness, exploratory score and feeder type as fixed effects. Significance of fixed- effects was tested using Type II ANOVAs and Kenward-Roger degrees of freedom. We evaluated terms using F-tests.

All analyses were conducted in R version 4.0.3 (R Core Team, 2022).

Results

Heritability and repeatability of associative and reversal learning performance

The significance and magnitude of fixed effects varied across task performances. These effects are not directly relevant to hypotheses being tested but are reported in full in Supplementary Table 2.2. Feeder type had a significant effect and was therefore controlled for all in subsequent models. Repeatability (with SE) of associative learning performance was low 0.06 ± 0.06, and likelihood ratio tests (LRT) showed no significant evidence for among-individual variation in performance (χ^2_1 = 0.85, p = 0.36), estimated under model 1 as $V_{ind}/V_p = V_{ind}/(V_{ind} + V_R)$. The addition of a random genetic intercept (χ^2_1 = 0, p = 1) or permanent environment effect (χ^2_1 = 0.00, p = 0.98) did not lead to a significantly improved model fit, but there was support for a small maternal effect (χ^2_1 = 3.95, p = 0.05) (Table 2.1). For reversal learning, LRT support presence of among-individual variation in performance, though repeatability (with SE) was low 0.14 ± 0.07, χ^2_1 = 5.1, p = 0.02). The addition of a random genetic intercept (χ^2_1 = 0, p = 1), maternal

effect (χ^2_1 = 1.4, p = 0.23), or permanent environment effect (χ^2_1 = 1.96, p = 0.16) did not lead to significantly improved model fit (Table 2.1). These results indicate there is no support for additive genetic variance in associative and reversal learning performance. For boldness (χ^2_1 = 11.9, p < 0.001) as well as exploration (χ^2_1 = 16.1, p < 0.001), there was evidence for significant heritable variation with estimates of $h^2 = 0.32 \pm 0.11$ for boldness and $h^2 = 0.34 \pm 0.10$ for exploration (Table 2.1).

Table 2.1 *Variance components, repeatability and heritability of cognitive and personality traits. Chi-square test statistics and p-values are provided for the individual term, testing for the presence of significant among-individual variation ($V_{ind} = V_A + V_M + V_{PE}$), and for the pedigree term, testing for the presence of significant additive genetic variance (V_A). Permanent environment (V_{PE}), maternal effects (V_M) and residual variances (V_R) are also given. Variance components for cognitive traits were obtained from a random regression animal model, corrected for feeder type. Variance components for personality traits were obtained from a single measure animal model.*

Trait	V_A (SE)	V_M (SE)	V_{PE} (SE)	V_R (SE)	R (SE)	χ^2_1	h^2 (SE)	χ^2_1
Associative learning	0.00 (0.00)	0.02 (0.01)	0.00 (0.03)	0.46 (0.04)	0.06 (0.06)	0.85, p = 0.36	0.00 (0.00)	0.00, p = 1.00
Reversal learning	0.00 (0.00)	0.01 (0.01)	0.04 (0.03)	0.34 (0.03)	0.14 (0.07)	**5.1, p = 0.02**	0.00 (0.00)	0.00, p = 1.00
Exploration	4.54 (1.59)	0.06 (0.57)	-	8.94 (1.17)	-	-	0.34 (0.10)	**16.1, p< 0.001**
Boldness	2.88 (1.09)	0.00 (0.00)	-	6.23 (0.00)	-	-	0.32 (0.11)	**11.9, p < 0.001**

Realized heritability of reversal learning performance

Great tits from the 'fast' and 'slow' line did not differ in reversal learning performance after one (t-test: t_{151} = 0.46, p = 0.65) and two (t-test: t_{129} = -0.89, p = 0.37) generations of selection. The realized heritability (response to selection as proportion to selection differential) was 0.02 and did not differ significantly from zero after two generations (p = 0.50, Figure 2.1, Table 2.2).

Table 2.2 *Realized heritability estimates (h^2) for reversal learning performance, calculated as the slope of the linear regression between cumulative selection differential and response to selection for fast reversal learning and slow reversal learning, calculating the average as well as realized heritability separately for each line.*

Line	Realized heritability	SE	p-value	R^2	F-statistic	Residual df
Average	0.02	0.027	0.50	0.122	0.554	4
Fast	-0.02	0.067	0.82	0.075	0.081	1
Slow	0.10	0.067	0.38	0.687	2.20	1

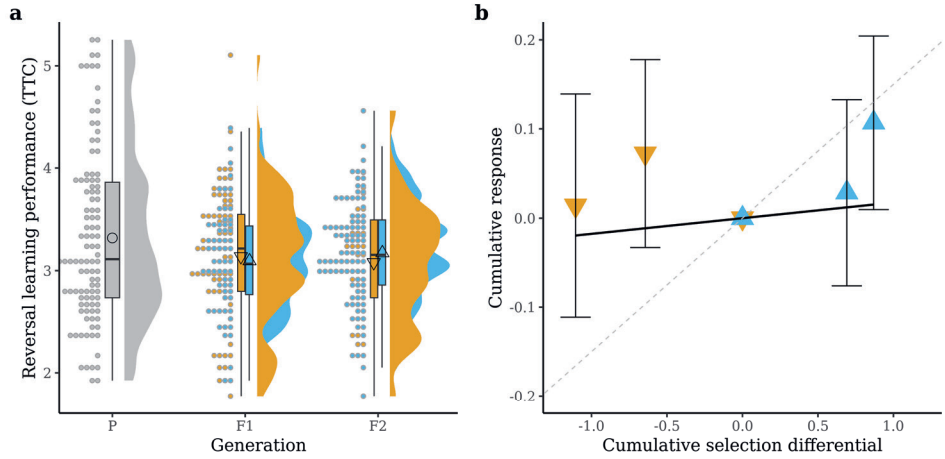

Figure 2.1 Response to selection per generation. *(a) Boxplot with horizontal lines representing median and interquartile range of reversal learning performance as trials to criterion (TTC), circle and triangles indicate mean trials to criterion, corrected for feeder type. Eye plots represent density distributions for trials to criterion. Dots indicate number of individuals within each bin. (b) Realized heritability (h^2) of reversal learning performance in an artificial selection experiment. Cumulative response to selection (R) is plotted as function of the cumulative selection differential (S) for each line selected on number of trials to reach learning criterion for two generations. The realized heritability (h^2) was calculated as the slope of the linear regression between R and S (black solid line). Error bars represent standard errors. Dashed line indicates expected function if slope (h^2) were 0.15. Yellow, downward pointing arrows: fast line; blue, upward pointing arrows: slow line.*

Relationship between associative and reversal learning performance

Reversal learning performance varied with associative learning performance, but the effect depended on feeder type (LM; TTC associative * Feeder type: $F = 11.23$, $p < 0.01$). Post hoc analysis indicated that for feeder type one, there was a trend for a positive relationship between associative learning and reversal learning performance (0.12 ± 0.08 $t = 1.56$, $p = 0.13$), whereas for feeder type two, this relationship was significantly negative (-0.21 ± 0.06 $t = -3.64$ $p < 0.01$), indicating that individuals that were slow during associative learning showed fast reversal learning (Figure 2.2a, Table 2.3).

The two feeder types differed in whether the first (preferred) choice was rewarded for associative learning or whether a random feeder was rewarded. Using data from feeder type 1, we explored whether the fact that an individual needed to learn that a preferred or a random feeder was rewarded could explain the difference in direction of the relationship between associative and reversal learning. Indeed, there was a trend that the effect of associative learning on reversal learning performance depended on the latency to the first correct visit that was made during associative learning (LM; TTC associative * Correct visit lag number: $F = 3.58$, $p = 0.06$). Post hoc comparisons show a significant positive relationship between associative learning and reversal learning performance when the 'correct visit lag number' is high (not learning initial choice, at mean +SD 0.5 ± 0.21 $t = 2.30$, $p =$

0.02), but that the slope flattens out as this number decreases (learning initial choice, at mean -SD -0.08 ± 0.18 t = -0.42, p = 0.67) (Figure 2.2b, Table 2.4).

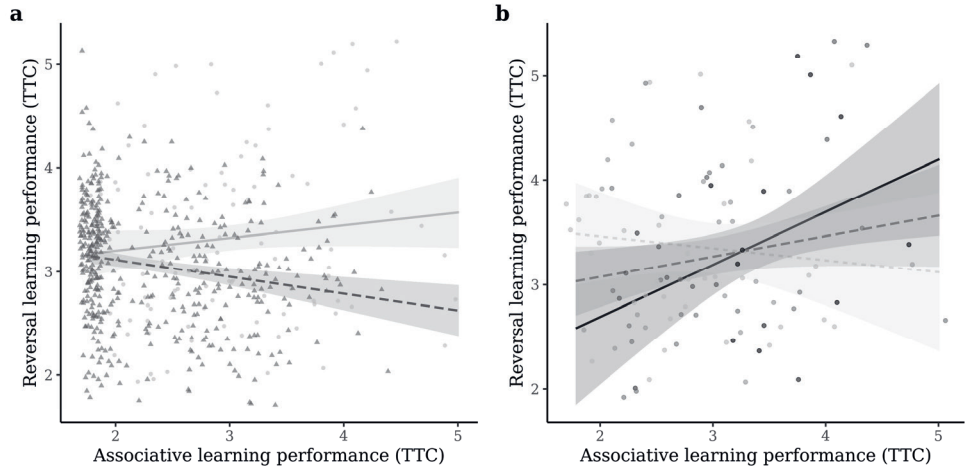

Figure 2.2 Relationship between the number of trials to criterion (TTC) (ln-transformed) in the reversal learning phase and the number of trials to criterion (ln-transformed) in the associative learning phase. *Data is from the first testing round (higher values = more trials needed/slower learning). This is shown for a) feeder type 1 (Light grey, continuous line and dots) and type 2 (dark grey, dashed line and triangles) and for b) the interaction between associative learning and the 'correct visit lag number' (grouping levels based on standard deviation; +1 SD is dark grey solid line and -1 SD is light grey dashed line). Darker dots reflect a higher 'correct visit lag number'. For both a) and b), plotted lines are marginal effects of the interactions term. Lines and shaded regions represent the model prediction (± 95 % confidence interval). The points of the scatterplot represent the actual data points.*

Table 2.3 *Trials to criterion (TTC) of associative learning phase in the first testing round in interaction with feeder type (one/two) as predictor of reversal learning performance (n = 384), fitted with a linear mixed effect model.*

Variable	Estimate	SE	F-statistic	p-value
(Intercept)	3.29	0.14		
TTC associative	-0.05	0.05	0.84	0.36
Feeder type	-0.33	0.14	5.43	**0.02**
TTC associative * Feeder type	0.17	0.05	11.23	**<0.01**

Table 2.4 *Trials to criterion (TTC) of associative learning phase in the first testing round as predictor of reversal learning performance for only feeder type 1 (n = 104), fitted with a linear mixed effect model with 'correct visit lag number' as fixed effect.*

Variable	Estimate	SE	F-statistic	p-value
(Intercept)	3.79	0.59		
TTC associative	-0.14	0.19	0.56	0.46
Correct visit lag number	-0.37	0.20	3.33	**0.07**
TTC associative * Correct visit lag number	0.11	0.06	3.59	**0.06**

Relationship between learning performance and personality traits

Associative learning performance in the first testing round associated with boldness score (Estimate: 0.03 ± 0.012, p = 0.021), with bolder individuals requiring more trials to reach learning criterion (Figure 2.3). When including repeated measures, this relationship was also apparent, but as trend (Estimate: 0.02 ± 0.010, p = 0.076). Exploration score did not predict trials to reach learning criterion during the associative learning task (Estimate: 0.00 ± 0.009, p = 0.72). Reversal learning performance did not associate with boldness score (Estimate: -0.01 ± 0.011, p = 0.52) or exploration score (Estimate: -0.01 ± 0.009, p = 0.18). See also Table 2.5.

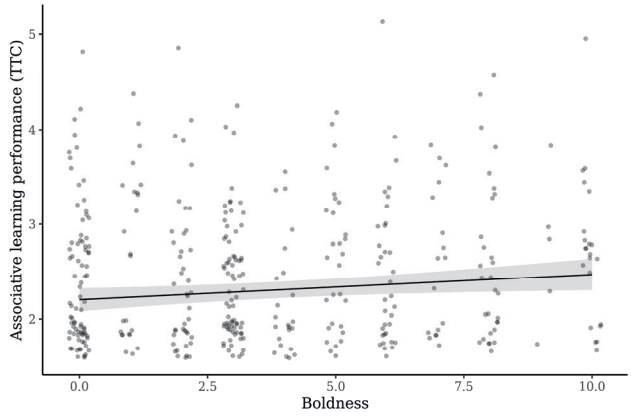

Figure 2.3 Significant relationship between boldness and associative learning performance. *Higher boldness values = faster to approach novel object. Higher trials to criterion (TTC) = more trials needed/slower learning. Line and shaded region represent the model prediction (± 95% confidence interval). The points of the scatterplot represent the actual data points.*

Table 2.5 *Predictors of the log transformed restricted mean trials to criterion for associative learning (n = 383; including repeats = 602 trials) and reversal learning performance (n = 378; including repeats = 559 trials). Data of only the first rounds was fitted with a linear model with apparatus type (one/two), exploration score and boldness as fixed effects. Data on all rounds was fitted with a linear mixed effect model with apparatus type (one/two), test round (one/two/three), exploration score and boldness as fixed effects and with bird ID included as random intercept.*

		Associative learning				Reversal learning			
Group	**Variable**	**N**	**Estimate**	**SE**	**p-value**	**N**	**Estimate**	**SE**	**p-value**
Round 1	**Apparatus type**	383	-0.67	0.079	**<0.001**	378	-0.18	0.075	**0.015**
	Exploration score		0.00	0.009	0.72		-0.01	0.009	0.18
	Boldness		0.03	0.012	**0.021**		-0.01	0.011	0.52
All rounds	**Apparatus type**	602	-0.66	0.079	**<0.001**	559	-0.19	0.072	**0.009**
	Round				0.11				**0.027**
	R1		-0.05	0.045			0.11	0.043	
	R2		0.08	0.048			-0.02	0.046	
	R3		—	—			—	—	
	Exploration score		0.00	0.008	0.94		-0.01	0.008	0.23
	Boldness		0.02	0.010	**0.076**		0.00	0.009	0.75

Discussion

To investigate the evolutionary potential of cognitive flexibility, we here used great tits to test the extent of among-individual variation and additive genetic variation of reversal learning and related traits using a bi-directional selection experiment of reversal learning performance. We found significant, but low, repeatability of reversal learning performance, but our artificial selection showed no evidence for narrow-sense heritability of reversal learning performance. We argue that this suggests a relatively low evolutionary potential of cognitive flexibility, but also points to difficulties with obtaining measures of cognitive flexibility.

The fact that reversal learning performance has a significant repeatable component, even though our repeatability estimates were relatively low, shows that performance on this task is to some extent consistent. This is in line with other studies finding repeatability of reversal learning performance in great tits (Cauchoix et al., 2018; Reichert et al., 2020; Morand-Ferron et al., 2022). Low to moderate estimates of repeatability on cognitive traits are common (Cauchoix et al., 2018). Individual experiences and the environment play a large role in shaping cognitive abilities (Lambert and Guillette, 2021), which is why individuals typically show plastic cognitive phenotypes. This is especially true in reversal learning tasks, because subsequent reversals can induce a change in prior knowledge, essentially changing the trait that is measured (Izquierdo et al., 2017). Furthermore, because we used relatively long measurement intervals (mean = 345 days), our repeatability estimates may be somewhat conservative. Over longer time periods, the environment of an individual is more likely to change relative to the last measurement, increasing within-individual variation in performance (Ashton et al., 2022). The fact that we find repeatability over long time intervals indicates that among-individual differences in reversal learning performance truly exist and can be stable across longer time periods.

Contrary to our predictions, and despite the detected repeatability, reversal learning performance did not respond to artificial selection over generations, and we found no evidence for heritable variation. The fact that in line with previous research, we found evidence for heritability of both personality traits we measured, boldness towards a novel object and exploratory behaviour, shows that our pedigree data was sufficient to pick up moderate heritabilities (Drent et al., 2003; Quinn et al., 2009; Class et al., 2019). The low heritability estimates and lack of response to selection as we found here, suggest that reversal learning performance has little to no evolutionary potential. Potentially, genetic variation may have been selected against for cognitive flexibility, since traits closely linked to fitness are expected to have little additive genetic variance, possibly lost through strong directional selection (Houle, 1992), but considering the wide phenotypic variation in trials to criterion, that does not seem to be the explanation for the results in this study. Instead, considering the high contribution of residual variance, there is still a lot of individual variation unaccounted for, and we speculate on some possible sources of variation in the discussion below.

Other studies did find moderate heritability in reversal learning performance, in red junglefowl (*Gallus gallus*) and house mice (*Mus musculus*), (Laughlin et al., 2011; Sorato et al., 2018; Bailey et al., 2021), although no heritability was found in Aegean wall lizards (*Podarcis erhardii*) (De Meester et al., 2022b). What can explain the different findings among studies? In other work on the great tit, problem solving was shown to be a moderately repeatable composite behaviour (Cole et al., 2011) but not heritable (Quinn et al., 2016). Furthermore, repeatability in problem solving was shown to be explained entirely by the underlying behaviours (motivation, experience, selective attention; (Cooke et al., 2021)), possibly explaining the lack of heritability in problem solving performance. Similarly, reversal learning performance is a composite trait made up of different cognitive components (Nilsson et al., 2015); its heritability is therefore dependent on the additive genetic variation of each of these components, and on their covariance (as detailed below). We summarized reversal learning performance as the number of trials to reach a learning criterion. This is a commonly used performance measure, but it does not allow to disentangle the different cognitive components that determine performance. If different task types, experimental setups, or species, lean more towards usage of one of the components, our chosen performance measure, trials to criterion, might be the cause of the differences between our and other studies. Furthermore, since each cognitive component itself may also be influenced by environmental variation, total additive genetic variation on a summary measure like trials to criterion may be masked.

Reversal learning performance tests a combination of cognitive components, that trials to criterion may not adequately capture (Pravosudov, 2022) such as: (1) the degree of proactive interference, where previously learnt, but now irrelevant, information interferes with learning and remembering newly relevant information (Tello-Ramos et al., 2019; Tsakanikos and Reed, 2022). Proactive interference results in perseverative choices and explained a large part of the among-individual variation in reversal learning performance in great tits (Morand-Ferron et al., 2022); (2) attentional allocation, the ability to notice that the change has occurred, resulting in a potential failure to detect task transitions (Izquierdo et al., 2017). For example, high resistance against external sources of interference (external attention) impairs reversal learning performance (Sauce et al., 2014); and (3) learning the new cue-reward association through reinforcement learning (Morand-Ferron et al., 2022). Reinforcement learning is involved in both associative and reversal learning performance since both phases require individuals to learn from positive reinforcements, increasing the excitatory strength of a stimulus, and to learn from non-reinforcements, decreasing approach towards non-rewarded locations (Nilsson et al., 2015). Sensitivity to negative as well as to positive feedback are stable traits (Noworyta-Sokolowska et al., 2019). Each of these constituents may be separate components of reversal learning performance that selection can act upon, but the extent to which these components make up reversal learning and the heritabilities of these traits remain an important avenue of further study.

These different cognitive components are also important for understanding our findings on the relationships between associative learning and reversal learning performance. The relative importance of proactive interference suggests that reversal learning performance can be strongly dependent upon the outcome of the associative learning task. We found that associative and reversal learning performance are negatively correlated, in line with a hypothesized trade-off between learning and cognitive flexibility, in which animals that are quick at forming initial associations learn subsequent similar information less well (Amy et al., 2012; Del Giudice and Crespi, 2018; Tello-Ramos et al., 2019). However, we only observed this negative correlation when individuals were rewarded for their first choice during the associative learning task, which may be their preferred feeder. Individuals that were quick to learn their initial choice possibly had a stronger preference for this feeder, developed a stronger memory, and experienced more proactive interference during the reversal task. Strong preferences are difficult to reverse (Aljadeff and Lotem, 2021), and faster and stronger associative learning might make it more difficult to inhibit the response towards that cue (Griffin et al., 2013; Bebus et al., 2016). On the other hand, when a randomly allocated feeder was rewarded first, there was a trend for a positive correlation between associative learning and reversal learning performance, if individuals were forced to learn a non-preferred feeder during the associative learning phase. Perhaps a stronger memory is formed if an individual takes a long time to learn a feeder to which it does not have a strong initial tendency to visit, causing more proactive interference of that memory, explaining the positive correlation between associative and reversal learning performance (Nettle et al., 2015).

Following the speed-accuracy trade-off hypothesis (Sih and Del Giudice, 2012), we predicted that more exploratory and bolder individuals, who are supposedly less sensitive to new information, would therefore be worse at reversal learning performance while being better at associative learning tasks. However, contrary to other studies (Guillette *et al.*, 2011; Marchetti and Drent, 2000; Mazza *et al.*, 2018; van Oers, Klunder and Drent, 2005; but see Guillette *et al.*, 2015), our findings do not support a speed-accuracy trade-off. We found a positive correlation between associative learning performance and boldness, but not exploratory behaviour. Importantly, a relationship between boldness or exploratory behaviour and reversal learning performance was absent. More proactive individuals have a stronger tendency to sample novel information (Arvidsson and Matthysen, 2016; Smit and van Oers, 2019; Rojas-Ferrer et al., 2020; Coomes et al., 2022), and may therefore need more trials to learn the associative learning task because they sample more before committing to one feeder. Considering the negative correlation between associative and reversal learning performance, there is a small potential for variation in reversal learning performance to be maintained through heritable among-individual variation in boldness. However, why this tendency does not persist in a relationship between reversal learning performance and boldness in our study is unclear. Perhaps these differences cannot be identified at the resolution of the performance criterion we used here. For example, bolder sticklebacks performed better during associative learning and made more mistakes

during reversal learning, but only during the first few trials, whereas these differences were not visible at trials to criterion (Bensky and Bell, 2020). This again suggests that dissecting the different mechanisms underlying reversal learning performance and relating them to associative learning and personality traits will be a crucial step towards a better understanding of any trade-offs between learning, flexibility and personality. We do however, not find a general tendency for personality differences to be the cause for consistent individual differences in reversal learning. Here, we only used single measures of our validated personality traits to associate with associative and reversal learning performance. Future studies should aim at associating multiple measures of a battery of cognitive functions to a battery of repeated personality traits, to see if these correlations hold at the among-individual level.

In summary, our results demonstrate that reversal learning performance is repeatable over longer time periods but seems to have no additive genetic variation. Although this suggests a limited evolutionary potential, the intricate relationships with other behavioural measures such as associative learning performance and boldness suggest a more complex interplay of experiences and personality that together result in task performance, possibly explaining the lack of additive genetic variation here. For future studies, it will be crucial to disentangle the different components that likely underlie individual variation in reversal learning performance; reinforcement learning, proactive interference, and attentional allocation. This will allow for separately quantifying the repeatability and heritability of these components as well as their covariances, and their relationships with other behavioural traits and ultimately fitness. This should preferably be done across a range of environmental conditions to explore the possibility that selection acts on the level of reaction norms rather than on the reversal learning performance itself.

Supplement to Chapter 2

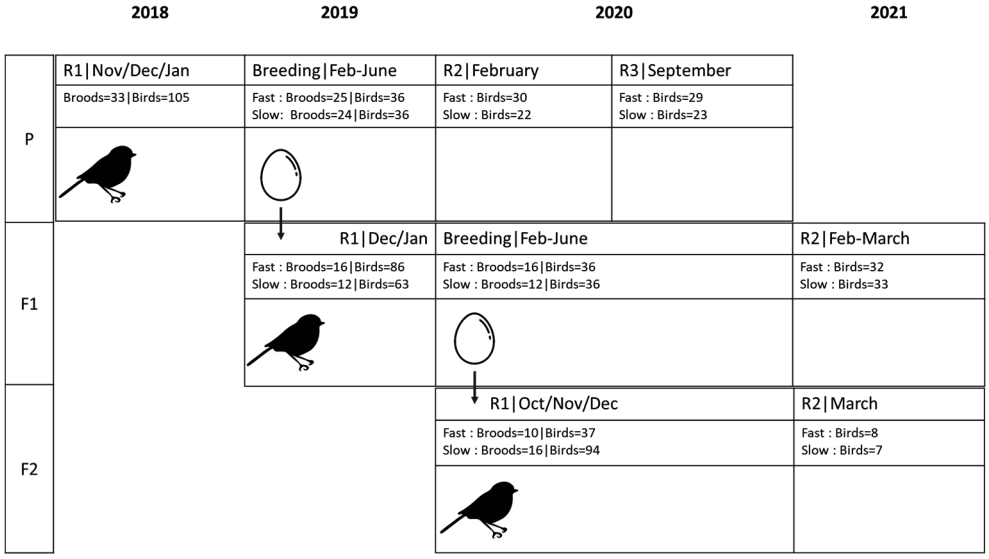

Supplementary Figure 2.*1 Timeline of the artificial selection procedure for fast and slow reversal learning in great tits. For generation P, we used great tits that were hand reared as nestlings and that originated from a wild nest box population. We tested 105 birds for reversal learning performance and selected 36 individuals for fast and slow reversal learning to set up 18 breeding pairs for each line. From the 18 pairs of each line, the eggs were incubated by foster parents from the nest box population and we hand-reared the nestlings. From this F1 generation, we tested 86 birds from 16 pairs from the fast line, and 63 birds from 12 pairs for the slow line for reversal learning performance. We selected 36 individuals respectively from the fast and slow reversal learning line to again set up 18 breeding pairs. Their offspring was also fostered and hand reared and from this F2 generation, we tested we tested 37 birds from 10 pairs from the fast line, and 94 birds from 16 pairs for the slow line for reversal learning performance. Timing of repeated measures (R1=Round 1, R2=Round 2, R3=Round 3) and number of birds with repeated measures are also indicated in the table.*

Supplementary Table 2.1 *The number of individuals that reached learning criterion (Y/N) and were selected for breeding (Y/N) for each generation (P, F1, F2), each line (FRL: fast reversal learning; SRL: slow reversal learning) and each round of testing.*

	Line		**FRL**			**SLR**		
	Reached criterion	**Y N Sum**	**Y N Sum**			**Y N Sum**	**Y N Sum**	
Round 1	**Selected for breeding**	N	Y	N		Y	N	
	P	27 6 33	36 - 36			30 6 36		
	Broods	*25*	*25*			*24*		
	F1		36 - 36	47 3 50		36 - 36	24 3 27	
	Broods		*16*	*16*		*12*	*10*	
	F2			34 3 37			78 15 93	
	Broods			*10*			*16*	
	Total	33	72	87		72	120	
Round 2	**P**		29 1 30			20 2 22		
	F1		31 1 32			30 3 33		
	F2			7 1 8			6 1 7	
	Total		62	8		55	7	
Round 3	**P**		28 1 29			19 4 23		
	F1							
	F2							
	Total		29			23		

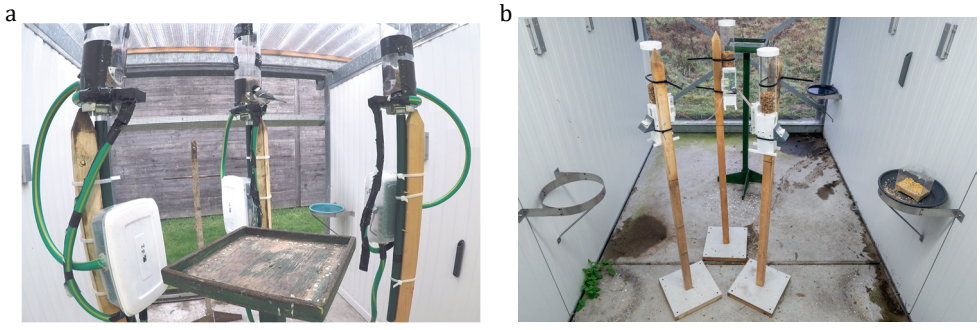

Supplementary Figure 2.2 Test setups*. Aviary with water bowl, dry food bowl, perching trees and test devices: a) apparatus type one, with doors facing inwards and flat landing platforms for tag registration b) apparatus type two, with doors facing outwards and white landing perches for tag registration.*

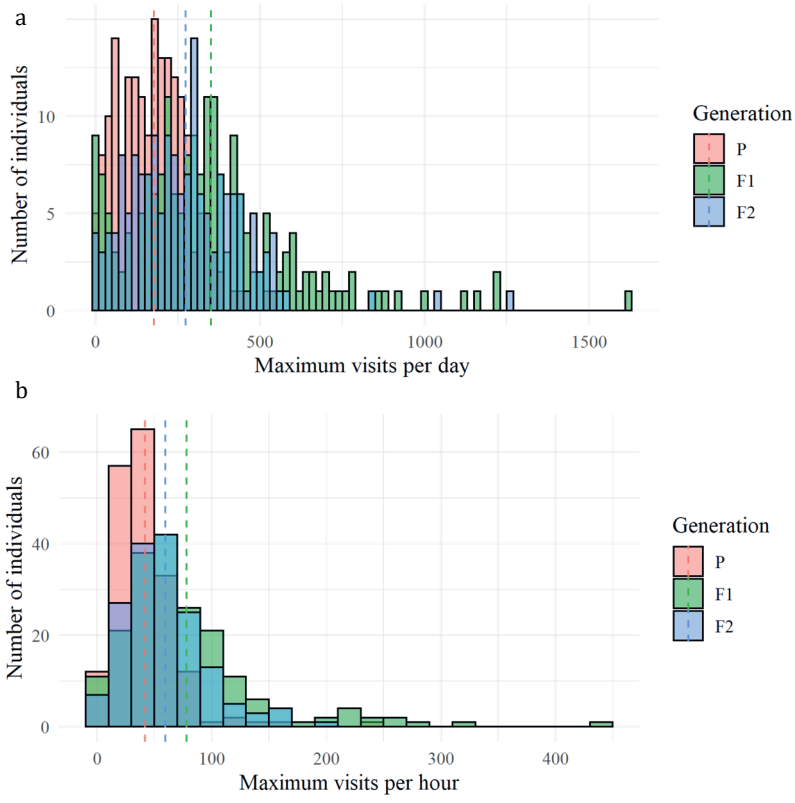

Supplementary Figure 2.3 *Histograms of individual habituation visits. a) number of visits for the day an individual had the most visits b) number of visits for the hour in which an individual had the most visits. Colours indicate generation.*

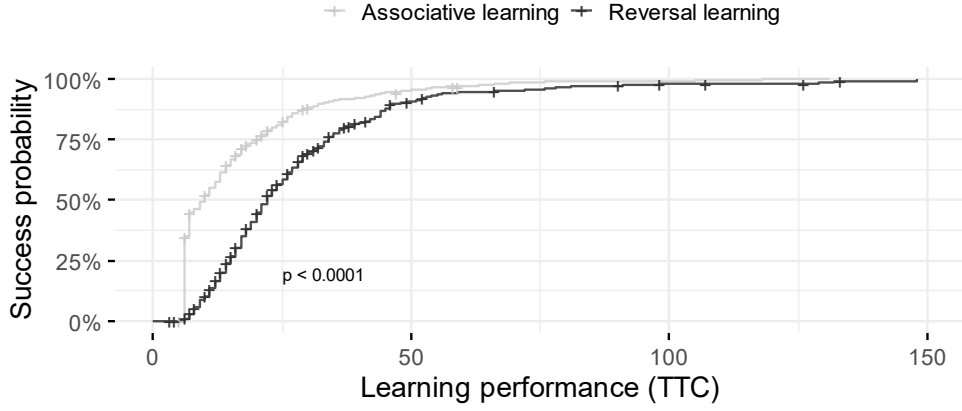

Supplementary Figure 2.4 *Kaplan Meier plots of the trials to reach learning criterion during the associative and reversal learning task. "Time" is number of trials, and "event" is reaching trials to criterion. Every time an individual reaches learning criterion, the proportion of individuals succeeding at the task on the Y-axis increases. The effect of learning task was significant (log-rank test P < 0.001). TTC=trials to criterion.*

Supplementary Table 2.2 *Predictors of the log transformed restricted mean trials to criterion for associative learning (n = 387; n = 559 trials) and reversal learning performance (n = 383; n = 549 trials), fitted with a linear mixed effect model with apparatus type (one/two), test round (one/two/three), sex (male/female), body condition and start time as fixed effects. Bird ID was included as a random intercept. Apparatus type significantly affected both associative learning performance (p < 0.001), and reversal learning performance (p = 0.016), trials to criterion being lower with apparatus type 2. For associative learning, males needed significantly less trials (p=0.015) but there were no significant effects of other control variables (test round, start time, body condition). For reversal learning, there was an effect of test round, with animals requiring less trials to complete the reversal phase over increasing rounds (p = 0.013) There was no effect of other control variables.*

	Associative learning			**Reversal learning**		
Variable	**Estimate**	**SE**	**p-value**	**Estimate**	**SE**	**p-value**
Apparatus type (Two)	-0.66	0.077	**<0.001**	-0.18	0.073	**0.016**
Round			0.71			**0.013**
R2	-0.05	0.075		-0.17	0.070	
R3	0.03	0.099		-0.20	0.094	
Sex (Male)	-0.14	0.057	**0.015**	-0.06	0.056	0.25
Body condition	0.00	0.000	0.62	0.00	0.000	0.60
Start time	-0.04	0.034	0.22	-0.03	0.028	0.36

5-22
5-22
5-22
5-22
5-22
5-22
5-22

Chapter 3.

Cell type- and brain region-specific patterns of differential gene expression and chromatin accessibility in great tits (*Parus major*)

Krista van den Heuvel, Beril Yildiz, Ilia Timpanaro, Aleksandra Badura, Chris de Zeeuw, Ingo Willuhn, Alexander Kotrschal, Menno Creyghton, Kees van Oers

Abstract

Epigenetic states are important mechanisms shaping both stable and dynamic transcriptional patterns in the brain that are involved in development, activity-dependent gene regulation, and hormonal and environmental responses. One such important regulatory mechanism is chromatin organization, however there is a lack of studies on the role of epigenetic mechanisms in ecologically relevant species. One of such model species for ecological and evolutionary questions is the great tit (*Parus major*). To understand how chromatin state modulates transcription in the great tit brain, we used the Assay for Transposase Accessible Chromatin followed by sequencing (ATAC-seq) combined with transcriptome analyses on this species. Since there is a lack of a reference for our results, we validated our findings in two widely studied species, mouse and rat. We used brain tissue from great tit striatum, cerebellum and hippocampus to study how brain region- and cell type-specific open chromatin relates to gene expression. We found pronounced differences in chromatin accessibility between neuronal and non-neuronal populations from the great tit striatum, that were associated with differences in gene expression. Interestingly, these differences were similar to transcriptomic cell type differences in the mouse striatum. Furthermore, we created maps of chromatin accessibility across three brain regions (hippocampus, cerebellum, and striatum), and found that differences in chromatin accessibility between pairs of these regions were associated with differential gene expression between those regions. For the comparison between striatum and cerebellum we validated these findings in mouse and rat. We show that ATAC-seq can be used to study cell type-specific chromatin accessibility in relevant brain tissues in the avian brain. This opens up new avenues for studying the relation between epigenetic states and ecologically relevant traits in an ecological model species.

To be submitted to Journal of Comparative Neurology

Introduction

The neuronal control of cognitive processes is organised in a cell type- and brain region-specific manner. Identifying how those brain structures control normal functions is crucial to understand the causes of individual differences in cognitive abilities. To gain insights into the functional differences between these anatomical structures, we should study the identity and function of the genes with localized expression patterns, as well as their regulatory elements. The epigenome is particularly important for controlling chromatin organization as a regulatory mechanism of cell type- and brain region-specific gene expression (Rizzardi et al., 2019). Epigenetic modifications, such as DNA and histone modifications, control the accessibility of chromatin to transcription factors (Klemm et al., 2019). In mammals, recent analyses have revealed extensive differences in both transcriptome and epigenome across brain regions (Strand et al., 2007; Negi and Guda, 2017; Fullard et al., 2018), and across cell types by making use of the nuclear neuronal marker (NeuN) to distinguish neurons from non-neurons (Rizzardi et al., 2019; Rocks et al., 2022). Transcriptomic analysis has also been crucial in gaining understanding of the molecular and functional organization of the avian brain, specifically the zebra finch (*Taeniopygia guttata*) (Jarvis et al., 2013; Lovell et al., 2020), with most recently a whole transcriptome study performed to compare the molecular profiles of avian pallial subdivisions (Gedman et al., 2021). However, thus far there has been no attempt to explore cell type and brain region-specific transcriptome and epigenome in ecological model species such as the great tit, and to what extent those mechanisms are similar to more widely studied species. This will be crucial in order to be able to make future predictions of the applicability of findings in laboratory model species in ecological species and vice versa.

The epigenetic landscape in the brain not only functions in the development and maintenance of cellular identity but is also modified upon neuronal activity (Su et al., 2017). Therefore, understanding the molecular profiles of specific brain regions will provide an important baseline for the comparison of cognitive and behavioural phenotypes of which the regulation is situated in these regions. There is an increasing interest in studying epigenetic mechanisms in ecological and evolutionary model species to understand its involvement of in behavioural, ecological and evolutionary processes, but because of the ease of sampling, current knowledge is mostly limited to the function of DNA methylation in accessible tissues (Sepers et al., 2019). Because epigenetic regulation can be explained by chromatin accessibility changes, assessing chromatin state provides a good starting point for understanding the regulatory mechanisms underlying gene expression differences (Grandi et al., 2022). Differences in chromatin accessibility can be compared using the Assay for Transposase Accessible Chromatin followed by sequencing (ATAC-seq) (Buenrostro et al., 2015; Corces et al., 2017).

We focus on three brain regions that are relevant to cognitive variation, have similar functions in birds and mammals, and are homologous between the two: the cerebellum, striatum and hippocampus. The striatum functions in decision making

and reward-based reinforcement learning as shown in mammals (Burton et al., 2015) and birds (Rose et al., 2013b). The striatum is of subpallial origin, and has uncontroversial homology across mammals and birds (Jarvis et al., 2005; Belgard et al., 2013). The hippocampus functions in spatial learning and navigation in mammals (Morris et al., 1982) as well as birds (Mayer et al., 2013), with a crucial role for adult neurogenesis especially in the avian brain (Herold et al., 2019). The function of the cerebellum lies primarily in motor control (Manto et al., 2012), but it also plays a role in higher cognitive functions, such as emotion, reward, and memory as mostly shown in mammals (Strata, 2015; Adamaszek et al., 2017; Heffley and Hull, 2019; Pierce and Péron, 2022), but evidence for similar roles for the cerebellum in birds is accumulating (Ebneter et al., 2016; Katajamaa et al., 2021; Stingo-Hirmas et al., 2022). The avian cerebellum is equivalent to the hemispheres of the mammalian cerebellum (Yopak et al., 2017). As other studies have reported that most variance in gene expression and chromatin accessibility between brain regions is due to neuronal cells (Fullard et al., 2018), we use fluorescent activated cell sorting (FACS) to purify neuronal nuclei from the striatum and hippocampus, where less than 60% of cells is neuronal, but we use bulk cells for the cerebellum, where over 80% of cells is neuronal (Olkowicz et al., 2016).

We here present cell type-specific transcriptome (RNA-seq) and open chromatin (ATAC-seq) analyses across three anatomically distinct brain regions of an ecological model species, the great tit (*Parus major*). In order to validate the generality of our findings, we additionally analysed the transcriptome of the striatum and cerebellum of mouse (*Mus* musculus) and rat (*Rattus norvegicus*) and performed species comparisons of regional expression patterns. Collectively, our results show distinct patterns of gene expression across brain regions and between cell types within brain regions, which correlate well across species. We show that these differences are accompanied by unique patterns of chromatin accessibility and reflect the functions of the respective cell types and regions.

Materials and Methods

Sample origins

Great tit

Tissue samples were collected from 16 male and female great tits (1–2 years old) originating from a captive population derived from wild-caught birds from the Netherlands and artificially selected for reversal learning performance for two generations (Chapter 1). Eight male birds originated from the parental generation, and 4 females and 4 males originated from the second generation of selection. Individuals were caught from their cage or aviary and deeply anaesthetized with isoflurane (IsoFlo, Zoetis, Kalamazoo, MI, USA). After decapitation, the brain was dissected out and placed in ice-cold PBS for further micro dissection of the cerebellum, and bilateral dissection of striatum (including area X) and hippocampus. Brain regions were located by the use of the online zebra finch brain atlas (Karten et al., 2013) ZEBrA (Oregon Health & Science University, Portland, OR,

USA; http://www.zebrafinchatlas.org). Isolated tissue was flash-frozen in liquid nitrogen in 1.5 ml RNA-free tubes and stored at −80°C until RNA isolation.

Mouse
Eight wild-type C57BL6/6JRj male mice (4 months old) were sacrificed using CO_2 followed by cervical dislocation. Their brains were rapidly dissected from the skull and whole cerebellum and striatum were further bilaterally dissected. Isolated tissue was flash-frozen using dry ice in 2 ml RNA-free tubes and stored at −80°C until RNA isolation.

Rat
Eight outbred Long-Evans (Janvier) male rats (4 months old) were sacrificed using CO_2 followed by cervical dislocation. Their brains were rapidly dissected from the skull and whole cerebellum and striatum (ventromedial, dorsomedial, dorsolateral) were further bilaterally dissected. Isolated tissue was flash-frozen using dry ice in 2 ml RNA-free tubes and stored at −80°C until RNA isolation.

Nuclei isolation
Frozen brain tissue (great tit: 8x cerebellum, 8x hippocampus, 16x striatum; mouse: 8x cerebellum, 8x striatum; rat: 8x cerebellum, 8x striatum) was pulverized with mortar and pestle on dry ice to yield ~0.2 mL of tissue powder. Tissue powder was homogenized in a glass douncer (Kontes Glass Co.) in 0.5 ml EZ buffer (Nuclei Isolation Kit, Sigma NUC101) and incubated for 5 min on ice. Subsequently samples were centrifuged for 15 min at 65 × g at 4 °C, resuspended in 0.5 mL EZ buffer and incubated on ice for 5 min. Samples were again centrifuged for 15 min at 65 × g at 4 °C, resuspended in 0.5 mL nuclear suspension buffer (NSB; 0.01% BSA, 1× complete protease inhibitor cocktail in PBS) and filtered through a 40 µm cell strainer. Samples were centrifuged for 15 min at 65 × g at 4 °C and resuspended in 0.5 mL NSB.

Striatum and hippocampus
For nuclei collected from the striatum and hippocampus, 1:1000 Hoechst 34580 (1 µg/ml, Fisher Scientific H21486) was added to blocking solution (1% BSA, 10% normal mouse serum (NMS) in PBS) and incubated light shielded at 4 °C for 20 min. 10% of the blocked sample was used as unstained control, the remaining 90% was stained with 1:1500 anti-NeuN antibody conjugated with Alexa488 (1:1000, Merck Millipore MAB377X) without washing and incubated for 1 h at 4 °C on a roller, protected from light. Stained nuclei were then transferred to FACS tubes precoated with 3% BSA and FACS-sorted on NeuN signal using a BD FACSAria II (BD Bioscience) (Supplementary Figure 3.1). We collected 5,000 neuronal (NeuN+ stained) and 5,000 non-neuronal (NeuN− stained) nuclei in 100 µl Trizol each for RNA-sequencing. 60,000 NeuN+ and NeuN− stained nuclei were collected in NSB and processed further for ATAC-sequencing.

Cerebellum
Bulk nuclei from cerebellar tissue were stained with trypan blue and counted on a

hemacytometer. 50,000 nuclei were processed further for ATAC-sequencing, 5,000 nuclei were pelleted by 10 minutes centrifugation at 500g and resuspended in 100 µl Trizol for RNA-sequencing.

RNA-sequencing

RNA-sequencing was performed at Single Cell Discoveries, a (single cell) sequencing provider located in the Netherlands using an adapted version of the CEL-seq protocol. In brief: Total RNA was extracted using the standard TRIzol (Invitrogen) protocol and used for library preparation and sequencing. mRNA was processed as described previously, following an adapted version of the single-cell mRNA seq protocol of CEL-Seq (Simmini et al., 2014; Hashimshony et al., 2016). In brief, samples were barcoded with CEL-seq primers during a reverse transcription and pooled after second strand synthesis. The resulting cDNA was amplified with an overnight In vitro transcription reaction. From this amplified RNA, sequencing libraries were prepared with Illumina Truseq small RNA primers. Paired-end sequencing was performed on the Illumina Nextseq500 platform with a sequencing depth of 10 million reads/sample. All reads were trimmed of adapters and low quality bases using *fastx* and sequencing quality was checked using the software *FastQC* v0.11.9 (Andrews, 2010). Trimmed reads were mapped to the *Parus major* reference genome (Ensembl Assembly Parus_major1.1: GCA_001522545.2), *Mus musculus* reference genome (Ensembl Assembly GRCm38.p6: GCA_000001635.8) and *Rattus norvegicus* reference genome (Ensembl Assembly Rnor_6.0: GCA_000001895.4) using *Hisat2* v2.2.1 (Kim et al., 2019) with default parameters. To summarize gene level read counts, we used the *featureCounts* program from the *Subread* package v2.0.2 (Liao et al., 2014).

Principal component analysis on RNA-seq data

Using *DESeq2* v1.38.0 (Love et al., 2014), low count genes were pre-filtered using a cut-off of 10 normalised counts in >75% of the samples (for pairwise comparisons) or at least 10 normalized counts in at least three samples in one brain region (for three wise comparisons). Mitochondrial and ribosomal RNA reads were removed from the gene expression matrix. The final matrix consisted of the following number of genes: great tit striatum cell type; 11,177, mouse striatum cell type; 13,128, great tit brain regions; 13,499, mouse brain regions; 16293, rat brain regions; 13,939. Remaining read counts were normalized with post-filtering library sizes and log2 transformed using the rlog function. Following normalization, we performed Principle Component Analysis (PCA) using *DEseq2* with the function *plotPCA* to visualize clustering of the samples and to spot individual sample outliers that separated significantly based on size factor (reflecting library size and/or RNA composition bias). These samples were then removed and the filtering and normalization steps were repeated. Sample sizes were therefore different than what we initially started with. We used the following samples for further analysis. Great tit: 4 striatal NeuN- (2F/2M) and 9 striatal NeuN+ (4F/5M), 8 hippocampal NeuN+ (all male) and 5 cerebellar bulk (all male) nuclei. Mouse: 5 striatal NeuN-, 5 striatal NeuN+, 5 cerebellar bulk nuclei (all males). Rat: 3 striatal NeuN+ and 2 cerebellar bulk (all male). An overview of included samples including library

quality can be found in Supplementary Table 3.1. In order to visualize principal sources of variation in the data, we performed final PCA analyses and visualized the first two principal components (PCs) with the DEseq2 function plotPCA, applying the default setting limiting the analysis to the top 500 most variable genes. Additional PCs were obtained using the *prcomp* function in R. We also plotted the percent variance explained by each PC. We tested for cell type or brain region differences in principal components using the correlate PCs functions in *pcaExplorer*, which computes the significance of correlations between PCA scores and the experimental covariates.

Differential gene expression analysis
Differences in gene expression (as log2Foldchange) were calculated using *DESeq2*. We tested for differential expression of genes in the following comparisons: (1) great tit striatal NeuN+ versus great tit striatal NeuN-; (2) mouse striatal NeuN+ versus mouse striatal NeuN-; (2) great tit striatal NeuN+ vs great tit hippocampal NeuN+ vs great tit cerebellar bulk (three pairwise comparisons); (3) mouse striatal NeuN+ vs mouse cerebellar bulk; (4) rat striatal NeuN+ vs rat cerebellar bulk. To control for the false discovery rate due to multiple testing, p-values were adjusted using the Benjamini-Hochberg (BH) procedure. Genes were considered as statistically differentially expressed if they displayed a 1-fold enrichment with adjusted p-values < 0.05. Volcano plots were generated using *EnhancedVolcano* v1.16.0 (Blighe, 2018). For the great tit brain region comparison, we continued the filtering to find regional differences in gene expression. To identify sets of genes that are enriched in one of the three regions only, we selected genes that showed significantly higher expression in a brain region in both pairwise comparisons with the other two regions. We summed the log2Foldchange of both comparisons to create a ranked set of top-regionally expressed genes.

Comparison between cell type- and brain region-specific differences in gene expression across species
To assess to what extent differences in gene expression were correlated across species, we obtained one-to-one orthologs using the *getLDS* function from *BiomaRt* v2.54.0 (Durinck et al., 2005, 2009). If multiple gene IDs of one species map to the on single gene ID of the other species, we retained only the gene ID with the highest base mean expression. We then trimmed the dataset by excluding genes with a change in expression of log2Foldchange < 1, plotted the log2Foldchange of one species against the log2Foldchange of another species and calculated Pearson correlation scores, comparing great tit with mouse in striatal neuronal and non-neuronal nuclei and comparing great tit, mouse and great in striatal neuronal versus bulk cerebellar nuclei. Orthologous genes were also used to create Venn diagrams to visualize intersections between differentially accessed genes across species.

Gene ontology analyses on differential gene expression
To identify significantly enriched gene ontology (GO) terms, we used *clusterProfiler* v4.6.0 (Yu et al., 2012) to perform Gene Set Enrichment Analysis (GSEA). GSEA does

not require delineation of DEGs from non-differential genes. We ranked the test statistic of all assessed genes to test for significantly coordinated shifts in gene pathways, as suggested by (Zyla et al., 2017). For all gene sets, we retained only those with 15-500 genes. We used the human, mouse and rat gene ontology database, for great tit, mouse and rat data, respectively. Great tit genes were mapped to their corresponding human orthologs based on HUGO Gene Nomenclature Committee (HGNC) symbol. Genes that could not be assigned to a human gene were excluded, and therefore great tit-specific genes are missing from these analyses. We kept all GO terms, namely biological process (BP), cellular component (CC) and molecular function (MF) and considered an adjusted p-value < 0.05 after BH correction and 10,000 permutations to be significant. We used enrichment map plot (*emapplot*) to visualize overlap in significant GO terms as well as interactions among terms.

Assay for transposase-accessible chromatin using sequencing (ATAC-seq)

OMNI-ATAC was performed on great tit samples: 8x cerebellar bulk, 8x hippocampus NeuN+, 8x hippocampus NeuN-, 16x striatum NeuN+ and 16 striatum NeuN- nuclei, according to an adapted protocol from (Corces et al., 2017). In short, 0.1% NP-40 was added to the nuclei and samples were centrifuged for 15 min at 500 × g at 4 °C. Nuclei were resuspended in 50 µl transposition mix (25 µl TD buffer (20 mM Tris-HCl pH 7.6, 10 mM $MgCl_2$, 20% dimethyl formamide in MQ), 2.5 µl Tn5 transposase, 16.5 µl PBS, 0.5 µl NP-40 1%, 10% Tween-20 / Triton-X, 0.5 µl, 5 µl MQ) and incubated for 30 min at 37 °C while shaking at 1000 rotations per minute. Samples were purified using Qiagen MinElute PCR purification kit (Qiagen 28004) and eluted in 21 µl MQ. Purified DNA was amplified with NEBnext High-Fidelity PCR master mix (NEB M0541S) and appropriate sequencing adapters for five PCR cycles. Library complexity was determined by qPCR on 5 µl of the PCR sample and the number of extra PCR cycles determined (Buenrostro et al., 2015). PCR samples were purified using AMPure XP beads (Agencount A63881), eluted in 12 µl MQ and sequenced at USEQ on a high-output NextSeq500, 1× 75 bp.

We trimmed reads of the Nextera adapter sequences using *trim-galore* v0.6.6 (Krueger, 2023). We then mapped trimmed reads to the *Parus major* reference genome (NCBI Assembly Parus_major1.1: GCF_001522545.3) using *Bowtie2* v2.4.4 (Langmead and Salzberg, 2012), with standard parameters and a maximum fragment length of 2,000. *Samtools* v1.12 (Danecek et al., 2021) was then used to remove unmapped, low quality (keeping MAPQ ≥ 20), duplicate and mitochondrial reads from further analysis. We only continued analysis with samples of which the data was of high enough quality, measured as fraction of reads in peaks (FRiP) scores exceeding the 0.8% threshold. Sample sizes were therefore different than what we initially started with and included 7 striatal NeuN- (3F/4M), 8 striatal NeuN+ (3F/5M), 6 hippocampal NeuN+ (all male) and 3 cerebellar bulk (all male) samples. The mean percentage of unique reads of the final selected samples was 79.4%, an overview of the final sample selection can be found in Supplementary Table 3.2. Accessible regions were defined using *MACS2* (MACS: Model-based Analysis for ChIP-Seq, 2023) on each bam file to call narrow peaks (with options -g

1.00229e9 -q 0.01). Identified open chromatin regions were extended to a minimum size of 1000 bp (peak center ± 500 bp). Lists of open chromatin regions were obtained by merging the identified regions of each sample, with regions overlapping at least 1 bp being stitched together, to construct a 'consensus' set of open chromatin regions. This resulted in 115,266 regions for the consensus set for the striatal neuronal versus non-neuronal comparison and 150,371 regions for the consensus set for the brain region comparison. For each sample, we then counted the number of reads overlapping each of the 'consensus' regions using the *coverageBed* function in the *BEDtools* package v2.24.0 (Quinlan and Hall, 2010), with higher read counts indicating more open chromatin at a given region.

Principal component analyses on ATAC-seq data
Using *DESeq2* v1.38.0 (Love et al., 2014), read counts were normalized with post-filtering library sizes and log2 transformed using the rlog function. Following normalization, we performed Principle Component Analysis (PCA) using the *DEseq2* function *plotPCA* to visualize principal sources of variation in the data, applying the default setting limiting the analysis to the top 500 most variable peaks. Additional PCs were obtained using the *prcomp* function in R. We also plotted the percent variance explained by each PC. We tested for cell type or brain region differences in principal components using the correlate PCs functions in *pcaExplorer*, which computes the significance of correlations between PCA scores and the experimental covariates.

Differential chromatin accessibility analysis
To define cell type- and brain region-specific accessible regions, we performed differential chromatin analysis using *DESeq2*. We tested for differential accessibility in the following comparisons: (1) great tit striatal NeuN+ versus great tit striatal NeuN-; (2) great tit striatal NeuN+ vs great tit hippocampal NeuN+ vs great tit cerebellar bulk (three pairwise comparisons). ATAC-seq peaks were considered differentially accessible regions if they displayed a 1-fold enrichment with an Benjamini-Hochberg adjusted p-value <0.05. Volcano plots were generated using *EnhancedVolcano* v1.16.0 (Blighe, 2018).

Association of chromatin accessibility with gene expression
We used *annotatePeak* from the *ChIPseeker* package v1.34.0 (Wang et al., 2022) to annotate ATAC-seq peaks to closest gene and genomic context, based on *Parus major* genome assembly and following the priority order: Promoter (1000 bp upstream to 1000 bp downstream of the annotated transcription starting position), 5'UTR, 3'UTR, Exon, Intron, Downstream (the downstream of gene end) and Intergenic. Based on rlog-transformed read counts of open chromatin regions that were annotated (to closest gene) to the 30 genes with the most regional expression patterns, we visualized the separation of brain regions by hierarchical clustering using Ward's linkage method and plotting the heatmap using the *complexHeatmap* package v2.14.0 (Zuguang Gu, 2017). In order to evaluate the association between differential chromatin accessibility and differential gene expression, we plotted the log2Foldchange in gene expression against log2Foldchange in chromatin

accessibility and calculated Pearson correlation scores, after trimming the dataset by excluding regions with a change in accessibility (log2Foldchange) <1, adjusted p-value > 0.05 and genes with a change in expression (log2Foldchange) <1, adjusted p-value > 0.05. To understand the effect of the genomic context on the relationship between differential chromatin accessibility and gene expression, we differentiated between genomic regions.

Gene ontology analyses on differentially accessible regions
Gene ontology analysis on differentially expressed genes that contained differentially accessible regions was performed using *clusterProfiler* v4.6.0 (Yu et al., 2012) to perform Over Representation Analysis (ORA) of GO pathways (biological process, molecular function and cellular component). We used the human, mouse and rat gene ontology database, for great tit, mouse and rat data, respectively. Great tit genes were mapped to their corresponding human orthologs based on HUGO Gene Nomenclature Committee (HGNC) symbol. Genes that could not be assigned to a human gene were excluded, and therefore great tit-specific genes are missing from these analyses. All functional category enrichment analyses considered an adjusted p-value < 0.05 after BH correction to be significant.

Results

Cell type differences in gene expression in the striatum of great tit compared with mouse

A PCA analysis showed that striatal neuronal and non-neuronal nuclei of great tit and mouse could be distinguished based on gene expression (Supplementary Figure 3.2a,b), and differential gene expression analysis showed many statistically significant differences (Supplementary Figure 3.4a, Supplementary Figure 3.5a), which were correlated between great tit and mouse (pearson correlation r = 0.41, p < 0.0001) (Figure 3.1a). In the great tit striatum, we found 826 genes to be expressed at a higher level in neuronal nuclei, of which 552 genes were one to one orthologs to mouse genes, in the mouse striatum, 1,734 genes were expressed at a higher level in neuronal nuclei, of which 1120 were orthologs to great tit genes. Of these one-to one orthologs, 267 genes overlapped across the two species (Figure 3.1b). Of the 1,100 great tit genes expressed at a higher level in non-neuronal nuclei, 799 genes were one to one orthologs to mouse genes, and of the 1,583 mouse genes expressed at a higher level in non-neuronal nuclei, 950 genes were orthologs to great tit genes. Of these one-to-one orthologs, 274 genes overlapped across the two species (Figure 3.1c). A table with a subset of the top 30 most differentially expressed genes for each cell type in the great tit can be found in (Supplementary Tables 3.3 and 3.4).

Genes that were expressed at a higher level in great tit neuronal nuclei, were enriched in GO categories with clear relevance to neuronal function, such as chemical synaptic transmission, synaptic signalling, dendritic tree. In contrast, genes that were expressed at a higher level in great tit non-neuronal nuclei were enriched in GO categories that are relevant to the functions of other cell types

residing in the striatum: including blood vessel development, regulation of cell migration, oligodendrocyte differentiation and gliogenesis (Supplementary Table 3.7). Mouse GO terms for which gene expression differentiated between neuronal and non-neuronal cells (1164 in total) were highly similar compared to GO terms in great tits (1081 in total): 532 were common between great tit and mouse (Figure 3.1d,e).

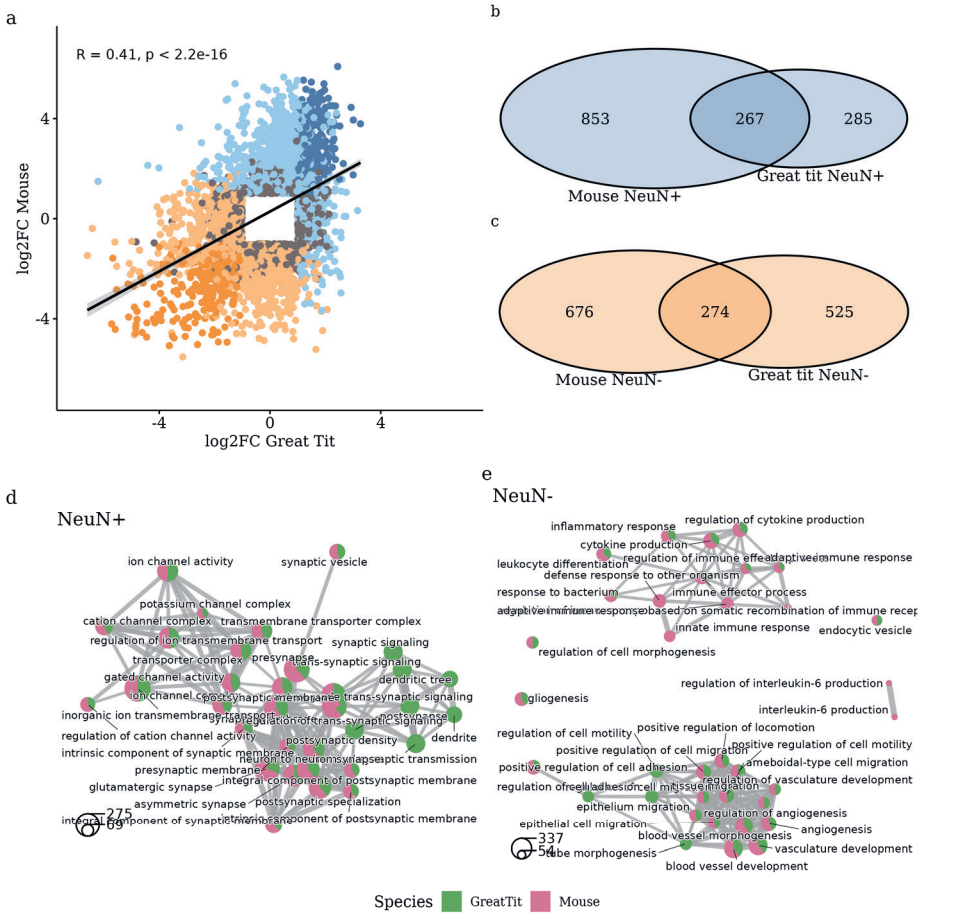

Figure 3.1 Cell type-specific gene expression in neuronal vs non-neuronal nuclei of the striatum of great tit and mouse. *a) Pearson correlation of log2FoldChange (log2FC) of differentially expressed genes between striatal neuronal (NeuN+) (blue dots) and non-neuronal (NeuN-) nuclei (orange dots) in the great tit versus the mouse. Darker dots indicate differentially expressed genes that overlap between the two species. b,c) Venn diagrams of genes differentially expressed between striatal neuronal and non-neuronal nuclei in both species, highlighting the overlap among species in the identities of differentially expressed genes. d,e) Comparisons of significantly enriched GO categories in cell type-specific expressed genes reveals many common terms across great tit and mouse. Shown are the 20 most enriched categories for each species. The size of the circle indicates the number of genes under that category, the proportion in the pie chart indicates the relative contribution of each species in case of overlapping GO categories.*

Brain regional differences in gene expression in great tit, mouse and rat

A PCA analysis showed that brain regions in great tit, mouse and rat could be distinguished based on gene expression (Supplementary Figure 3.3a-c), and differential gene expression analysis on pairwise comparisons showed strong statistically significant differences (Supplementary Figure 3.4b-d, Supplementary Figure 3.5b, Supplementary Figure 3.6). In the great tit, genes that were expressed at a higher level in striatum neuronal nuclei when compared to both cerebellum (n = 1,641) and hippocampus (n = 1,623), were enriched in GO categories with clear relevance to striatal neuronal function: synaptic membrane, dendrite, GABA-ergic synapse and glutamatergic synapse (Figure 3.2, Supplementary Table 3.9). Genes that were expressed at a higher level in hippocampal neuronal nuclei (n = 2,644) when compared to striatal neuronal nuclei were enriched in GO categories with more general cellular functions such as angiogenesis and tissue migration, whereas when compared to bulk cerebellar nuclei (n = 1,647), GO categories such as neuron differentiation and signalling receptor activity were enriched (Figure 3.2, Supplementary Table 3.9). Genes that were expressed at a higher level in bulk cerebellum nuclei are enriched for ribosomal functions and blood vessel morphogenesis reflecting the heterogeneous origin of these cells, especially when compared to striatal neuronal nuclei (n=2019), but also midbrain development and neurotransmitter secretion are enriched when compared to hippocampal neuronal nuclei (n = 1,747) (Figure 3.2, Supplementary Table 3.8). By taking the overlap in differentially expressed genes for each brain region (in the two comparisons striatum = 868 genes, hippocampus = 816 genes, cerebellum = 815 genes) and summing the log2Fold change, we created lists of genes specifically upregulated in each region. A table with a subset of the top 30 most differentially expressed genes for each brain region in the great tit can be found in Supplementary Tables 3.4-6. Among the top most regionally expressed genes were for example *DRD2*, *DRD5* and *PENK* in the striatum; *EN2*, *CBLN1*, *GRIN2C* and *ZIC1* in the cerebellum; *IFI30*, *C1QC* and *FEZF2* in the hippocampus, the expression of which we confirmed in online datasets with regional gene expression data available from https://www.proteinatlas.org/ and http://www.zebrafinchatlas.org/.

Quantitative differences in gene expression between striatal neuronal nuclei and cerebellar bulk nuclei correlated well between great tit and mouse ($r = 0.42$, $p < 0.0001$) and rat ($r = 0.28$, $p < 0.0001$) (Figure 3.3a-c). Of the 3,360 genes differentially expressed between striatal neuronal nuclei and cerebellar nuclei, 2,137 genes were one to one orthologs to mouse and rat genes, of which 347 differentially expressed genes overlapped between these regions with both mouse and rat (Figure 3.3d). Also at the level of GO terms, brain region differentiation in the three species was highly similar: Of the GO categories differentially represented in striatal neuronal and cerebellar bulk nuclei, 257 were common between great tit (492 in total) and mouse (525 in total) and 222 were common between great tit and rat (654 in total), 184 terms were common among all species (Figure 3.3e,f).

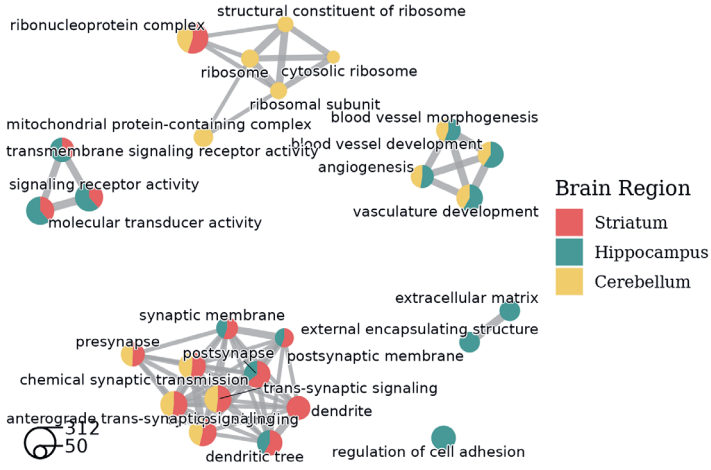

Figure 3.2 Enriched GO categories in brain region-specific expressed genes in the great tit reveals specific function of regionally expressed genes. *Shown are the 10 most enriched categories for each brain region in each pairwise comparison. The size of the circle indicates the number of genes under that category, the proportion in the pie chart indicates the relative contribution of each brain region in case of overlapping GO categories.*

Cell type- and brain region-specific patterns of chromatin accessibility in the great tit

Cluster analyses using PCA based on chromatin accessibility data grouped the samples according to striatal cell type (Supplementary Figure 3.7a) and brain region (Supplementary Figure 3.7b). 41,823 of the 114,885 open chromatin regions tested were differentially accessible (adjusted p-value < 0.05) between neuronal and non-neuronal nuclei (Supplementary Figure 3.8a). Out of the 150,371 open chromatin regions used for the brain regions dataset, we identified 51,597 differentially accessible regions (DARs) between striatal neuronal nuclei and hippocampal neuronal nuclei, 56,327 DARs between striatal NeuN+ nuclei and cerebellar bulk nuclei and 49,800 DARs between hippocampal neuronal nuclei and cerebellar bulk nuclei (Supplementary Figure 3.8b-d). We found that DARs were not evenly distributed across genomic regions: open chromatin regions resided more often in intronic, distal intergenic, promoter and exonic regions, in decreasing numbers. On the contrary, the neuron-specific DARs were located more distally to promoter regions, with more regions being located in exonic than promoter regions (within 1,000 kb of a TSS) (Figure 3.4a). Furthermore, the proportion of striatal and hippocampal neuronal nuclei-specific open chromatin regions that is located in promoters is less compared to the proportion of bulk cerebellar open chromatin regions residing in promoter regions (Figure 3.7a, Figure 3.8a, Figure 3.9a).

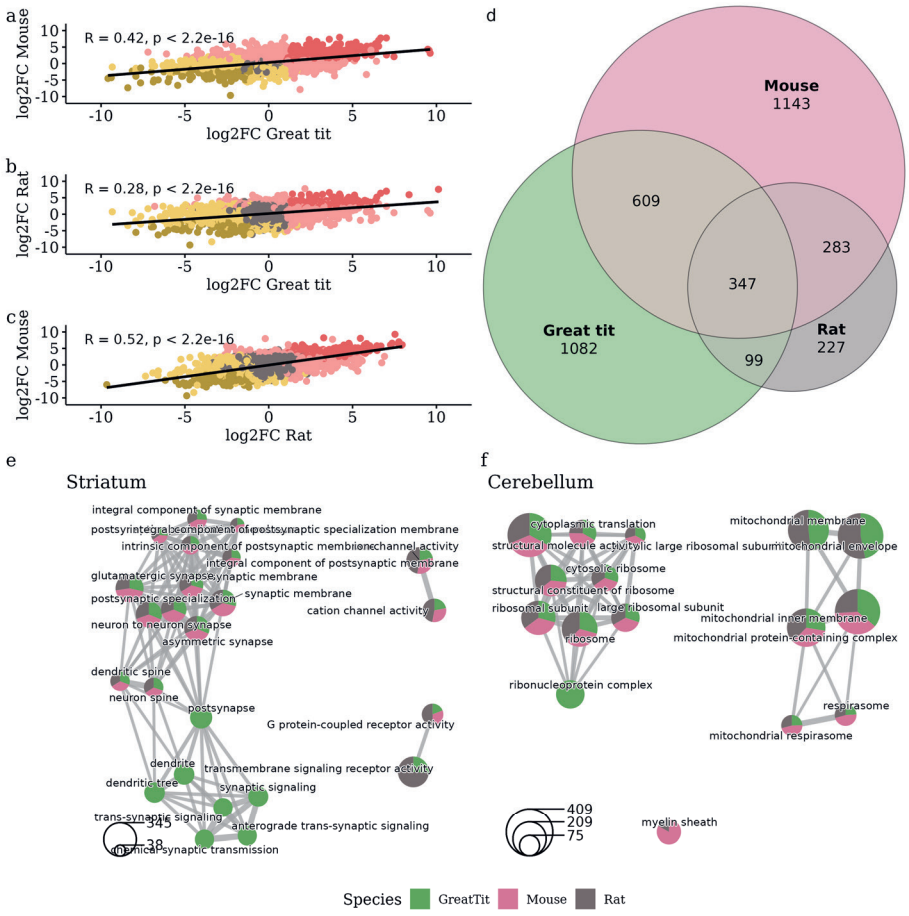

Figure 3.3 Brain region-specific gene expression in striatal neuronal nuclei versus cerebellum bulk nuclei of great tit, mouse and rat. *a-c) Pearson correlations of log2FoldChange (log2FC) of gene expression differences between striatal (red dots) compared to cerebellar (yellow dots) nuclei in the great tit versus mouse, great tit versus rat and rat versus mouse using one to one ortholog genes. Darker dots indicate differentially expressed genes that overlap between each two species. d) Venn diagram of genes differentially expressed between the two brain regions in each species, highlighting the overlap among species in the identities of differentially expressed genes. e,f) Comparison of significantly enriched GO categories in genes specifically expressed in striatal neuronal nuclei versus bulk cerebellar nuclei reveals many common terms across great tit, mouse and rat. Shown are the 10 most enriched categories for each species in each brain region. The size of the circle indicates the number of genes under that category, the proportion in the pie chart indicates the relative contribution of each species in case of overlapping GO categories.*

Relationship between gene expression and chromatin expression

Differences in chromatin accessibility are overall strongly correlated with expression of the closest gene, although this relationship varied across cell type and brain region comparisons and genomic contexts. The overall correlation between differential gene expression and differential openness was the strongest when comparing neuronal and non-neuronal nuclei from the striatum (r = 0.67, p <

0.0001; Figure 3.4b), with DARs in 5'UTR, intronic and promoter regions being most predictive of gene expression, and distal intergenic DARs being the least predictive, although still significantly correlated (Figure 3.4c-f, Supplementary Figure 3.9a,b).

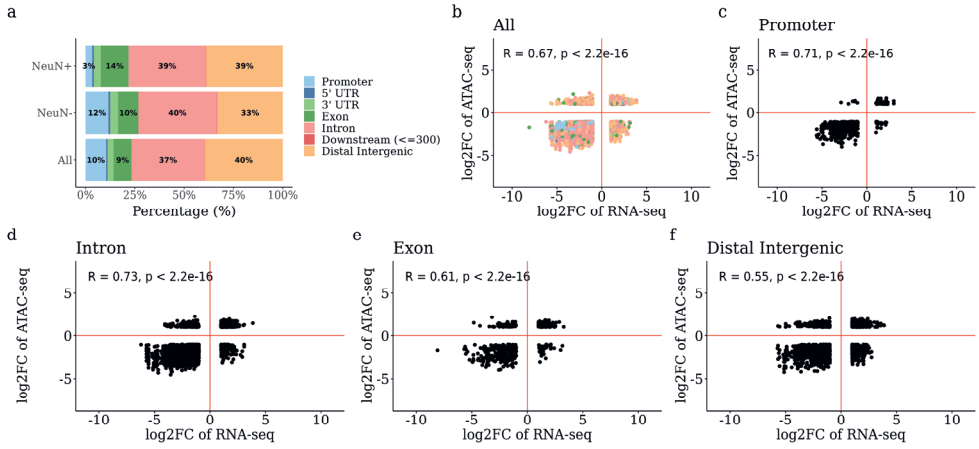

Figure 3.4 Relationship between differential chromatin accessibility and gene expression in neuronal vs non-neuronal nuclei of the striatum of great tits. *a) Bar plot representing the fraction of accessible regions assigned to each genomic region, split in all accessible regions, neuronal-specific regions and non-neuronal-specific regions. b-f) Pearson correlation of differentially expressed genes and differentially accessible chromatin regions (in log2FC) between neuronal compared to non-neuronal nuclei in the great tit striatum for the indicated genomic regions (Promoter; Intron; Exon; Distal Intergenic).*

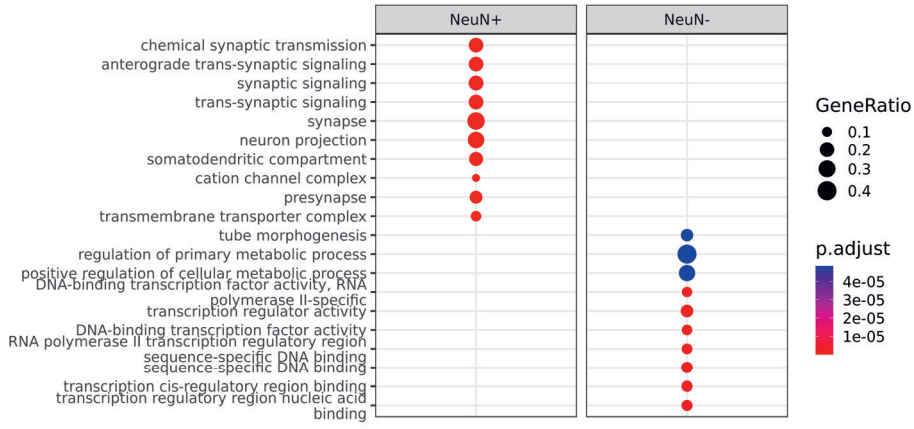

Figure 3.5 Over representation analysis of GO terms enriched in neuronal and non-neuronal-specific differentially expressed genes that contain differentially accessible regions. *Top 10 GO terms (biological process, molecular function and cellular component) are shown for each cell type. Colours indicate p-values (Benjamini–Hochberg-corrected) and dot size corresponds to gene ratio.*

Striatal neuronal-specific DEGs that contained DARs (n= 425), were enriched in GO categories with clear relevance to neuronal function (e.g., chemical synaptic transmission, synaptic signalling, neuron projection), whereas striatal non-neuronal nuclei DEGs containing DARs (n = 702) were enriched in transcription regulation, tube morphogenesis and metabolic process (Figure 3.5), indicating that differential expression of genes with these functions is related to the accessibility of their chromatin.

Accessibility of chromatin regions located in a subset of genes (90 genes) that showed the most regional expression across the three brain regions (30 genes per brain region, ranked as described in materials and methods) accurately clustered the brain regions (Figure 3.6). When comparing gene expression and chromatin openness between brain regions, the strength of this relationship is about equally high in the comparison between cerebellar nuclei with striatal neuronal nuclei ($r = 0.53$, $p < 0.0001$, Figure 3.7b-f, Supplementary Figure 3.9c,d) as when compared to hippocampal neuronal nuclei ($r = 0.51$, $p < 0.0001$, Figure 3.8b-f, Supplementary Figure 3.9e,f). The strength is lower when comparing striatal with hippocampal neuronal nuclei ($r = 0.36$, $p < 0.0001$, Figure 3.9b-f, Supplementary Figure 3.9g,h), likely reflecting a stronger similarity in gene regulatory mechanisms across neuronal cells from two brain regions relative to when purified neuronal cells are compared to bulk cerebellar nuclei.

Striatal neuronal-specific DEGs containing DARs in the comparison with hippocampal neuronal nuclei (n = 811) and cerebellar bulk nuclei (n= 958) showed enrichment of neuron-general terms (Figure 3.10) as well as striatal-specific functions, such as associative learning (adjusted p-value < 0.0001), response to dopamine (adjusted p-value = 0.003) and striatum development (adjusted p-value = 0.027). Genes that contained regions with higher accessibility as well as higher expression in hippocampal neuronal nuclei when compared to striatal neuronal (n=925) or to cerebellar nuclei (n=746), were enriched in neurogenesis-related GO categories such as regulation of neuron projection development (adjusted p-value <0.0001) and DNA-binding transcription factor activity (adjusted p-value <0.0001), but also gliogenesis (adjusted p-value <0.0001) and vasculature development (adjusted p-value <0.0001) and categories related to hippocampal neurotransmitters such as glutamatergic synapse (adjusted p-value <0.0001) and GABA-ergic synapse (adjusted p-value <0.0015) (Figure 3.10). When comparing cerebellar nuclei to striatal neuronal nuclei (n= 769) or to hippocampal neuronal nuclei (n=937), most terms related to ribosome functioning (Figure 3.10), but also trans-synaptic signalling (adjusted p-value < 0.0001), parallel fiber to Purkinje cell synapse (adjusted p-value < 0.001) and glutamatergic synapse (adjusted p-value < 0.001) were enriched.

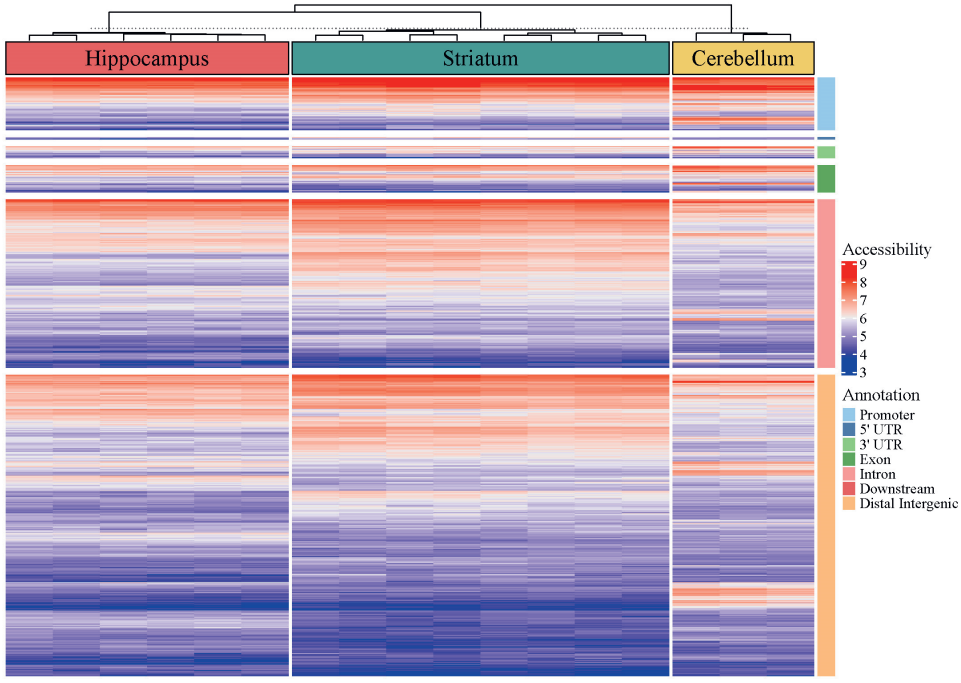

Figure 3.6 Hierarchical clustering of brain regions in the great tit by chromatin accessibility using the 90 genes with the most regional expression patterns (30 per brain region). *Chromatin accessibility was rlog normalized across samples. Accessibility as read count is coloured by standard deviation from the within-group mean. Columns represent samples with red, blue and yellow bars on top indicating brain regions. Rows represent accessible regions, with bars on the right indicating genomic localizations of chromatin regions.*

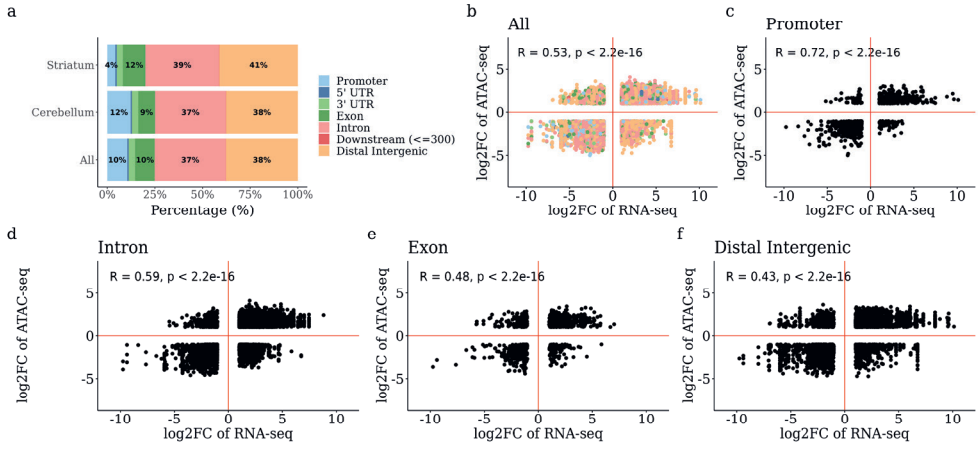

Figure 3.7 Relationship between differential chromatin accessibility and gene expression in striatal vs cerebellar nuclei of great tits. *a) Bar plot representing the fraction of accessible regions assigned to each genomic region, split in all accessible regions, striatum-specific regions and cerebellum-specific regions. b-f) Pearson correlation of differentially expressed genes and differentially accessible chromatin regions (in log2FC) between striatal compared to cerebellar nuclei for the indicated genomic regions (Promoter; Intron; Exon; Distal Intergenic).*

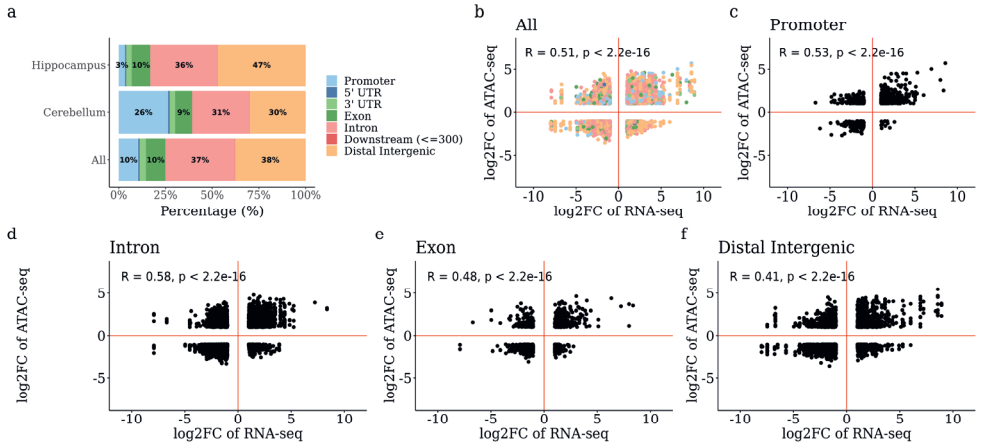

Figure 3.8 Relationship between differential chromatin accessibility and gene expression in hippocampal vs cerebellar nuclei of great tits. *a) Bar plot representing the fraction of accessible regions assigned to each genomic region, split in all accessible regions, hippocampus-specific regions and cerebellum-specific regions. b-f) Pearson correlation of differentially expressed genes and differentially accessible chromatin regions (in log2FC) between hippocampal compared to cerebellar nuclei for the indicated genomic regions (Promoter; Intron; Exon; Distal Intergenic).*

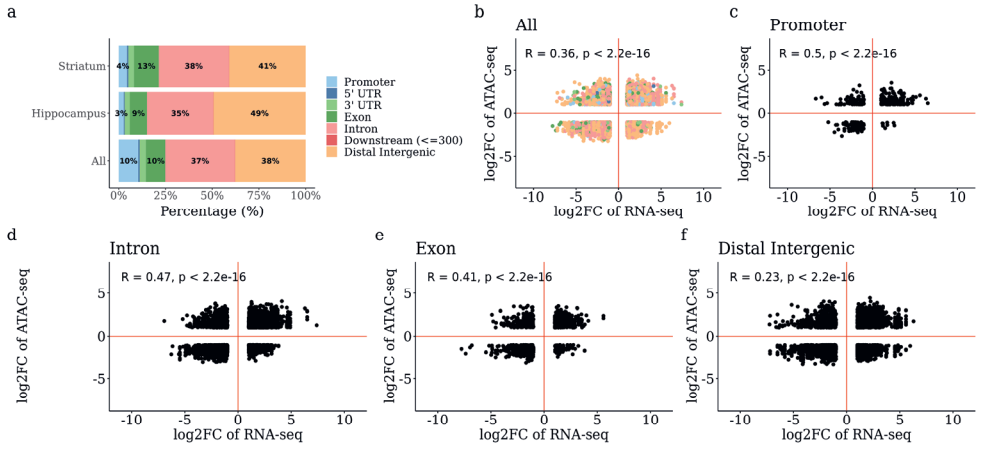

Figure 3.9 Relationship between differential chromatin accessibility and gene expression in striatal vs hippocampal nuclei of great tits. *a) Bar plot representing the fraction of accessible regions assigned to each genomic region, split in all accessible regions, striatum-specific regions and hippocampus-specific regions. b-f) Pearson correlation of differentially expressed genes and differentially accessible chromatin regions (in log2FC) between striatal compared to hippocampal nuclei for the indicated genomic regions (Promoter; Intron; Exon; Distal Intergenic).*

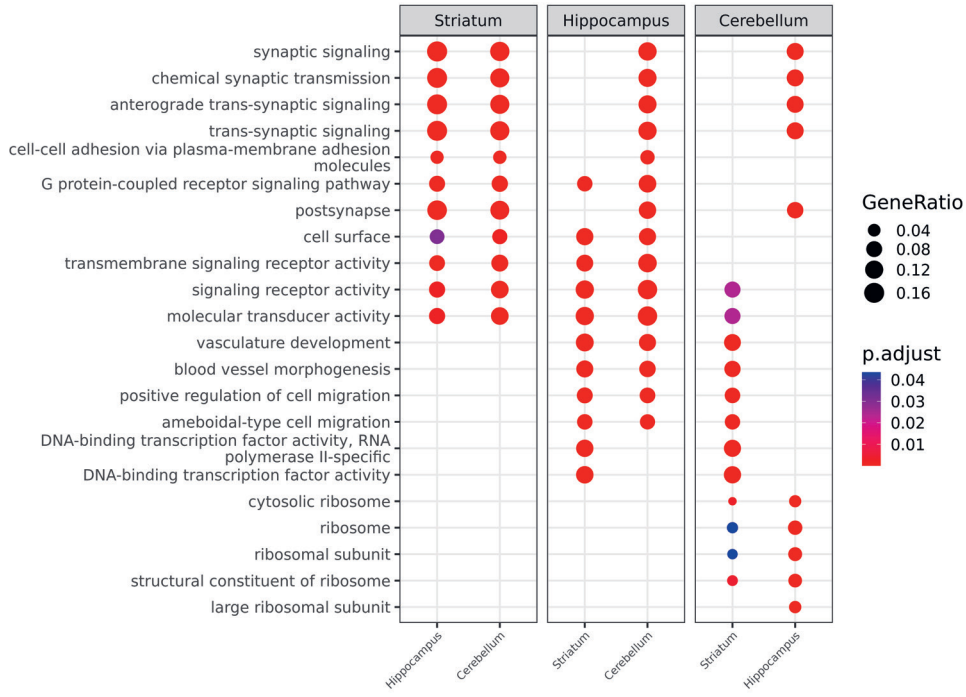

Figure 3.10 Over representation analysis of GO terms enriched in differentially expressed genes that contain differentially accessible regions in each pairwise brain region comparison. *Top 10 GO terms (biological process, molecular function and cellular component) are shown for each comparison. Colours indicate p - values (Benjamini–Hochberg-adjusted) and dot size corresponds to gene ratio.*

Discussion

In this study, we performed an integrated analysis of gene expression and genome-wide chromatin accessibility to characterize cell type- and brain region-specific mechanisms of gene expression in the great tit brain. Our data indicate clear patterns of differential gene expression that were conserved across homologous regions and cell types in mouse and rat brains after validation in those species. This is consistent with other comparative neuroanatomical studies that find strong similarities between the transcriptomes of these regions, such as conserved patterns of gene expression in the striatum (Belgard et al., 2013) and shared differentially expressed genes between cerebellar cell types (Kebschull et al., 2020) of chicken and mouse. Differential chromatin accessibility analysis showed that the genomic localization of accessible chromatin regions in relation to the gene, varied across cell types and brain regions, and correlated positively with differential gene expression in all comparisons. Altogether, these findings provide the first insights into the cell type-specific regulatory mechanisms underlying gene expression in the brain of an ecological model species, the great tit.

Using fluorescence-activated nuclear sorting (FANS) we were able to isolate striatal neuronal from non-neuronal nuclei based on the neuronal marker NeuN. Functional enrichment analysis of the differentially expressed genes between these cell types confirmed successful separation of these cell types, as enriched terms for genes with higher expression in in the neuronal population included categories with neuronal function, such as chemical synaptic transmission, synaptic signalling and dendritic tree, whereas enriched terms in the non-neuronal populations included blood vessel development, regulation of cell migration, oligodendrocyte differentiation and gliogenesis. Furthermore, in line with the known evolutionary homology of this region (Medina and Reiner, 1995; Reiner et al., 1998), differences in gene expression between the two cell populations correlated with differentially expression patterns of samples collected from the mouse striatum, with enrichment of highly similar gene ontologies.

Striatal-specific genes such as *DRD2*, *PPP1R1B*, *PENK* and *TAC1* (Strand et al., 2007; Negi and Guda, 2017) were upregulated in striatal neuronal nuclei compared to hippocampal neuronal nuclei and cerebellar nuclei. These expression patterns likely largely reflect the GABAergic medium spiny neurons that constitute the majority of striatal neuronal nuclei (Kemp and Powell, 1971; Person et al., 2008). Genes that were expressed at a higher level in hippocampal neuronal nuclei showed not only hippocampal-specific genes, such as *FEZF2* (Shimizu and Hibi, 2009; Berberoglu et al., 2014) and *PPP1R9B* (Allen et al., 1997), and functions, such as neuron differentiation and signalling receptor activity, but also other functions such as angiogenesis and tissue migration, especially when compared with the striatal neuronal nuclei. Additionally, several of the genes that were differentially expressed in hippocampal nuclei also showed high expression in non-neuronal nuclei from the striatum (e.g., *SLC4A1* and *SALL3*). *SLC4A1* is expressed in erythrocytes (Sahr et al., 1994), and *SALL3* is a marker of GABAergic precursor neurons (Bocchi et al., 2021). This suggests that hippocampal neuronal nuclei express these genes at a higher level than striatal neurons, or that also some non-neuronal nuclei or neuronal precursors were stained with the NeuN antibody. Further work to confirm the specificity of these genes to hippocampal neuronal nuclei is therefore necessary. Even though we used bulk cerebellar samples, and found according enrichment of functions like angiogenesis and ribosome, we also found high regional expression of known cerebellum-specific genes, including *CBLN1*, *GRIN2C* and *ZIC1* (Strand et al., 2007; Negi and Guda, 2017) as well as enrichment of functions associated with these genes like synaptic signalling. Furthermore, differences between striatal neuronal nuclei and cerebellar nuclei were consistent across great tits, mouse and rats with highly similar ontologies being enriched. Further validation of these cell type and brain region patterns of gene expression may in the future be validated via real-time PCR (qPCR) or in situ hybridization experiments, as well as more detailed cell-type specific analysis using cell-type specific markers and single-cell sequencing approaches (Mo et al., 2015; Yu et al., 2023).

By performing differential chromatin accessibility analyses we revealed cell type– and brain region–specific patterns of open chromatin. Generally, gene promotors are broadly accessible across cell types, whereas the accessibility of distal enhancers is expected to be more cell type-specific (Klemm et al., 2019). Indeed, we found that compared to the distribution of all accessible regions, a smaller fraction of differentially accessible regions was associated with the promoter. This difference was most pronounced in neuronal nuclei-specific regions, both when comparing different cell types of the striatum, as well as when comparing striatal and hippocampal neuronal nuclei with the bulk of cerebellar nuclei. This is in accordance with findings in humans (Fullard et al., 2018) and mice (Mo et al., 2015), showing that gene regulation in neurons occurs distally, with a greater fraction of promoter-associated peaks being shared across cell types. Additionally, the non-neuronal cell population likely includes a heterogeneous variety of glial cell types (microglia, astrocytes and oligodendrocytes), which are more diverse in cell function than neuronal subtypes (e.g., inhibitor and excitatory neurons), explaining why the observe more open chromatin regions in the promoters, which are generally less variable than enhancers and other regulatory elements. This likely also explains the higher fraction of DARs in the promoter regions of cerebellar bulk data.

To assess if and when open chromatin relates to gene expression, we tested whether genes with high variance of expression across the three brain regions would cluster the chromatin accessibility dataset by brain region, which was indeed the case, indicating that genes with brain region-specific expression also show brain region-specific chromatin accessibility. Furthermore, differences in gene expression correlated positively with chromatin accessibility. Functional enrichment of cell type or regionally expressed genes that also contained DARs showed enrichment of functions relevant to the respective regions indicating that functional variation in gene expression is explained by chromatin accessibility. Nonetheless, for each comparison, we also observed DARs that were mapped to genes that did not show expression differences. This can be explained by the fact that that some genes require multiple enhancers or additional epigenetic regulators to affect their expression (Ong and Corces, 2011). Alternatively, these might be false positives, or our approach to assign genes to the nearest TSS might not have linked to region to the gene(s) that it actually acts on. This is especially true for distal intergenic regions, which generally showed the lowest relationship with differential gene expression. To resolve these standing questions, a logical next step will be to characterize the transcription factors that are responsible for these open chromatin patterns by predicting transcription factor binding sites in open chromatin regions using e.g., HOMER motif enrichment analysis (Heinz et al., 2010), followed by expression analysis of the transcription factors for which the binding sites are enriched. Further work should focus on studying coordinated patterns of chromatin accessibility and known other regulatory mechanisms brain-region specific patterns of gene expression such as lncRNAs (Meléndez-Ramírez et al., 2021), histone modifications and DNA methylation (Mo et al., 2015, 2), which

especially in a non-CpG context is a strong predictor of brain-region specific gene expression (Rizzardi et al., 2019).

In conclusion, our findings add to the standing evidence that distinct patterns in cell type and brain region-specific transcriptional activity are regulated by chromatin accessibility, and our study is the first to so in an ecological model species, the great tit. As neuron-specific regulatory regions are enriched for behavioural traits (Rizzardi et al., 2019), neuronal activity can induce epigenetic changes (Su et al., 2017), and gene regulatory mechanisms are a fundamental mechanism underlying individual variation in behaviour (Sweatt, 2019), these findings provide a basis for using brain regulatory mechanisms to understand differences in behaviour and cognition.

Supplement to Chapter 3

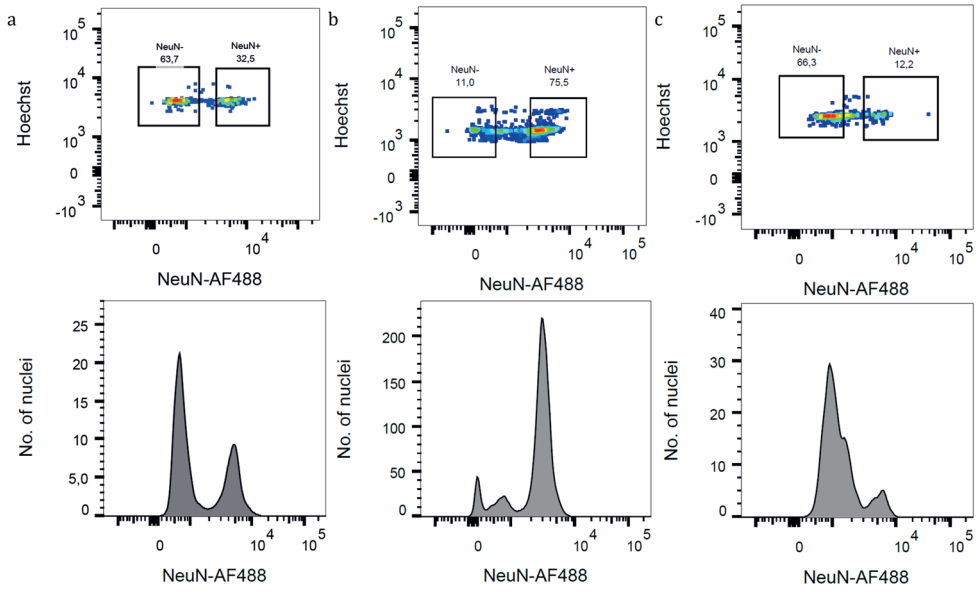

Supplementary Figure 3.1 *Striatal nuclei in these representative examples were isolated by fluorescence activated nuclei sorting (FANS). Nuclei were separated based on detection of AlexaFluor 488-conjugated anti-NeuN antibody. a) Mouse b) Great tit c) Rat.*

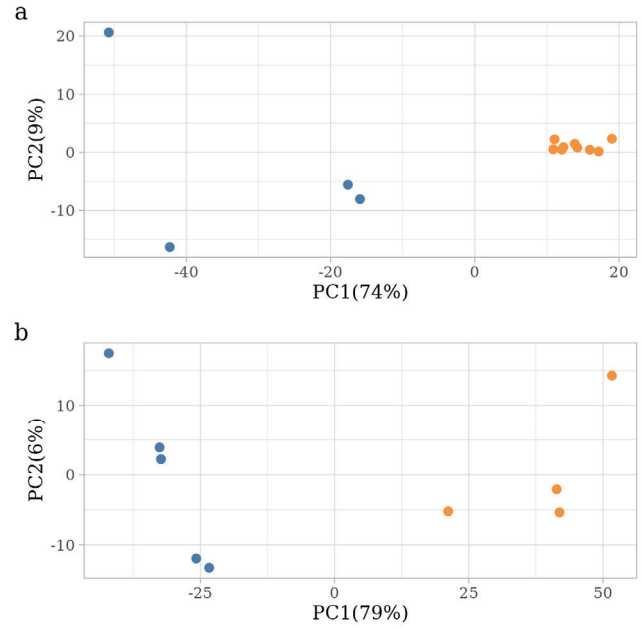

Supplementary Figure 3.2 *PCA plot showing clustering of neuronal (NeuN+, orange) and non-neuronal (NeuN-, blue) nuclei from the striatum along PC1 based on gene expression levels a) Great tit. PC1 explained 74% of the variance, PC2 8.7% and PC3 5.8%. Cell types separate significantly along PC1 (p = 0.0054) b) Mouse. PC1 explained 79% of the variance, PC2 6.2% and PC3 5.8%. Cell types separate significantly along PC1 (p = 0.014)*

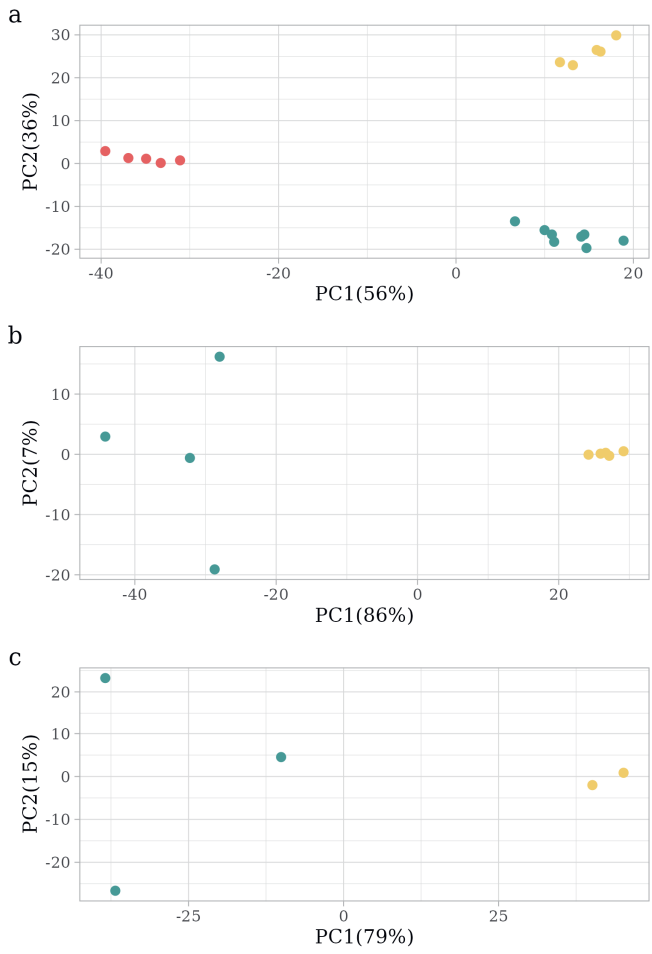

Supplementary Figure 3.3 *PCA plot showing clustering of brain regions based on gene expression levels. a) Great tit. PC1 explained 56% of the variance, PC2 36% and PC3 1.5%. Brain regions separate significantly along PC1 (p = 0.004) and PC2 (p<0.001) b) Mouse. PC1 explained 86% of the variance, PC2 6.7% and PC3 3.8%. Brain regions separate significantly along PC1 (p = 0.014) c) Rat. PC1 explained 79% of the variance, PC2 15% and PC3 5.2%. Brain regions separate along PC1, though not significantly (p = 0.08). Yellow = cerebellum, turquoise = hippocampus, red = striatum.*

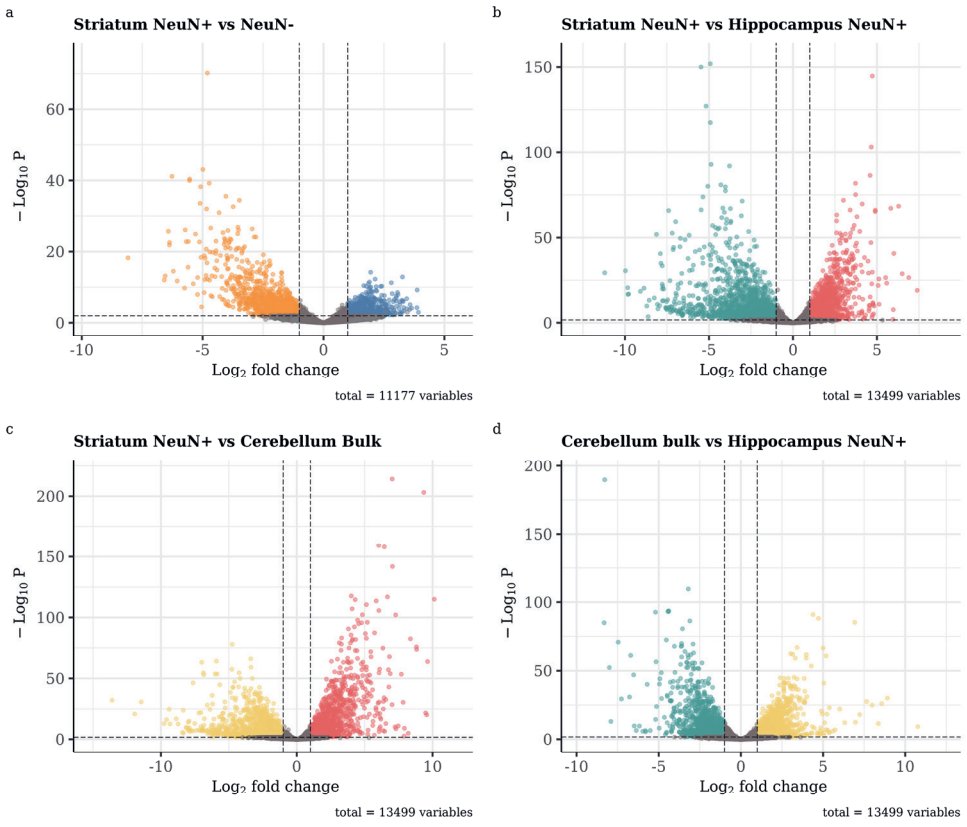

Supplementary Figure 3.4 *Volcano plots highlighting genes that are differentially expressed in the great tit, where the cut-off for significance (coloured dots beyond the dashed lines) is $p < 0.05$ with false-discovery rate correction and a log-fold change of one or greater. a) neuronal versus non-neuronal nuclei from the striatum b) striatal neuronal versus hippocampal neuronal nuclei c) striatal neuronal versus bulk cerebellar nuclei d) bulk cerebellar nuclei versus hippocampal neuronal nuclei. Orange = neuronal (NeuN+), blue = non-neuronal (NeuN-), yellow = cerebellum, turquoise = hippocampus, red = striatum.*

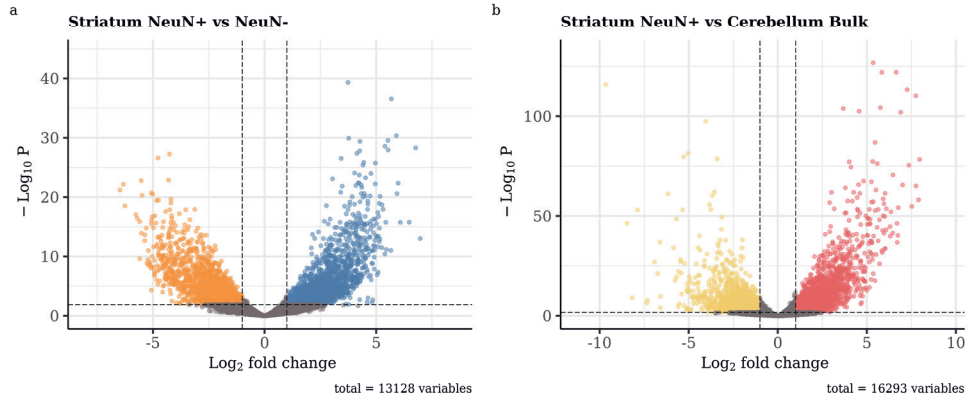

Supplementary Figure 3.5 *Volcano plots highlighting genes that are differentially expressed in the mouse, where the cut-off for significance (coloured dots beyond the dashed lines) is p < 0.05 with false-discovery rate correction and a log-fold change of one or greater. a) neuronal versus non-neuronal nuclei from the striatum b) striatal neuronal versus bulk cerebellar nuclei. Orange = neuronal (NeuN+), blue = non-neuronal (NeuN-), yellow = cerebellum, red = striatum.*

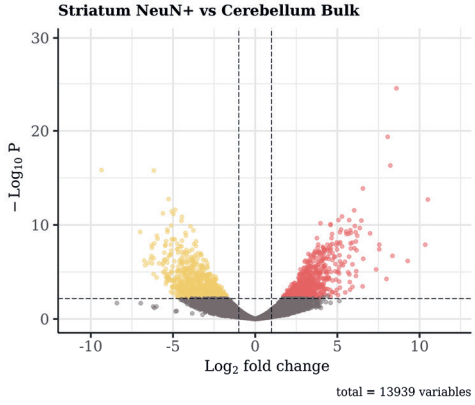

Supplementary Figure 3.6 *Volcano plots highlighting genes that are differentially expressed in the rat striatal neuronal versus bulk cerebellar nuclei, where the cut-off for significance (coloured dots beyond the dashed lines) is p < 0.05 with false-discovery rate correction and a log-fold change of one or greater.*

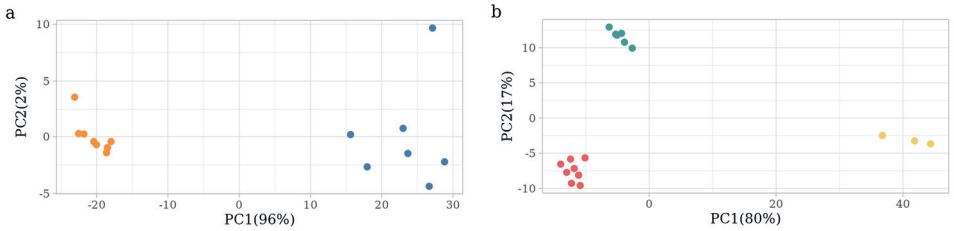

Supplementary Figure 3.7 *PCA plot showing clustering cell types based on chromatin accessibilty a) Clustering of neuronal (NeuN+, orange) and non-neuronal (NeuN-, blue) nuclei from the striatum along PC1. PC1 explained 96% of the variance, PC2 2% and PC3 0.6%. Cell types separate significantly along PC1 (p = 0.001) b) Clustering of striatal neuronal (red), hippocampal neuronal (turquoise) and cerebellar (yellow) bulk nuclei. PC1 explained 80% of the variance, PC2 17% and PC3 0.6%. Cell types separate significantly along PC1 (p = 0.001) and PC2 (p = 0.001).*

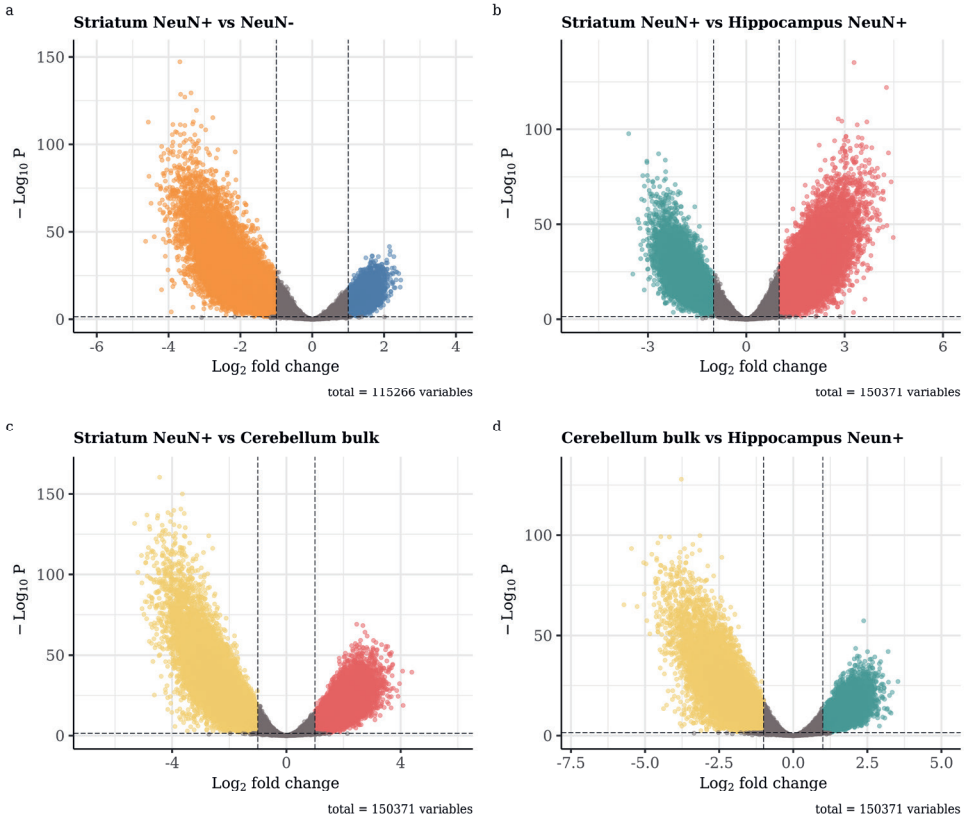

Supplementary Figure 3.8 *Volcano plots highlighting differentially accessible regions in the great tit, where the cut-off for significance (coloured dots beyond the dashed lines) is p < 0.05 with false-discovery rate correction and a log-fold change of one or greater. a) neuronal versus non-neuronal nuclei from the striatum b) striatal neuronal versus hippocampal neuronal nuclei c) striatal neuronal versus bulk cerebellar nuclei d) bulk cerebellar nuclei versus hippocampal neuronal nuclei. Orange = neuronal (NeuN+), blue = non-neuronal (NeuN-), yellow = cerebellum, turquoise = hippocampus, red = striatum.*

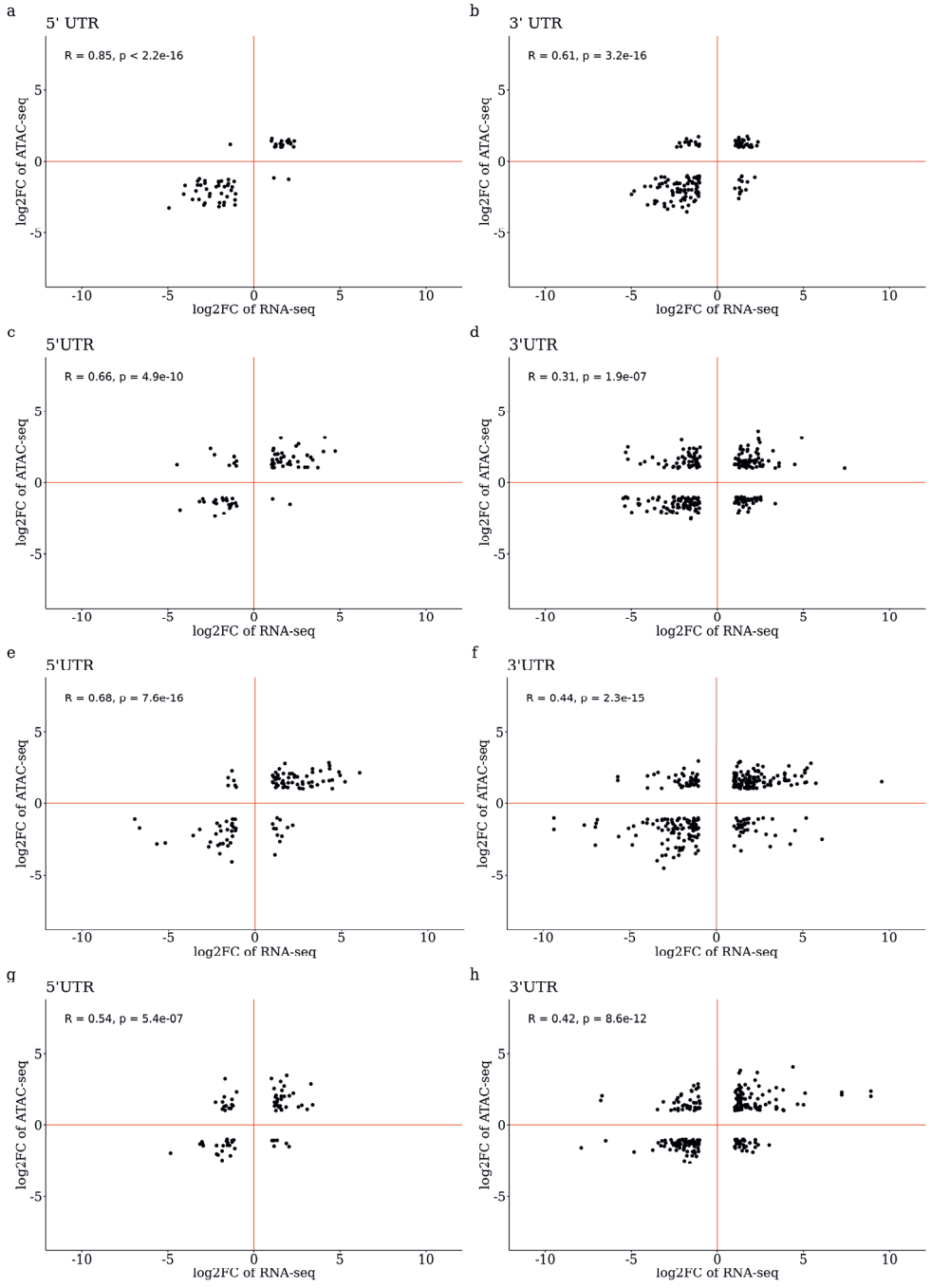

Supplementary Figure 3.9 *Pearson correlations of differentially expressed genes and differentially accessible chromatin regions for 5'UTR and 3'UTR. a,b) Striatal neuronal versus non-neuronal nuclei; c,d) Striatal neuronal+ versus cerebellar bulk nuclei; e,f) Cerebellar bulk versus hippocampal neuronal nuclei; g,h) Striatal neuronal versus hippocampal neuronal nuclei.*

Supplementary Table 3.1 *Summary of sequencing and alignment of included RNA-seq libraries.*

ID	Sex	Brain region	Cell type	#raw reads	%Aligned 1X	#Aligned 1X	#Aligned To Genes
GT021	M	Cerebellum	Bulk	25,722,205	75.64	19,456,678	10,912,056
GT081	M	Cerebellum	Bulk	16,972,169	72.42	12,290,472	7,511,182
GT157	M	Cerebellum	Bulk	21,155,242	75.00	15,865,407	9,386,363
GT216	M	Cerebellum	Bulk	12,261,508	74.08	9,083,617	5,425,060
GT237	M	Cerebellum	Bulk	20,130,748	74.18	14,933,841	8,608,710
GT021	M	Hippocampus	NeuN+	18,759,090	74.90	14,050,942	7,673,207
GT038	M	Hippocampus	NeuN+	19,655,441	71.13	13,980,115	7,855,229
GT081	M	Hippocampus	NeuN+	18,159,772	73.30	13,310,627	7,379,186
GT096	M	Hippocampus	NeuN+	34,247,747	72.87	24,956,962	13,970,889
GT149	M	Hippocampus	NeuN+	34,124,867	74.57	25,448,068	13,663,424
GT157	M	Hippocampus	NeuN+	27,493,335	76.87	21,133,874	11,740,772
GT216	M	Hippocampus	NeuN+	22,240,767	71.76	15,959,308	8,965,101
GT237	M	Hippocampus	NeuN+	29,025,622	73.24	21,258,136	11,888,550
GT662	F	Striatum	NeuN-	14,216,172	75.65	10,754,659	6,869,445
GT738	F	Striatum	NeuN-	13,792,366	71.24	9,825,725	6,047,811
GT216	M	Striatum	NeuN-	12,662,264	66.06	8,538,706	5,317,141
GT237	M	Striatum	NeuN-	26,059,168	68.21	18,291,994	10,603,427
GT662	F	Striatum	NeuN+	22,634,029	74.49	16,860,420	10,763,548
GT676	F	Striatum	NeuN+	12,482,360	74.26	9,269,665	5,643,241
GT711	F	Striatum	NeuN+	26,474,877	76.38	20,221,976	11,241,205
GT738	F	Striatum	NeuN+	17,563,656	73.38	12,887,964	7,847,225
GT592	M	Striatum	NeuN+	16,443,711	75.54	12,422,028	7,554,204
GT038	M	Striatum	NeuN+	27,956,839	78.13	21,841,806	12,470,514
GT096	M	Striatum	NeuN+	60,259,538	80.14	48,294,457	26,958,249
GT149	M	Striatum	NeuN+	56,860,753	77.74	44,201,536	24,504,588
GT237	M	Striatum	NeuN+	27,180,653	69.31	18,836,513	11,471,278
Mouse1	M	Cerebellum	Bulk	8,633,819	73.48	6,344,474	5,250,415
Mouse2	M	Cerebellum	Bulk	28,667,824	73.03	20,937,436	17,166,645
Mouse3	M	Cerebellum	Bulk	16,773,547	74.18	12,443,378	10,192,388
Mouse4	M	Cerebellum	Bulk	36,905,336	73.56	27,148,287	22,471,799
Mouse7	M	Cerebellum	Bulk	20,284,564	73.32	14,872,656	12,197,289
Mouse2	M	Striatum	NeuN-	9,825,991	75.90	7,458,199	6,368,202
Mouse3	M	Striatum	NeuN-	37,104,300	72.68	27,015,030	22,864,991
Mouse4	M	Striatum	NeuN-	18,412,840	54.64	9,999,162	8,463,786
Mouse7	M	Striatum	NeuN-	33,593,668	60.66	20,378,245	6,469,051
Mouse8	M	Striatum	NeuN-	59,409,397	66.25	39,356,084	15,415,578
Mouse2	M	Striatum	NeuN+	33,707,254	77.17	26,011,829	21,844,337
Mouse3	M	Striatum	NeuN+	41,534,881	74.08	30,768,161	25,847,563
Mouse8	M	Striatum	NeuN+	60,633,785	79.63	48,281,831	17,418,156
Mouse9	M	Striatum	NeuN+	17,484,978	68.40	11,960,115	5,864,833
Rat4	M	Cerebellum	Bulk	9,475979	67.34	6,381,130	4,357,285
Rat5	M	Cerebellum	Bulk	25,654213	66.84	17,147,337	11,988,922
Rat7	M	Striatum	NeuN+	30,752119	31.13	9,893,481	6,402,967
Rat14	M	Striatum	NeuN+	26,993065	63.04	17,015,379	5,449,934
Rat16	M	Striatum	NeuN+	37,194246	56.97	21,190,638	12,345,767

Supplementary Table 3.2 *Summary of sequencing and alignment of included ATAC-seq libraries.*

ID	Sex	Brain region	Cell type	#raw reads	%Aligned 1X	#Aligned 1X	#Peaks	FRiP	TSSE
GT038	M	Cerebellum	Bulk	64,732,036	85.04	55,047,165	31,373	0.09	4.69
GT096	M	Cerebellum	Bulk	41,000,053	86.52	35,473,283	28,255	0.11	6.9
GT149	M	Cerebellum	Bulk	47,130,607	85.69	40,383,998	29,927	0.11	6.4
GT021	M	Hippocampus	NeuN+	36,614,777	71.53	26,189,992	99,882	0.19	6.56
GT038	M	Hippocampus	NeuN+	36,845,692	60.24	22,195,509	70,044	0.13	4.88
GT081	M	Hippocampus	NeuN+	58,100,302	90.50	52,578,300	86,225	0.13	3.49
GT096	M	Hippocampus	NeuN+	21,859,014	65.68	14,357,813	54,272	0.12	7.53
GT149	M	Hippocampus	NeuN+	24,057,085	69.56	16,734,233	60,606	0.12	6.34
GT237	M	Hippocampus	NeuN+	40,905,652	90.30	36,936,483	74,505	0.13	4.26
GT157	M	Striatum	NeuN-	51,033,930	68.03	34,718,570	48,816	0.12	7.86
GT216	M	Striatum	NeuN-	55,688,192	61.53	34,262,459	48,290	0.13	8.29
GT612	M	Striatum	NeuN-	30,332,682	82.59	25,051,503	56,539	0.15	9.46
GT237	M	Striatum	NeuN-	49,481,805	52.36	25,909,720	42,325	0.12	8.88
GT662	F	Striatum	NeuN-	31,737,032	85.57	27,156,332	60,653	0.15	8.19
GT711	F	Striatum	NeuN-	24,525,396	81.85	20,074,639	50,186	0.15	11.17
GT738	F	Striatum	NeuN-	24,916,107	85.97	21,421,298	47,799	0.2	8.48
GT612	M	Striatum	NeuN+	31,012,186	88.42	27,420,873	66,464	0.18	7.41
GT662	F	Striatum	NeuN+	32,930,013	90.41	29,770,525	97,262	0.21	6.91
GT711	F	Striatum	NeuN+	31,069,589	88.51	27,500,460	83,377	0.22	10.66
GT738	F	Striatum	NeuN+	37,899,756	89.92	34,080,403	98,832	0.21	6.83
GT081	M	Striatum	NeuN+	78,267,531	69.97	54,764,139	88,842	0.17	3.79
GT157	M	Striatum	NeuN+	64,007,565	86.74	55,519,451	83,210	0.18	4.34
GT216	M	Striatum	NeuN+	65,662,557	86.23	56,623,089	89,701	0.2	4.77
GT237	M	Striatum	NeuN+	56,267,933	82.46	46,396,622	79,522	0.14	3.84

Supplementary Table 3.3 *Top 30 differentially expressed genes with higher expression in neuronal nuclei compared to non-neuronal nuclei in great tit striatum.*

Geneid	Gene symbol	Gene description	log2FC
ENSPMJG00000008365	METRN	meteorin, glial cell differentiation regulator	3.87
ENSPMJG00000002073	NXNL2	nucleoredoxin like 2	3.86
ENSPMJG00000008960	VIP	vasoactive intestinal peptide	3.58
ENSPMJG00000008896	IGF1	insulin like growth factor 1	3.28
ENSPMJG00000010075	TAC1	tachykinin precursor 1	3.26
ENSPMJG00000000787	STARD5	StAR related lipid transfer domain containing 5	3.16
ENSPMJG00000000740	TMC3	transmembrane channel like 3	3.16
ENSPMJG00000016819	ALDH1A2	aldehyde dehydrogenase 1 family member A2	3.08
ENSPMJG00000017611	CYB561	cytochrome b561	3.01
ENSPMJG00000014374	DGKZ	diacylglycerol kinase zeta	3.00
ENSPMJG00000016079	PLK2	polo like kinase 2	2.93
ENSPMJG00000010978	NPY1R	neuropeptide Y receptor Y1	2.91
ENSPMJG00000007716	ADAM19	ADAM metallopeptidase domain 19	2.91
ENSPMJG00000010133	CFTR	CF transmembrane conductance regulator	2.88
ENSPMJG00000008533	MPZL2	myelin protein zero-like protein 2	2.86
ENSPMJG00000016398	OTOP1	otopetrin 1	2.84
ENSPMJG00000012689	NTS	neurotensin	2.81
ENSPMJG00000010854	RXFP1	relaxin family peptide receptor 1	2.75
ENSPMJG00000007895	TAF9	TATA-box binding protein associated factor 9b	2.74
ENSPMJG00000014674	TYMS	thymidylate synthetase	2.68

Supplementary Table 3.3 (continued).

ENSPMJG00000007216	ITGA3	integrin subunit alpha 3	2.64
ENSPMJG00000018485	ONECUT1	one cut homeobox 1	2.64
ENSPMJG00000010142	WNT2	Wnt family member 2	2.63
ENSPMJG00000016147	CRHBP	corticotropin releasing hormone binding protein	2.61
ENSPMJG00000003284	KATNAL2	katanin catalytic subunit A1 like 2	2.60
ENSPMJG00000006342	TMEM50B	transmembrane protein 50B	2.58
ENSPMJG00000011494	VEGFD	vascular endothelial growth factor D	2.57
ENSPMJG00000005685	GRAMD2B	GRAM domain containing 2B	2.56
ENSPMJG00000005544	ARL6IP5	ADP ribosylation factor like GTPase 6 interacting protein 5	2.56

Supplementary Table 3.4 *Top 30 differentially expressed genes with higher expression in non-neuronal compared to neuronal nuclei in great tit striatum.*

Geneid	Gene symbol	Gene description	log2FC
ENSPMJG00000017680	SLC4A1	solute carrier family 4 member 1 (Diego blood group)	-8.09
ENSPMJG00000007903	H1-0	histone H5	-6.42
ENSPMJG00000017149	APOH	apolipoprotein H	-6.27
ENSPMJG00000003988	SPTB	spectrin beta, erythrocytic	-6.21
ENSPMJG00000006128	NKX6-2	NK6 homeobox 2	-5.72
ENSPMJG00000010520	PRAG1	PEAK1 related, kinase-activating pseudokinase 1	-5.68
ENSPMJG00000011873	NID2	nidogen 2	-5.60
ENSPMJG00000014118	PLLP	plasmolipin	-5.59
ENSPMJG00000005686	FGFR2	fibroblast growth factor receptor 2	-5.54
ENSPMJG00000019877	SLC15A2	solute carrier family 15 member 2	-5.54
ENSPMJG00000001716	FETUB	fetuin B	-5.39
ENSPMJG00000015591	VAMP8	vesicle associated membrane protein 8	-5.21
ENSPMJG00000014813	GPR157	G protein-coupled receptor 157	-5.21
ENSPMJG00000013325	PRDM16	PR/SET domain 16	-5.13
ENSPMJG00000005922	C10orf90	chromosome 6 C10orf90 homolog	-5.10
ENSPMJG00000015806	SLC1A3	solute carrier family 1 member 3	-5.08
ENSPMJG00000004298	SLC13A3	solute carrier family 13 member 3	-5.06
ENSPMJG00000010131	FMO5	dimethylaniline monooxygenase N-oxide-forming] 5-like	-5.04
ENSPMJG00000018157	SALL3	spalt like transcription factor 3	-4.99
ENSPMJG00000012544	SLC38A3	solute carrier family 38 member 3	-4.94
ENSPMJG00000013845	MERTK	MER proto-oncogene, tyrosine kinase	-4.93
ENSPMJG00000014349	CDH19	cadherin 19	-4.89
ENSPMJG00000015611	RASGRP3	RAS guanyl releasing protein 3	-4.86
ENSPMJG00000002204	SALL1	spalt like transcription factor 1	-4.85
ENSPMJG00000005820	UGT8	UDP glycosyltransferase 8	-4.84
ENSPMJG00000014137	NRN1L	neuritin 1 like	-4.82
ENSPMJG00000003779	ZCCHC24	zinc finger CCHC-type containing 24	-4.80
ENSPMJG00000009957	SLC1A2	solute carrier family 1 member 2	-4.73
ENSPMJG00000014056	ADGRG1	adhesion G protein-coupled receptor G1	-4.71
ENSPMJG00000007492	ABTB2	ankyrin repeat and BTB domain containing 2	-4.66

Supplementary Table 3.4 *Top 30 genes uniquely expressed in striatum neuronal nuclei compared to hippocampal neuronal nuclei and cerebellar bulk nuclei.*

Geneid	Gene symbol	Gene description	Sum log2FC
ENSPMJG00000001995	TMEM61	transmembrane protein 61	15.11
ENSPMJG00000008548	DRD2	dopamine receptor D2	13.52
ENSPMJG00000004576	MATK	megakaryocyte-associated tyrosine kinase	12.8
ENSPMJG00000010682	TMEM158	transmembrane protein 158 (gene/pseudogene)	12.63
ENSPMJG00000017909	PPP1R1B	protein phosphatase 1 regulatory inhibitor subunit 1B	12.37
ENSPMJG00000017012	DLK1	delta like non-canonical Notch ligand 1	12.17
ENSPMJG00000015877	ISL1	ISL LIM homeobox 1	11.95
ENSPMJG00000005180	CAMKV	CaM kinase like vesicle associated	11.92
ENSPMJG00000010075	TAC1	tachykinin precursor 1	11.67
ENSPMJG00000007047	PDYN	prodynorphin	11.28
ENSPMJG00000015717	PENK	proenkephalin	11.25
ENSPMJG00000007811	PDE7B	phosphodiesterase 7B	11.11
ENSPMJG00000002600	KCNA4	potassium voltage-gated channel subfamily A member 4	11.09
ENSPMJG00000011014	SOSTDC1	sclerostin domain containing 1	10.9
ENSPMJG00000012178	GABRA3	gamma-aminobutyric acid type A receptor alpha3 subunit	10.75
ENSPMJG00000015254	GABRA5	gamma-aminobutyric acid type A receptor alpha5 subunit	10.74
ENSPMJG00000010051	DLX6	distal-less homeobox 6	10.47
ENSPMJG00000018260	PHACTR1	phosphatase and actin regulator 1	10.44
ENSPMJG00000016397	DRD5	dopamine receptor D5	10.42
ENSPMJG00000006121	ADGRB2	adhesion G protein-coupled receptor B2	10.4
ENSPMJG00000010310	PCP4	Purkinje cell protein 4	10.37
ENSPMJG00000006340	HTR4	5-hydroxytryptamine receptor 4	10.1
ENSPMJG00000010496	IAPP	islet amyloid polypeptide	9.98
ENSPMJG00000006225	SH3RF2	SH3 domain containing ring finger 2	9.94
ENSPMJG00000016993	BCL11B	BAF chromatin remodeling complex subunit BCL11B	9.92
ENSPMJG00000001519	EVX1	even-skipped homeobox 1	9.88
ENSPMJG00000006555	DRD1	dopamine receptor D1	9.78
ENSPMJG00000001137	KCNH4	potassium voltage-gated channel subfamily H member 4	9.77
ENSPMJG00000008150	RASD2	RASD family member 2	9.77
ENSPMJG00000016588	RASGRP1	RAS guanyl releasing protein 1	9.7

Supplementary Table 3.5 *Top 30 genes uniquely expressed in cerebellar bulk nuclei compared to striatal neuronal nuclei and hippocampal neuronal nuclei.*

Geneid	Gene symbol	Gene description	Sum log2FC
ENSPMJG00000005161	EN2	engrailed homeobox 2	22.16
ENSPMJG00000007883	BAIAP2L2	BAR/IMD domain containing adaptor protein 2 like 2	19.44
ENSPMJG00000019848	LHX1	LIM homeobox 1	19.17
ENSPMJG00000005131	INKA1	inka box actin regulator 1	18.25
ENSPMJG00000002660	CBLN1	cerebellin 1 precursor	18.12
ENSPMJG00000006706	BARHL1	BarH like homeobox 1	16.62
ENSPMJG00000017592	GNG13	G protein subunit gamma 13	16.56
ENSPMJG00000000130	GRIN2C	glutamate ionotropic receptor NMDA type subunit 2C	15.92
ENSPMJG00000018977	HSPB1	heat shock protein family B (small) member 1	13.41
ENSPMJG00000011955	KCNA10	potassium voltage-gated channel subfamily A member 10	13.38
ENSPMJG00000018609	ZIC1	zinc finger protein ZIC 1	12.93
ENSPMJG00000019403	BARHL2	BarH like homeobox 2	12.33
ENSPMJG00000004661	LBX1	ladybird homeobox 1	11.18
ENSPMJG00000009299	KCNJ5	potassium inwardly rectifying channel subfamily J member 5	10.95
ENSPMJG00000017767	BMP1	bone morphogenetic protein 1	10.68
ENSPMJG00000004274	R3HDML	R3H domain containing like	10.62
ENSPMJG00000016606	GJD2	gap junction protein delta 2	10.42
ENSPMJG00000016712	NPTX1	neuronal pentraxin 1	10.31
ENSPMJG00000013751	CD93	CD93 molecule	10.02
ENSPMJG00000019064	RSKR	ribosomal protein S6 kinase related	9.96
ENSPMJG00000006032	RNF19B	ring finger protein 19B	9.91
ENSPMJG00000008011	PVALB	parvalbumin	9.89
ENSPMJG00000006043	HPCA	hippocalcin	9.61
ENSPMJG00000009325	TH	tyrosine hydroxylase	9.6
ENSPMJG00000018608	ZIC4	Zic family member 4	9.53
ENSPMJG00000013956	WFDC1	WAP four-disulfide core domain 1	9.42
ENSPMJG00000007123	EOMES	eomesodermin	9.38
ENSPMJG00000016405	MSX1	msh homeobox 1	9.27
ENSPMJG00000006576	RGS5	regulator of G protein signaling 5	9.02
ENSPMJG00000010453	PLEKHG5	pleckstrin homology and RhoGEF domain containing G5	8.76

Supplementary Table 3.6 *Top 30 genes uniquely expressed in cerebellar bulk nuclei compared to striatal neuronal nuclei and hippocampal neuronal nuclei.*

Geneid	Gene symbol	Gene description	Sum log2FC
ENSPMJG00000017680	SLC4A1	solute carrier family 4 member 1 (Diego blood group)	12.34
ENSPMJG00000010828	IFI30	IFI30 lysosomal thiol reductase	12.2
ENSPMJG00000002789	C1QC	complement C1q subcomponent subunit C-like	11.51
ENSPMJG00000007903	H1-0	histone H5	11.33
ENSPMJG00000001168	OSGIN1	oxidative stress induced growth inhibitor 1	11.24
ENSPMJG00000007556	CDHR2	cadherin related family member 2	11.23
ENSPMJG00000005019	FEZF2	FEZ family zinc finger 2	11.17
ENSPMJG00000002787	C1QB	complement C1q B chain	11.14
ENSPMJG00000016531	NEU4	neuraminidase 4	10.84
ENSPMJG00000006408	LPXN	leupaxin	10.81
ENSPMJG00000003005	CSPG5	chondroitin sulfate proteoglycan 5	10.77
ENSPMJG00000005539	EMX2	empty spiracles homeobox 2	10.59
ENSPMJG00000007055	P2RY12	P2Y purinoceptor 12-like	10.56
ENSPMJG00000003988	SPTB	spectrin beta, erythrocytic	10.5
ENSPMJG00000007978	RAC2	Rac family small GTPase 2	10.41
ENSPMJG00000005422	RFESD	Rieske Fe-S domain containing	10.31
ENSPMJG00000000238	TAL1	TAL bHLH transcription factor 1, erythroid differentiation factor	10.15
ENSPMJG00000014812	SLC2A5	solute carrier family 2, facilitated glucose transporter member 5	10
ENSPMJG00000016251	TREM2	triggering receptor expressed on myeloid cells 2	9.98
ENSPMJG00000014054	ADGRG3	adhesion G protein-coupled receptor G3	9.85
ENSPMJG00000016248	APOBEC2	apolipoprotein B mRNA editing enzyme catalytic subunit 2	9.72
ENSPMJG00000013281	PPP1R9B	protein phosphatase 1 regulatory subunit 9B	9.69
ENSPMJG00000001311	P2RY6	pyrimidinergic receptor P2Y6	9.67
ENSPMJG00000018157	SALL3	spalt like transcription factor 3	9.62
ENSPMJG00000000087	HBEGF	heparin binding EGF like growth factor	9.54
ENSPMJG00000017574	ADORA3	adenosine A3 receptor	9.34
ENSPMJG00000009957	SLC1A2	solute carrier family 1 member 2	9.31
ENSPMJG00000016474	KLHL6	kelch like family member 6	9.3
ENSPMJG00000014702	METTL7A	methyltransferase like 7A	9.14
ENSPMJG00000012545	SEMA3B	semaphorin 3B	9.13

Supplementary Table 3.7 *List of significantly enriched (adjusted p values) GO terms (Biological Processes, Molecular Function, Cellular Components) from GSEA on gene expression differences between neuronal and non-neuronal nuclei in the great tit. Shown are top 15 terms per cell type. ES: enrichment score. NES: normalized enrichment score.*

Cell_Type	Ontology	ID	Description	setSize	ES	NES	p.adjust	rank
Neuronal	BP	GO:0007268	chemical synaptic transmission	409	0.44	2.4	1.44E-19	1438
Neuronal	BP	GO:0098916	anterograde trans-synaptic signaling	409	0.44	2.4	1.44E-19	1438
Neuronal	BP	GO:0099537	trans-synaptic signaling	416	0.44	2.37	5.02E-19	1438
Neuronal	BP	GO:0099536	synaptic signaling	429	0.43	2.34	8.98E-19	1438
Neuronal	CC	GO:1902495	transmembrane transporter complex	196	0.53	2.66	2.79E-16	1720
Neuronal	CC	GO:1990351	transporter complex	212	0.51	2.6	3.72E-16	1720
Neuronal	CC	GO:0097060	synaptic membrane	248	0.47	2.46	8.24E-15	1447
Neuronal	CC	GO:0098794	postsynapse	413	0.39	2.14	1.91E-14	1630
Neuronal	CC	GO:0034702	ion channel complex	158	0.55	2.67	2.16E-14	1720
Neuronal	CC	GO:0034703	cation channel complex	114	0.6	2.78	7.96E-14	1570
Neuronal	CC	GO:0097447	dendritic tree	393	0.39	2.1	1.1E-12	1461
Neuronal	CC	GO:0098793	presynapse	321	0.42	2.23	1.1E-12	1336
Neuronal	MF	GO:0005216	ion channel activity	230	0.46	2.33	1.79E-12	1766
Neuronal	CC	GO:0030425	dendrite	392	0.39	2.1	3.11E-12	1461
Neuronal	BP	GO:0034765	regulation of ion transmembrane transport	247	0.44	2.27	7.15E-12	1569
Non-neuronal	BP	GO:0001568	blood vessel development	364	-0.5	-2.2	7.66E-15	1095
Non-neuronal	BP	GO:0048514	blood vessel morphogenesis	315	-0.52	-2.27	7.75E-15	1095
Non-neuronal	BP	GO:0001944	vasculature development	382	-0.5	-2.17	9.97E-15	1095
Non-neuronal	BP	GO:0035239	tube morphogenesis	456	-0.47	-2.08	5.88E-14	1095
Non-neuronal	BP	GO:0030334	regulation of cell migration	471	-0.46	-2.06	1.01E-13	1263
Non-neuronal	BP	GO:2000145	regulation of cell motility	494	-0.45	-2.02	2.91E-13	1263
Non-neuronal	BP	GO:0001525	angiogenesis	263	-0.52	-2.22	1.19E-12	1069
Non-neuronal	BP	GO:0030155	regulation of cell adhesion	356	-0.48	-2.09	3.35E-12	1278
Non-neuronal	BP	GO:0001667	ameboidal-type cell migration	253	-0.52	-2.2	8.71E-12	1290
Non-neuronal	BP	GO:0090132	epithelium migration	180	-0.53	-2.19	3.54E-09	1116
Non-neuronal	BP	GO:0090130	tissue migration	181	-0.53	-2.19	3.75E-09	1116
Non-neuronal	BP	GO:0010631	epithelial cell migration	179	-0.53	-2.19	6.67E-09	1116
Non-neuronal	BP	GO:0022604	regulation of cell morphogenesis	193	-0.5	-2.09	2.13E-08	1117
Non-neuronal	BP	GO:0030335	positive regulation of cell migration	265	-0.47	-1.99	2.69E-08	1038
Non-neuronal	BP	GO:1901342	regulation of vasculature development	132	-0.56	-2.22	4.39E-08	1474

Supplementary Table 3.8 *List of significantly enriched (adjusted p values) GO terms (Biological Processes, Molecular Function, Cellular Components) from GSEA on gene expression differences between striatum, hippocampus and cerebellum in the great tit. Shown are top 10 terms per brain region. ES: enrichment score. NES: normalized enrichment score.*

Brain_Region	Ontology	ID	Description	setSize	ES	NES	p.adjust	rank
Striatum	CC	GO:0098794	postsynapse	435	0.54	2.55	3.96E-27	1172
Striatum	BP	GO:0099536	synaptic signaling	456	0.53	2.52	1.13E-26	1553
Striatum	CC	GO:0097447	dendritic tree	417	0.54	2.54	2.68E-26	1172
Striatum	BP	GO:0007268	chemical synaptic transmission	437	0.53	2.52	2.68E-26	1398
Striatum	BP	GO:0098916	anterograde trans-synaptic signaling	437	0.53	2.52	2.68E-26	1398
Striatum	CC	GO:0030425	dendrite	416	0.54	2.54	3.02E-26	1172
Striatum	BP	GO:0099537	trans-synaptic signaling	444	0.53	2.51	3.94E-26	1398
Striatum	CC	GO:0097060	synaptic membrane	267	0.59	2.68	1.08E-23	1165
Striatum	CC	GO:0045211	postsynaptic membrane	191	0.63	2.71	1.28E-20	1108
Striatum	CC	GO:0098793	presynapse	341	0.53	2.44	4.99E-20	1362
Hippocampus	BP	GO:0048514	blood vessel morphogenesis	368	-0.49	-2.31	3.33E-16	1736
Hippocampus	BP	GO:0001944	vasculature development	440	-0.46	-2.2	5.1E-16	1719
Hippocampus	BP	GO:0001568	blood vessel development	421	-0.46	-2.2	1.51E-15	1719
Hippocampus	MF	GO:0038023	signaling receptor activity	464	-0.46	-2.15	7.06E-15	1538
Hippocampus	MF	GO:0060089	molecular transducer activity	464	-0.46	-2.15	7.06E-15	1538
Hippocampus	MF	GO:0004888	transmembrane signaling receptor activity	359	-0.48	-2.18	4.36E-13	1615
Hippocampus	CC	GO:0030312	external encapsulating structure	300	-0.48	-2.22	1.77E-12	1642
Hippocampus	CC	GO:0031012	extracellular matrix	300	-0.48	-2.22	1.77E-12	1642
Hippocampus	BP	GO:0030155	regulation of cell adhesion	404	-0.43	-2.07	5.56E-12	1648
Hippocampus	BP	GO:0001525	angiogenesis	310	-0.47	-2.17	6.65E-12	1736
Cerebellum	CC	GO:0044391	ribosomal subunit	115	0.74	2.99	2E-24	2079
Cerebellum	CC	GO:0005840	ribosome	136	0.71	2.97	2E-24	2079
Cerebellum	CC	GO:1990904	ribonucleoprotein complex	446	0.52	2.47	2E-24	2662
Cerebellum	MF	GO:0003735	structural constituent of ribosome	99	0.75	2.98	1.53E-21	2007
Cerebellum	CC	GO:0022626	cytosolic ribosome	60	-0.85	-3.11	2.37E-21	1188
Cerebellum	CC	GO:0098798	mitochondrial protein-containing complex	171	0.64	2.76	4.61E-20	2449
Cerebellum	CC	GO:0044391	ribosomal subunit	115	-0.69	-2.85	1.51E-17	2025
Cerebellum	CC	GO:0005743	mitochondrial inner membrane	281	0.53	2.42	8.4E-17	2030
Cerebellum	CC	GO:0015934	large ribosomal subunit	75	0.75	2.83	3.84E-16	2007
Cerebellum	CC	GO:0019866	organelle inner membrane	312	0.51	2.33	5E-16	2030

Chapter 4.

Transcriptomic correlates of cognitive flexibility in two homologue brain regions of songbirds and rodents

Krista van den Heuvel, Beril Yildiz, Ilia Timpanaro, Bastijn J.G. van den Boom, Aleksandra Badura, Chris I. De Zeeuw, Ingo Willuhn, Alexander Kotrschal, Menno Creyghton, Kees van Oers

Abstract

Cognitive flexibility allows animals to adapt to environmental challenges, and this ability varies considerably within species. Understanding the causal mechanisms that underlie such individual variation is key for understanding the evolution of cognitive traits. However, both the genetic underpinnings of variation in cognitive flexibility and whether between-individual differences have the same origin across species, have not been established. Cognitive flexibility is enabled by neuronal functions mediated by gene expression. Therefore, we assessed baseline gene expression profiles in the brains of individuals differing in reversal learning performance. With this we aimed to test for conserved patterns of differential gene expression between extreme fast and slow reversing individuals in birds (great tit, *Parus major*) and mammals (mouse, *Mus musculus*). While we did find subtle transcriptomic differences between fast and slow reversing individuals, these differences were largely dissimilar between species at the gene level, suggesting different origins of individual differences in cognitive flexibility. Nonetheless, reversal learning-associated transcriptional changes, albeit different at the level of genes, converge on biological processes in functional analyses, indicating that some core functions may be consistently altered between brains of individuals in birds and mammals, underlying their differing reversal learning performance.

To be submitted to Behavioural Brain Research

Introduction

Understanding how individual differences in behaviour are regulated is crucial for understanding how they are maintained in populations and to predict when certain behaviours are adaptive (Fawcett et al., 2012). Across species, between-individual differences in behavioural phenotypes may either have evolved from convergent genetic and developmental mechanisms, or from divergent (sets of) genes (Arendt and Reznick, 2008; Rittschof and Robinson, 2014). Between-individual behavioural differences have been linked to polymorphisms of the same gene across species (Laine and van Oers, 2017), but only few overlapping genes might be differentially expressed in relation to a certain behavioural phenotype, even though many of their functional pathways are likely to be shared between species (Rey et al., 2021; Demin et al., 2022). The same is likely true for cognitive traits, the mechanisms by which animals acquire, process, store and act on information from the environment (Shettleworth, 2010). However, currently it is unclear to what extent the molecular causes of individual cognitive variation are universal across species or even taxonomic classes. Individual differences in cognition might originate from convergent molecular mechanisms or from convergent neurobiological pathways, emerging from different genes. In other words, there might be variation across species in the genes that drive a correlation between a biological process and task performance, while the functionality in the biological processes that underlie the individual differences is conserved.

Complex behavioural traits are generally influenced by many genes; yet, they are not only regulated by heritable differences at the DNA sequence level, but also by environmental and epigenetic changes (Rittschof and Robinson, 2014). The latter is crucial, because repeatability and heritability estimates of cognitive abilities are relatively low, probably because the contribution of heritable genetic components is masked by influence from the environment and the individual's previous experiences, as described in Chapter 2 (Laughlin et al., 2011; Croston et al., 2015a; Bailey et al., 2021; Lambert and Guillette, 2021; Bagley et al., 2022; De Meester et al., 2022b). To better understand the molecular mechanisms that contribute to individual variation in cognition, we can study the dynamic genome by using transcriptomic analysis to assess whether and how individual variation in performance correlates with differences in genome-wide gene-expression (Bell and Robinson, 2011; Rittschof and Robinson, 2014; Bengston et al., 2018). For instance, black-capped chickadees (*Poecile atricapillus*) that exhibit population differences in spatial memory performance and hippocampal neurogenesis also exhibit differential hippocampal gene expression (Pravosudov et al., 2013). More than half of those differentially expressed genes are known to be involved in regulation of hippocampal processes in mammals, potentially pointing towards similar functions of these genes between birds and mammals (Pravosudov et al., 2013). However, whether between-individual differences in cognition rely on the same cognitive architecture across animal classes remains enigmatic. To our knowledge, such a direct comparison between birds and mammals has not yet been conducted in this context.

Animals not only need to be able to discriminate among stimuli, they also constantly need to learn new discriminations (Shettleworth, 2010). Cognitive flexibility describes this ability of an organism to flexibly update learned predictions about cue-reward contingencies when those are altered (Izquierdo et al., 2017). Whereas differential cognitive flexibility is commonly studied in the context of altered cognitive functioning in neuropsychiatric disorders (Uddin, 2021), proximate variables that determine natural individual variation in cognition remain unexplored (Matzel and Sauce, 2017). We know that the ability to show flexibility in learned responses is determined by brain regions involved in reward processing and decision making, and on neurotransmitter functioning and synaptic plasticity in these circuits (Izquierdo et al., 2017; Gao et al., 2018). However, in order to understand how natural selection acts on any behavioural trait, we must study its genetic relationship (Rittschof and Robinson, 2014).

Individual differences in brain functioning and cognitive performance are known to be regulated by transcriptomic differences in the brain (Ji et al., 2014; Konopka, 2017). However, it is less clear which genes or molecular pathways are specifically crucial for cognitive flexibility. Cognitive flexibility is classically measured using discrimination and reversal learning tasks, where a firstly rewarded option becomes non-rewarding and vice versa, and the ability of animals to correctly respond to this change is measured (Izquierdo et al., 2017). Using this paradigm, several genes have been uncovered that might play a role in cognitive flexibility. In rhesus macaques, structural variants of the serotonin transporter gene affect expression levels the transporter in the brain and associate with reversal learning performance (Izquierdo et al., 2007; Vallender et al., 2009). Using recombinant inbred mouse strains, genome-wide QTLs have been mapped that were associated with reversal learning performance leading to the identification of *Syn3* and *Wdr73* as candidate genes, associated with striatal dopamine receptor expression (Laughlin et al., 2011; Bagley et al., 2022). Dopamine D2 receptor expression in the midbrain negatively correlated with reversal learning in mice (Laughlin et al., 2011). These findings highlight an important role for genes involved in neurotransmitters trafficking.

Any distinct patterns of gene expression that relate to differences in behavioural phenotypes are likely brain region- or species-specific (Izquierdo et al., 2017). In red junglefowl (*Gallus gallus*) chicks, expression levels of the serotonin receptor genes 5HT2A and 5HT2b in the caudal telencephalon were associated with reversal learning performance, but the dopamine D1 and D2 receptors were not, despite their implicated role in mammals (Boddington et al., 2020). The caudal telencephalon contains the nidopallium caudolaterale (NCL), which has similar functions as the mammalian prefrontal cortex. These higher order brain regions have been implicated in reversal learning performance (Rudebeck and Izquierdo, 2022) but they are not homologous between the mammalian and avian brain (Güntürkün et al., 2021) and have a different genetic profile (Puelles et al., 2000). These structural differences could explain why different genes correlate with reversal learning in different species.

Two potential brain region candidates involved in regulating reversal learning performance in both birds and mammals are the striatum and the cerebellum. The mammalian striatum plays a prominent role in reward-based (reinforcement) learning (Day et al., 2007; Stuber et al., 2008). The avian striatum is considered homologous to the mammalian striatum based on developmental and anatomical data (Kuenzel et al., 2011), and is similarly involved in reward processing (Rose et al., 2013a; Seki et al., 2014) and complex behaviour (Rook et al., 2020). There is a crucial role for striatal dopamine and glutamate signalling in the ability of mammals to alter their response following a change in stimulus-reward contingencies (Groman et al., 2014, 2016; Linden et al., 2018; Liu et al., 2020; Sala-Bayo et al., 2020), and individual variation in reversal learning performance is linked to the extent of cue-induced dopamine release in the striatum of rats (*Rattus norvegicus*) (Klanker et al., 2015). In homing pigeons (*Columba livia*), administration of dopaminergic D2 and glutamatergic NMDA receptor antagonists impair reversal learning performance (Herold, 2010). Another region of interest is the cerebellum. Although it has received comparatively little attention in the field of (comparative) cognition, there is evidence in mammals that the cerebellum is involved in reversal learning (Badura et al., 2018; Peterburs et al., 2018; Shipman and Green, 2020; Pierce and Péron, 2022). Loss of Purkinje cells leads to impairment of reversal learning performance in mice (Dickson et al., 2017), and granule cells respond to reward delivery and anticipation as well as to reward omission (Wagner et al., 2017). The avian and mammalian cerebellum are homologous (Yopak et al., 2017). Similar to mammals (Caligiore et al., 2017; Pierce and Péron, 2020), neural pathways through the thalamus connect the cerebellum with the basal ganglia and cortical regions in the zebra finch (*Taeniopygia castanotis*) (Pidoux et al., 2018). Thus, although there is no direct evidence for contribution of the avian cerebellum to reversal learning, its homology and connectivity suggests a similar involvement as the mammalian cerebellum.

Here, we performed a cross-species/cross-taxon analysis of brain transcriptomic data in great tits and mice, in order to identify both shared and unique molecular targets for individual variation in reversal learning performance. We assessed baseline gene expression in two homologous brain regions in an ecological model species, the great tit (*Parus major*), and in the mouse (*Mus musculus C57BL/6J*), a well-studied model organism in respect to genetic and environmental sources of variation in reversal learning performance. We tested the hypothesis that genes that are differentially expressed in these brain regions between fast and slow reversal learners would not necessarily include conserved genes, but rather conserved functionality in the biological processes such as neurotransmitter trafficking, synaptic plasticity and neurogenesis across the two species.

Materials and Methods

Sample origins – Great tit

Study subjects

In May and June of 2018, 322 10-day old great tit nestlings were captured in a consort from in total 42 broods and transported to the aviary facilities at the NIOO-KNAW. They originated from the nest box population Boslust (Groot Warnsborn) near Arnhem, Netherlands (5°850 E, 52°010 N), a 70 ha field site, consisting of mixed pine-deciduous forest. We hand-reared the nestlings until independence according to established methods (Drent et al., 2003). Briefly, we transferred nestlings in sibling groups of three to four birds to a compartment within a wooden box, each box containing three compartments and each compartment containing a natural parasite-free nest. Upon fledging, around 17-20 days after hatching, birds were transferred to small wire-mesh cages in groups of three. Around day 35 after hatching, they were completely independent and we transferred them to standard individual cages of 0.9 m × 0.4 m × 0.5 m with solid bottom, top, side, and rear walls, a wire-mesh front and three perches. Birds were kept under natural light conditions with acoustic and visual contact to each other.

In July, we took a blood sample for sex determination. In September, after their first moult, we transferred individuals to single-sex groups in semi-open outdoor aviaries (2 m x 4 m x 2.5 m). Food consisted of a homemade mixture of ground beef heart, egg, calcium and a multivitamin solution, supplemented with mealworms, apple, and sunflower seeds and fat balls in winter, and was available ad libitum. Birds were kept under natural light conditions, with vocal and visual contact to other birds. In October, when birds were full-grown, we measured their tarsus.

Reversal learning assessment

From October 2018-February 2019, birds were tested for associative and reversal learning performance to assess their cognitive flexibility. As part of a larger study (Chapter 2), all individuals were subjected to two additional rounds of testing, in February 2020 and September 2020. We used automated feeders to assess learning performance, using a three-choice spatial learning procedure as described in Chapter 2. Briefly, eight days prior to testing, individuals were habituated to use the feeders under standard housing conditions in semi-open outdoor aviaries. After habituation, we caught individuals from the group, weighed them, and released them individually in a testing aviary. In the testing aviary, water was available ad libitum while no food was available during the test, in order to maintain motivation to take part in the learning test.

During the experiment, one feeder at a time provided a reward (freeze-dried mealworm) in a triangular array with two other unrewarding feeders, requiring individuals to learn the location of the rewarded feeder. Individuals were first trained to go to an assigned feeder, which was reinforced until individuals reached a criterion level of six correct trials out of seven. This success rate is significantly different from the expectation if birds selected feeders at random (binomial test, p

< 0.01). A trial was defined as a landing on the perch with the RFID antenna. After completing the associative learning phase, the reversal learning task began as the reward contingencies were reversed to one of the other two feeders. Again, birds had to reach the learning criterion of six correct visits across seven trials to the new feeder. Individuals had from 09:00 until 15:00 to complete both phases of the test. For further details of the test setup, see Chapter 2.

Reversal learning performance was scored as the total number of trials required to reach the learning criterion (six correct visits out of seven subsequent trials). Selected slow individuals needed more trials to finish the reversal learning task compared to fast individuals ($p = 0.007$, Supplementary Figure 4.1)**.** After the last reversal learning test, the birds were housed under standard group housing conditions without handling.

Tissue collection
Based on their mean performance across the three reversal learning tests, four unrelated fast and slow performing males were selected for comparative gene expression analysis. Four weeks after the last reversal learning task, individuals were caught from the aviaries and deeply anaesthetized with isoflurane (IsoFlo, Zoetis, Kalamazoo, MI, USA). After decapitation, the brain was dissected out and placed in ice cold PBS for further micro dissection of the cerebellum, and bilateral dissection of striatum (including area X) and hippocampus (the latter for future use). Brain regions were located by the use of the online zebra finch brain atlas (Karten et al., 2013) ZEBrA (Oregon Health & Science University, Portland, OR, USA; http://www.zebrafinchatlas.org). Isolated tissue was flash-frozen in liquid nitrogen in 1.5 ml RNA-free tubes and stored at −80°C until RNA isolation.

Sample origins – Mouse
Study subjects
Wild-type C57BL6/6JRj male[1] offspring from two nests (nest 1 born on 28-10-2019, nest 2 born on 05-11-2019) were socially housed with food and water ad libitum and kept on a 12-h light and dark cycle. On 24-01-2020, the light-dark cycle was reversed and individuals were food restricted to 85% of their free-feeding body weight. All behavioural procedures were performed during the dark phase. Behavioural testing took place from 12-02-2020 until 12-03-2020.

Reversal learning assessment
Behavioural training and testing were conducted in operant-conditioning chambers (Med-Associates, ENV-307, 21.6 × 17.8 × 12.7 cm) equipped with two nose-poke holes flanking a food magazine and a house light (3 W, 24 V). Cue lights were positioned inside the nose-poke holes. The food magazine was connected to a pellet dispenser delivering one food pellet per trial (Bio-Serv dustless precision sucrose pellet; 20 mg). The nose-poke holes and food magazine could be illuminated internally. Food magazine and nose-poke holes contained infra-red beams for the detection of the animals' responses. Animal behaviour was

videotaped. All task programming and data acquisition was performed with Med-PC-IV software (Med-Associates).
Mice were habituated to reward delivery in the magazine (two sessions, 20 rewards delivered with 60 s intervals), followed by nose-poke training. After habituation, mice were trained to nose poke for a food reward during shaping sessions. Mice received six shaping sessions (session 1-6), one session per day. Mice were randomly presented with the right or left nose-poke cue light and responding in either of the two illuminated nose pokes resulted in the delivery of one sucrose pellet in the food dispenser. Shaping sessions consisted of trials with a 10 or 20 s interval and continued until mice had received 30 (first 4 sessions) or 40 rewards (last 2 sessions), or when the session lasted 60 min, whichever came first.

After six shaping sessions, mice progressed to spatial discrimination learning (60 trials per session, variable inter-trial intervals (15/25/35/45 s), or 70 min, whichever came first). On every trial both cue lights were illuminated, thus, cue lights did not signal which side was rewarded, but indicated that reward was available - provided the correct choice was made. A nose poke on one side was rewarded, while the other side was never rewarded. The rewarded side was counterbalanced between mice. If mice did not make a nose-poke response within 10 s, the trial was scored as omission. Mice received one session per day, with in total eight spatial discrimination sessions (session 7-14). In session eight, all mice had reached an 85% response criterion (excluding omissions), measured across the entire session.

The reversal session (session 15) consisted of 100 trials, with variable inter-trial intervals (15/25/35/45 s). The reversal was presented at the 16th trial in the session, so that a response to the previously non-rewarded nose-poke hole was now rewarded and vice versa. The reversal was not cued to the animals; instead, animals had to use the change in feedback to adapt their responding. The reversed conditions continued in sessions 16-20 with 60 trials per session.

After the reversal, the number of rewarded responses decreased, whereas nonrewarded responses increased (Supplementary Figure 4.2a). Reversal learning was based on performance in the reversal session and scored as total number of correct responses in the 86 trials that directly followed the reversal (Supplementary Figure 4.2b). This corresponded with individuals with the highest proportion of correct responses across incorrect responses (both when in- and excluding omissions). Based on the number of correct responses, two fast and two slow performing mice were selected from each family (four fast and slow performing mice in total) for comparative gene expression analysis.

Tissue collection
On 12 March 2020, maximally 6 hours after completing the last reversal learning test, mice were sacrificed using CO_2 followed by cervical dislocation. Their brains were rapidly dissected from the skull and whole cerebellum and striatum were

further bilaterally dissected. Isolated tissue was flash-frozen using dry ice in 2 ml RNA-free tubes and stored at −80°C until RNA isolation.

Nuclei isolation

For both species, frozen brain tissue was pulverized with mortar and pestle on dry ice to yield ~0.2 mL of tissue powder, homogenized in a glass douncer (Kontes Glass Co.) in 0.5 ml EZ buffer (Nuclei Isolation Kit, Sigma NUC101) and incubated for 5 min on ice. Subsequently samples were centrifuged for 15 min at 65 × g at 4 °C, resuspended in 0.5 mL EZ buffer and incubated on ice for 5 min. Samples were again centrifuged for 15 min at 65 × g at 4 °C, resuspended in 0.5 mL nuclear suspension buffer (NSB; 0.01% BSA, 1× complete protease inhibitor cocktail in PBS) and filtered through a 40 µm cell strainer. Samples were centrifuged for 15 min at 65 × g at 4 °C and resuspended in 0.5 mL NSB.

Cerebellar tissues

Bulk nuclei from cerebellar tissue cerebellar tissue (which consists of >80% neurons (Olkowicz et al., 2016)) were stained with trypan blue and counted on a hemacytometer. 5,000 nuclei were pelleted by 10 minutes centrifugation at 500g and resuspended in 100 µl Trizol for RNA-sequencing.

Striatal tissues

1:1000 Hoechst 34580 (1 µg/ml, Fisher Scientific H21486) was added to blocking solution (1% BSA, 10% normal mouse serum (NMS) in PBS) and incubated light shielded at 4 °C for 20 min. 10% of the blocked sample was used as unstained control, the remaining 90% was stained with 1:1500 anti-NeuN antibody conjugated with Alexa488 (1:1000, Merck Millipore MAB377X) without washing and incubated for 1 h at 4 °C on a roller, protected from light. Stained nuclei were then transferred to FACS tubes precoated with 3% BSA and FACS-sorted on NeuN signal using a BD FACSAria II (BD Bioscience). We collected 5,000 neuronal (NeuN+ stained) and 5,000 non-neuronal (NeuN− stained) nuclei in 100 µl Trizol each for RNA-sequencing. In this study, we only used neuronal cells for further analysis.

RNA-sequencing

RNA-sequencing was performed at Single Cell Discoveries (Utrecht, the Netherlands), a (single cell) sequencing provider using an adapted version of the CEL-seq protocol. In brief: Total RNA was extracted using the standard TRIzol (Invitrogen) protocol and used for library preparation and sequencing. mRNA was processed as described previously, following an adapted version of the single-cell mRNA seq protocol of CEL-Seq (Simmini et al., 2014; Hashimshony et al., 2016). In brief, samples were barcoded with CEL-seq primers during a reverse transcription and pooled after second strand synthesis. The resulting cDNA was amplified with an overnight In vitro transcription reaction. From this amplified RNA, sequencing libraries were prepared with Illumina Truseq small RNA primers. Paired-end sequencing was performed on the Illumina Nextseq500 platform with a sequencing

depth of 10 million reads/sample. All reads were trimmed of adapters and low quality bases using *fastx* and sequencing quality was checked using the software *FastQC* v 0.11.9 (Andrews, 2010). Trimmed reads were mapped respectively to the *Parus major* reference genome build v1.1 (GCA_001522545.2, (Laine et al., 2016)) and to the *Mus musculus* reference genome build GRCm39 (GCA_000001635.9) using Hisat2 v 2.2.1 (Kim et al., 2019) with default parameters. To summarize gene level read counts, we used the *featureCounts* program from the *Subread* package v 2.0.2 (Liao et al., 2014).

Statistical analyses

Principal component analysis

Using *DESeq2* v 1.38.0 (Love et al., 2014), low count genes were pre-filtered using a cut-off of 10 normalised counts in >75% of the samples, before they were normalized with post-filtering library sizes and log2 transformed using the *rlog* function. Following normalization, we performed Principle Component Analysis (PCA) using *DEseq2* with the function *plotPCA* to visualize clustering of the samples and to spot individual sample outliers that separated significantly based on size factor (reflecting library size and/or RNA composition bias). These samples were then removed and the filtering and normalization steps were repeated. These samples were removed and the filtering and normalization steps were repeated. Sample sizes were therefore different than what we initially started with and included two fast and two slow reversal learners for the striatum of both species and cerebellum of mice. For the great tit cerebellum samples, three fast and two slow reversal learners were included. An overview of the final sample selection can be found in Supplementary Tables 4.1-3.

In order to visualize principal sources of variation in the data, we performed a final PCA analysis on one-to-one ortholog genes and visualized the first two principal components (PCs) with the *DEseq2* function *plotPCA*, applying the default setting limiting the analysis to the top 500 most variable genes. Additional PCs were obtained using the *prcomp* function in R. We also plotted the percent variance explained by each PC. We tested for species, brain region and reversal phenotype differences in principal components using the *correlate PCs* functions in *pcaExplorer*, which computes the significance of correlations between PCA scores and the experimental covariates.

Differential gene expression analysis

Differences in gene expression in log2FoldChange (log2FC) within each species and brain region were calculated using *DESeq2*. To control for the false discovery rate due to multiple testing, p-values were adjusted using the Benjamini-Hochberg (BH) procedure. Genes were considered statistically differentially expressed when adjusted p-values were < 0.05. The volcano plots were generated using *EnhancedVolcano* v 1.16.0 (Blighe, 2018) and boxplots for a subset of the differentially expressed genes (DEGs) were prepared using *ggplot2* v 3.4.0 (Wickham, 2016).

Gene ontology analyses

To identify significantly enriched gene ontology (GO) and Kyoto Encyclopedia of Genes and Genomes (KEGG) terms, we used *clusterProfiler* v 4.6.0 (Yu et al., 2012) to perform Gene Set Enrichment Analysis (GSEA) of GO and KEGG pathways. GSEA does not require delineation of DEGs from non-differential genes. Instead, we ranked the test statistic of all assessed genes to test for significantly coordinated shifts in gene pathways, as suggested by (Zyla et al., 2017). We used the human and mouse gene ontology database, for great tit and mouse data, respectively. Great tit genes were mapped to their corresponding human orthologs based on HUGO Gene Nomenclature Committee (HGNC) symbol. Genes that could not be assigned to a human gene were excluded, and therefore great tit-specific genes are missing from these analyses. All functional category enrichment analyses considered an adjusted p-value < 0.05 after BH correction to be significant.

Results

Brain region- and species-specific differences in gene expression between fast and slow reversal learning individuals

Using principal component analysis (PCA) on gene expression data from the striatum and cerebellum of both species, principal component (PC)1 explained 94% of the variance, PC2 3% and PC3 1.5% (Figure 4.1). Species separated significantly along PC1 ($p < 0.001$) and brain regions separated along PC2 ($p < 0.001$). Fast and slow reverser groups did not separate significantly in any of the PCs.

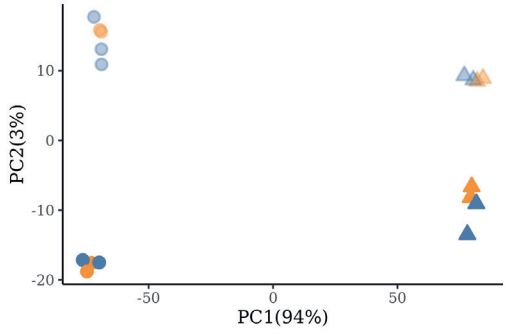

Figure 4.1 Clustering of RNA-seq samples based on principal component analysis (PCA). *Species cluster along PC1 (circles = great tit; triangles = mouse) and brain regions along PC2 (solid= striatum; transparent = cerebellum) but reverser phenotypes (blue = fast, orange = slow) do not cluster based on gene expression levels.*

We found significant gene expression differences between fast and slow reversal learners in three genes in the striatum of great tits (Figure 4.2a) and 37 genes in the striatum of mice (Figure 4.2b), see Supplementary Table 4.4 for full list. In the striatum of great tits, two genes were upregulated and one downregulated in fast compared to slow learning individuals. The expression of ubiquitin-specific peptidase 5 (*USP5*) (log2FC = -4.71, adjusted p-value = 0.020) and polycystic kidney disease-like ion channel (*PKD2L1*) (log2FC = -5.34, adjusted p-value = 0.002) was

upregulated in fast learning individuals, whereas ENSPMJG00000015246, which overlaps the VWA domain-containing protein 3B (*VWA3B)* (log2FC = 4.45, adjusted p-value = 0.002) was upregulated in slow learning individuals (Figure 4.2c). In the mouse striatum, four genes were upregulated and 33 were downregulated in fast learning individuals compared to slow individuals. Of these, eva-1 homolog A (*Eva1a*) (logFC = 6.41, adjusted p-value < 0.001) has a log fold change greater than 5 (Figure 4.2d).

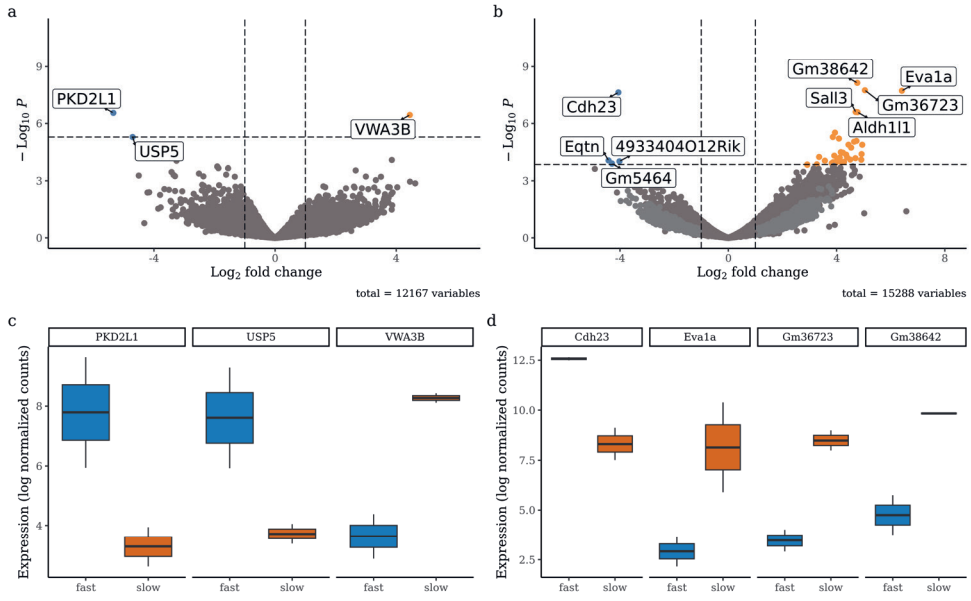

Figure 4.2 Striatal gene expression in fast and slow reversal learning great tits and mice. *Volcano plots highlight the genes that are differentially expressed in the great tit striatum a) and mouse striatum b), where the cut-off for significance (dots beyond the dashed lines) is p < 0.05 with false-discovery rate correction and a log2FoldChange of 1 or greater. c) Highlighted differentially expressed genes in the great tit striatum and d) mouse striatum are shown as boxplots, with rectangles as the lower and upper quartiles (with the median as the line) and whiskers that indicate the maximum and minimum values. Blue = higher expressed in fast reversers, orange = higher expressed in slow reversers.*

We found significant gene expression differences between fast and slow reversal learners in four genes in the cerebellum of great tits and two genes in the cerebellum of mice (Figure 4.3a), see Supplementary Table 4.4 for full list. In the great tit cerebellum, the four DEGs were all upregulated in slow learners (Figure 4.3b): alpha-L-iduronidase *IDUA* (log2FC = 1.66, adjusted p-value = 0.03), aldehyde dehydrogenase *ALDH1A3* (log2FC = 1.97, adjusted p-value = 0.035), forkhead box *FOXC2* (log2FC = 2.29, adjusted p-value = 0.01) and the fourth is a transcript (ENSPMJG00000000917) that overlaps the keratin, type I cytoskeletal 14 gene (NCBI *LOC107215137;* log2FC = 3.57, adjusted p-value < 0.001) (Figure 4.3c). In the mouse cerebellum, two genes were upregulated in slow learners (Figure 4.3d): pseudogene *Gm29216* (log2FC = 5.33, adjusted p-value < 0.001) and inositol

phosphatase *Inpp5d* (log2FC = 1.75, adjusted p-value < 0.001). There was no overlap in DEGs across the brain regions or species.

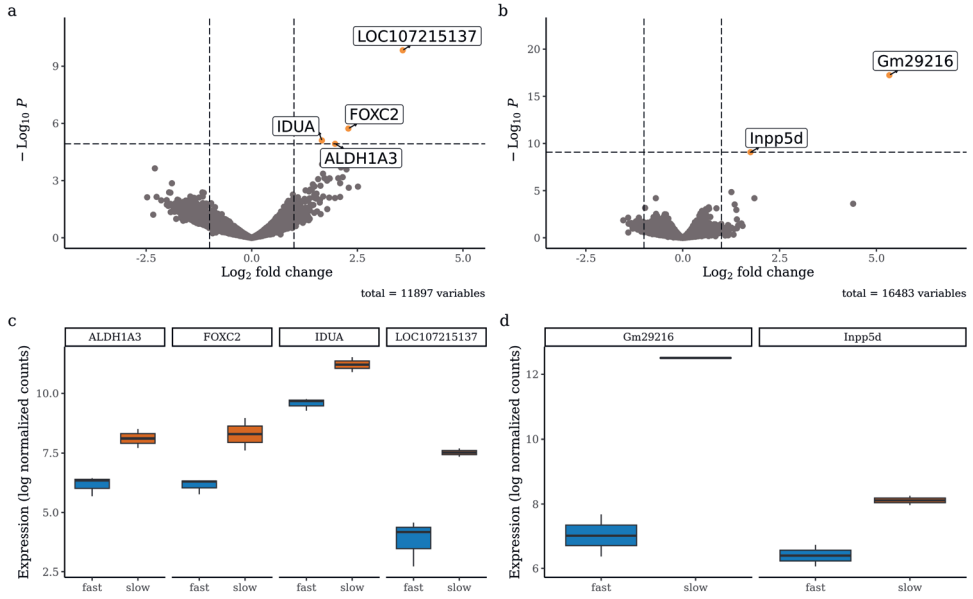

Figure 4.3 Cerebellar gene expression in fast and slow reversal learning great tits and mice. *Volcano plots highlight the genes that are differentially expressed in the great tit cerebellum a) and mouse cerebellum b), where the cut-off for significance (dots beyond the dashed lines) is p < 0.05 with false-discovery rate correction and a log-fold change of one or greater. c) Highlighted differentially expressed genes in the great tit cerebellum and d) mouse cerebellum are shown as boxplots, with rectangles as the lower and upper quartiles (with the median as the line) and whiskers that indicate the maximum and minimum values. Blue = higher expressed in fast reversers, orange = higher expressed in slow reversers.*

G*O enrichment analysis of differentially expressed genes*

Gene set enrichment analysis identified 63 enriched GO and 13 enriched KEGG sets in the great tit striatum, 92 GO and 13 KEGG in the great tit cerebellum, 223 GO and 27 KEGG in the mouse striatum and 143 GO and 27 KEGG in the mouse cerebellum (Figure 4.4 and Supplementary Tables 4.5-12). We found large overlap in these enriched GO and KEGG sets when comparing mouse and great tit, especially in the cerebellum. Sets that were enriched in the striatum of both species include the GO terms “neuron to neuron synapse”, “glutamate receptor binding”, “gated channel activity” and KEGG terms “pathways of neurodegeneration”, “prion disease” and “huntington disease”. Sets that were enriched in the cerebellum of both species include GO terms “oxidative phosphorylation”, “ribosome”, “mitochondrial-containing complex”, “structural constituent of ribosome”, “unfolded protein binding” and KEGG terms “prion disease”, “huntington disease” and “Parkinson disease”.

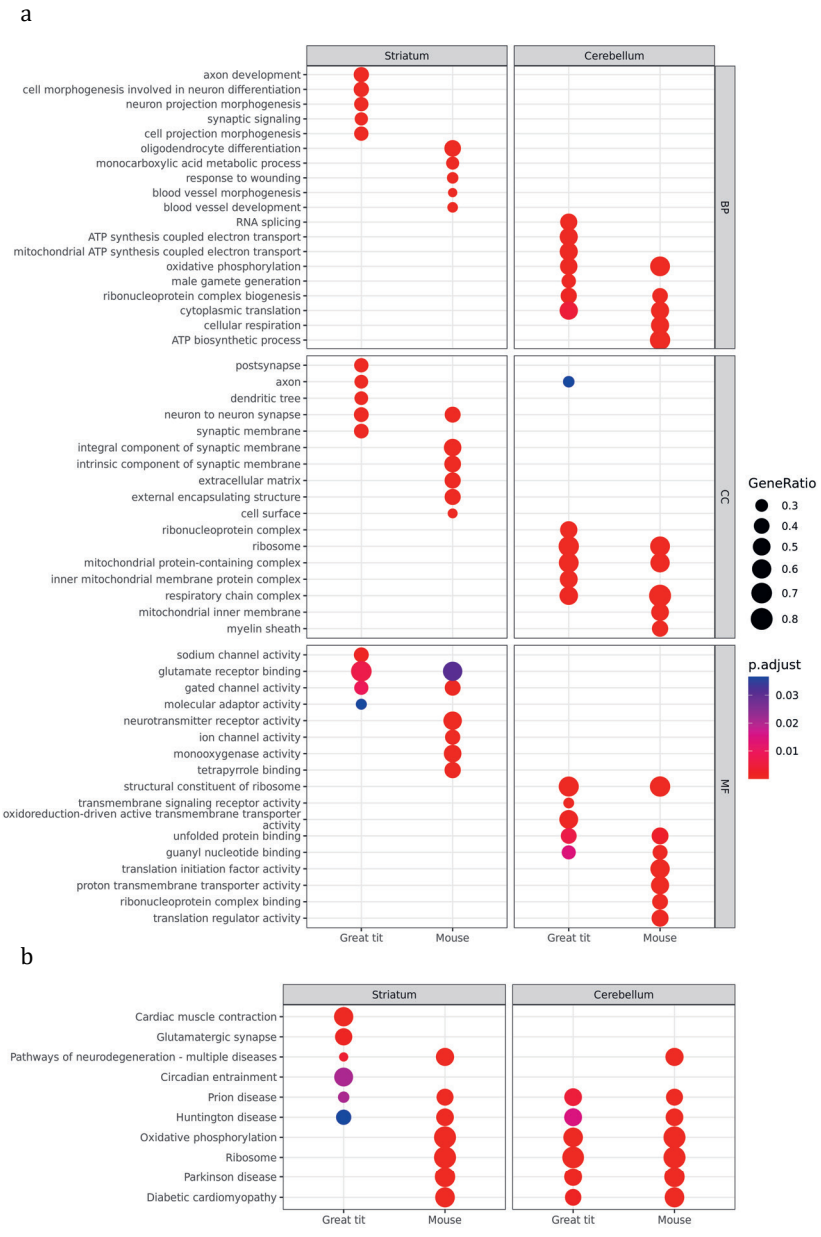

Figure 4.4 Gene-set enrichment analysis of differential expression between fast and slow reversers. *(a) Enriched GO terms (biological process, molecular function and cellular component) terms and (b) KEGG terms in the transcriptome of striatum and cerebellum of fast and slow reversal learning mice and great tits. Gene ratio (dot size) represents percentage of core enrichment genes in the given term, and significance (colours) is based on Benjamini-Hochberg adjusted p-values (FDR).*

Discussion

To better understand individual differences in cognitive flexibility and cross-species molecular causes of these differences, we compared brain gene expression of fast and slow reversal learners in mice and birds. We identified several differentially expressed genes in two brain regions in great tits that are relevant to reversal learning. When testing for conserved functionality across taxonomic classes by comparing these results to transcriptomic differences in homologous regions of mice that were fast and slow at reversal learning, we found that most of the variation in gene expression was explained by species, followed by brain region (cerebellum vs striatum). Accordingly, we found no overlap in transcriptomic differences between fast and slow learning individuals when comparing great tit and mouse. Nonetheless, gene set enrichment analysis showed striking parallels in the cross-taxa RNA-sequencing results that are relevant to the function of the striatum and cerebellum in reversal learning performance.

In each brain region, we found unique genes to be differentially expressed between fast and slow reversal learners, of which some of the most interesting we will discuss below. The striatum plays a particularly important role in feedback-driven learning (Schultz, 2006), including rapidly shifting feedback as occurs in reversal learning assays (Cools et al., 2002; Klanker et al., 2015). In the striatum of great tits, we found overexpression of *PKD2L1* in fast reversal learners. *PKD2L1* contributes to sour taste responses in mice (Horio et al., 2010). A possible indication how *PKD2L1* relates to reversal learning performance, is that it is up-regulated in rats with high emotional reactivity in comparison to less emotional rats (Sabariego et al., 2013). In addition, the ubiquitin-specific peptidase 5 (*USP5*) was upregulated in fast learning individuals. This gene encodes a protein that controls ubiquitin levels. The ubiquitin-proteasome system enables rapid protein changes, and, as such, ubiquitin-dependent remodelling of the synaptic proteome is an important process for synaptic plasticity and memory storage (Mabb and Ehlers, 2010). In the mouse striatum, most genes were overexpressed in slow learners, including Eva-1 Homolog A (*Eva1a*), which plays an important role in neurogenesis (Zhong et al., 2017), Spalt Like Transcription Factor 3 (*Sall3*), a transcription factor gene that is expressed in precursors of GABAergic neurons (Morello et al., 2020), and peroxisome proliferator-activated receptor-alpha *(PPARα*), disruption which caused cognitive inflexibility in a spatial reversal-learning task in mice (D'Agostino et al., 2015).

Cerebellar neurons also show a response to reward delivery, anticipation, and to shifting feedback (Pierce & Péron, 2022; Wagner et al., 2017). In the great tit cerebellum, the gene *ALDH1A3* is overexpressed in slow reversal learners and encodes an aldehyde dehydrogenase enzyme, which oxidizes retinal to retinoic acid. Retinoic acid plays a regulatory role in nervous system development including the cerebellum (Durston et al., 1989; Matsumoto et al., 1998; Parenti and Cicirata, 2004). Alpha-L-iduronidase (*IDUA*) encodes an enzyme that is required for the lysosomal degradation of glycosaminoglycans, which play a crucial role in the cell

signalling process, including regulation of cell growth and proliferation. Long-term memory for aversive training is impaired in mice with targeted disruption of *IDUA* (Reolon et al., 2006). In the mouse cerebellum, *INPP5D* was overexpressed in slow reversal learners. *INPP5D* encodes inositol polyphosphate-5-phosphatase which metabolizes inositol phospholipids, which play a key role in signal transfer between the cell membrane and the nucleus (Viernes et al., 2014). Specifically, *INPP5D* negatively regulates immune signalling, positively correlates with amyloid plaque density, and its´ expression increases as Alzheimer's disease progresses (Tsai et al., 2021). This disease has been linked to reduced cognitive flexibility. Interestingly, an intronic SNP in *INPP5D* that has been associated with a lowered risk of Alzheimer's disease, was also associated with lower protein expression of *IDUA* (Heath et al., 2022), providing a link between *IDUA*, which had higher expression levels in slow reversal learners in the great tit, and *INPP5D*, which had higher expression levels in slow reversal learners in the mouse.

One explanation for the low number of genes that showed differences in expression between the fast and slow reversal learners is that the differences in performance in the individuals that we used in our study were not sufficiently extreme to allow for the detection of correlated differences in gene expression. Earlier studies that linked transcriptional variation with cognitive flexibility phenotypes generally did so by examining experience-dependent gene expression following task execution (Guzowski et al., 2001), or by comparing manipulated individuals or disease models with controls (Wang et al., 2015a, 2015b; eIanov et al., 2016; Lander et al., 2017). Also, from the work in Chapter 2 we know that repeatability of this trait is relatively low (0.14) in great tits, as is common for measures of cognition (Cauchoix et al., 2018). Subtle behavioural differences may be accompanied by small expressions change, which may be difficult to pick up (Benowitz et al., 2019). Indeed, it is not uncommon to find relatively low numbers of differentially expressed genes when comparing baseline behavioural states (Kabelik et al., 2021; Lattin et al., 2022).

Nonetheless, these studies find large variation in the number of trait-related differentially expressed genes across brain regions, and it is likely that the magnitude of transcriptional differences within a brain region reflects its relative importance to the studied trait. Normal functioning of the cerebellum and striatum is crucial for cognitive flexibility (Klanker et al., 2015; Groman et al., 2016; Linden et al., 2018; Peterburs et al., 2018; Sala-Bayo et al., 2020; Shipman and Green, 2020; Pierce and Péron, 2022). However, based on our findings it seems that differences in gene expression in these regions explain individual performance differences only to a small degree. Perhaps there are other brain regions that play more crucial roles for individual differences in reversal learning performance, other candidates are for instance the hippocampus (Thompson et al., 2015; Vilà-Balló et al., 2017) and amygdala (Izquierdo et al., 2013; Keefer and Petrovich, 2020). We also know that higher order brain regions, like cortical regions in mammals and the NCL in birds, play important roles (Brigman and Rothblat, 2008; Izquierdo et al., 2017). However, as these regions are not homologous between birds and mammals

(Belgard et al., 2013; Güntürkün and Bugnyar, 2016), we choose not to focus on these regions here.

On the level of differentially expressed genes, the causes of between-individual differences in reversal learning performance seem not universal but rather the result of convergent molecular mechanisms. Because we studied baseline states of a highly complex trait, we expected that small but coordinated changes in sets of functionally related genes might be equally impactful on the behavioural phenotype as the genes that have large expression changes. Therefore, we also performed gene set enrichment analysis to look for pathways that display significantly co-ordinated differences in gene expression. On doing so, we found overlap in biological function of significantly enriched gene sets. Generally, there was more overlap within brain region across species rather than within species, across brain regions. Two enriched pathways that overlapped across all four groups, were the KEGG terms prion disease and Huntington disease. Both are neurodegenerative diseases that affect neuronal dysfunction and experience-dependent plasticity (Murphy et al., 2000; Moreno and Mallucci, 2010; Murmu et al., 2015), and therefore it is no surprise that genes in these pathways link to reversal learning performance. Specifically in the case of Huntington disease, striatal-dependent cognitive flexibility is affected (Nickchen et al., 2017; Padron-Rivera et al., 2022). The GO category "axon", was enriched in both striatum and cerebellum of great tits, but otherwise there were no overlapping terms within the two different brain regions in either species. This affirms the importance of studying brain region-specific patterns of gene expression.

In both striatum and cerebellum, GO and KEGG pathway analysis showed a functional similarity between genes differentially expressed in mice and great tits. In the striatum, overlapping terms were relevant to striatal functioning, such as neuron to neuron synapse, glutamate receptor binding, and pathways of neurodegeneration. The striatum receives glutamatergic projections from the cortex and thalamus (Paraskevopoulou et al., 2019), and there is ample evidence that glutamate signalling is important for reversal learning performance (Izquierdo et al., 2017; Liu et al., 2020). There were also some notable differences in the striatum of both species, in the great tit several pathways related to neuronal differentiation were differentially upregulated, whereas in the mouse, we found differential regulation of angiogenetic and cardiovascular processes. In mice, these processes were found to be differentially upregulated in the striatum following learning, and angiogenesis, rather than neurogenesis was shown to be critical for learning and memory acquisition in rats (Kerr et al., 2010; Lousada et al., 2023). Neurogenesis occurs much more broadly in the avian brain than in the mammalian brain (Barnea and Pravosudov, 2011). Together, this apparent discrepancy between the two species may reflect a true difference of importance of neurogenesis versus angiogenesis to reversal learning performance between great tits and mice that would be an interesting avenue for further study.

In the cerebellum, the ribosome pathway was significantly activated in fast learners of both species. Ribosomes are crucial complexes for protein synthesis, suggesting that slow learners have altered protein translations compared to fast learners. Local protein synthesis is crucial for memory formation and synaptic plasticity (Costa-Mattioli et al., 2009; Moncada et al., 2015; Chen et al., 2017), and age-linked dysregulation of protein synthesis correlate with deterioration of spatial memory and behavioural flexibility (Yang et al., 2019). Also, the oxidative phosphorylation pathway was significantly activated in fast learners. This term refers to the process that takes place in the mitochondria, where nutrients are oxidized to produce ATP. Neural tissue development and function is very dependent on mitochondrial dynamics (Chen et al., 2007). Lower oxidative phosphorylation activity can cause increased production of reactive oxygen species, which have a modulatory role in synaptic plasticity, but can impair LTP at too high concentrations (Serrano and Klann, 2004). The KEGG term Parkinson's disease was significantly activated in the cerebellum of fast learners in both species as well as in the striatum of mice. Notably, many genes that are associated with Parkinson's disease have a function in the oxidative phosphorylation, providing a link between these two pathways (Ali and Dholaniya, 2022). Parkinson's disease is a progressive neurodegenerative disorder causing pathological alterations in the cerebellum (Wu and Hallett, 2013), primarily resulting from dopamine neuronal loss (Tolosa et al., 2006). In that sense, it is surprising that differences related to genes in the Parkinson's disease pathway were not found in the striatum of great tits, where dopamine is also an important neuromodulator. In general it is surprising that we did not find any differences in genes specifically related to dopamine signalling, considering the known importance of the dopaminergic system for reward processing and cognitive flexibility, although we did find enrichment of pathways related to neurotransmitter signalling (Laughlin et al., 2011; Groman et al., 2014, 2016; Klanker et al., 2015; Linden et al., 2018; Sala-Bayo et al., 2020).

The gene expression patterns highlighted above only reflect a molecular phenotype and not necessarily a genotype. Variation in gene expression can have genetic origins, but we know that the estimated heritability of reversal learning performance equals zero in great tits (Chapter 2), and ranges from 0.17-0.3 in mice (Laughlin et al., 2011; Bailey et al., 2021), meaning that the contribution of other regulatory factors is high. Environmental interventions, such as social isolation (Han et al., 2011; Benner et al., 2014) and neonatal handling (Noschang et al., 2012; Río-Álamos et al., 2019), are known to affect reversal learning performance and brain gene expression, and these external influences are among others mediated by epigenetic mechanisms such as histone acetylation (Li et al., 2016). Therefore, to better understand what underlies individual differences in gene expression and cognition, it will be worthwhile to assess whether those differences coexist with epigenetic variation. And, to explore potential environmental causes of individual variation, it would be very interesting to manipulate early life (e.g., adversity or enrichment) and study how that affects gene expression and epigenetic marks.
To conclude, we found no overlap in the genes that were differentially expressed between brain regions and between species. However, when summarising these

genes in differentially enriched gene sets, we did find overlapping GO and KEGG categories. Most overlapping terms between species occurred within the same brain region, suggesting that individual differences in reversal learning performance are highly brain region-specific, but this pattern is consistent even across-taxa. In the striatum, we found overlap in terms related to synaptic plasticity, glutamate signalling and pathways of neurodegeneration. In the cerebellum, we mostly found overlapping pathways related to metabolism, such as protein metabolic processes, oxidative phosphorylation and ribosome functioning. Considering the high energetic costs of information processing in the cerebellum, most neurons of which show extremely high intrinsic activity that is modulated during learning (De Zeeuw et al., 2011; De Zeeuw, 2021), and given the energetic costs that come with associated learning and memory performance (Laughlin, 2001), it seems intuitive that individual differences in energy metabolism or allocation may underlie individual differences in cognitive performance. Overall, our findings suggests that although the identity of differentially expressed genes are highly brain region- and species-specific, some core functions related to reversal learning performance are conserved across mammals and birds.

Supplement to Chapter 4

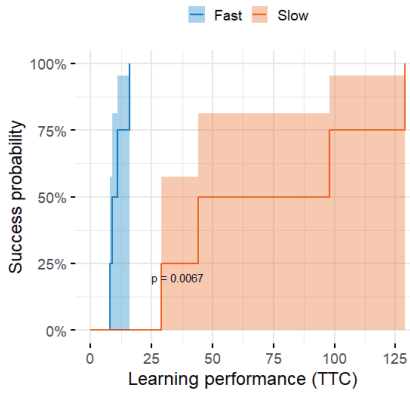

Supplementary Figure 4.1 *Kaplan Meier plots of the trials to reach learning criterion (TTC) during the reversal learning task for great tits. "Time" is number of trials, and "event" is reaching trials to criterion. Every time an individual reaches learning criterion, the proportion of individuals succeeding at the task on the Y-axis increases. The fast and slow learning individuals differ significantly on success probability (log-rank test p = 0.007).*

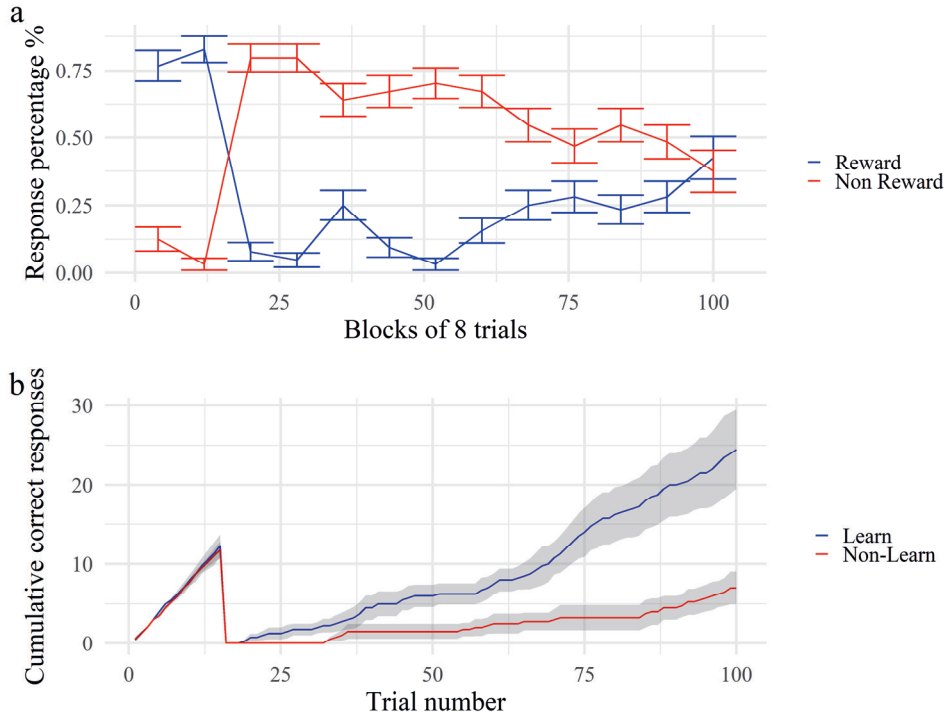

Supplementary Figure 4.2 *a) Behavioural performance across reversal learning session for mice. Lines show percent response during rewarded (blue) and non-rewarded (red) trials across consecutive blocks of trials before and after reversal (block 3). b) Cumulative response curves for learners (blue, n = 4) and non-learners (red, n = 4).*

Supplementary Table 4.1 *Sample origins, reversal learning scores, and samples (Y) included in final analysis. TTC = trials to criterion.*

Species	Phenotype	Individual	Brood/ Nest	TTC R1	TTC R2	TTC R3	Mean TTC	Total correct	STR NeuN+	CB Bulk
Great tit	Fast	BD...76237	70664	8	25	7	13.33	-	Y	Y
		BD...76021	70154	9	26	9	14.67	-		Y
		BD...76157	70156	11	15	8	11.33	-		Y
		BD...76096	70132	16	23	8	15.67	-	Y	
	Slow	BD...76081	70145	29	16	30	25	-		Y
		BD...76038	70115	53	21	24	32.67	-	Y	
		BD...76216	70361	98	81	45	74.67	-		Y
		BD...76149	70155	164	8	45	72.33	-	Y	
Mouse	Fast	1	1		-	-	-	12		Y
		3	1		-	-	-	32	Y	Y
		6	2		-	-	-	21		
		8	2		-	-	-	33	Y	
	Slow	2	1		-	-	-	4	Y	Y
		4	1		-	-	-	11		Y
		7	2		-	-	-	3		
		9	2		-	-	-	10	Y	

Supplementary Table 4.2 *Summary of sequencing and alignment of included great tit libraries.*

Brain region	Phenotype	Individual	#Raw reads	%Aligned 1X	#Aligned 1X	#Aligned to genes
Striatum	Fast	BD...76237	27,180,653	69.31	18,836,513	11,471,278
		BD...76096	60,259,538	80.14	48,294,457	26,958,249
	Slow	BD...76038	27,956,839	78.13	21,841,806	12,470,514
		BD...76149	56,860,753	77.74	44,201,536	24,504,588
Cerebellum	Fast	BD...76237	20,130,748	74.18	14,933,841	8,608,710
		BD...76021	25,722,205	75.64	19,456,678	10,912,056
		BD...76157	21,155,242	75.00	15,865,407	9,386,363
	Slow	BD...76081	16,972,169	72.42	12,290,472	7,511,182
		BD...76216	12,261,508	74.08	9,083,617	5,425,060

Supplementary Table 4.3 *Summary of sequencing and alignment of included mouse libraries.*

Brain region	Phenotype	Individual	#Raw reads	%Aligned 1X	#Aligned 1X	#Aligned to genes
Striatum	Fast	3	41,534,881	74.08	30,768,161	25,847,563
		8	60,633,785	79.63	48,281,831	17,418,156
	Slow	2	33,707,254	77.17	26,011,829	21,844,337
		9	17,484,978	68.40	11,960,115	5,864,833
Cerebellum	Fast	1	8,633,819	73.48	6,344,474	5,250,415
		3	16,773,547	74.18	12,443,378	10,192,388
	Slow	2	28,667,824	73.03	20,937,436	17,166,645
		4	36,905,336	73.56	27,148,287	22,471,799

Supplementary Table 4.4 *List of differentially expressed genes between fast and slow reversal learners for each brain region and species.*

Geneid	log2FC	padj	Gene Name	Description
Great tit – Striatum				
ENSPMJG00000015246	4.45	0.002		
ENSPMJG00000016012	-5.34	0.002	PKD2L1	polycystin 2 like 1, transient receptor potential cation channel
ENSPMJG00000007267	-4.71	0.021	USP5	ubiquitin specific peptidase 5
Great tit -Cerebellum				
ENSPMJG00000000917	3.57	1.75E-06		keratin, type I cytoskeletal 14
ENSPMJG00000013927	2.29	0.011	FOXC2	forkhead box C2
ENSPMJG00000003485	1.66	0.031	IDUA	alpha-L-iduronidase
ENSPMJG00000009765	1.97	0.035	ALDH1A3	aldehyde dehydrogenase 1 family member A3
Mouse - Striatum				
ENSMUSG00000012819	-4.06	7.36E-05	Cdh23	cadherin 23 (otocadherin)
ENSMUSG00000035104	6.41	7.36E-05	Eva1a	eva-1 homolog A (C. elegans)
ENSMUSG00000111219	4.77	7.36E-05	Gm38642	predicted gene, 38642
ENSMUSG00000113669	5.05	7.36E-05	Gm36723	predicted gene, 36723
ENSMUSG00000024565	4.7	0.00053	Sall3	spalt like transcription factor 3
ENSMUSG00000030088	4.78	0.00053	Aldh1l1	aldehyde dehydrogenase 1 family, member L1
ENSMUSG00000112112	3.94	0.0055	Gm48508	predicted gene, 48508
ENSMUSG00000005958	3.86	0.0081	Ephb3	Eph receptor B3
ENSMUSG00000100147	4.09	0.0087	1700047M11Rik	RIKEN cDNA 1700047M11 gene
ENSMUSG00000031385	4.74	0.010	Plxnb3	plexin B3
ENSMUSG00000040260	4.65	0.010	Daam2	dishevelled associated activator of morphogenesis 2
ENSMUSG00000007682	4.44	0.013	Dio2	deiodinase, iodothyronine, type II
ENSMUSG00000097881	4.95	0.013	Celrr	cerebellum expressed regulatory RNA
ENSMUSG00000032281	4.54	0.017	Acsbg1	acyl-CoA synthetase bubblegum family member 1
ENSMUSG00000030235	4.16	0.027	Slco1c1	solute carrier organic anion transporter family, member 1c1
ENSMUSG00000052914	4.23	0.027	Cyp2j6	cytochrome P450, family 2, subfamily j, polypeptide 6
ENSMUSG00000048424	4.92	0.030	Ranbp3l	RAN binding protein 3-like
ENSMUSG00000116885	4.35	0.031	4930420G21Rik	RIKEN cDNA 4930420G21 gene
ENSMUSG00000050721	3.92	0.033	Plekho2	pleckstrin homology domain containing, family O member 2
ENSMUSG00000046240	4.39	0.036	Hepacam	hepatocyte cell adhesion molecule
ENSMUSG00000048402	4.12	0.036	Gli2	GLI-Kruppel family member GLI2

Supplementary Table 4.4 (continued).

ENSMUSG00000051729	3.36	0.036	Gm5087	predicted gene 5087
ENSMUSG00000026170	4.7	0.037	Cyp27a1	cytochrome P450, family 27, subfamily a, polypeptide 1
ENSMUSG00000004892	3.57	0.041	Bcan	brevican
ENSMUSG00000014361	4.5	0.041	Mertk	MER proto-oncogene tyrosine kinase
ENSMUSG00000022383	4.91	0.041	Ppara	peroxisome proliferator activated receptor alpha
ENSMUSG00000026424	4.02	0.041	Gpr37l1	G protein-coupled receptor 37-like 1
ENSMUSG00000028575	-4.42	0.041	Eqtn	equatorin, sperm acrosome associated
ENSMUSG00000097908	-4.02	0.043	4933404O12Rik	RIKEN cDNA 4933404O12 gene
ENSMUSG00000022382	4.28	0.044	Wnt7b	wingless-type MMTV integration site family, member 7B
ENSMUSG00000010064	3.87	0.044	Slc38a3	solute carrier family 38, member 3
ENSMUSG00000030351	4.17	0.044	Tspan11	tetraspanin 11
ENSMUSG00000047216	3.96	0.045	Cdh19	cadherin 19, type 2
ENSMUSG00000036634	3.83	0.045	Mag	myelin-associated glycoprotein
ENSMUSG00000075553	-4.3	0.045	Gm5464	predicted gene 5464
ENSMUSG00000032220	2.92	0.049	Myo1e	myosin IE
ENSMUSG00000048782	3.27	0.049	Insc	INSC spindle orientation adaptor protein
Mouse - Cerebellum				
ENSMUSG00000101249	5.33	9.47E-14	Gm29216	predicted gene 29216
ENSMUSG00000026288	1.75	6.83E-06	Inpp5d	inositol polyphosphate-5-phosphatase D

Supplementary Table 4.5 *List of 25 most significantly enriched (adjusted p values) GO terms for great tit, striatum. ES: enrichment score. NES: normalized enrichment score.*

Ontology	ID	Description	setSize	ES	NES	p.adjust	Rank
BP	GO:0061564	axon development	333	-0.46	-1.87	4.43E-06	1899
BP	GO:0048667	cell morphogenesis involved in neuron differentiation	384	-0.44	-1.84	4.43E-06	2028
BP	GO:0048812	neuron projection morphogenesis	431	-0.42	-1.78	4.43E-06	1899
CC	GO:0098794	postsynapse	422	-0.43	-1.82	4.43E-06	1901
BP	GO:0099536	synaptic signaling	441	-0.42	-1.77	4.56E-06	1829
BP	GO:0048858	cell projection morphogenesis	445	-0.42	-1.77	4.56E-06	1899
CC	GO:0030424	axon	422	-0.43	-1.79	4.56E-06	1903
CC	GO:0097447	dendritic tree	409	-0.42	-1.75	1.17E-05	1901
CC	GO:0098984	neuron to neuron synapse	246	-0.47	-1.89	1.55E-05	1899
CC	GO:0097060	synaptic membrane	255	-0.46	-1.83	3.75E-05	1899

Supplementary Table 4.5 (continued).

BP	GO:0061387	regulation of extent of cell growth	75	-0.62	-2.11	6.65E-05	1972
CC	GO:1902495	transmembrane transporter complex	210	-0.47	-1.86	0.00013	1834
CC	GO:1990351	transporter complex	228	-0.46	-1.81	0.00013	1769
BP	GO:0050804	modulation of chemical synaptic transmission	271	-0.43	-1.74	0.00020	1829
BP	GO:0050807	regulation of synapse organization	139	-0.51	-1.92	0.00023	1899
CC	GO:0098978	glutamatergic synapse	235	-0.46	-1.81	0.00024	1855
BP	GO:0034330	cell junction organization	425	-0.39	-1.64	0.00029	2075
CC	GO:0044309	neuron spine	122	-0.53	-1.95	0.00035	1852
BP	GO:0034329	cell junction assembly	249	-0.43	-1.73	0.00038	1941
BP	GO:0050803	regulation of synapse structure or activity	142	-0.51	-1.89	0.00043	1899
MF	GO:0005272	sodium channel activity	27	-0.73	-2.07	0.00097	929
BP	GO:0048588	developmental cell growth	151	-0.48	-1.82	0.0013	1899
BP	GO:0019433	triglyceride catabolic process	16	0.82	2.15	0.0013	506
BP	GO:0007215	glutamate receptor signaling pathway	35	-0.68	-2.04	0.0029	1574
CC	GO:0030532	small nuclear ribonucleoprotein complex	45	-0.64	-2.01	0.0035	1487

Supplementary Table 4.6 *List of 25 most significantly enriched GO terms for great tit, cerebellum. ES: enrichment score. NES: normalized enrichment score.*

Ontology	**ID**	**Description**	**setSize**	**ES**	**NES**	**p.adjust**	**rank**
CC	GO:1990904	ribonucleoprotein complex	439	0.37	2.05	5.37E-10	2839
CC	GO:0005840	ribosome	136	0.47	2.26	1.54E-06	3419
CC	GO:0098798	mitochondrial protein-containing complex	184	0.42	2.07	1.06E-05	3571
BP	GO:0008380	RNA splicing	280	0.37	1.96	1.06E-05	2842
CC	GO:0098800	inner mitochondrial membrane protein complex	89	0.52	2.28	2.43E-05	2360
MF	GO:0003735	structural constituent of ribosome	99	0.48	2.18	7.89E-05	3248
MF	GO:0004888	transmembrane signaling receptor activity	309	-0.36	-1.82	0.00010	1229
BP	GO:0042773	ATP synthesis coupled electron transport	57	0.56	2.28	0.00015	2178
BP	GO:0042775	mitochondrial ATP synthesis coupled electron transport	57	0.56	2.28	0.00015	2178
BP	GO:0006119	oxidative phosphorylation	80	0.5	2.16	0.00015	2360
CC	GO:0098803	respiratory chain complex	47	0.59	2.27	0.00026	2178
BP	GO:0048232	male gamete generation	250	-0.37	-1.82	0.00026	1831
BP	GO:0044782	cilium organization	226	-0.38	-1.84	0.00049	1827
BP	GO:0060271	cilium assembly	211	-0.38	-1.82	0.00049	1827

Supplementary Table 4.6 (continued).

BP	GO:0022613	ribonucleoprotein complex biogenesis	301	0.32	1.71	0.00051	2832
MF	GO:0015453	oxidoreduction-driven active transmembrane transporter activity	42	0.6	2.27	0.00051	2087
BP	GO:0009201	ribonucleoside triphosphate biosynthetic process	70	0.5	2.12	0.00064	2392
CC	GO:0070469	respirasome	52	0.54	2.15	0.00086	2178
BP	GO:0060445	branching involved in salivary gland morphogenesis	16	-0.76	-2.2	0.00095	690
BP	GO:0022412	cellular process involved in reproduction in multicellular organism	182	-0.38	-1.82	0.0012	1864
BP	GO:0030336	negative regulation of cell migration	160	0.37	1.82	0.0012	1590
BP	GO:0006457	protein folding	131	0.4	1.87	0.0016	1730
CC	GO:0005929	cilium	353	-0.32	-1.62	0.0018	1827
CC	GO:0005681	spliceosomal complex	126	0.39	1.85	0.0028	2932

Supplementary Table 4.7 *List of 25 most significantly enriched GO terms for mouse, striatum. ES: enrichment score. NES: normalized enrichment score.*

Ontology	ID	Description	setSize	ES	NES	p.adjust	rank
CC	GO:0099699	integral component of synaptic membrane	178	-0.46	-2.4	6.84E-10	2848
CC	GO:0099240	intrinsic component of synaptic membrane	197	-0.44	-2.34	6.84E-10	2497
CC	GO:0031012	extracellular matrix	241	0.49	2.13	3.10E-09	2486
CC	GO:0030312	external encapsulating structure	242	0.49	2.13	3.10E-09	2486
BP	GO:0048709	oligodendrocyte differentiation	94	0.62	2.44	6.26E-09	1697
CC	GO:0009986	cell surface	454	0.42	1.91	6.59E-09	1596
BP	GO:0032787	monocarboxylic acid metabolic process	352	0.42	1.87	5.26E-07	2640
CC	GO:0034702	ion channel complex	207	-0.38	-2.04	7.48E-07	2499
CC	GO:0099572	postsynaptic specialization	378	-0.31	-1.76	1.42E-06	3307
CC	GO:0098984	neuron to neuron synapse	385	-0.31	-1.77	1.47E-06	3307
CC	GO:0032279	asymmetric synapse	359	-0.31	-1.76	1.47E-06	3307
CC	GO:0098793	presynapse	483	-0.29	-1.67	1.47E-06	2543
CC	GO:0098978	glutamatergic synapse	460	-0.29	-1.69	1.64E-06	3178
MF	GO:0030594	neurotransmitter receptor activity	60	-0.57	-2.49	3.81E-06	2444
CC	GO:0009897	external side of plasma membrane	161	0.48	2.04	3.89E-06	2020
MF	GO:0005216	ion channel activity	273	-0.33	-1.84	5.18E-06	2541
BP	GO:0009611	response to wounding	274	0.41	1.82	7.99E-06	2040
BP	GO:0048514	blood vessel morphogenesis	368	0.4	1.78	1.40E-05	1994
BP	GO:0001568	blood vessel development	428	0.38	1.72	1.40E-05	2241

Supplementary Table 4.7 (continued).

BP	GO:0006954	inflammatory response	330	0.39	1.75	1.91E-05	**2436**
MF	GO:0004497	monooxygenase activity	40	0.67	2.27	2.35E-05	1972
MF	GO:0046906	tetrapyrrole binding	65	0.58	2.16	5.51E-05	2053
BP	GO:0007272	ensheathment of neurons	129	0.48	1.97	5.86E-05	2532
BP	GO:0008366	axon ensheathment	129	0.48	1.97	5.86E-05	2532
MF	GO:0022836	gated channel activity	213	-0.34	-1.82	6.61E-05	2535

Supplementary Table 4.8 *List of 25 most significantly enriched GO terms for mouse, cerebellum. ES: enrichment score. NES: normalized enrichment score.*

Ontology	ID	Description	setSize	ES	NES	p.adjust	rank
CC	GO:0005840	ribosome	193	0.6	2.81	8.11E-21	4072
MF	GO:0003735	structural constituent of ribosome	142	0.61	2.75	3.79E-16	4147
CC	GO:0098798	mitochondrial protein-containing complex	244	0.5	2.41	8.73E-14	5186
CC	GO:0005743	mitochondrial inner membrane	453	0.42	2.16	8.73E-14	5186
CC	GO:0043209	myelin sheath	193	0.5	2.34	1.58E-10	3146
BP	GO:0002181	cytoplasmic translation	129	0.56	2.49	5.10E-10	3460
CC	GO:0098803	respiratory chain complex	64	0.63	2.51	3.84E-08	5033
BP	GO:0022613	ribonucleoprotein complex biogenesis	381	0.38	1.92	8.59E-08	4262
BP	GO:0006119	oxidative phosphorylation	108	0.54	2.36	8.78E-08	4536
BP	GO:0045333	cellular respiration	189	0.46	2.18	8.94E-08	4597
BP	GO:0006754	ATP biosynthetic process	83	0.58	2.42	1.95E-07	4344
BP	GO:0009206	purine ribonucleoside triphosphate biosynthetic process	90	0.57	2.39	1.95E-07	3478
BP	GO:0007005	mitochondrion organization	460	0.36	1.85	2.27E-07	3992
CC	GO:0070469	respirasome	71	0.6	2.41	2.78E-07	5033
CC	GO:0016469	proton-transporting two-sector ATPase complex	42	0.68	2.47	9.47E-07	3937
MF	GO:0003743	translation initiation factor activity	43	0.67	2.45	3.38E-06	3373
MF	GO:0015078	proton transmembrane transporter activity	85	0.53	2.22	7.97E-06	3549
CC	GO:1990204	oxidoreductase complex	97	0.52	2.21	1.02E-05	5033
CC	GO:0005844	polysome	69	0.56	2.27	1.80E-05	4231
MF	GO:0043021	ribonucleoprotein complex binding	145	0.45	2.05	2.21E-05	3504
BP	GO:0046390	ribose phosphate biosynthetic process	183	0.42	1.96	2.57E-05	4344
BP	GO:0030433	ubiquitin-dependent ERAD pathway	77	0.54	2.2	4.60E-05	3732
CC	GO:0005761	mitochondrial ribosome	85	0.51	2.12	6.52E-05	5063

Supplementary Table 4.8 (continued).

BP	GO:0046034	ATP metabolic process	179	0.41	1.93	7.19E-05	4536
BP	GO:2000112	regulation of cellular macromolecule biosynthetic process	400	0.34	1.72	8.47E-05	3567

Supplementary Table 4.9 *List of enriched (adjusted p values) KEGG terms for great tit, striatum. ES: enrichment score. NES: normalized enrichment score.*

ID	Description	setSize	ES	NES	p.adjust	rank
04260	Cardiac muscle contraction	44	-0.6278185	-2.25541213	0.00019	1753
04724	Glutamatergic synapse	70	-0.5114918	-2.02373806	0.00076	1868
05022	Pathways of neurodegeneration - multiple diseases	273	-0.34433229	-1.66039069	0.0042	1786
04713	Circadian entrainment	59	-0.47773798	-1.82020038	0.023	2142
05020	Prion disease	151	-0.36928257	-1.65857507	0.023	1766
05010	Alzheimer disease	216	-0.33734724	-1.58715168	0.026	1766
04261	Adrenergic signaling in cardiomyocytes	86	-0.42267361	-1.73883851	0.033	1753
04961	Endocrine and other factor-regulated calcium reabsorption	28	-0.58329686	-1.8911123	0.034	1099
04934	Cushing syndrome	84	-0.42505377	-1.74480715	0.034	1538
04721	Synaptic vesicle cycle	46	-0.48526431	-1.76928566	0.042	1835
04024	cAMP signaling pathway	129	-0.3627778	-1.59194245	0.042	1749
05016	Huntington disease	184	-0.33127145	-1.52425667	0.042	1860
04979	Cholesterol metabolism	30	0.53422673	1.85036993	0.042	855

Supplementary Table 4.10 *List of enriched (adjusted p values) KEGG terms for great tit, cerebellum. ES: enrichment score. NES: normalized enrichment score.*

ID	Description	setSize	ES	NES	p.adjust	rank
03010	Ribosome	84	0.51029616	2.23716443	3.19E-05	3235
00190	Oxidative phosphorylation	77	0.50548827	2.16750103	0.00020	2493
05012	Parkinson disease	150	0.39318663	1.90276093	0.00045	2526
05415	Diabetic cardiomyopathy	120	0.40405424	1.8878908	0.0016	2245
05020	Prion disease	153	0.35681865	1.72658467	0.0054	2729
00980	Metabolism of xenobiotics by cytochrome P450	11	0.79957934	2.09903433	0.0064	550
04080	Neuroactive ligand-receptor interaction	119	-0.39425454	-1.76361067	0.0064	1169
05010	Alzheimer disease	214	0.31886904	1.60045875	0.0066	2729
05016	Huntington disease	180	0.31863586	1.56969323	0.017	2741
05014	Amyotrophic lateral sclerosis	221	0.30412361	1.53838948	0.017	2503

Supplementary Table 4.10 (continued).

00500	Starch and sucrose metabolism	16	-0.68802614	-1.93200672	0.022	1177
04141	Protein processing in endoplasmic reticulum	118	0.35127438	1.63855599	0.027	1722
05208	Chemical carcinogenesis - reactive oxygen species	123	0.33914844	1.59603129	0.048	2526

Supplementary Table 4.11 *List of enriched (adjusted p values) KEGG terms for mouse, striatum. ES: enrichment score. NES: normalized enrichment score.*

ID	Description	setSize	ES	NES	p.adjust	rank
00190	Oxidative phosphorylation	101	0.64060436	2.76341674	4.68E-09	3633
03010	Ribosome	118	0.61921626	2.72735399	4.68E-09	4017
05012	Parkinson disease	217	0.52389765	2.5165294	4.68E-09	4449
05016	Huntington disease	248	0.47787596	2.33267805	4.68E-09	3697
05020	Prion disease	209	0.48750876	2.32819455	4.68E-09	2942
05014	Amyotrophic lateral sclerosis	294	0.42591365	2.11397353	4.68E-09	4915
05010	Alzheimer disease	307	0.42109842	2.10398656	4.68E-09	4760
05022	Pathways of neurodegeneration - multiple diseases	377	0.38295611	1.94440536	9.26E-09	4729
05415	Diabetic cardiomyopathy	160	0.46302993	2.13074338	2.27E-07	4387
05208	Chemical carcinogenesis - reactive oxygen species	171	0.45119553	2.10116653	4.45E-07	3298
05171	Coronavirus disease - COVID-19	164	0.44979494	2.08203431	7.15E-07	3137
04932	Non-alcoholic fatty liver disease	126	0.47776057	2.1270435	1.34E-06	4387
04141	Protein processing in endoplasmic reticulum	151	0.44915848	2.04623231	1.34E-06	3952
04714	Thermogenesis	186	0.4091782	1.92834235	1.46E-05	4611
03040	Spliceosome	119	0.4263635	1.87919261	0.00026	4806
03050	Proteasome	41	0.58408404	2.06891756	0.00041	2455
05132	Salmonella infection	213	0.35242778	1.68617077	0.0014	3663
04020	Calcium signaling pathway	176	-0.32299597	-1.66018853	0.0029	3417
05414	Dilated cardiomyopathy	77	-0.40668959	-1.82377319	0.0037	1849
05410	Hypertrophic cardiomyopathy	71	-0.41809359	-1.84231705	0.0049	1849
04217	Necroptosis	98	0.40731087	1.73779991	0.0067	2800
05211	Renal cell carcinoma	64	0.44152346	1.72682792	0.013	1336
04964	Proximal tubule bicarbonate reclamation	16	0.6645232	1.87897761	0.016	2389
03250	Viral life cycle - HIV-1	52	0.46955629	1.76028704	0.018	4066
04721	Synaptic vesicle cycle	64	0.43441051	1.69900871	0.019	2514
04140	Autophagy - animal	124	0.35193928	1.56848476	0.039	2066

Supplementary Table 4.11 (continued).

04066	HIF-1 signaling pathway	89	0.39161615	1.64231698	0.042	1415

Supplementary Table 4.12 *List of enriched (adjusted p values) KEGG terms for mouse, cerebellum. ES: enrichment score. NES: normalized enrichment score.*

ID	Description	setSize	ES	NES	p.adjust	rank
00190	Oxidative phosphorylation	101	0.64060436	2.76341674	4.68E-09	3633
03010	Ribosome	118	0.61921626	2.72735399	4.68E-09	4017
05012	Parkinson disease	217	0.52389765	2.5165294	4.68E-09	4449
05016	Huntington disease	248	0.47787596	2.33267805	4.68E-09	3697
05020	Prion disease	209	0.48750876	2.32819455	4.68E-09	2942
05014	Amyotrophic lateral sclerosis	294	0.42591365	2.11397353	4.68E-09	4915
05010	Alzheimer disease	307	0.42109842	2.10398656	4.68E-09	4760
05022	Pathways of neurodegeneration - multiple diseases	377	0.38295611	1.94440536	9.26E-09	4729
05415	Diabetic cardiomyopathy	160	0.46302993	2.13074338	2.27E-07	4387
05208	Chemical carcinogenesis - reactive oxygen species	171	0.45119553	2.10116653	4.45E-07	3298
05171	Coronavirus disease - COVID-19	164	0.44979494	2.08203431	7.15E-07	3137
04932	Non-alcoholic fatty liver disease	126	0.47776057	2.1270435	1.34E-06	4387
04141	Protein processing in endoplasmic reticulum	151	0.44915848	2.04623231	1.34E-06	3952
04714	Thermogenesis	186	0.4091782	1.92834235	1.46E-05	4611
03040	Spliceosome	119	0.4263635	1.87919261	0.00026	4806
03050	Proteasome	41	0.58408404	2.06891756	0.00041	2455
05132	Salmonella infection	213	0.35242778	1.68617077	0.0014	3663
04020	Calcium signaling pathway	176	-0.32299597	-1.66018853	0.0029	3417
05414	Dilated cardiomyopathy	77	-0.40668959	-1.82377319	0.0037	1849
05410	Hypertrophic cardiomyopathy	71	-0.41809359	-1.84231705	0.0049	1849
04217	Necroptosis	98	0.40731087	1.73779991	0.0067	2800
05211	Renal cell carcinoma	64	0.44152346	1.72682792	0.013	1336
04964	Proximal tubule bicarbonate reclamation	16	0.6645232	1.87897761	0.016	2389
03250	Viral life cycle - HIV-1	52	0.46955629	1.76028704	0.018	4066
04721	Synaptic vesicle cycle	64	0.43441051	1.69900871	0.019	2514
04140	Autophagy - animal	124	0.35193928	1.56848476	0.039	2066
04066	HIF-1 signaling pathway	89	0.39161615	1.64231698	0.042	1415


HET GELDERSCH LANDSCHAP

Chapter 5.

Molecular and epigenetic mechanisms underlying individual differences in cognitive flexibility in a songbird

Krista van den Heuvel, Beril Yildiz, Ilia Timpanaro, A. Christa Mateman, Alexander Kotrschal, Menno Creyghton, Kees van Oers

Abstract

Cognitive flexibility allows animals to adapt to environmental challenges, and this ability varies considerably between individuals within species. Understanding the causal mechanisms that underlie such individual variation is key for understanding the evolution of cognitive traits. However, while the neural mechanisms involved in cognitive flexibility are revealed, the role of epigenetic mechanisms regulating gene transcription to cause individual cognitive variation is increasingly discussed but has not been established. To address this, we assessed how chromatin accessibility and DNA methylation associate with gene expression related to natural variation in cognitive flexibility using the great tit (*Parus major*) as our model species. For this, we compared gene expression in three brain regions (striatum, hippocampus and cerebellum) between individuals with previously established high and low performance on a reversal learning task. For two of these brain regions, the striatum and hippocampus, we assessed how differential gene expression correlates with differences in chromatin accessibility. In the striatum, we additionally assessed whole-genome DNA methylation. We found brain region-specific gene expression differences between high and low reversal learners. While in the striatum we found a positive relationship between differences in chromatin accessibility and gene expression, specifically for open regions in promoter and introns, there was no such association in the hippocampus. Consequently, we additionally assessed DNA methylation in the striatum, and found that DNA methylation was associated with gene expression for CpG sites situated in the promoter and around the transcription start site. Hence, our study revealed that reversal learning-specific differences in gene expression are epigenetically regulated in a brain- and genomic region-specific way. These new insights into the molecular epigenetic underpinnings of individual variation in cognitive flexibility, is an important step towards understanding how cognitive variation is involved in the adaptation to a rapidly changing environment without changing the DNA sequence.

To be submitted to Molecular Ecology

Introduction

Epigenetic mechanisms play an essential role in experience-dependent learning processes (Shumake et al., 2009; Cholewa-Waclaw et al., 2016; Duke et al., 2017; Sun et al., 2019; Shang and Bieszczad, 2022). Epigenetic processes, such as DNA methylation and post-translational histone modifications are molecularly linked (Vaissière et al., 2008; Hashimoto et al., 2010), and can alter the transcriptional state of DNA by influencing the accessibility of chromatin at gene promoters and enhancers to transcription factors (Gibney and Nolan, 2010; Klemm et al., 2019). DNA methylation and histone modifications are both required for memory formation and synaptic plasticity (Campbell and Wood, 2019; Herre and Korb, 2019). The encoding of new memories requires distinct profiles of gene expression to promote synaptic plasticity which involves altering epigenetic states of those genomic loci (Cortés-Mendoza et al., 2013; Campbell and Wood, 2019). As such, epigenetic alterations serve as a platform for early-life experiences to alter long-term behavioural output (Bedrosian et al., 2018; Raus et al., 2023). Therefore, epigenetic mechanisms have recently become the focus for understanding individual differences in behaviour (Ledon-Rettig et al., 2013; Phelps et al., 2017; Kilvitis et al., 2018; Sweatt, 2019).

In the wild, animals constantly need to learn to discriminate among stimuli and to learn new discriminations (Shettleworth, 2010). Cognitive flexibility describes this ability to flexibly update learned predictions about cue-reward contingencies when those are altered (Izquierdo et al., 2017). Individuals vary widely and consistently in their level of cognitive flexibility performance, see Chapter 2 and (Ashton et al., 2022; De Meester et al., 2022b; Morand-Ferron et al., 2022). Despite the critical involvement of epigenetic mechanisms in associative reward learning (Day et al., 2013), only few studies have specifically addressed their role in causing variation in reversal learning performance. There is evidence that environmental interventions such as social isolation (Han et al., 2011; Benner et al., 2014) and neonatal handling (Noschang et al., 2012; Río-Álamos et al., 2019) that affect reversal learning performance, do so via epigenetic mechanisms. For example, rats that were socially isolated during early adolescence display impaired spatial reversal learning as well as altered histone acetylation at the BDNF gene and BDNF expression (Li et al., 2016). More direct evidence for the critical involvement of epigenetic mechanisms in reversal learning, comes from manipulation studies. Inhibition of DNA methyltransferase negatively affected reversal learning but not associative learning performance in honey bees (*Apis mellifera*), most likely because long-term memory formation was affected (Biergans et al., 2016). Similarly, inhibition of histone deacetylase of the dorsal striatum following associative reward learning accelerated habit formation, which requires consolidation of long-term memories, suggesting a role for striatal histone acetylation in establishing inflexible responding (Malvaez et al., 2018). Epigenetic mechanisms may contribute to long-term individual differences in cognition. However, the extent to which natural variation in reversal learning performance can be explained by epigenetic variation is currently unknown.

To better understand the mechanisms that predispose individuals to exhibit a certain cognitive flexibility phenotype, we previously compared brain gene expression in the striatum and cerebellum of fast and slow reversal learning great tits (Chapter 4). The avian striatum is homologous to the mammalian striatum (Jarvis et al., 2005) and functions in reward-based reinforcement learning (Pennartz et al., 2009; Rose et al., 2013b). The avian cerebellum is equivalent to the hemispheres of the mammalian cerebellum and functions in motor coordination and locomotion (Hall et al., 2013; Yopak et al., 2017), but there is now increasing evidence for roles of the avian cerebellum in additional cognitive functions, such as emotion, reward, and memory (Ebneter et al., 2016; Edwards et al., 2020; Katajamaa et al., 2021; Stingo-Hirmas et al., 2022), although most evidence to date comes from mammals (Pierce and Péron, 2022). In both brain regions, we found transcriptomic differences between fast and slow learning individuals, with enriched pathways in synaptic functioning in the striatum, and metabolism in the cerebellum. Here, we build on our previous study and include the hippocampus, another frequently discussed candidate region for spatial reversal learning (Epp et al., 2016; Tello-Ramos et al., 2019). The avian hippocampus is a functional and developmental homologue of the mammalian hippocampus, and well known for its role in spatial navigation and stimulus-response learning (Colombo and Broadbent, 2000; Belgard et al., 2013; Herold et al., 2022). In mammals, it is postulated that the hippocampus encodes information about the reward location (Gauthier and Tank, 2018; Karlsson et al., 2018) and that hippocampal neurogenesis plays a role in cognitive flexibility (Toda and Gage, 2018).

Variation in gene expression can have genetic origins, but as there seems to be no heritability of reversal learning performance in great tits (Chapter 2), the contribution of regulatory factors, such as epigenetic mechanisms is likely high. In songbirds, DNA methylation changes are associated with neurodevelopmental gene expression dynamics (Diddens et al., 2021) and histone modifications are associated with developmental song learning (Kelly et al., 2018). This can likely be extended to other types of synaptic plasticity. Because epigenetic differences can be explained by chromatin accessibility changes, assessing chromatin state provides a good starting point for understanding the regulatory mechanisms underlying gene expression differences between phenotypes (Grandi et al., 2022). Differences in chromatin accessibility can be compared using the assay for transposase-accessible chromatin using sequencing (ATAC-seq) (Buenrostro et al., 2015; Corces et al., 2017). As epigenetic patterns are cell-type- and brain-region-specific (Brown et al., 2008; Rizzardi et al., 2019), the epigenetic differences that play a role in cognitive variation are likely similarly specific to those regions and cells that are involved in cognitive tasks. Neuron purification by fluorescent activated cell sorting (FACS) is a useful tool to investigate molecular mechanisms of defined cell types (Lobo et al., 2006). However, to our knowledge, no studies have examined both gene expression and epigenetic differences between cellular subpopulations isolated from avian brain tissue and linked that to natural cognitive variation. Here, we addressed this knowledge gap by associating gene expression differences between fast and slow reversers with chromatin accessibility in

neuronal nuclei isolated from the striatum and the hippocampus and DNA methylation using Enzymatic methyl sequencing (EM-seq) in bulk striatal tissue of great tits (*Parus major*), selected for fast and slow reversal learning performance. We expect that differential chromatin accessibility and methylation can explain, in part, differences in gene expression between fast and slow reversal learners, mainly in the striatum.

Materials and Methods

Sample origins

Study subjects and housing

In May and June of 2018, 322 10-day old great tit nestlings were captured in a consort from in total 42 broods and transported to the aviary facilities at the NIOO-KNAW. They originated from the nest box population Boslust (Groot Warnsborn) near Arnhem, the Netherlands (5°850 E, 52°010 N), a 70 ha field site, consisting of mixed pine-deciduous forest. We hand-reared the nestlings until independence according to established methods (Drent et al., 2003). Briefly, we transferred nestlings in sibling groups of three to four birds to a compartment within a wooden box, each box containing three compartments and each compartment containing a natural parasite-free nest. Upon fledging, around 17-20 days after hatching, birds were transferred to small wire-mesh cages in groups of three. Around day 35 after hatching, they were completely independent and we transferred them to standard individual cages of 0.9 m × 0.4 m × 0.5 m with solid bottom, top, side, and rear walls, a wire-mesh front and three perches. Birds were kept under natural light conditions in acoustic and visual contact with each other.

In July, we took a blood sample for sex determination. In September, after their first moult, we transferred individuals to single-sex groups in semi-open outdoor aviaries (2 m x 4 m x 2.5 m). Food consisted of a homemade mixture of ground beef heart, egg, calcium and a multivitamin solution, supplemented with mealworms, apple, and sunflower seeds and fat balls in winter, and was available ad libitum. Birds were kept under natural light conditions, with vocal and visual contact to other birds. In October, when birds were full-grown, we measured tarsus.

Reversal learning assessment

From October 2018-February 2019, birds were tested for associative and reversal learning performance to assess their cognitive flexibility. As part of a larger study (Chapter 2), all individuals were subjected to two additional rounds of testing, in February 2020 and September 2020. We used automated feeders to assess learning performance, using a three-choice spatial learning procedure as described in Chapter 2. Briefly, eight days prior to testing, individuals were habituated to use the feeders under standard housing conditions in semi-open outdoor aviaries. After habituation, we caught individuals from the group, weighed them, and released them individually in a testing aviary. In the testing aviary, water was available ad libitum while no food was available during the test, in order to maintain motivation to take part in the learning test.

During the experiment, one feeder at a time provided a reward (freeze-dried mealworm) in a triangular array with two other unrewarding feeders, requiring individuals to learn the location of the rewarded feeder. Individuals were first trained to go to an assigned feeder, which was reinforced until individuals reached a criterion level of six correct trials out of seven. This success rate is significantly different from the expectation if birds selected feeders at random (binomial test, $p < 0.01$). A trial was defined as a landing on the perch with the RFID antenna. After completing the associative learning phase, the reversal learning task began as the reward contingencies were reversed to one of the other two feeders. Again, birds had to reach the learning criterion of six correct visits across seven trials to the new feeder. Individuals had from 09:00 until 15:00 to complete both phases of the test. For further details of the test setup, see Chapter 2.

Reversal learning performance was scored as the total number of trials required to reach the learning criterion (six correct visits out of seven subsequent trials). Selected slow individuals needed more trials to finish the reversal learning task compared to fast individuals ($p = 0.007$, Supplementary Figure 5.1). After the last reversal learning test, animals were housed under standard group housing conditions without handling.

Tissue collection

Based on their mean performance across the three reversal learning tests, four unrelated fast and slow performing males were selected for comparative gene expression analysis. Four weeks after the last reversal learning task, individuals were caught from the aviaries and deeply anaesthetized with isoflurane (IsoFlo, Zoetis, Kalamazoo, MI, USA). After decapitation, the brain was dissected out and placed in ice cold PBS for further micro dissection of the cerebellum, and bilateral dissection of striatum (including area X) and hippocampus. Brain regions were located by the use of the online zebra finch brain atlas (Karten et al., 2013) ZEBrA (Oregon Health & Science University, Portland, OR, USA; http://www.zebrafinchatlas.org). Isolated tissue was flash-frozen in liquid nitrogen in 1.5 ml RNA-free tubes and stored at −80°C until RNA isolation.

Nuclei isolation

Frozen brain tissue was pulverized with mortar and pestle on dry ice to yield ~0.2 mL of tissue powder, the rest of the tissue powder was saved for DNA extraction. Tissue powder was homogenized in a glass douncer (Kontes Glass Co.) in 0.5 ml EZ buffer (Nuclei Isolation Kit, Sigma NUC101) and incubated for 5 min on ice. Subsequently samples were centrifuged for 15 min at 65 × g at 4 °C, resuspended in 0.5 mL EZ buffer and incubated on ice for 5 min. Samples were again centrifuged for 15 min at 65 × g at 4 °C, resuspended in 0.5 mL nuclear suspension buffer (NSB; 0.01% BSA, 1× complete protease inhibitor cocktail in PBS) and filtered through a 40 µm cell strainer. Samples were centrifuged for 15 min at 65 × g at 4 °C and resuspended in 0.5 mL NSB.

Striatum and hippocampus
For nuclei collected from the striatum and hippocampus, 1:1000 Hoechst 34580 (1 µg/ml, Fisher Scientific H21486) was added to blocking solution (1% BSA, 10% normal mouse serum (NMS) in PBS) and incubated light shielded at 4 °C for 20 min. 10% of the blocked sample was used as unstained control, the remaining 90% was stained with 1:1500 anti-NeuN antibody conjugated with Alexa488 (1:1000, Merck Millipore MAB377X) without washing and incubated for 1 h at 4 °C on a roller, protected from light. Stained nuclei were then transferred to FACS tubes precoated with 3% BSA and FACS-sorted on NeuN signal using a BD FACSAria II (BD Bioscience). 5,000 neuronal (NeuN+ stained) and 5000 non-neuronal (NeuN− stained) nuclei were collected in 100 µl Trizol each for RNA-sequencing. 60,000 NeuN+ and NeuN− stained nuclei were collected in NSB and processed further for ATAC-sequencing (see below). In this study, we only used neuronal cells for further analysis.

Cerebellum
Bulk nuclei from cerebellar tissue (which consists of >80% neurons (Olkowicz et al., 2016)) were stained with trypan blue and counted on a hemacytometer. 50,000 nuclei were processed further for ATAC-sequencing, 5,000 nuclei were pelleted by 10 minutes centrifugation at 500g and resuspended in 100 µl Trizol for RNA-sequencing.

RNA-sequencing
RNA-sequencing was performed at Single Cell Discoveries, a (single cell) sequencing provider located in the Netherlands using an adapted version of the CEL-seq protocol. In brief: Total RNA was extracted using the standard TRIzol (Invitrogen) protocol and used for library preparation and sequencing. mRNA was processed as described previously, following an adapted version of the single-cell mRNA seq protocol of CEL-Seq (Simmini et al., 2014; Hashimshony et al., 2016). In brief, samples were barcoded with CEL-seq primers during a reverse transcription and pooled after second strand synthesis. The resulting cDNA was amplified with an overnight In vitro transcription reaction. From this amplified RNA, sequencing libraries were prepared with Illumina Truseq small RNA primers. Paired-end sequencing was performed on the Illumina Nextseq500 platform with a sequencing depth of 10 million reads/sample. All reads were trimmed of adapters and low quality bases using *fastx* and sequencing quality was checked using the software *FastQC* (v0.11.9) (Andrews, 2010). Trimmed reads were mapped to the *Parus major* reference genome (Ensembl Assembly Parus_major1.1: GCA_001522545.2, (Laine et al., 2016)) using *Hisat2* v2.2.1 (Kim et al., 2019) with default parameters. To summarize gene level read counts, we used the *featureCounts* program from the *Subread* package v2.0.2 (Liao et al., 2014).

Principal component analyses on RNA-seq data
Using *DESeq2* v1.38.0 (Love et al., 2014), low count genes were pre-filtered using a cut-off of 10 normalised counts in >75% of the samples, before they were normalized with post-filtering library sizes and log2 transformed using the *rlog*

function. Following normalization, we performed Principle Component Analysis (PCA) using *DEseq2* with the function *plotPCA* to visualize clustering of the samples and to spot individual sample outliers that separated significantly based on size factor (reflecting library size and/or RNA composition bias). These samples were then removed and the filtering and normalization steps were repeated. Sample sizes were therefore different than what we initially started with and included two fast and two slow reversal learners for the striatum, four fast and four slow for the hippocampus and three fast and two slow for the cerebellum. An overview of the final sample selection and the library qualities can be found in Supplementary Table 5.1 and 5.2. In order to visualize principal sources of variation in the data, we performed a final PCA analysis and visualized the first two principal components (PCs) with the *DEseq2* function *plotPCA*, applying the default setting limiting the analysis to the top 500 most variable genes. Additional PCs were obtained using the *prcomp* function in R. We also plotted the percent variance explained by each PC. We tested for brain region and learning group differences in principal components using the *correlate PCs* functions in *pcaExplorer*, which computes the significance of correlations between PCA scores and the experimental covariates.

Differential gene expression analysis
Differences in gene expression within each brain region were calculated using *DESeq2*. To control for the false discovery rate due to multiple testing, p-values were adjusted using the Benjamini-Hochberg (BH) procedure. Genes were considered as statistically differentially expressed if they displayed a 1-fold enrichment with adjusted p-values < 0.05. The volcano plots were generated using *EnhancedVolcano* v1.16.0 (Blighe, 2018), boxplots for a subset of the differentially expressed genes (DEGs) were prepared using *ggplot2* v3.4.0 (Wickham, 2016) and a heatmap of differential expression of DEGs across brain regions was prepared using *pheatmap* 1.0.12 (Kolde, 2019).

Correlation between differences in gene expression across brain regions
To assess to what extent differences in gene expression were correlated across brain regions, we plotted the log2Foldchange in one brain region against both other brain regions in each pairwise comparison and calculated Pearson correlation scores, after trimming the dataset by excluding genes with a change in expression (in log2FoldChange) of smaller than 1.

Gene ontology analyses on differential gene expression
To identify significantly enriched gene ontology (GO) and Kyoto Encyclopedia of Genes and Genomes (KEGG) terms, we used *clusterProfiler* v4.6.0 (Yu et al., 2012) to perform Gene Set Enrichment Analysis (GSEA) of GO "Biological Processes" and KEGG pathways. GSEA does not require delineation of DEGs from non-differential genes. Instead, we ranked the test statistic of all assessed genes to test for significantly coordinated shifts in gene pathways, as suggested by (Zyla et al., 2017). We used the human gene ontology database. Great tit genes were mapped to their corresponding human orthologs based on HUGO Gene Nomenclature Committee (HGNC) symbol. Genes that could not be assigned to a human gene were

excluded, and therefore great tit-specific genes are missing from these analyses. All functional category enrichment analyses considered an adjusted p-value < 0.05 after BH correction to be significant.

Assay for transposase-accessible chromatin using sequencing (ATAC-seq)
OMNI-ATAC was performed according to an adapted protocol from Corces *et al.*, (2017). In short, 0.1% NP-40 was added to the nuclei and samples were centrifuged for 15 min at 500 × g at 4 °C. Nuclei were resuspended in 50 µl transposition mix (25 µl TD buffer (20 mM Tris-HCl pH 7.6, 10 mM $MgCl_2$, 20% dimethyl formamide in MQ), 2.5 µl Tn5 transposase, 16.5 µl PBS, 0.5 µl NP-40 1%, 10% Tween-20 / Triton-X, 0.5 µl, 5 µl MQ) and incubated for 30 min at 37 °C while shaking at 1000 rotations per minute. Samples were purified using Qiagen MinElute PCR purification kit (Qiagen 28004) and eluted in 21 µl MQ. Purified DNA was amplified with NEBnext High-Fidelity PCR master mix (NEB M0541S) and appropriate sequencing adapters for five PCR cycles. Library complexity was determined by qPCR on 5 µl of the PCR sample and the number of extra PCR cycles determined (Buenrostro et al., 2015). PCR samples were purified using AMPure XP beads (Agencount A63881), eluted in 12 µl MQ and sequenced at USEQ on a high-output NextSeq500, 1× 75 bp.

We trimmed reads of the Nextera adapter sequences using *trim-galore* v0.6.6 (Krueger, 2023). We then mapped trimmed reads to the *Parus major* reference genome (NCBI Assembly Parus_major1.1: GCF_001522545.3) using *Bowtie2* v2.4.4 (Langmead and Salzberg, 2012), with standard parameters and a maximum fragment length of 2,000. *Samtools* v1.12 (Danecek et al., 2021) was then used to remove unmapped, low quality (keeping MAPQ ≥ 20), duplicate and mitochondrial reads from further analysis. We only continued analysis with samples with fraction of reads in peaks (FRiP) scores exceeding the 1% threshold. Sample sizes were therefore different than what we initially started with and included two fast and two slow reversal learners for the striatum and three fast and three slow reversers for the hippocampus. An overview of the final sample selection can be found in Supplementary Table 5.3. The mean percentage of unique reads of the final selected samples was 77.32%. Accessible regions were defined using *MACS2* (Zhang et al., 2008) on each bam file to call narrow peaks (with options -g 1.00229e9 -q 0.01). Identified open chromatin regions were extended to a minimum size of 1000 bp (peak center ± 500 bp). Lists of open chromatin regions per brain region were obtained by merging the identified regions of the individuals per tissue, with regions overlapping at least 1 bp being stitched together, to construct a 'consensus' set of open chromatin regions. This resulted in 89,385 peaks for neuronal nuclei from the striatum and 104,635 peaks for neuronal nuclei from the hippocampus. For each sample, we then counted the number of reads overlapping each of the 'consensus' peaks using the *coverageBed* function in the *BEDtools* package v2.24.0 (Quinlan and Hall, 2010).

Principal component analyses on ATAC-seq data
Using *DESeq2* v1.38.0 (Love et al., 2014), read counts were normalized with post-filtering library sizes and log2 transformed using the *rlog* function. Following normalization, we performed Principle Component Analysis (PCA) using the *DEseq2* function *plotPCA* to visualize clustering of the samples and spot individual sample outliers. In order to visualize principal sources of variation in the data, we performed a final PCA analysis and visualized the first two principal components (PCs) with the *DEseq2* function *plotPCA*, applying the default setting limiting the analysis to the top 500 most variable peaks. Additional PCs were obtained using the *prcomp* function in R. We also plotted the percent variance explained by each PC. We tested for brain region and learning group differences in principal components using the *correlate PCs* functions in *pcaExplorer*, which computes the significance of correlations between PCA scores and the experimental covariates.

Differential chromatin accessibility analysis
Phenotype-specific accessible regions within each brain region were calculated using *DESeq2*. ATAC-seq peaks were considered differentially accessible regions (DARs) if they displayed a 1-fold enrichment with an Benjamini-Hochberg adjusted p-value <0.05. Volcano plots were generated using *EnhancedVolcano* v1.16.0 (Blighe, 2018).

Association of chromatin accessibility with gene expression
We used *annotatePeak* from the *ChIPseeker* package v1.34.0 (Wang et al., 2022) to annotate ATAC-seq peaks to genomic regions, following the priority order: Promoter (1,000 bp upstream to 1,000 bp downstream of the annotated transcription starting position), 5'UTR, 3'UTR, Exon, Intron, Downstream (the downstream of gene end) and Intergenic. Peaks were assigned to the nearest gene based on *Parus major* genome assembly. In order to evaluate the association between differential chromatin accessibility and differences in gene expression, we plotted the difference in gene expression (in log2Foldchange) against log2Foldchange in chromatin accessibility and calculated Pearson correlation scores, after trimming the dataset by excluding regions with a change in accessibility (log2Foldchange) < 0.5 and genes with a change in expression (log2Foldchange) < 0.5. To understand the effect of the genomic location on the relationship between differential chromatin accessibility and gene expression, we differentiated between genomic locations. Furthermore, we divided each plot in four quadrants of association: higher accessibility and gene expression in fast learners (NE), higher accessibility and lower gene expression in fast learners (NW), higher accessibility and gene expression in slow learners (SW) higher accessibility and lower gene expression in slow learners (SE). As the NE and SW quadrant would relate to changes in the predicted directions (based on the expectation that accessibility and expression are positively correlated), we tested whether the number of accessible regions in the NE and SW quadrant significantly exceeded the total number of accessible regions using binomial tests for each genomic region.

Gene ontology analyses on differentially accessible regions
Gene ontology analysis was performed using *clusterProfiler* v4.6.0 (Yu et al., 2012) to perform Over Representation Analysis (ORA) of GO pathways on genes that contained DARs. Additionally, we performed ORA to determine which biological functions were enriched in genes in the NE and SW quadrants for each genomic region. We used the human gene ontology database. Great tit genes were mapped to their corresponding human orthologs based on HUGO Gene Nomenclature Committee (HGNC) symbol. Genes that could not be assigned to a human gene were excluded, and therefore great tit-specific genes are missing from these analyses. All functional category enrichment analyses considered an adjusted p-value < 0.05 after BH correction to be significant.

Enzymatic Methyl-sequencing (EM-seq)
We assessed genome-wide DNA methylation levels of bulk striatal tissue using EM-seq. We extracted DNA from tissue powder (as described under *Nuclei isolation*) using the MagAttract HMW DNA Kit (Qiagen) according to manufacturer's protocol. Sample libraries were prepared by Roy J. Carver Biotechnology Centre, University of Illinois at Urbana-Champaign with the NEBNext Enzymatic Methyl-seq Kit (Vaisvila et al., 2021). The libraries were pooled, quantitated by qPCR and paired-end sequenced on an Illumina NovaSeq 6000 (Modi et al., 2021) in two SP lanes with 2x150nt reads.

Demultiplexing, quality control and trimming
Raw reads were demultiplexed with Illumina's *bcl2fastq* v2.20 Conversion Software (RRID: SCR_015058), and adapters and short reads (<20 bp) were removed. An additional three bp were removed from the 5' end of the forward and reverse reads. Quality improvement of the reads was verified by *FastQC* v0.11.9 (Andrews, 2010), *FastQ-Screen* v0.15.0 (Wingett, 2022) and *MultiQC* v1.11 (Ewels et al., 2016). An overview of reads and mapping efficiency is provided in Supplementary Table 5.4.

Alignment and methylation calling
Bismark v0.22.3 (Krueger and Andrews, 2011) was used to align the trimmed reads to the *Parus major* reference genome (Ensembl Assembly Parus_major1.1: GCA_001522545.2) and to call methylation. We aligned the reads in paired-end mode. Methylation calling was also done using *Bismark* in paired-end mode and overlap between read pairs was using the -no overlap option to prevent double scoring or overlapping methylation calls. Methylation was called in CpG context.

Filtering of methylation calls
The R package *methylKit* v1.16.1 (Akalin et al., 2012) was used to read the datafiles into Rstudio, to merge complementary CpG dinucleotides. Next, CpG sites (CpGs) with a low coverage (<10x), a mean methylation level (the number of methylated Cs divided by the coverage of that site) of lower than 5% or higher than 95% and very high coverage (> 99.9th percentile) were removed, in that order. This resulted

in a total of 6.035.888 CpGs out of 15.116.607 that remained after filtering (Supplementary Table 5.5).

Differential methylation analysis
To check for outliers, we generated a correlation matrix using the *getCorrelation* function, performed hierarchical cluster analysis using the *clusterSamples* function, and conducted a principal component analysis (PCA) the default settings of the *PCASamples* function in *methylKit* (Supplementary Figure 5.5a-d). To test for differentially methylated sites (DMS) between fast and slow reversal learning individuals, we conducted a differential methylation analysis, using the *calculateDiffMeth* function in *methylKit*. We considered a site significantly differentially methylated when the difference in methylation between groups> 25% and a padj value < 0.05.

Gene annotation
Using USCS' *gff3toGenePred* and *GenePredtoBed* command-line applications, Ensembl's great tit GFF3 genome annotation file was converted to BED format. This was used as input for genomation's *readTranscriptFeatures* function to create a gene annotation object. The gene annotation object was used as input for genomation's *annotateWithGeneParts*, *getAssociationWithTSS* and *getMembers* functions function to annotate the overlap of CpGs to genomic regions (TSS (300 bp upstream - 50 bp downstream of the annotated transcription start site), promoter region (2000 bp upstream - 200 bp downstream of the annotated transcription start site) and gene body (exons and introns).

Association of gene body methylation with gene expression and chromatin accessibility
We used *pheatmap* 1.0.12 (Kolde, 2019) to create a heatmap to display the average methylation difference for CpG sites located with the TSS region of each DEG, as well as the average log2Foldchange of the peaks located within the promoter of each respective DEG. In addition, we created a heatmap to display the average methylation difference for CpG sites located within DARs.

In order to evaluate the association between differential gene expression and differential methylation we calculated Pearson correlation scores. We trimmed the dataset by excluding CpG sites with a methylation difference <25% and genes with a change in expression (log2Foldchange) <1. To understand the effect of the genomic location on the relationship between differential chromatin accessibility and gene expression, we differentiated between TSS region, promoter region and gene body. Furthermore, we divided each plot into four quadrants of association: hypomethylation and higher gene expression in slow learners (NE), hypomethylation and lower gene expression in slow learners (SE), hypomethylation and higher gene expression in fast learners (SW), and hypomethylation and lower gene expression in fast learners (NW). As the NE and SW quadrant would relate to changes in the predicted directions (based on the expectation that DNA methylation and gene expression are negatively correlated),

we tested whether the number of observations in the NE and SW quadrants significantly exceeded the total number of methylation-gene associations using binomial tests, for each genomic region.

Gene ontology analyses on differentially methylated sites
We performed ORA analysis on the DMS to explore which functional groups (GO terms) are over-represented in fast and slow reversal learners and possibly linked to reversal learning performance. GO analysis was performed using *ClusterProfiler* as described above. We used human gene ontologies with three background gene set lists, which were all the genes covered by filtered CpG sites (14832 genes), promoter regions covered by CpG sites (13562 genes) and TSS regions covered by CpG sites (7385 genes).

Results

Brain region specific differences in gene expression between fast and slow reversal learning individuals

A PCA analysis showed that gene expression data from striatal neurons, hippocampal neurons and cerebellar bulk nuclei clustered the samples strongly by brain region for PC1 (p = 0.006) and PC2 (p=0.001), but not by reversal learning performance (Supplementary Figure 5.2). Also, in PCA analyses for each brain region separately we found no significant clustering of reversal learning types (Supplementary Figure 5.3), indicating no global gene expression differences between fast and slow reversal learning types. In a differential gene expression analysis, we found more subtle differences between fast and slow reversal learners. Three transcripts in striatum, three in hippocampus, and four in the cerebellum were differentially expressed between the reversal learning types (Figure 5.1).

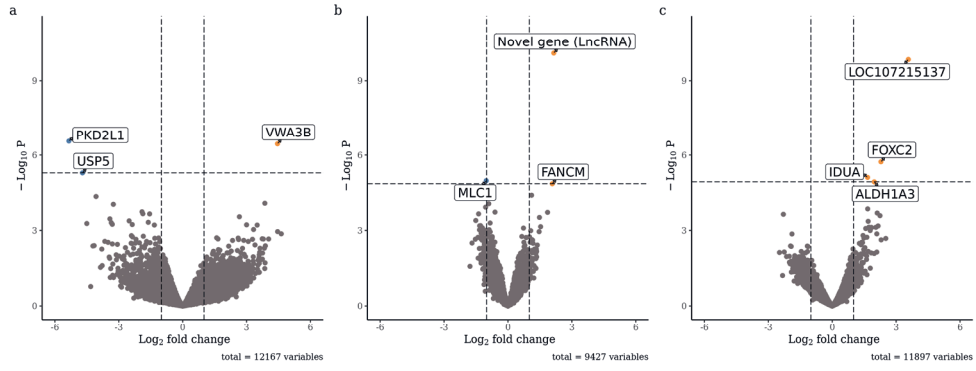

Figure 5.1 Gene expression differences in three brain regions of fast and slow reversal learning great tits. *Volcano plots highlighting the genes that are differentially expressed between fast and slow reversal learning great tits in three brain regions, where the cut-off for significance (red dots beyond the dashed lines) is p < 0.05 with false-discovery rate correction and a log-fold change of one or greater. (a) Striatum, (b) Hippocampus, (c) Cerebellum*

In the striatum, expression of *USP5* (log2FC = -4.71, adjusted p-value = 0.020) and *PKD2L1* (log2FC = -5.34, adjusted p-value = 0.002) was upregulated in fast learning individuals, whereas ENSPMJG00000015246, which overlaps the gene *VWA3B* (log2FC = 4.45, adjusted p-value = 0.002), was upregulated in slow learning individuals (Figure 5.2a). In the hippocampus, *MLC1* was upregulated (log2FC = -1.02, adjusted p-value = 0.04) and two novel genes downregulated in fast compared to slow learning individuals; one long non-coding RNA (LncRNA; ENSPMJG00000013724: log2FC = 2.15, adjusted p-value < 0.001); and ENSPMJG00000013908, which overlaps the gene *FANCM*: log2FC = 2.08, adjusted p-value = 0.04) (Figure 5.2b). In the cerebellum, the four DEGs were all upregulated in slow learners: *IDUA* (log2FC = 1.66, adjusted p-value = 0.03), *ALDH1A3* (log2FC = 1.97, adjusted p-value = 0.035), *FOXC2* (log2FC = 2.29, adjusted p-value = 0.01) and a transcript (ENSPMJG00000000917) that overlaps the keratin, type I cytoskeletal 14 gene (NCBI *LOC107215137;* log2FC = 3.57, adjusted p-value < 0.001; Figure 5.2c).

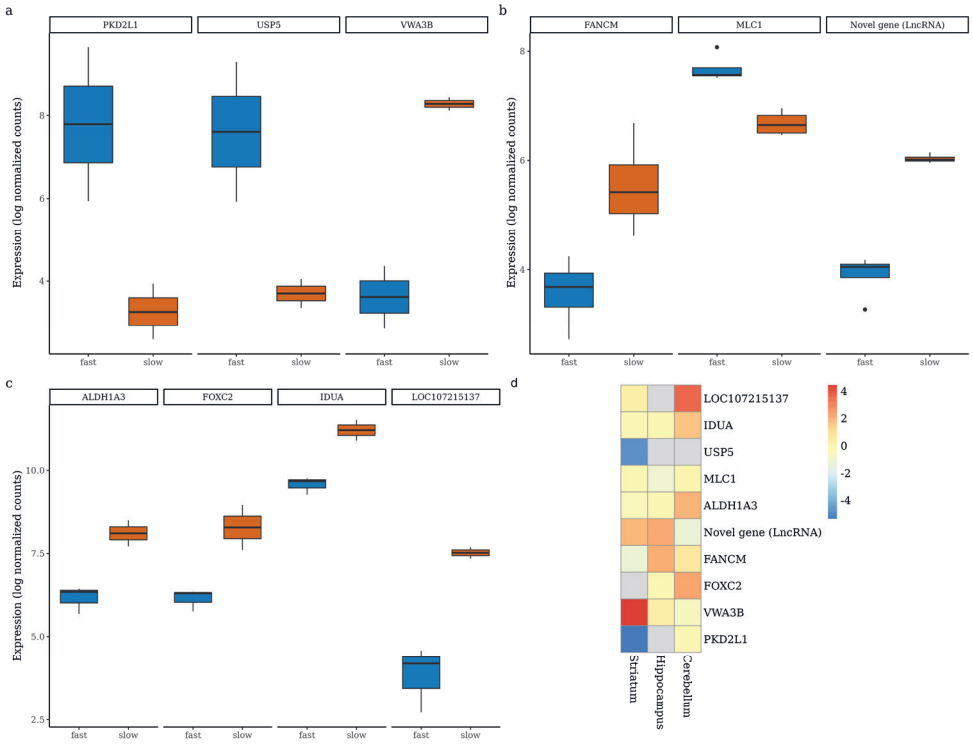

Figure 5.2 Differentially expressed genes between fast and slow reversal learning great tits in three brain regions. *Shown as boxplots, with rectangles as the lower and upper quartiles (with the median as the line) and whiskers that indicate the maximum and minimum values. (a) Striatum, (b) Hippocampus, (c) Cerebellum. Blue = higher expressed in fast reversers, orange = higher expressed in slow reversers. (d) A heatmap shows log fold change of differentially expressed genes across all brain regions.*

There was no overlap in DEGs across the brain regions (Figure 5.2d) indicating brain region-specific differences between reversal learning types. Nonetheless, gene expression differences between slow and fast reversal learners showed correlations across the three brain regions. Expression differences in the striatum were positively correlated with expression differences in the hippocampus (r = 0.25, p < 0.001, Figure 5.3a), but negatively correlated with expression differences in the cerebellum (r = -0.25, p < 0.001, Figure 5.3b). Similarly, gene expression differences in the hippocampus neurons were negatively correlated with expression differences in the cerebellum (r = -0.19, p < 0.0001, Figure 5.3c). This suggests opposite involvement of genes in the hippocampus and striatum with the cerebellum.

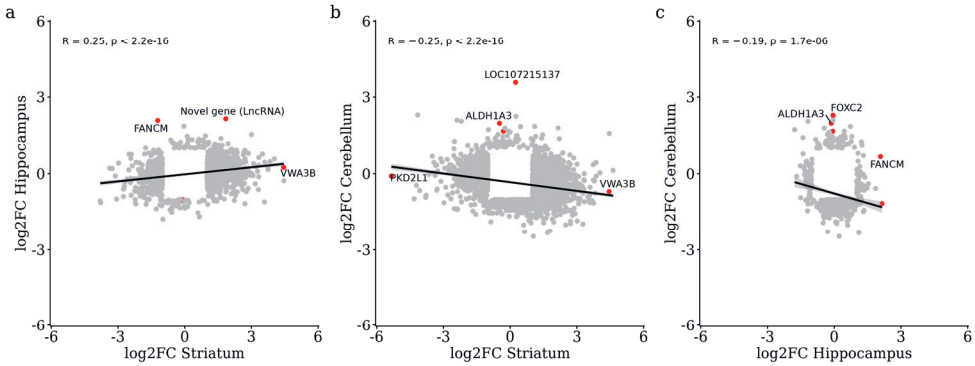

Figure 5.3 Relationship between differences in gene expression between fast and slow reversal learners across brain regions. *Pearson correlation of differences in gene expression (log2Foldchange >1) in (a) striatum versus hippocampus, (b) striatum versus cerebellum and (c) hippocampus versus cerebellum. Genes with adjusted p-value < 0.05 are depicted in red. R and p values are based on Pearson correlation, line is the regression line.*

Gene ontology analyses of differentially expressed genes

To gain insight into the biological relevance of reversal learning-related transcriptional profiles from the different tissues, we performed Gene Set Enrichment Analysis (GSEA) to test for significantly enriched GO and KEGG terms. Enriched terms were rather different across brain regions (summarized in Figure 5.4; top 30 GO and KEGG terms are reported in Supplementary Tables 5.13-16). Significant terms unique to the striatum and upregulated in fast learners (102 terms in total) were GO terms related to axon development, neuron differentiation and glutamate signalling, upregulated in slow learners (12 terms) were GO terms related to lipid metabolism. The striatum KEGG terms were related to glutamatergic synapse and neurodegeneration in fast learners and cholesterol metabolism in slow learners. Unique GO terms to the hippocampus and upregulated in fast learners (2 terms in total) were fatty acid and monocarboxylic acid metabolic process, and the KEGG term spliceosome, GABAergic synaptic transmission was uniquely upregulated in the hippocampus slow learners (3 terms in total). Unique to the cerebellum of fast learners (53 terms in total) were GO enrichments related to axoneme assembly and sensory perception, and KEGG

terms neuroactive ligand-receptor interaction and starch and sucrose metabolism. Unique to slow learners (31 terms in total) were GO enrichments related to mRNA processing and ATP synthesis and KEGG enrichments related to ribosome, oxidative phosphorylation and Parkinson disease. The striatum and hippocampus overlapped in two terms related to synaptic signalling, though the direction of change is opposite. The striatum and cerebellum overlapped in GO terms related to RNA splicing, cilium assembly and cell projection assembly, as well as KEGG term prion disease, both with an opposite direction of change. There was no overlap in GO or KEGG enrichments between hippocampus and cerebellum.

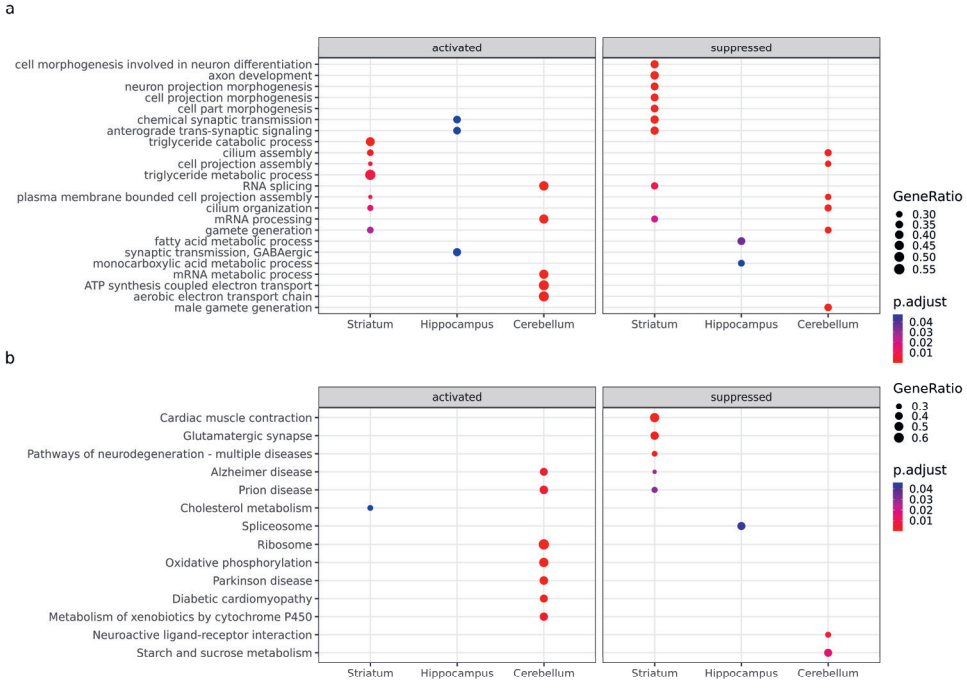

Figure 5.4 Gene-set enrichment analysis of differential expression between fast and slow reversers *(a) Enriched GO terms (biological process) and (b) KEGG terms in the transcriptome of striatum, hippocampus and cerebellum of fast and slow reversal learning great tits. Gene ratio (dot size) represents percentage of core enrichment genes in the given term, and significance (colours) is based on Benjamini-Hochberg adjusted p-values (FDR).*

Brain region-specific differences in chromatin accessibility between fast and slow reversal learning individuals

A PCA analysis showed that PC1 explained 49% and 54%, and PC2 explained 32% and 14% of the variation in chromatic openness respectively for striatum and hippocampus, but we found no clustering among reversal learning types (Supplementary Figure 5.4). Most called peaks fall within distal intergenic, introns and promoter regions. These patterns were very comparable between hippocampus and striatum. (Figure 5.6a and Figure 5.7a, Supplementary Table 5.7 and 5.8). In both brain regions, we evaluated each of the open chromatin regions

for differences in accessibility between phenotypes. In the striatum, 14 chromatin regions were differentially accessible between fast and slow reversing individuals (Figure 5.5a, Supplementary Table 5.6). We found no significant differences between fast and slow reversing individuals in chromatin accessibility in the neurons of the hippocampus (Figure 5.5b).

To examine the function of the 14 DARs in the striatum, we related them to the nearest annotated gene in order to identify biological functions associated with the open chromatin regions. Two regions fell into an intron; one in lysine demethylase 4C (*KDM4C*), and one in secreted phosphoprotein 2 (*SPP2*). The other 11 regions fall into distant intergenic regions, which we annotated to the nearest gene: *DHX35*, *GALNT9*, *NT5E*, *FCHO2*, *CHMP2B* and several LOC genes of which two partially overlap a gene (LOC117244170 overlaps *DUSP10*, LOC107202428 overlaps *TMEM18*), three overlap a lncRNA (LOC117244115, LOC107201404, LOC107209066) and one does not overlap any known gene (LOC117245467). Performing over-representation GO analyses on the total set of 14 genes with DARs in the striatum, did not result in any significantly enriched GO terms. Furthermore, there was no overlap between genes that contain differentially accessible regions and DEGs.

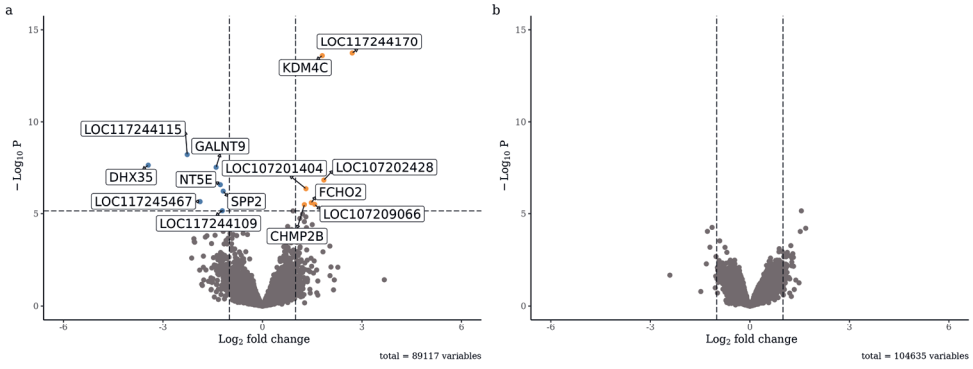

Figure 5.5 Chromatin accessibility differences in the striatum and hippocampus of fast and slow reversal learning great tits. *Volcano plots highlighting regions that are differentially accessible between fast and slow reversal learning great tits, where the cut-off for significance (red dots beyond the dashed lines) is $p < 0.05$ with false-discovery rate correction and a log-fold change of one or greater. (a) Striatum, (b) Hippocampus.*

Associations between differences in chromatin accessibility and gene expression in striatum and hippocampus

To evaluate the impact of phenotype-specific chromatin accessibility on gene regulation, we examined the correlation between gene expression and open chromatin regions on a global level as well as at each genomic functional region (Figure 5.6 and Figure 5.7 for respectively striatum and hippocampus). We distinguished between open chromatin regions mapped to different functional elements such as gene bodies, promoters, and distal regulatory elements.

For striatum, we observed a low but significant positive correlation between differential gene expression and chromatin accessibility when we combined data from all functional regions (r = 0.096, p = 0.023; Figure 5.6b), with significantly more points falling into the two quartiles (NE and SW) with a positive relationship between gene expression and accessibility (Supplementary Table 5.9). When including only promoter regions, we found a trend for a positive correlation at the promoter region (r = 0.35, p = 0.062; Figure 5.6c), but not significantly more associations fall in to the expected quartiles. The same pattern is visible for DARs of the intron region (r = 0.14, p = 0.047; Figure 5.6d), with significantly more regions falling into the expected quartiles. In contrast, there is no evidence that these patterns are present for the DARs that were present in distal intergenic regions, exons, 5 'UTR or 3' UTRs (Supplementary Table 5.9).

No terms were enriched when restricting GO analysis on the striatal neuronal genes that were in the expected quartiles (NE and SW), when including all functional regions. When focusing on the promoter regions, we find eight significantly enriched terms, all related to neurotransmitter receptor activity (Supplementary Table 5.17). For genes that were in the expected quadrants of the intron regions, we found one enriched term, muscle structure development (Supplementary Table 5.17). For hippocampus, we find no evidence for any correlation between chromatin accessibility and gene expression (Figure 5.7b-e, Supplementary Table 5.10).

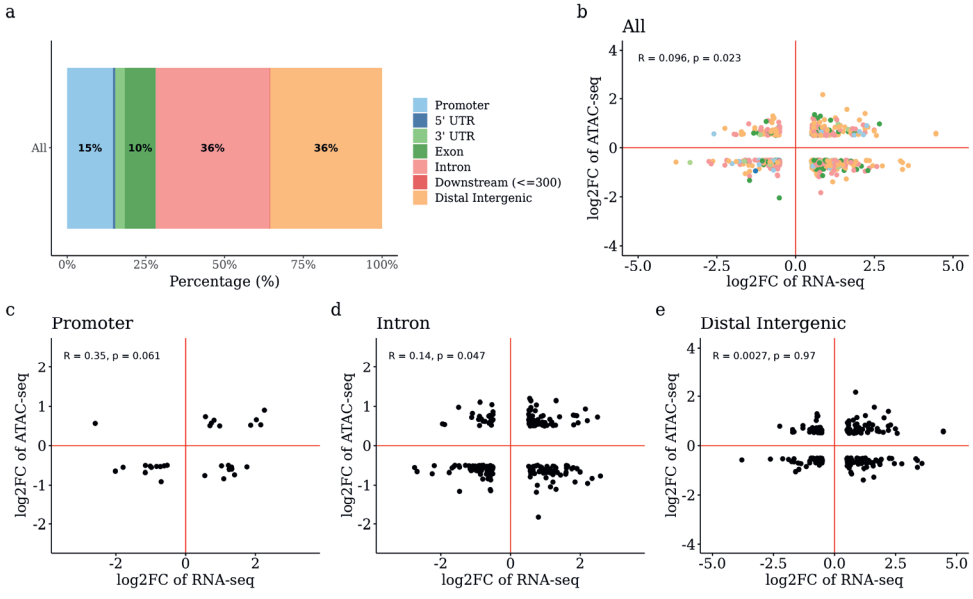

Figure 5.6 Relationship between differential chromatin accessibility and gene expression in striatum. *a) Bar plot representing the fraction of accessible regions assigned to each genomic region b-e) Pearson correlation of differences in gene expression (log2Foldchange >0.5) and chromatin accessibility (log2Foldchange >0.5) in the striatum for the indicated genomic regions (Promoter; Intron; Distal Intergenic). Each plot is divided into four quadrants corresponding to*

distinct functional groups of DARs. The NE and SW quadrants represented slow- and fast-specific DARs, respectively, associated with high expression. By contrast, the SE and NW quadrants comprised slow- and fast -specific DARs, respectively, associated with low expression. Note the different x and y axis in frames b and e versus c and d.

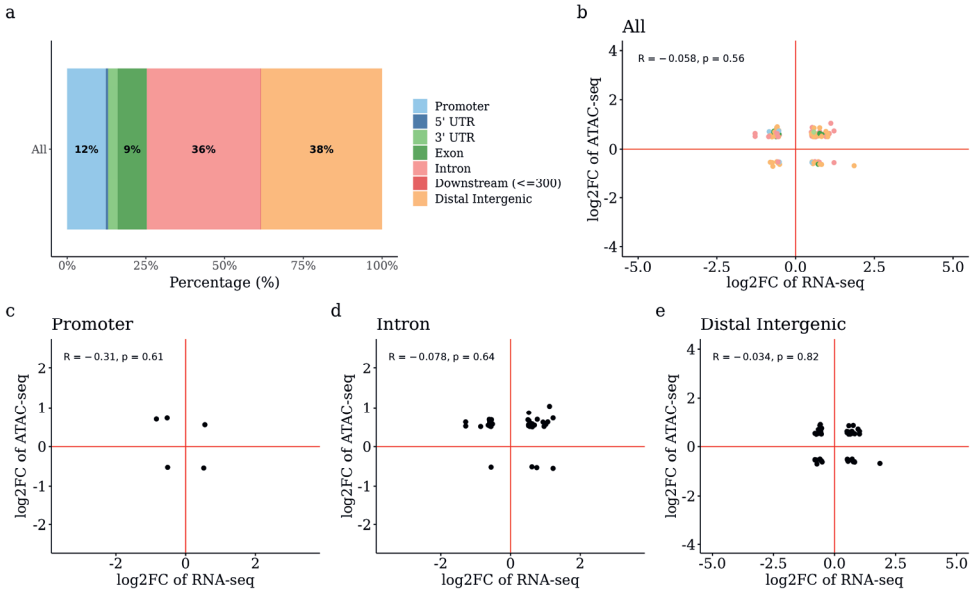

Figure 5.7 Relationship between differential chromatin accessibility and gene expression in hippocampus. *a) Bar plot representing the fraction of accessible regions assigned to each genomic region b-e) Pearson correlation of differences in gene expression (log2Foldchange >0.5) and chromatin accessibility (log2Foldchange >0.5) in the striatum for the indicated genomic regions (Promoter; Intron; Distal Intergenic). Each plot is divided into four quadrants corresponding to distinct functional groups of DARs. The NE and SW quadrants represented slow- and fast-specific DARs, respectively, associated with high expression. By contrast, the SE and NW quadrants comprised slow- and fast -specific DARs, respectively, associated with low expression. Note the different x and y axis in frames b and e versus c and d.*

DNA methylation

To evaluate how DNA methylation variation associates with gene expression, we identified reversal learning phenotype-specific CpG site methylation of bulk striatal tissue. A PCA analysis of methylation information revealed that PC1 explained 37% of the variance, PC2 33% and PC3 30%, but samples did not cluster strongly by reversal learning type (Supplementary Figure 5.5). Regardless of the lack of a global methylation difference between the reversal learning types, 4.551 of the 2,816,097 CpG sites that we covered in this dataset showed a significant difference in DNA methylation between fast and slow reversing individuals. Of these, 133 CpG sites were situated near the promoter, of which 15 CpG sites were situated near the transcription start site of a gene, these are reported in Supplementary Table 5.12.

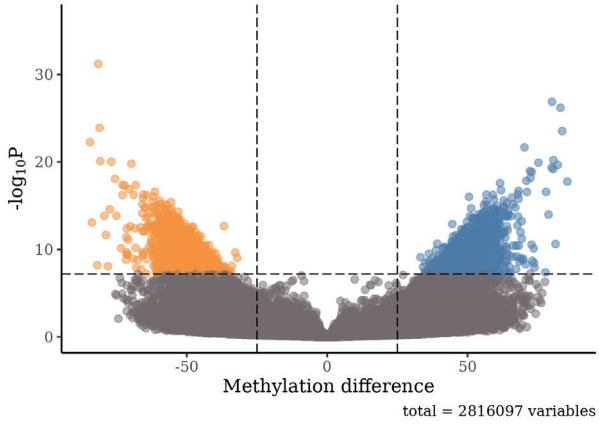

Figure 5.8 DNA methylation differences in the striatum and hippocampus of fast and slow reversal learning great tits. *Volcano plot highlighting the CpG sites that are differentially methylated between fast and slow reversal learning great tits in the striatum, where the cut-off for significance is p < 0.05 with false-discovery rate correction and a methylation difference of 25 or greater. Blue = hypermethylated in fast versus slow reversers. Orange = hypermethylated in slow versus fast reversers.*

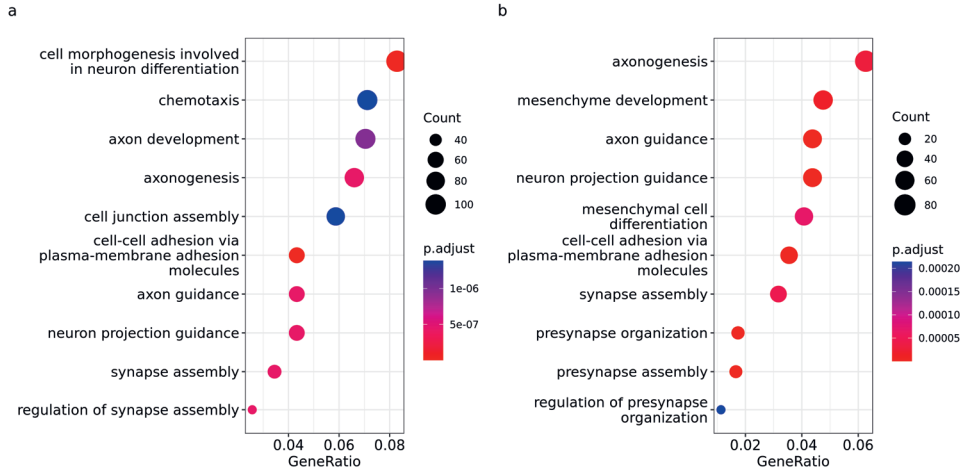

Figure 5.9 Over representation analysis of GO terms enriched in genes related to differentially methylated sites. *Top 10 GO terms (biological process) are shown for genes related to CpG sites that are hypermethylated in (a) fast reversers and (b) slow reversers. Colours indicate p-values (Benjamini–Hochberg-corrected) and dot size corresponds to gene ratio.*

Gene ontology analyses of differentially methylated sites

The differentially methylated sites (DMS) covered in total 2925 unique great tit genes. Using the human gene ontology (GO) database, we found 252 (hypermethylated in fast reversers) and 140 (hypermethylated in slow reversers) significantly enriched GO terms that associated with the genes carrying DMS between fast and slow reversal learning individuals. We found many terms that potentially have a role in neural system functioning. These included the GO terms;

'axon guidance', 'neuron projection guidance', and 'cell morphogenesis involved in neuron differentiation' (Figure 5.9, Supplementary Tables 5.18 and 5.19). Performing GO analyses on sets of genes where DMS were located in the promoter (132 unique genes) or the TSS region (15 unique genes) did not result in any significantly enriched GO terms.

Associations between differences in methylation, gene expression and chromatin accessibility in striatum

We find no overlap with DEGs and DMSs or DARs between fast and slow reversal learners. Of the DEGs in the striatum, we see that TSS methylation differences and promoter accessibility differences are small and not significant. For *USP5* we do not have data on TSS methylation and for VWA3B we do not have data on promoter accessibility (Figure 5.10a). We also find no overlap with DARs and differentially methylated sites between fast and slow reversal learners, but the average methylation difference of DARs mostly follows the expected pattern of lower methylation in regions with higher accessibility (Figure 5.10b).

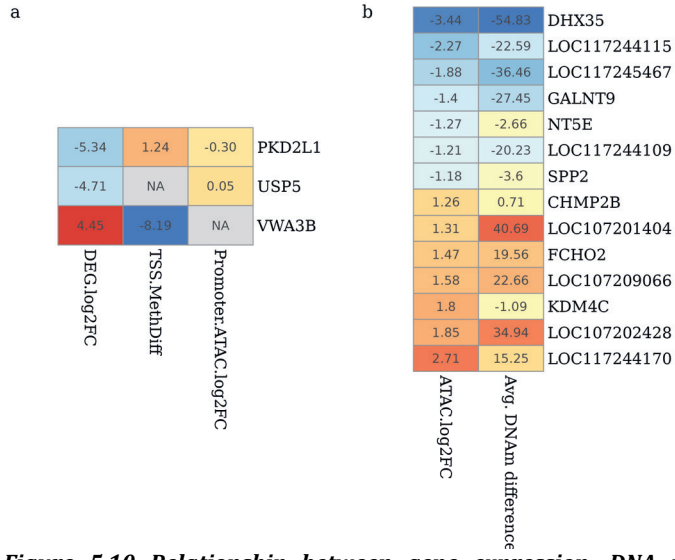

Figure 5.10 Relationship between gene expression, DNA methylation and chromatin accessibility *a) Heatmap indicating the log2Foldchange estimates of striatal DEGs between fast and slow reversal learners, the average methylation difference for CpG sites located with the TSS region of each respective DEG, and the average log2Foldchange of the peaks located within the promoter of each respective DEG. b) Heatmap indicating the 2Foldchange estimates of striatal DARs between fast and slow reversal learners (negative sign indicates higher accessibility in fast), and the average methylation difference for CpG sites located within that region (negative sign indicates hypomethylated in fast).*

We tested the association between differential gene expression in neuronal striatal nuclei between the reversal learning types and CpG site methylation differences in (bulk) striatal nuclei between the reversal learning types. When including CpG sites from all genomic regions, associations between differential gene expression and

differential DNA methylation differences were mostly randomly distributed across all four quadrants (r=0.05, p <0.001 (pearson), p = 0.012 (binomial), Figure 5.11, Supplementary Table 5.11). For CpGs situated in promoters and TSS, we observed significant relations between differential gene expression and differences in DNA methylation (Promoter: r = 0.12, p = 0.0018 (pearson), p = 0.002 (binomial); TSS: r = 0.26, p = 0.012 (pearson), p = 0.055 (binomial), Figure 5.11, Supplementary Table 5.11), with significantly more points falling into the two expected quartiles (NE and SW), indicating that specifically promotor/TSS methylation seems important for epigenetic regulation of differentially expressed genes between the reversal learning types.

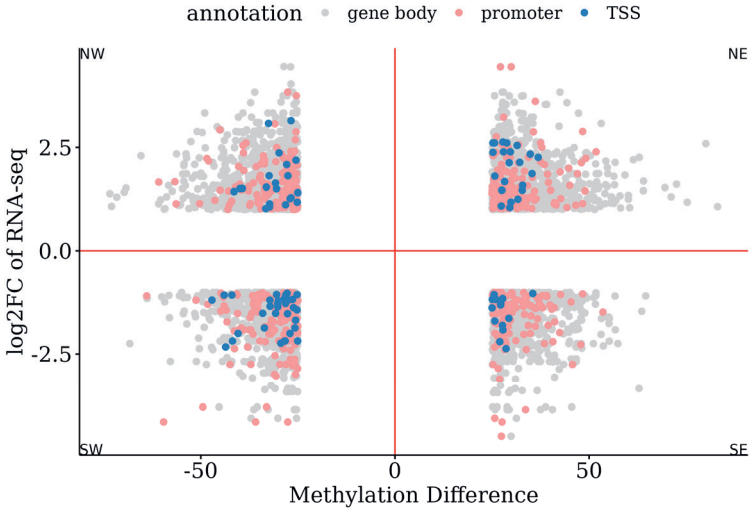

Figure 5.11 Relationship between differential DNA methylation and gene expression in striatum *Differences in gene expression (log2Foldchange >1) in relation to differences in DNA methylation (methylation difference >25%) in the striatum between fast and slow reversers. Plot is divided into four quadrants corresponding to distinct associations between DNA methylation and gene expression. The SW quadrants represents higher gene expression and hypomethylation in fast learners, the NE quadrant represents higher gene expression and hypomethylation in slow learners. TSS = transcription start site.*

Discussion

Gene regulatory mechanisms are critically involved in individual differences in cognitive abilities and here we explored to what extent differences in reversal learning performance are explained by brain region-specific individual differences in gene expression and underlying epigenetic regulatory mechanisms. We compared gene expression of neuronal nuclei from the striatum and hippocampus, and bulk cerebellar nuclei, of fast versus slow reversal learners. Our findings indicate that all regions have a function in reversal learning, but that these functions vary between region and are regulated differently within each region. In the striatum, but not in the hippocampus, differences in gene expression are partially explained by chromatin accessibility. Furthermore, promoter DNA methylation explained differences in striatal gene expression. The results of this

study therefore give a first glimpse of brain-region specific involvement of epigenetic mechanisms in individual differences in reversal learning performance.

The striatum, hippocampus and cerebellum each have a different function in relation to reversal learning ability. Accordingly, we found unique sets of differentially expressed genes for each brain region. The striatum is known to play an important role in feedback-driven learning (Schultz, 2006), including rapidly shifting feedback as occurs in reversal learning assays (Cools et al., 2002; Klanker et al., 2015). Ubiquitin-specific peptidase 5 (*USP5*) was upregulated in the striatum of fast learning individuals. This gene encodes a protein that controls ubiquitin levels. The ubiquitin-proteasome system enables rapid protein changes, and as such, ubiquitin-dependent remodelling of the synaptic proteome is an important process for synaptic plasticity and memory storage (Mabb and Ehlers, 2010), and downregulation of this system is involved in the pathogenesis of neurodegenerative diseases (Hol et al., 2005). The polycystic kidney disease-like ion channel (*PKD2L1*) was likewise overexpressed in the striatum of fast reversal learners. This gene contributes to sour taste responses in mice (Horio et al., 2010) and is up-regulated in rats with high emotional reactivity in comparison to less emotional rats (Sabariego et al., 2013). The VWA domain-containing protein 3B (*VWA3B*), which is overexpressed in slow reversal learners, is likely involved in the apoptotic signalling pathway in neuronal cells (Kawarai et al., 2016). Gene set enrichment analysis revealed upregulation of genes involved in axon development, synaptic signalling and neurogenesis in fast compared to slow individuals in the striatum as well as the KEGG categories cardiac muscle contraction, glutamatergic synapse, circadian entrainment and pathways of neurodegeneration. Very similar functions were found to be enriched in genes that were differentially expressed following a learning task in the striatum of mice, confirming their relevance in striatal functioning (Lousada et al., 2023). Indeed, the avian striatum receives glutamatergic projections from the pallium, glutamate receptors are involved in reward and extinction learning (Gao et al., 2019) and glutamatergic neurotransmission in the striatum is crucial for reversal learning performance (Liu et al., 2020). In slow reversal learners, genes involved in triglyceride metabolic processes were upregulated in the striatum. Dietary triglycerides moderate dopamine-dependent food-seeking and reward-associated behaviours through dopamine receptor type 2-expressing neurons (Berland et al., 2020). Differences in circulating triglycerides can lead to differences in reward sensitivity, possibly explaining why differential expression of genes related to triglyceride metabolism are linked to differences in reversal learning performance.

The avian hippocampus functions in spatial learning and navigation (Colombo and Broadbent, 2000; Mayer et al., 2013), stimulus-response learning (Herold et al., 2022) and emotional behaviour and stress response (Smulders, 2017). Neurogenesis is a significant feature of avian hippocampal-dependent cognitive processes (Barnea and Pravosudov, 2011; Herold et al., 2019). In line with this, we found that the gene Fanconi anemia complementation group M (*FANCM*) was upregulated in slow learning individuals. The Fanconi DNA repair pathway plays a

role during neurogenesis and is important for survival and maintenance of neural progenitor cells, which give rise to glia and neurons (Sii-Felice et al., 2008). *MLC1* was upregulated in fast compared to slow learning individuals, a gene that is predominantly expressed in astrocytes (Teijido et al., 2007) and predicts dementia status (Simon et al., 2018). Few GO or KEGG terms were significantly enriched in the hippocampus, but several signalling-related GO terms were upregulated is slow learners. Although the hippocampus plays a crucial role in spatial navigation, it is, at least in mammals, likely less crucial for shifting behavioural strategies (Regier et al., 2015; Seib et al., 2020). In a spatial navigation task with shifting reward contingencies, activity of hippocampal neuron mostly reflect the searching process, whereas striatal neurons more specifically respond to the change of contingency (Regier et al., 2015). A limited contribution of hippocampal functioning to reversal learning ability could explain the relatively small effect sizes and limited enrichment of pathways compared to the striatum.

Like striatal neurons, cerebellar neurons also play a role in the processing of rewards and encode prediction errors (Wagner et al., 2017; Pierce and Péron, 2022). Therefore, it was surprising to find contrasting patterns of differential gene expression and involved pathways across the striatum and cerebellum. The gene *ALDH1A3* is overexpressed in slow reversal learners and encodes an aldehyde dehydrogenase enzyme, which oxidizes retinal to retinoic acid. Retinoic acid plays a regulatory role in nervous system development including the cerebellum (Durston et al., 1989; Matsumoto et al., 1998; Parenti and Cicirata, 2004). Also, Alpha-L-iduronidase (*IDUA*) is overexpressed in slow individuals and encodes an enzyme that is required for the degradation of glycosaminoglycans, which play a crucial role in the cell signalling process, including regulation of cell growth and proliferation. Long-term memory for aversive training is impaired in mice with targeted disruption of *IDUA* due to neuronal deficits (Reolon et al., 2006). Enrichment analysis showed that genes that are upregulated in slow compared to fast learning individuals in the cerebellum are involved in ribosomal functions like RNA splicing, mRNA metabolism as well as ATP synthesis and oxidative phosphorylation. Defective mitochondrial oxidative phosphorylation causes malfunctioning energy production, metabolism and amino acid biosynthesis leading to neuronal cell death, which happens in neurodegenerative disorders such as Alzheimer's, Parkinson's, and Huntington's diseases (Lin and Beal, 2006; Sharanek and Jahani-Asl, 2022). Considering the high energetic costs of information processing in the cerebellum (De Zeeuw et al., 2011; De Zeeuw, 2021), and given the energetic costs that come with associated learning and memory performance (Laughlin, 2001), individual differences in cerebellar energy metabolism may underlie individual differences in reversal learning performance. Uniquely upregulated in the cerebellum of fast learning individuals are genes related to the KEGG term "neuroactive ligand-receptor interaction". The neuroactive ligand receptor interaction pathway is made up of mainly neuroreceptor genes and is involved in environmental information processing (Lauss et al., 2007). When comparing differentially enriched terms found in the cerebellum with the striatum, categories related to cilium functioning and cell projection assembly show opposite

enrichment patterns, suggesting opposing roles of intracellular cilia in reversal learning performance across the two brain regions. In the striatum, the length of primary cilia is dependent on the extent of dopaminergic inputs (Miyoshi et al., 2014) and cilia are essential for establishing synaptic connectivity in striatal interneurons (Guo et al., 2017). Knock-out of cilia function also causes degenerative changes to cerebellar Purkinje cells (Bowie and Goetz, 2020). Perhaps upregulation of these pathways in the striatum in slow learners causes stronger stimulus-reward memories to be formed which are more difficult to reverse (Aljadeff and Lotem, 2021), whereas upregulation of these pathways in the cerebellum of fast learners ascertain proper normal cerebellar error sensitivity. It could also be that these opposite patterns are due to the fact that we used bulk cerebellar nuclei, but neuronal striatal nuclei. Perhaps these processes have opposing roles in neuronal versus non-neuronal cells in relation to reversal learning performance. Whether this means an opposite requirement of these pathways in different brain regions in relation to the reversal learning process, or whether this differences is caused by the more heterogenous cell population from bulk cerebellar nuclei remains to be studied.

To summarize, we found that each great tit brain region has its own unique set of differentially expressed genes when comparing slow and fast reversal learners. We saw the largest expression differences between the types in the striatum, with enrichment of pathways required for neuronal signalling and the processing of rewards. This suggest that the striatum is a promising brain region for further study on the neural mechanisms of cognitive flexibility in great tits. In the cerebellum we found an enrichment of pathways related to oxidative phosphorylation and mitochondrial ribosomes. The expression differences between fast and slow learners in the hippocampus showed correlated expression with differences in the striatum, pointing to correlated functional differences in the great tit. The striatum receives projections from the hippocampus (Atoji et al., 2002; Husband and Shimizu, 2011), possibly explaining the positive correlation in direction of gene expression. The lack of overlap in differentially expressed genes between these tissues despite the positive correlation in fold change, suggests that the limited number of differentially expressed genes is perhaps due to a lack of power that could potentially be resolved by deeper sequencing depth, more individuals, or stronger phenotypic differences.

In the striatum, we found a positive correlation between gene expression differences between fast and slow reversal learners, and differential chromatin accessibility, especially when focusing on promoter and intronic regions. This means that genes associated with chromatin opening are more likely to be upregulated, and vice versa, in relation to reversal learning performance. We found fourteen differentially accessible peaks, which all resided in intronic and intergenic genomic regions, rather than promoter regions, consistent with the functional significance of distal regulatory elements for gene expression (Corces et al., 2018; Sigalova et al., 2020). Restricting gene ontology analysis to genes that show concordant patterns of gene expression and open chromatin in promoter regions

revealed eight striatum-relevant molecular functions such as postsynaptic membrane potential and neurotransmitter receptor activity to be enriched, suggesting that genes in pathways relevant to the function of the striatum in a reversal learning task are potentially regulated by differential chromatin accessibility of the promoter. On the contrary, we found little variation in chromatin accessibility between fast and slow reversal learners in hippocampal neurons and likely consequently, no evidence for a correlation between chromatin accessibility and gene expression. The small differences in gene expression in the hippocampus that we observed are thus not explained by chromatin accessibility. This is surprising, as there is ample evidence that modified chromatin accessibility underlies the gene expression changes that occur in the hippocampus following neuronal activation (Su et al., 2017; Fernandez-Albert et al., 2019).

When focussing on differentially expressed genes only, we did not observe a significant differential accessibility or no significant differential expression when focussing on the genes that contained a differentially accessible region. Differential gene expression can be induced by a variety of mechanisms, and differentially accessible peaks might have an effect on other genes than those of which they are closest to, explaining the discrepancy between the ATAC-seq and RNA-seq results in this analysis. Although accessibility of gene regulatory regions, such as promoters and distal enhancers, has transcriptional impact, also inactive promoters and enhancers can be open (Klemm et al., 2019). Such 'poised' regions require additional regulatory manipulations to affect gene expression. Distal intergenic and intronic genomic regions harbour elements such as active cis-regulatory enhancers, which can be located very distant from the TSS of the gene they control (Perenthaler et al., 2019). Indeed, whereas we see a significant relationship between differential chromatin accessibility of promoter regions and gene expression, most of the differentially accessible peaks reside in distal intergenic regions. Enhancers can be located in other genes, and can also regulate multiple genes, explaining why the association between chromatin accessibility in these regions is less predictive of the accessibility of its nearest gene. Altogether, our results suggest that although, at least in the striatum, differential chromatin accessibility partially explains the variation in gene expression patterns that correlate with reversal learning performance, chromatin accessibility alone does not explain the majority of the variation in gene expression and that likely other regulatory mechanisms are also at play.

When considering the genes that harboured a differentially accessible peak in the striatum, no gene ontology term was enriched. An intronic region of the gene Lysine Demethylase 4C (*KDM4C*) showed significantly higher chromatin accessibility in slow reversal learners. This gene encodes a trimethylation-specific demethylase, an enzymatic action that regulates gene expression. This epigenetic regulator contributes to neurogenesis, as it can induce *BDNF* expression by demethylating its regulatory regions, while blocking astrogliogenesis by demethylating *GFAP* exonic regions (Cascante et al., 2014). Interestingly, stress-enhanced reversal learning ability was prevented by *BDNF* infusion (Graybeal et al., 2011), and activation of

BDNF-TrkB signaling of *BDNF* induced behavioural inflexibility (McCarthy et al., 2016), a similar effect might be reached if there was an effect of *KDM4C* intronic openness on *BDNF* expression. Notably, an intronic region of the gene secreted phosphoprotein 2 (*SPP2*), which degrades S1P levels, was significantly more accessible in fast reversal learners. S1P enhances cell proliferation and activates neuronal progenitor cells (O'Sullivan and Dev, 2013; Motyl and Strosznajder, 2018) and crucially, S1P receptor activation increased BDNF levels (Deogracias et al., 2012), again suggesting that negative regulation of BDNF is linked to reversal learning ability in the striatum of great tits. Among the genes that showed increased accessibility in distant intergenic regions in fast reversal learners was *GALNT9*, a brain-specific O-glycosylase which is enriched for H3K27ac enhancer mark and contains a binding site for *EGR1*, a transcription factor that is induced by BDNF following neuronal activity and can regulate *GALNT9* by DNA demethylation (Sun et al., 2019). O-Glycans are important mediators of neural cell interactions (Toba et al., 2000; Zhang et al., 2003; Kleene and Schachner, 2004), and differential regulation of *GALNT9* may thus be causal to reversal learning performance. *NT5E* is a plasma membrane protein responsible for the production of adenosine, an important modulator of neuronal plasticity, especially in the striatum (Cunha, 2001; Zimmermann et al., 2012; Ena et al., 2013a). *NT5E* knock-out mice exhibit enhanced spatial working memory and open field habituation (Ena et al., 2013b), and our results suggests that *NT5E* might also be a candidate gene for reversal learning performance.

Among the genes that showed increased accessibility in distant intergenic regions in slow reversal learners were Dual specificity protein phosphatase 10 (*DUSP10*), Charged Multivesicular Body Protein 2B (*CHMP2B*) and transmembrane protein 18 (*TMEM18*). *DUSP10* is part of a large family of protein tyrosine phosphatases and is an activity-regulated signalling molecule that is upregulated during neurogenesis (Kim et al., 2016). *CHMP2B* is expressed in neurons and encodes a component of the ESCRT-III complex, which functions in the recycling or degradation of cell surface receptors. Transgenic mice expressing mutant *CHMP2B* develop neurodegeneration and synaptic dysfunction (Ghazi-Noori et al., 2012; Clayton et al., 2022). *CHMP2B* was among the top ranked significant genes from a genome-wide association study on spatial cognitive variation (Branch et al., 2022), suggesting a role for this gene in avian spatial learning ability. Both *DUSP10* and *CHMP2B* suggest differential neurodevelopment underlying reversal leaning ability. *TMEM18* is a hypothalamic gene that has been linked to obesity and eating disorders in genome wide association studies (Almén et al., 2010; Chermon and Birk, 2023), and exerts its role in the control of appetitive behaviour through its effect on energy balance (Larder et al., 2017). As our task is an appetitive learning task, the involvement of this gene suggests that individual variation in reward sensitivity may underlie variation in reversal learning performance.

Although annotation of differentially accessible regions provides us with an interpretation of the functional impact, it does not explain how transcription is affected. Differentially accessible regions are likely to harbour motifs, specific

sequences that transcription factors can bind to (Klemm et al., 2019). Assessing which motifs are enriched in differentially accessible regions, can provide a prediction about the transcription factors that are involved, which could be linked to the expression patterns of those genes (Yan et al., 2020). This will be a crucial next step in understanding the gene regulatory networks that underlie differences in chromatin accessibility.

DNA methylation is an additional epigenetic mechanism that contributes to regulation of gene transcription. DNA methylation functions as a transcriptional inhibitor (Siegfried et al., 1999) and associates negatively with chromatin accessibility (Thurman et al., 2012). We found multiple differentially methylated sites in relation to reversal learning performance and explored how DNA methylation differences associated with changes in gene expression and chromatin accessibility. Most chromatin regions that showed increased accessibility in one group, showed lower average CpG methylation, although none of these regions harbored significant differentially methylated sites. Furthermore, genome-wide, we found an expected correlation between low CpG site methylation and high expression of the associated gene, mostly in TSS and promoter regions. This means that differential expression of genes with these functions in relation to reversal learning performance is at least to some extent established by differences in DNA methylation. Considering that we performed EM-seq on bulk striatal cells rather than neuronal nuclei, this relationship between DNA methylation and gene expression is likely to be stronger than we present here.

Genes carrying DMS showed enrichment for GO terms related to biological processes involved in neuronal functions, such as neuron differentiation, axon development and synapse assembly. No terms and pathways were found to be enriched when looking at functional enrichment of significantly methylated sites located in the TSS region, indicating that these genes are relevant to a wide range of functions. Still, several of these genes have a clear link with learning differences in the literature. The thyroid hormone receptor *THRB*, is crucial for brain development and is associated with learning and cognitive abilities and plays a modulatory role in striatal gene expression (Bernal, 2000). *APBB2* is involved in the formation of β-amyloid (Aβ), the main constituent of the senile plaques that are characteristic for Alzheimer's disease, and the gene is linked to cognitive impairment (Golanska et al., 2008, 2013). Other genes were less strongly linked to cognition, but have a direct link to behaviour. For example *BCAS1* is involved in myelination and is associated with schizophrenia-like behaviour. (Ishimoto et al, 2017). *SLC35F2* is a solute transporter functioning in transmembrane transport and was among the top SNPs for anxious temperament in brain areas relevant both for emotional reactivity and affection. Interestingly, this was also including the striatum (Gonda et al., 2021). Yet other genes are associated with neural system development (*LRTM1, FLCN*) (Kenyon et al., 2016; Samata et al., 2016) and neuronal signalling (*SLC35A48*) (Richard et al., 2001). Together, this indicates a functional role for DNA methylation in regulating gene expression variation in relation to learning and behaviour, as well as neuronal structure and development.

Overall, our approach revealed molecular (epi)genetic candidates for further studies to demonstrate causal relationships between specific genes and their function in reversal learning ability, which will provide insights into the origin of individual cognitive differences. Collectively, our data supports the idea that transcriptomic and epigenomic signatures differ between individuals that vary in their reversal learning performance, and that these differences correlate across genomic and epigenetic functions, especially in the striatum. The identity and function of the involved genes are brain region-specific. Our study is among the first to make use of innovative transcriptomic and epigenomic sequencing tools to reveal brain region-specific functioning of neurons on reversal learning performance in an ecological model species. This study is a first step towards understanding the genomic and epigenetic functioning of cognitive ability in a wild vertebrate.

Supplement to Chapter 5

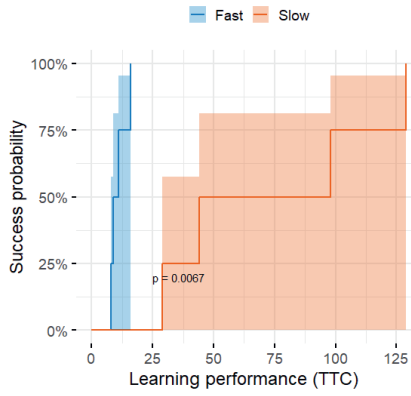

Supplementary Figure 5.1 *Kaplan Meier plots of the trials to reach learning criterion (TTC) during the reversal learning task for great tits. "Time" is number of trials, and "event" is reaching trials to criterion. Every time an individual reaches learning criterion, the proportion of individuals succeeding at the task on the Y-axis increases. The fast and slow learning individuals differ significantly on success probability (log-rank test P = 0.007).*

Supplementary Table 5.1 *Sample origins, reversal learning scores, and samples included in final analysis. TTC = trials to criterion.*

Phenotype	ID	Brood	TTC R1	TTC R2	TTC R3	Mean TTC	Striatum NeuN+		Hippocampus NeuN+		Cerebellum Bulk
Fast	BD...76021	70154	9	26	9	14,67			RNA	ATAC	RNA
	BD...76096	70132	16	23	8	15,67	RNA		RNA	ATAC	
	BD...76157	70156	11	15	8	11,33		ATAC EM	RNA		RNA
	BD...76237	70664	8	25	7	13,33	RNA	ATAC EM	RNA	ATAC	RNA
Slow	BD...76081	70145	29	16	30	25		ATAC EM	RNA	ATAC	RNA
	BD...76038	70115	53	21	24	32,67	RNA		RNA	ATAC	
	BD...76149	70155	164	8	45	72,33	RNA		RNA	ATAC	
	BD...76216	70361	98	81	45	74,67		ATAC EM	RNA		RNA

Supplementary Table 5.2 *Summary of sequencing and alignment of included RNA-seq libraries.*

ID	Type	Brain region	Cell type	#Raw reads	%Aligned 1X	#Aligned 1X	#Aligned toGenes
GT021	Fast	Cerebellum	Bulk	25,722,205	75.64	19,456,678	10,912,056
GT081	Slow	Cerebellum	Bulk	16,972,169	72.42	12,290,472	7,511,182
GT157	Fast	Cerebellum	Bulk	21,155,242	75.00	15,865,407	9,386,363
GT216	Slow	Cerebellum	Bulk	12,261,508	74.08	9,083,617	5,425,060
GT237	Fast	Cerebellum	Bulk	20,130,748	74.18	14,933,841	8,608,710
GT021	Fast	Hippocampus	NeuN+	18,759,090	74.90	14,050,942	7,673,207
GT038	Slow	Hippocampus	NeuN+	19,655,441	71.13	13,980,115	7,855,229
GT081	Slow	Hippocampus	NeuN+	18,159,772	73.30	13,310,627	7,379,186
GT096	Fast	Hippocampus	NeuN+	34,247,747	72.87	24,956,962	13,970,889
GT149	Slow	Hippocampus	NeuN+	34,124,867	74.57	25,448,068	13,663,424
GT157	Fast	Hippocampus	NeuN+	27,493,335	76.87	21,133,874	11,740,772
GT216	Slow	Hippocampus	NeuN+	22,240,767	71.76	15,959,308	8,965,101
GT237	Fast	Hippocampus	NeuN+	29,025,622	73.24	21,258,136	11,888,550
GT038	Slow	Striatum	NeuN+	27,956,839	78.13	21,841,806	12,470,514
GT096	Fast	Striatum	NeuN+	60,259,538	80.14	48,294,457	26,958,249
GT149	Slow	Striatum	NeuN+	56,860,753	77.74	44,201,536	24,504,588
GT237	Fast	Striatum	NeuN+	27,180,653	69.31	18,836,513	11,471,278

Supplementary Table 5.3 *Summary of sequencing and alignment of included ATAC-seq libraries.*

ID	Type	Brain region	Cell type	#Raw reads	%Aligned 1X	#Aligned 1X	#Peaks	FRiP	TSSE
GT038	Slow	Cerebellum	Bulk	64,732,036	85.04	55,047,165	31373	0.09	4.69
GT096	Fast	Cerebellum	Bulk	41,000,053	86.52	35,473,283	28255	0.11	6.9
GT149	Slow	Cerebellum	Bulk	47,130,607	85.69	40,383,998	29927	0.11	6.4
GT021	Fast	Hippocampus	NeuN+	36,614,777	71.53	26,189,992	99882	0.19	6.56
GT038	Slow	Hippocampus	NeuN+	36,845,692	60.24	22,195,509	70044	0.13	4.88
GT081	Slow	Hippocampus	NeuN+	58,100,302	90.50	52,578,300	86225	0.13	3.49
GT096	Fast	Hippocampus	NeuN+	21,859,014	65.68	14,357,813	54272	0.12	7.53
GT149	Slow	Hippocampus	NeuN+	24,057,085	69.56	16,734,233	60606	0.12	6.34
GT237	Fast	Hippocampus	NeuN+	40,905,652	90.30	36,936,483	74505	0.13	4.26
GT081	Slow	Striatum	NeuN+	78,267,531	69.97	54,764,139	88842	0.17	3.79
GT157	Fast	Striatum	NeuN+	64,007,565	86.74	55,519,451	83210	0.18	4.34
GT216	Slow	Striatum	NeuN+	65,662,557	86.23	56,623,089	89701	0.2	4.77
GT237	Fast	Striatum	NeuN+	56,267,933	82.46	46,396,622	79522	0.14	3.84

Supplementary Table 5.4 *Summary of sequencing and alignment of EM-seq libraries.*

ID	Type	Brain region	Cell type	#Raw reads	%Aligned 1X	#Aligned 1X
GT081	Slow	Striatum	Bulk	163,841,906	52.7%	86,325,091
GT157	Fast	Striatum	Bulk	225,488,123	52.1%	117,407,638
GT216	Slow	Striatum	Bulk	252,342,399	56.7%	142,988,987
GT237	Fast	Striatum	Bulk	259,955,928	57.4%	149,226,883

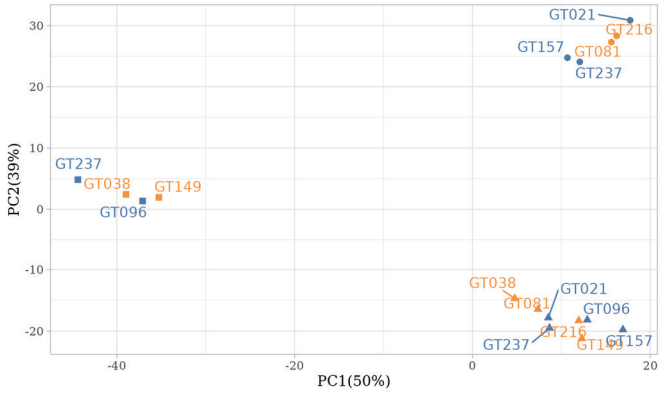

Supplementary Figure 5.2 *Clustering of RNA-seq samples based on PCA. Samples collected from fast (blue) and slow (orange) reversal learners and from Striatum (squares), Hippocampus (triangles) and Cerebellum (circles). PC1 explained 50% of the variance, PC2 39% while PC3 explained 2.2% (all eigenvalue > 1.0).*

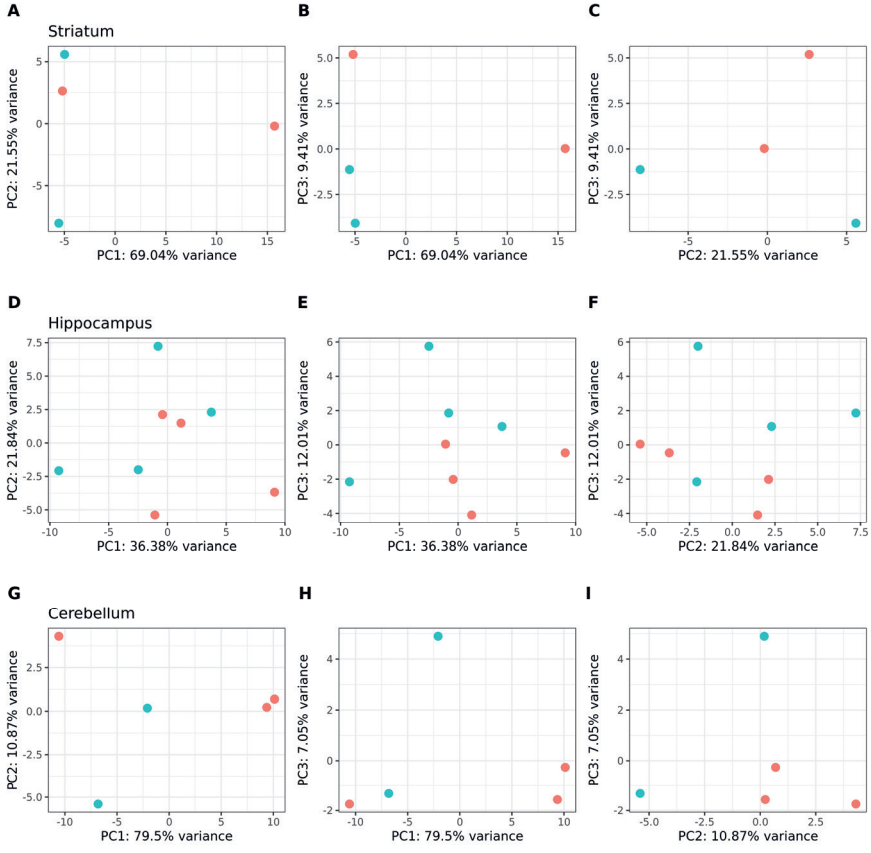

Supplementary Figure 5.3 *Clustering of RNA-seq samples based on PCA. Samples collected from fast (red dots) and slow (blue dots) reversal learners and from three different brain regions: a-c) Striatum, d-f) Hippocampus and g-i) Cerebellum.*

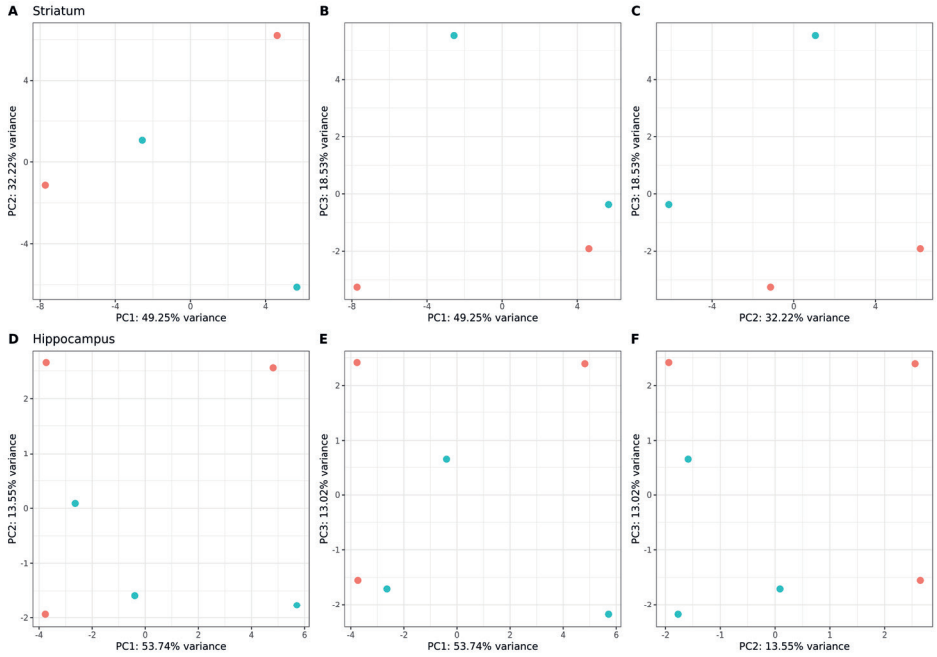

Supplementary Figure 5.4 *Clustering of ATAC-seq samples based on PCA. Samples collected from fast (red dots) and slow (blue dots) reversal learners and from three different brain regions: A. Striatum, B. Hippocampus and C. Cerebellum.*

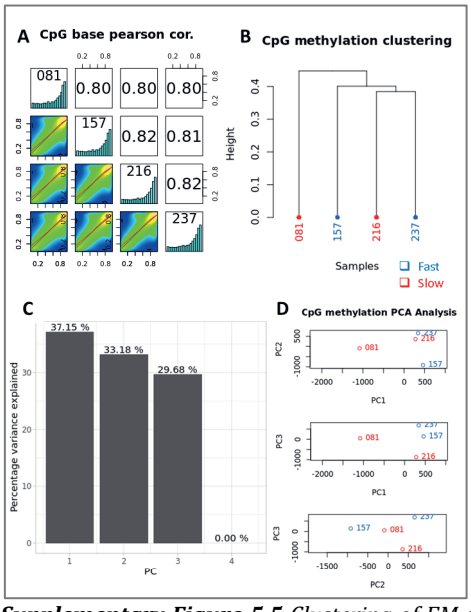

Supplementary Figure 5.5 *Clustering of EM-seq samples shows no apparent clustering between the two phenotypes. Fast reversal-learning individuals are coloured blue and slow individuals are coloured red. a) Sample correlation matrix b) Hierarchical clustering. The distance method is correlation and the clustering method is ward. c) Percentage of variance explained per PC. d) PCA for DNA methylation for PCs 1-3, containing all functional variance.*

Supplementary Table 5.5 *Number of CpGs before and after filtering.*

Filtering step	# of methylated sites
Raw/no filtering	15.116.607
Uniting	7.626.028
Coverage ≥10x	7.467.562
5% ≥ mean meth ≤ 95%	6.036.195
Percentile filtering of 0.01%	6.035.888

Differential methylation analysis	
Overdispersion correction (Bonferroni)	4.772.866
Overdispersion + complete cases (the site occurred in all four individuals)	2.830.107
Difference >25% and padj < 0.05	11.418
Overdispersion + significant + complete	4.551

Supplementary Table 5.6 *Gene name, annotation, distance to TSS (in bp), adjusted p-value (padj) and log2Foldchange (log2FC) associated with differentially accessible regions between fast and slow reversal learners.*

Phenotype	Gene name	annotation	distanceToTSS	log2FC	padj
Fast	DHX35	Distal Intergenic	95,688	-3.44	0.00
	LOC117244115	Distal Intergenic	-183,552	-2.27	0.00
	LOC117245467	Distal Intergenic	20,788	-1.88	0.02
	GALNT9	Distal Intergenic	-32,036	-1.40	0.00
	NT5E	Distal Intergenic	-112,940	-1.27	0.00
	LOC117244109	Distal Intergenic	6,216	-1.21	0.04
	SPP2	Intron	-9,968	-1.18	0.01
Slow	CHMP2B	Distal Intergenic	-7,519	1.26	0.02
	LOC107201404	Distal Intergenic	-16,399	1.31	0.00
	FCHO2	Distal Intergenic	-5,501	1.47	0.02
	LOC107209066	Distal Intergenic	110,117	1.58	0.02
	KDM4C	Intron	153,406	1.80	0.00
	LOC107202428	Distal Intergenic	-146,226	1.85	0.00
	LOC117244170	Distal Intergenic	-17,876	2.71	0.00

Supplementary Table 5.7 *Distribution of accessible chromatin regions in striatum.*

Feature (Striatum)	Frequency
Promoter	12.27
5' UTR	0.71
3' UTR	3.05
Exon	9.27
Intron	36.06
Downstream (<=300)	0.19
Distal Intergenic	38.45

Supplementary Table 5.8 *Distribution of accessible chromatin regions in hippocampus.*

Feature (Hippocampus)	Frequency
Promoter	14.54
5' UTR	0.73
3' UTR	3.03
Exon	9.82
Intron	36.13
Downstream (<=300)	0.19
Distal Intergenic	35.55

Supplementary Table 5.9 *Relationship between differential chromatin accessibility and differential gene expression in the striatum.*

Region	NE + SW	All quadrants	Binom p.value	Pearson Correlation	p.value
All	306	564	0.048	0.096	0.023
Promoter	20	30	0.099	0.35	0.061
Intron	126	211	0.006	0.14	0.047
Exon	41	80	0.911	0.056	0.62
DistalIntergenic	105	220	0.544	0.00027	0.97
UTR5	3	3	0.25	0.98	0.12
UTR3	10	19	1	0.31	0.2

Supplementary Table 5.10 *Relationship between differential chromatin accessibility and differential gene expression in the hippocampus.*

Region	NE + SW	All quadrants	Binom p.value	Pearson Correlation	p.value
All	56	102	0.37	-0.58	0.56
Promoter	2	5	1	-0.31	0.61
Intron	23	39	0.34	-0.078	0.64
Exon	2	7	0.45	-0.45	0.31
DistalIntergenic	26	48	0.67	-0.034	0.82
UTR5	NA	NA	NA	NA	NA
UTR3	3	3	0.25	0.83	0.38

Supplementary Table 5.11 *Relationship between differential DNA methylation and differential gene expression in the striatum.*

Region	NE + SW	All quadrants	Binom p.value	Pearson Correlation	p.value
All	5531	10802	0.013	0.05	<0.001
Gene body	2248	4330	0.012	0.04	0.0072
Promoter	364	650	0.0025	0.12	0.0018
TSS	54	89	0.055	0.26	0.012

Supplementary Table 5.12 *Distance to TSS,, chromosome number or unplaced scaffold, q-value, Δ of % methylation level, gene name and TSS annotation Y/N associated with DMS between fast and slow reversal learners.*

Dist.to.TSS	Chrom/Scaf	Gene name	q-value	Δ Meth.	TSS
-282	chrZ	FAM169A	5.46E-08	56	Y
5	chr3	CGA	7.07E-07	-57	Y
-48	chr2	THRB	3.21E-06	49	Y
25	chr12	ENSPMJG00000012560	0.000832	-46	Y
-288	chr1	SLC35F2	0.001242	44	Y
46	chr14	ENSPMJG00000017423	0.002213	44	Y
-281	chr1	ENSPMJG00000012243	0.00271	46	Y
-130	chr1A	CHPT1	0.003025	51	Y
49	chr13	ENSPMJG00000007638	0.011436	-51	Y
-166	chr15	ENSPMJG00000018778	0.014024	-42	Y
48	chr4	APBB2	0.014517	-48	Y
9	chr20	ENSPMJG00000009107	0.024431	-40	Y
-29	chr13	SLC25A48	0.027101	-41	Y
-100	chr12	LRTM1	0.029643	-46	Y
-175	scaffold	HADHB	0.049596	48	Y
-639	chr12	GXYLT2	3.41E-10	-62	N
-345	chr13	ENSPMJG00000014455	6.39E-08	-60	N
-1453	chr4	RBM46	1.05E-07	-61	N
-692	chr1	ALKBH8	1.72E-07	57	N
-1490	chr15	SRRM4	1.77E-07	68	N
-1801	chr15	KSR2	2.03E-07	-64	N
-1181	chr3	DUSP10	2.28E-07	-56	N
-1891	chr7	GORASP2	3.42E-07	-59	N
-1388	chr3	RHOQ	4.07E-07	-71	N
-1017	chr1	EPHB6	7.54E-07	60	N
-1600	chr10	TIPIN	2.76E-06	-55	N
-1688	chr4	TAPT1	2.89E-06	-55	N
-1975	chrZ	SLC46A2	3.27E-06	-53	N
-1294	chr13	GRXCR2	3.35E-06	48	N
-1210	chr14	RBBP6	4.61E-06	-59	N
-1133	chr3	TDRP	4.68E-06	58	N
-1240	chr9	ENSPMJG00000002756	8.7E-06	-54	N
-1175	chr5	ASB2	1.17E-05	-53	N
-1394	chr2	ENSPMJG00000018140	1.45E-05	-49	N
63	chr15	CIT	1.62E-05	-53	N
-1844	chr7	BIN1	1.92E-05	-51	N
-359	chr26	LRRN2	2.06E-05	-52	N
-515	chr5	ENSPMJG00000003343	2.25E-05	-47	N
-372	chr28	MATK	2.26E-05	-51	N
128	chr14	POLR3E	2.54E-05	51	N
-1977	chr21	TAS1R1	2.71E-05	60	N
-591	chr27	IKZF3	2.97E-05	-56	N
-791	chrZ	RFESD	3.11E-05	-56	N
-450	chr24	CHEK1	3.18E-05	60	N
-1632	chr6	PCDH15	3.47E-05	-54	N
-1981	chr20	CDH4	4.9E-05	50	N
-1507	chr4	FGFR3	5.65E-05	-44	N
-401	chr27	ENSPMJG00000004130	8.54E-05	-56	N
-499	chr4	C1QTNF7	8.65E-05	62	N

Supplementary Table 5.12 (continued).

Dist.to.TSS	Chrom/Scaf	Gene name	q-value	Δ Meth.	TSS
-1849	chr5	BTBD10	8.71E-05	54	N
-1793	chr8	DAB1	8.92E-05	-47	N
-908	chr1	DIAPH3	0.000104	49	N
-488	chr21	ENSPMJG00000009402	0.000106	48	N
81	chr9	IL1RAP	0.000127	-50	N
-303	chr2	MTCL1	0.000144	-48	N
149	chr12	ENSPMJG00000012782	0.000148	-56	N
-1360	chr2	TMUB1	0.000197	56	N
102	chr7	TFPI	0.000233	-53	N
-955	chr12	RYBP	0.000244	-50	N
-1710	chr1	ENSPMJG00000010675	0.000292	-50	N
-782	chrZ	DAB2	0.000344	-45	N
-1727	chr5	IPO7	0.000351	46	N
-1216	chr5	MARK3	0.000359	-48	N
-1492	chr1	SKA3	0.000359	50	N
-1796	chr14	ALKBH5	0.000406	50	N
-1266	chr17	ZBTB43	0.0006	49	N
-500	chr11	ADGRG1	0.000632	-49	N
-1887	chr3	KCNK1	0.000744	47	N
-1746	chr28	ELL	0.000807	56	N
-1704	chr9	ENSPMJG00000016471	0.000891	-49	N
-1098	chr4	HPSE	0.000942	-51	N
-366	chr1	CYBB	0.000984	48	N
-333	chr15	ENSPMJG00000001295	0.001019	46	N
-1247	chr7	DNPEP	0.001393	49	N
-1160	chr1A	GNPTAB	0.001568	46	N
-1743	chr3	TOMM20	0.001585	-48	N
-1224	chr7	C2orf88	0.001609	-45	N
-1305	chr1	PIGA	0.001621	44	N
-1374	chr8	DARS2	0.001835	-49	N
-1874	chr20	NCOA6	0.001981	49	N
-1656	chr9	PCOLCE2	0.00222	-42	N
-427	chr13	KLHL3	0.002313	46	N
-1915	scaffold	ENSPMJG00000001813	0.002535	-49	N
-1793	chr1	ENSPMJG00000011313	0.002632	-59	N
-754	chr3	C1orf115	0.002694	-54	N
-617	chr25LG2	PRPF3	0.002877	-51	N
-1658	chr1	CCDC83	0.003169	-45	N
-1161	chr4A	WDR44	0.003707	44	N
-1363	chr2	ANKIB1	0.005248	50	N
-761	chr3	WDCP	0.005272	54	N
-1110	scaffold	TMBIM6	0.005581	-55	N
189	chr4	MRPL1	0.00571	45	N
-1530	chr2	CARMIL1	0.006239	46	N
-1105	chr2	ENSPMJG00000014167	0.006993	-49	N
137	chr6	ANAPC16	0.007749	-52	N
-1375	chr1	ENSPMJG00000015013	0.007937	48	N
-1467	chr4A	CYSLTR1	0.008377	-47	N
-428	chr1A	LRRK2	0.009724	41	N
-642	chr13	ATP10B	0.010078	-51	N
-1425	chr1	C3AR1	0.010302	45	N

Supplementary Table 5.12 (continued).

Dist.to.TSS	Chrom/Scaf	Gene name	q-value	Δ Meth.	TSS
-816	chr4	HNRNPD	0.010844	47	N
-1579	chr1A	CDC123	0.012247	-40	N
-1262	chr1	CDK8	0.012476	46	N
-1652	chr4	IGFBP7	0.012958	46	N
-445	chr1A	SLC35E3	0.01317	-59	N
-347	chr9	ARL14	0.013237	41	N
-328	chr18	GAA	0.014018	-43	N
-1486	chr3	SPDYA	0.014397	44	N
-569	chr6	A1CF	0.016341	-45	N
-1237	chr4	IL21	0.017507	-45	N
-1370	chr4A	HS6ST2	0.017618	-39	N
-1207	chr1	SLC9A2	0.018816	-51	N
-1845	chr4A	AMOT	0.019417	41	N
-1673	chr6	MCU	0.019887	55	N
-1543	chr19	VEZF1	0.021729	48	N
-373	chr18	GAA	0.022743	-39	N
-917	chr1	MAOA	0.023164	-46	N
-558	chr8	KIAA1614	0.024	59	N
112	chrZ	ANKRD34B	0.024201	-48	N
-1508	chr1A	MGAT3	0.024378	-42	N
-923	chr10	PDCD7	0.02584	44	N
-1469	chr2	GATAD1	0.026167	42	N
-1689	chr3	XRN2	0.027007	48	N
75	chr4A	GLOD5	0.02748	-46	N
-814	chr14	ENSPMJG00000019245	0.027652	38	N
-898	chr14	SREBF1	0.028414	-44	N
-1080	chr4A	ENSPMJG00000012214	0.031261	49	N
-782	chr14	ENSPMJG00000000118	0.031625	-47	N
-991	chr11	CMTM4	0.032688	48	N
78	chr19	HEATR6	0.0337	-46	N
150	chr1	HIKESHI	0.04025	-45	N
-1869	chr11	PSMD7	0.041572	-52	N
-916	chr23	TENT5B	0.048388	59	N

Supplementary Table 5.13 *List of top 30 significantly enriched (adjusted p values) GO terms (Biological Processes) from GSEA on gene expression differences in the striatum. NES: normalized enrichment score.*

Cluster	ID	Description	setSize	NES	p.adjust	rank
Striatum	GO:0048667	cell morphogenesis involved in neuron differentiation	384	-1.99	1.69E-08	2028
Striatum	GO:0061564	axon development	333	-2.04	2.41E-08	2016
Striatum	GO:0048812	neuron projection morphogenesis	431	-1.92	6.55E-08	2028
Striatum	GO:0048858	cell projection morphogenesis	445	-1.9	8.83E-08	2028
Striatum	GO:0120039	plasma membrane bounded cell projection morphogenesis	442	-1.88	1.14E-07	2028
Striatum	GO:0032990	cell part morphogenesis	459	-1.87	1.14E-07	2028
Striatum	GO:0099536	synaptic signaling	441	-1.87	1.14E-07	2300
Striatum	GO:0099537	trans-synaptic signaling	428	-1.88	1.34E-07	2300
Striatum	GO:0007409	axonogenesis	300	-2	1.51E-07	2016
Striatum	GO:0007268	chemical synaptic transmission	421	-1.89	1.67E-07	2300
Striatum	GO:0098916	anterograde trans-synaptic signaling	421	-1.89	1.67E-07	2300
Striatum	GO:0061387	regulation of extent of cell growth	75	-2.33	2.66E-06	1972
Striatum	GO:0034330	cell junction organization	425	-1.79	3.43E-06	2075
Striatum	GO:0030516	regulation of axon extension	65	-2.36	3.92E-06	2068
Striatum	GO:0010975	regulation of neuron projection development	307	-1.89	3.92E-06	2075
Striatum	GO:0000904	cell morphogenesis involved in differentiation	481	-1.76	5.71E-06	2028
Striatum	GO:0050807	regulation of synapse organization	139	-2.08	9.25E-06	1899
Striatum	GO:0048675	axon extension	87	-2.2	9.31E-06	1972
Striatum	GO:0099177	regulation of trans-synaptic signaling	272	-1.86	9.31E-06	2300
Striatum	GO:0050803	regulation of synapse structure or activity	142	-2.05	1.01E-05	1999
Striatum	GO:0034329	cell junction assembly	249	-1.9	1.21E-05	2198
Striatum	GO:0050804	modulation of chemical synaptic transmission	271	-1.86	1.86E-05	2300
Striatum	GO:0050808	synapse organization	276	-1.85	2.54E-05	1899
Striatum	GO:0048588	developmental cell growth	151	-1.98	4.4E-05	1899
Striatum	GO:0050770	regulation of axonogenesis	116	-2.04	0.00010	1899
Striatum	GO:1990138	neuron projection extension	123	-1.97	0.00021	1899
Striatum	GO:0019433	triglyceride catabolic process	16	2.26	0.00061	506
Striatum	GO:0007215	glutamate receptor signaling pathway	35	-2.24	0.00073	2318
Striatum	GO:0050767	regulation of neurogenesis	240	-1.74	0.0010	2028
Striatum	GO:0051960	regulation of nervous system development	285	-1.68	0.0014	1899

Supplementary Table 5.14 *List of top 30 significantly enriched (adjusted p values) GO terms (Biological Processes) from GSEA on gene expression differences in the hippocampus. NES: normalized enrichment score.*

Cluster	ID	Description	setSize	NES	p.adjust	rank
Hippocampus	GO:0006631	fatty acid metabolic process	163	-1.84	0.035	1640
Hippocampus	GO:0051932	synaptic transmission, GABAergic	32	2.06	0.047	763
Hippocampus	GO:0032787	monocarboxylic acid metabolic process	266	-1.61	0.047	1614
Hippocampus	GO:0007268	chemical synaptic transmission	362	1.53	0.047	1872
Hippocampus	GO:0098916	anterograde trans-synaptic signaling	362	1.53	0.047	1872

Supplementary Table 5.15 *List of top 30 significantly enriched (adjusted p values) GO terms (Biological Processes) from GSEA on gene expression differences in the cerebellum. NES: normalized enrichment score.*

Cluster	ID	Description	setSize	NES	p.adjust	rank
Cerebellum	GO:0008380	RNA splicing	280	1.95	2.1E-05	2842
Cerebellum	GO:0006397	mRNA processing	294	1.91	2.1E-05	2839
Cerebellum	GO:0016071	mRNA metabolic process	427	1.76	2.1E-05	3068
Cerebellum	GO:0042773	ATP synthesis coupled electron transport	57	2.27	0.00033	2178
Cerebellum	GO:0042775	mitochondrial ATP synthesis coupled electron transport	57	2.27	0.00033	2178
Cerebellum	GO:0019646	aerobic electron transport chain	53	2.27	0.00033	2178
Cerebellum	GO:0044782	cilium organization	226	-1.84	0.00033	1827
Cerebellum	GO:0006119	oxidative phosphorylation	80	2.17	0.00046	2360
Cerebellum	GO:0048232	male gamete generation	250	-1.82	0.00046	1831
Cerebellum	GO:0000375	RNA splicing, via transesterification reactions	192	1.82	0.0012	2932
Cerebellum	GO:0007276	gamete generation	320	-1.69	0.0012	1831
Cerebellum	GO:0009060	aerobic respiration	113	1.97	0.0012	2914
Cerebellum	GO:0060271	cilium assembly	211	-1.82	0.0012	1827
Cerebellum	GO:0120031	plasma membrane bounded cell projection assembly	331	-1.7	0.0012	1827
Cerebellum	GO:0030031	cell projection assembly	334	-1.69	0.0013	1827
Cerebellum	GO:0009201	ribonucleoside triphosphate biosynthetic process	70	2.12	0.0013	2392
Cerebellum	GO:0009142	nucleoside triphosphate biosynthetic process	76	2.08	0.0013	2518
Cerebellum	GO:0022613	ribonucleoprotein complex biogenesis	301	1.71	0.0013	2832
Cerebellum	GO:0035082	axoneme assembly	46	-2.22	0.0014	1997
Cerebellum	GO:0022412	cellular process involved in reproduction in multicellular organism	182	-1.82	0.0014	1864

Supplementary Table 5.15 (continued).

Cerebellum	GO:0000377	RNA splicing, via transesterification reactions with bulged adenosine as nucleophile	190	1.79	0.0014	2932
Cerebellum	GO:0000398	mRNA splicing, via spliceosome	190	1.79	0.0014	2932
Cerebellum	GO:0007283	spermatogenesis	242	-1.75	0.0014	1831
Cerebellum	GO:0060445	branching involved in salivary gland morphogenesis	16	-2.21	0.0023	690
Cerebellum	GO:0022904	respiratory electron transport chain	70	2.07	0.0023	2178
Cerebellum	GO:0009206	purine ribonucleoside triphosphate biosynthetic process	66	2.05	0.0026	2392
Cerebellum	GO:0006754	ATP biosynthetic process	60	2.03	0.0026	2392
Cerebellum	GO:0006457	protein folding	131	1.87	0.0026	1730
Cerebellum	GO:0030336	negative regulation of cell migration	160	1.82	0.0026	1590
Cerebellum	GO:0019953	sexual reproduction	372	-1.59	0.0028	1864

Supplementary Table 5.16 *List of significantly enriched (adjusted p values) KEGG terms from GSEA on gene expression differences for all brain regions. NES: normalized enrichment score.*

Brain Region	ID	Description	setSize	NES	p.adjust	rank
Striatum	hsa04260	Cardiac muscle contraction	44	-2.28	0.00019	1753
Striatum	hsa04724	Glutamatergic synapse	70	-2.04	0.0021	1868
Striatum	hsa05022	Pathways of neurodegeneration - multiple diseases	273	-1.66	0.0031	1786
Striatum	hsa05010	Alzheimer disease	216	-1.58	0.027	1766
Striatum	hsa04713	Circadian entrainment	59	-1.86	0.031	2142
Striatum	hsa04261	Adrenergic signaling in cardiomyocytes	86	-1.75	0.031	1753
Striatum	hsa05020	Prion disease	151	-1.65	0.031	1766
Striatum	hsa04934	Cushing syndrome	84	-1.74	0.033	1538
Striatum	hsa04961	Endocrine and other factor-regulated calcium reabsorption	28	-1.9	0.042	1099
Striatum	hsa04979	Cholesterol metabolism	30	1.91	0.045	855
Striatum	hsa05016	Huntington disease	184	-1.51	0.048	1860
Hippocampus	hsa03040	Spliceosome	68	-1.93	0.042	1485
Cerebellum	hsa03010	Ribosome	84	2.23	5.32E-05	3235
Cerebellum	hsa00190	Oxidative phosphorylation	77	2.18	0.00016	2493
Cerebellum	hsa05012	Parkinson disease	150	1.89	0.00051	2526
Cerebellum	hsa05415	Diabetic cardiomyopathy	120	1.88	0.0011	2245
Cerebellum	hsa00980	Metabolism of xenobiotics by cytochrome P450	11	2.11	0.0046	550
Cerebellum	hsa05020	Prion disease	153	1.72	0.0058	2729

Supplementary Table 5.16 (continued).

Cerebellum	hsa04080	Neuroactive ligand-receptor interaction	119	-1.76	0.0061	1169
Cerebellum	hsa05010	Alzheimer disease	214	1.63	0.0061	2729
Cerebellum	hsa05014	Amyotrophic lateral sclerosis	221	1.55	0.015	2503
Cerebellum	hsa00500	Starch and sucrose metabolism	16	-1.98	0.016	1177
Cerebellum	hsa05016	Huntington disease	180	1.58	0.026	2741
Cerebellum	hsa04141	Protein processing in endoplasmic reticulum	118	1.64	0.037	1722
Cerebellum	hsa05208	Chemical carcinogenesis - reactive oxygen species	123	1.59	0.037	2526
Cerebellum	hsa04714	Thermogenesis	146	1.58	0.037	2729

Supplementary Table 5.17 *List of significantly enriched (adjusted p values) GO terms from ORA on genes showing concordant patterns of gene expression and chromatin accessibility in the striatum.*

Genomic Region	**Ontology**	**ID**	**Description**	**GeneRatio**	**BgRatio**	**p.adjust**
Promoter	MF	GO:0005231	excitatory extracellular ligand-gated ion channel activity	2/19	31/8537	0,047
Promoter	MF	GO:1904315	transmitter-gated ion channel activity involved in regulation of postsynaptic membrane potential	2/19	35/8537	0,047
Promoter	MF	GO:0099529	neurotransmitter receptor activity involved in regulation of postsynaptic membrane potential	2/19	36/8537	0,047
Promoter	MF	GO:0015075	ion transmembrane transporter activity	5/19	473/8537	0,047
Promoter	MF	GO:0022824	transmitter-gated ion channel activity	2/19	40/8537	0,047
Promoter	MF	GO:0022835	transmitter-gated channel activity	2/19	40/8537	0,047
Promoter	MF	GO:0005230	extracellular ligand-gated ion channel activity	2/19	44/8537	0,047
Promoter	MF	GO:0098960	postsynaptic neurotransmitter receptor activity	2/19	44/8537	0,047
Intron	BP	GO:0061061	muscle structure development	16/100	368/8423	0,013
Exon	CC	GO:0031093	platelet alpha granule lumen	3/37	33/8689	0,046

Supplementary Table 5.18 *List of top 30 significantly enriched (adjusted p values) GO terms (Biological Processes) from ORA on genes carrying DMS in striatum, hypermethylated in fast reversal learning individuals.*

ID	Description	GeneRatio	BgRatio	p.adjust
GO:0098742	cell-cell adhesion via plasma-membrane adhesion molecules	59/1363	149/10423	1.57E-12
GO:0048667	cell morphogenesis involved in neuron differentiation	113/1363	460/10423	1.55E-08
GO:0051963	regulation of synapse assembly	35/1363	88/10423	4.21E-07
GO:0007411	axon guidance	59/1363	198/10423	4.21E-07
GO:0097485	neuron projection guidance	59/1363	199/10423	4.21E-07
GO:0007416	synapse assembly	47/1363	142/10423	4.21E-07
GO:0007409	axonogenesis	90/1363	363/10423	4.21E-07
GO:0061564	axon development	96/1363	403/10423	9.57E-07
GO:0034329	cell junction assembly	80/1363	318/10423	1.39E-06
GO:0006935	chemotaxis	97/1363	413/10423	1.39E-06
GO:0042330	taxis	97/1363	415/10423	1.65E-06
GO:0099054	presynapse assembly	21/1363	41/10423	2.05E-06
GO:0099172	presynapse organization	21/1363	42/10423	3.28E-06
GO:0099174	regulation of presynapse organization	17/1363	29/10423	3.28E-06
GO:1905606	regulation of presynapse assembly	17/1363	29/10423	3.28E-06
GO:0050807	regulation of synapse organization	50/1363	170/10423	4.22E-06
GO:0021953	central nervous system neuron differentiation	45/1363	147/10423	5.54E-06
GO:0007157	heterophilic cell-cell adhesion via plasma membrane cell adhesion molecules	16/1363	27/10423	6.08E-06
GO:0050803	regulation of synapse structure or activity	50/1363	174/10423	8.23E-06
GO:0007156	homophilic cell adhesion via plasma membrane adhesion molecules	30/1363	81/10423	1.01E-05
GO:1901888	regulation of cell junction assembly	47/1363	161/10423	1.13E-05
GO:0050808	synapse organization	79/1363	333/10423	1.24E-05
GO:0021537	telencephalon development	56/1363	211/10423	2.14E-05
GO:0030900	forebrain development	74/1363	311/10423	2.67E-05
GO:0045165	cell fate commitment	56/1363	217/10423	5.46E-05
GO:0007389	pattern specification process	81/1363	358/10423	6.17E-05
GO:0051960	regulation of nervous system development	81/1363	359/10423	6.72E-05
GO:0010975	regulation of neuron projection development	81/1363	361/10423	8.26E-05
GO:0060411	cardiac septum morphogenesis	24/1363	63/10423	8.41E-05
GO:0060560	developmental growth involved in morphogenesis	51/1363	194/10423	8.41E-05

Supplementary Table 5.19 *List of top 30 significantly enriched (adjusted p values) GO terms (Biological Processes) from ORA on genes carrying DMS in striatum, hypermethylated in slow reversal learning individuals.*

ID	Description	GeneRatio	BgRatio	p.adjust
GO:0099172	presynapse organization	23/1325	42/10423	4.28E-07
GO:0007411	axon guidance	58/1325	198/10423	5.66E-07
GO:0099054	presynapse assembly	22/1325	41/10423	5.66E-07
GO:0097485	neuron projection guidance	58/1325	199/10423	5.66E-07
GO:0098742	cell-cell adhesion via plasma-membrane adhesion molecules	47/1325	149/10423	1.21E-06
GO:0060485	mesenchyme development	63/1325	245/10423	1.6E-05
GO:0007409	axonogenesis	83/1325	363/10423	2.85E-05
GO:0007416	synapse assembly	42/1325	142/10423	4.58E-05
GO:0048762	mesenchymal cell differentiation	54/1325	207/10423	6.65E-05
GO:0099174	regulation of presynapse organization	15/1325	29/10423	0.00021
GO:1905606	regulation of presynapse assembly	15/1325	29/10423	0.00021
GO:0061564	axon development	86/1325	403/10423	0.00023
GO:0030201	heparan sulfate proteoglycan metabolic process	16/1325	33/10423	0.00023
GO:0048667	cell morphogenesis involved in neuron differentiation	95/1325	460/10423	0.00025
GO:0050919	negative chemotaxis	18/1325	42/10423	0.00039
GO:0060411	cardiac septum morphogenesis	23/1325	63/10423	0.00039
GO:0050808	synapse organization	73/1325	333/10423	0.00043
GO:0034329	cell junction assembly	70/1325	318/10423	0.00058
GO:0007423	sensory organ development	92/1325	454/10423	0.00064
GO:0015012	heparan sulfate proteoglycan biosynthetic process	13/1325	25/10423	0.00064
GO:0072132	mesenchyme morphogenesis	19/1325	49/10423	0.00088
GO:0007156	homophilic cell adhesion via plasma membrane adhesion molecules	26/1325	81/10423	0.00097
GO:0003279	cardiac septum development	28/1325	92/10423	0.0013
GO:0051963	regulation of synapse assembly	27/1325	88/10423	0.0015
GO:0003231	cardiac ventricle development	30/1325	103/10423	0.0015
GO:0060412	ventricular septum morphogenesis	15/1325	36/10423	0.0027
GO:0003205	cardiac chamber development	36/1325	139/10423	0.0033
GO:0007585	respiratory gaseous exchange by respiratory system	19/1325	54/10423	0.0034
GO:0045596	negative regulation of cell differentiation	91/1325	471/10423	0.0035
GO:0003203	endocardial cushion morphogenesis	14/1325	33/10423	0.0035

Chapter 6.

General Discussion

Variable environments lead to predictable and unpredictable changes to which animals need to respond. The extent to which environmental changes are predictable will cause variation in the type of selection pressures that act on the cognitive mechanisms required for foraging behaviour (Dunlap and Stephens, 2012). Foraging in variable environments requires not only acquiring and storing information, but also the ability to use this information in a flexible manner, especially when changes occur unpredictably. Cognitive flexibility describes the ability of individuals to adaptively change a learned behaviour in response to changed contingencies in the environment. Human-induced climate change and urbanization drastically alter the environmental stability and predictability of habitats, leading to the question of how this will lead to altered selection on cognitive flexibility (Vardi and Berger-Tal, 2022). However, being able to make such predictions requires a better understanding of the causal mechanisms underlying variation in cognitive flexibility. Use of the reversal learning task to assess individual responses to a change in learned contingencies has contributed to our understanding of the neuroanatomical basis of cognitive flexibility in laboratory animals (Izquierdo et al., 2017; Highgate and Schenk, 2021) and environmental predictors and fitness consequences of cognitive flexibility (Ashton et al., 2018; Hermer et al., 2018; Madden et al., 2018; Tello-Ramos et al., 2018; Sonnenberg et al., 2019; Rochais et al., 2021), but studies on the causal mechanisms in ecological model species are still limited.

In this thesis, I explored the mechanisms underlying natural variation in cognitive flexibility in an ecological model species, the great tit. Where possible, I directly linked these findings to rodent models, to better understand the generality of findings in rodent species to make predictions in ecologically relevant species. I developed a high-throughput reversal learning task that allowed me to assess cognitive flexibility repeatedly across a wide range of individuals. First, I used performance of wild-caught captive great tits to assess to what extent reversal learning is repeatable and heritable in the great tit, and how reversal learning ability is linked to personality traits (**Chapter 2**). To explore the molecular mechanisms underlying cognitive flexibility, I first studied how chromatin accessibility contributes to cell type heterogeneity and tissue specificity of brain regions relevant to reversal learning performance (**Chapter 3**) and then assessed whether individual differences in reversal learning performance are explained by variation in chromatin accessibility and gene expression in these brain regions (**Chapter 4 and 5**). In this final chapter, I will discuss what can be concluded from these findings and how they relate to one another. The possibilities of automated learning devices (Griebling et al., 2022) have led to a rapid surge in the amount of data that is being collected on avian cognition. This has contributed to an increasing understanding of the molecular and neurobiological mechanisms as well as behavioural and fitness correlates of individual variation in cognitive performance. I will discuss the findings in this thesis in light of these recent developments and end this chapter with suggestions for promising directions for future research.

Consistency and heritability of cognitive flexibility

Limited repeatability of cognitive flexibility

In **Chapter 2** I first show that individuals display marginal repeatability in reversal learning performance, as expected and consistent with many recent publications on great and blue tits (Reichert et al., 2020; Morand-Ferron et al., 2022), mountain chickadees (Tello-Ramos et al., 2018), Aegean wall lizards (De Meester et al., 2022b), as well as several other datasets published in a metanalysis (Cauchoix et al., 2018), although there are also reports of exceptionally high repeatability, for example in Australian magpies (Ashton et al., 2022). Repeatability, the proportion of between-individual variance relative to the total phenotypic variance, can express the proportion of the variance of a measurement that is due to permanent differences between individuals, which can be genetic as well as environmental. Repeatability is therefore used to quantify whether multiple measures represent the same trait, and whether individuals show consistency in performance (Dohm, 2002). However, in the reversal learning task, individuals are likely to get better in the task as they are exposed to repeated measures, as initially shown by subjecting rats and pigeons to serial reversals (Bitterman, 1965; Mackintosh et al., 1968), and since then has been shown to occur in many avian species including corvids (Bond et al., 2007), great tits (Cauchoix et al., 2017), blue jays (Dunlap and Stephens, 2012) and mountain chickadees (Benedict et al., 2023). Interestingly, this is not the case in guppies (Boussard et al., 2020) and honeybees (Mota and Giurfa, 2010), possibly indicating differences in the ability to implement rule learning among animal classes. This gradual improvement over time can confound the meaning of repeatability in a reversal learning task. However, improvement will only affect repeatability estimates when improvement rates vary substantially between individuals. Australian magpies show high repeatability in reversal learning tasks despite improvement over repeated reversals (Ashton et al., 2022), which could indicate the tested individuals did not vary in improvement rate. The extent to which individuals show variation in improvement rate will be a useful addition to the current standing work on the repeatability of reversal learning performance.

No heritability of cognitive flexibility

Although the repeatability of a trait is generally considered to set an upper limit to its heritability (Falconer, 1989), when repeated measures reflect different traits genetically, repeatability can in fact underestimate heritability. Nonetheless, in our artificial selection experiment, I observed near-zero narrow-sense heritability of reversal learning performance, which I confirmed with an animal model approach. I was expecting to find low heritability estimates, considering the low repeatability and known low heritability of cognitive traits, but the absence of additive genetic variation in our results was striking. An absence of heritability of reversal learning performance (as well as low to moderate repeatability) was recently also reported in Aegean wall lizards (De Meester et al., 2022b). Assuming the phenotypic gambit, the belief that all traits are ultimately at least partly heritable (Grafen, 1984), our findings suggest that heritability of reversal learning performance in our study system is too small to detect. The narrow-sense heritability is, together with the

strength of selection, determinant of the level of evolutionary response (Falconer, 1989). This means that even if there would be selection on reversal learning ability, which ultimately acts on the phenotype, the consequence of such a small heritability is that reversal learning performance has a low evolutionary potential.

This finding contrast to other studies, including results of a pedigree-based animal model showing heritability of reversal learning performance in red junglefowl (Sorato et al., 2018), and a study on honey bees reporting divergence of performance in selection lines on reversal learning performance (Ferguson et al., 2001). Genome-wide quantitative trait locus (QTL) analysis on bees representing extreme phenotypes from the 'fast' and 'slow' reversing lines identified two QTLs that together explained 27% of the phenotypic variance (Chandra et al., 2001). In mice, strain-level heritability of reversal learning performance was estimated at 0.17 with a significant QTL explaining 12% of the variance (Bagley et al., 2022) and 0.3 in another study, with a significant QTL explaining 19% of the variance (Laughlin et al., 2011). Recently, the genetic basis of spatial learning and memory ability was explored in mountain chickadees using a genome-wide association study (GWAS), finding that 10 loci explained 87% of the variance (Branch et al., 2022). It could be fruitful to combine QTL or GWAS analyses with animal models to study not only heritability but also the contribution of genetic architecture and specific genes to reversal learning (Slate, 2005; Poissant et al., 2013). However, although such an approach would conceptually be very interesting, it may not be as useful in our study system, where heritability is too low to detect.

Choices

A low repeatability and heritability can also indicate that performance in the reversal task is strongly influenced by environmental factors and measurement errors, which can reduce estimates of repeatability and heritability (Falconer, 1989). I largely mitigated environmental sources of variation by rearing the great tits in a common environment. Some factors we could not control, such as experience with the feeders during habituation time, possibly also affected by dominance interactions. Furthermore, environmental sources of variation can also be stochastic. For example, genetically identical mice develop individual differences in exploratory behaviour and associated epigenetic marks, when reared under identical, but enriched environments (Kempermann et al., 2022). As extensively discussed in **Chapter 2**, reversal learning performance tests a combination of cognitive components, and trials to criterion may only capture the aggregate result. Such components include the degree of proactive interference resulting in perseverative choices (Tello-Ramos et al., 2019; Morand-Ferron et al., 2022; Tsakanikos and Reed, 2022); attentional allocation resulting in a potential failure to detect task transitions (Izquierdo et al., 2017); and reinforcement learning, to learn the new cue-reward association as well as learning from non-reinforcements, decreasing approach towards non-rewarded locations (Nilsson et al., 2015). Each of these constituents may be separate components of reversal learning performance that selection can act upon, but the extent to which these components

make up reversal learning and the heritabilities of these components remain an important avenue for further study.

One potential source of unaccounted for variation is the experience an individual has acquired during the associative phase immediately before initiation of the reversal learning phase. The strength of memories formed in the associative learning phase can induce individuals differences in preference for the previously rewarding cue at the start of the reversal phase (Anderson and Neely, 1996; Aljadeff and Lotem, 2021). A stronger memory can lead to more proactive interference, the degree to which previously learnt, but now irrelevant, information interferes with learning and remembering newly relevant information (Tello-Ramos et al., 2019). Extensive proactive interference can make it more difficult to inhibit a response towards the previously rewarded cue, and thus decreasing performance in the reversal learning task. Indeed, lower reversal performance followed associative learning tasks that included more trials, with most errors being made on the previously rewarded feeder (Tello-Ramos et al., 2018). Such results are suggestive for a trade-off between learning and cognitive flexibility, in which animals that are quick at forming initial associations learn subsequent similar information less well. I found that associative and reversal learning performance were negatively correlated, consistent with hypothesized limitations of proactive interference and memory load (Tello-Ramos et al., 2019; Hermer et al., 2021). However, it was particularly striking that I only observed this negative correlation when individuals were rewarded for their first choice during the associative learning task, not when one of the other two feeders was rewarded. This suggests that not only intrinsic differences play a role in the relationship between associative and reversal learning performance, but also experimental design choices, such as the cue that is initially rewarded. This finding indicates that randomly allocating cues contingencies to individuals, as is often done, may in fact experimentally induce individual differences in performance. This idea is further strengthened by findings that both learned and innate cue preferences can induce variation in difficulty with the reversal task (Dhawan et al., 2019; Aljadeff and Lotem, 2021).

Crucially, this means that study design choices can strongly affect an individual's starting state, and eventually the measure of reversal learning performance, not only between individuals, but also across studies. Another example is the moment of reversal onset. In this thesis, I used the moment of reaching a pre-defined learning criterion as starting point for the reversal phase, with the aim to standardize the individuals' state at the beginning of the reversal phase (Bond et al., 2007; Boogert et al., 2011; Guillette et al., 2015; Shaw et al., 2015; Cauchoix et al., 2017; Ashton et al., 2018, 2022; Buechel et al., 2018; Soravia et al., 2022). However, others have used a fixed number of trials (Raine and Chittka, 2012; Madden et al., 2018; van Horik et al., 2019) or a fixed number of days (Tello-Ramos et al., 2018; Reichert et al., 2020; Morand-Ferron et al., 2022; Benedict et al., 2023). This is a crucial difference in task design, because a fixed number of trials or a fixed number of days can lead to overtraining: receiving additional experience after an association has been learned. Overtraining can improve reversal learning

performance because it creates a greater attention towards the relevant cue (Dhawan et al., 2019). This means that overtraining can stimulate model-based (rule-) learning in the sense that it creates a mental set, allowing an individual to learn that it should 'focus' on a specific cue type (colour, location, shape). Differences in the amount of experience during the associative learning phase may therefore account for the wide range of relationships that have been observed between associative and reversal learning across studies, including positive (Nettle et al., 2015; Tello-Ramos et al., 2018; Bagley et al., 2022), negative (Bebus et al., 2016; Sorato et al., 2018) and an absence of associations (Ferguson et al., 2001; Benedict et al., 2023), but might also account for the differences in repeatability and heritability across studies. It would be highly informative to experimentally or meta-analytically test how differences in study design affect (the additive genetic component of) consistent individual variation.

Following the speed-accuracy trade-off hypothesis (Sih and Del Giudice, 2012), I predicted that more exploratory and bolder individuals would perform worse at reversal learning performance while being better at associative learning tasks. However, contrary to other studies (Guillette et al., 2011; Marchetti and Drent, 2000; Mazza et al., 2018; van Oers et al., 2005; but see Guillette et al., 2015), our findings do not support a speed-accuracy trade-off. I found a positive correlation between associative learning performance and boldness, but not exploratory behaviour. Importantly, a relationship between boldness or exploratory behaviour and reversal learning performance was absent. Considering the negative correlation between associative and reversal learning performance, there is a small potential for variation in reversal learning performance to be maintained through heritable among-individual variation in boldness. However, it seems that these differences cannot be identified at the resolution of the performance criterion I used in this study.

To conclude, cognitive flexibility is challenging to isolate, as it requires the combined used of several aspects of executive function. As a result, task performance will depend on task setups and scoring methods, possibly explaining not only the limited repeatability and heritability in our study, but also the highly variable findings across studies, as even the same performance measures (e.g. trials to criterion) can have different meanings across studies. In **Chapter 2** I argue that disentangling the different mechanisms underlying reversal learning performance, identifying the repeatability and heritability of each of these components and relating them to associative learning and personality traits will be a crucial step towards a better understanding of any trade-offs between learning, flexibility and personality. I then propose that future studies should aim at associating multiple measures of a battery of cognitive functions to a battery of repeated personality traits, to see if these correlations hold at the among-individual level. Additionally, researchers interested in individual variation in cognitive flexibility could focus on the ability to use knowledge to improve foraging efficiency (an improvement rate, or learning curve). For example, one could study how much experience (e.g. number of errors or number of visits) it takes for an individual to perform optimally

in the reversal learning task, meaning a shift towards a win-stay lose-shift strategy (needing only one non-rewarded visit to respond to the contingency switch) (Strang and Sherry, 2014; Benedict et al., 2023). To my knowledge, the repeatability and heritability of improvement rates have not been tested as of yet. Such a study would likely benefit from the recent suggestion to implement 'learning reaction norms': modelling the extent to which an individual gains cumulative experience by including an environmental axis representing an individual's cumulative experiences to the traditional reaction norm approach (Barron and Robinson, 2008; Wright et al., 2022). Such an approach would allow for the use of quantitative genetic approaches as I used in **Chapter 2,** combining the learning reaction norms with animal models to assess genetic variation in the reaction norm parameters.

The plastic brain

In **Chapter 2**, I focused on the stable and heritable components of cognitive flexibility, finding low contribution of additive genetic variation. However, I also expected a significant contribution of plastic interactions between an individual's genome and its environment to influence cognitive flexibility. Transcriptomics provide a useful tool to study plastic cognitive traits, because differences in gene expression can explain how the genome and epigenome interact with the environment to produce phenotypic differences. In **Chapter 3, 4 and 5** I therefore made a switch from genetics to genomics to specifically focus on the dynamic aspects of the genome. I compared gene expression and epigenetic state across reversal learning phenotypes in order to identify associations between the regulation and expression of genes and reversal learning performance. For this I applied transcriptional profiling with RNA-seq combined with chromatin profiling with ATAC-seq and methylation profiling using EM-seq.

Chromatin accessibility explains cell type heterogeneity in brain gene expression

The striatum, hippocampus and cerebellum were the brain regions of focus in this thesis because of their hypothesized relevance to reversal learning performance. In **Chapter 3**, I identified their molecular profiles and studied the identity and function of genes with localized expression patterns, as well as their regulatory elements. This to understand how differential regulation of genes in these brain structures control cognitive and behavioural functions. I observed strong differences in gene expression between the neuronal and non-neuronal nuclei from the striatum, which correlated well with differential expression patterns of samples collected from the mouse striatum, with enrichment of highly similar gene ontologies. Furthermore, I observed that the expression of genes with known relevance to the function of the striatum in reversal learning performance mostly showed significantly higher expression in the neuronal cell population. This included genes encoding receptors for dopamine, serotonin and glutamate, stressing the importance of cell type-specific gene expression analysis. Across brain regions I also found clear differences in gene expression, with differences between striatal neuronal nuclei and cerebellar nuclei being consistent across great tits,

mouse and rats, and genes with region-specific functions showing high localized expression patterns, such as *DRD2*, *DRD5* and *PENK* in the striatum, *EN2*, *CBLN1*, *GRIN2C* and *ZIC1* in the cerebellum and *IFI30*, *C1QC* and *FEZF2* in the hippocampus.

Generally, these differences in gene expression correlated strongly and positively with chromatin accessibility, indicating that chromatin accessibility underlies cell type heterogeneity within the striatum and across brain regions. Specifically, I observed that most cell type- and brain region-specific accessible regions were located in introns and distal intergenic regions rather than promoters. This is commonly observed in studies of (brain) tissue-specific chromatin accessibility (Fullard et al., 2018; Yin et al., 2020). This was most pronounced in neuronal nuclei-specific cell populations, consistent with patterns of chromatin accessibility in the human brain (Fullard et al., 2018), but can also be explained by a higher heterogeneity of cell types in the non-neuronal samples. Differentially accessible chromatin regions in introns and distal intergenic regions are indicative of enhancers: distantly located cis-regulatory regions that mediate transcription via long-distance interactions with promoter regions (Perenthaler et al., 2019). Enhancer regions are bound by transcription factors on transcription factor binding sites (Lambert et al., 2018) and enhancer function typically underlies tissue-specific gene regulation (Spitz and Furlong, 2012). The results of **Chapter 3** underscore the function of variable chromatin accessibility across the genome in driving gene expression, and provide a basis for further exploration of mechanisms underlying stable and dynamic regulation of gene expression.

Cognitive flexibility across taxa is explained by different genes underlying similar pathways

In **Chapter 4** and **Chapter 5,** I investigated the differences in gene expression between extreme 'slow' and 'fast' reversal learning great tits and mice. Despite a dissimilarity of differentially expressed genes between extreme 'fast' and 'slow' reversers across the two species, gene set enrichment showed parallels in the biological functions of these cross-taxa RNA-sequencing results. In the great tit striatum, genes related to taste response (*PKD2L1)* (Horio et al., 2010), the ubiquitin-protease system (*USP5*), important for synaptic plasticity (Mabb and Ehlers, 2010), and apoptotic signalling in neuronal cells (*VWA3B*) (Kawarai et al., 2016) were differentially expressed. In the mouse striatum, genes related to neurogenesis (*Eva1a*, *Sall3*) and lipid homeostasis *(PPARα*), linked to brain dopamine function and loss of which promotes cognitive inflexibility (D'Agostino et al., 2015) were differentially expressed. Gene sets relevant to striatal functioning were differentially enriched between the reversal phenotypes in both species, such as neuron to neuron synapse, pathways of neurodegeneration and glutamate receptor binding, consistent with the role of glutamate synaptic signalling in reversal learning in both taxa. Glutamate receptors are involved in reward and extinction learning (Gao et al., 2019) and glutamatergic neurotransmission in the striatum is crucial for reversal learning performance in both birds and mammals (Lissek et al., 2002; Herold, 2010; Thonnard et al., 2019; Liu et al., 2020). A crucial difference between the species was the involvement of neuronal differentiation in

great tits compared to the involvement of angiogenesis in the mouse. Interestingly, angiogenesis rather than neurogenesis, was shown to be critical for learning and memory acquisition in mice and rats (Kerr et al., 2010; Lousada et al., 2023). Neurogenesis occurs much more broadly in the avian brain than in the mammalian brain (Barnea and Pravosudov, 2011). Whether the relative importance of neurogenesis versus angiogenesis reflects a true difference between great tits and mice would be an interesting avenue for further study.

In the cerebellum, I also found involvement of different genes between the species, but with similar functions. In the great tit cerebellum, *ALDH1A3,* related to retinoic acid function and crucial for neurodevelopment (Durston et al., 1989; Matsumoto et al., 1998; Parenti and Cicirata, 2004), and *IDUA,* lack of which causes neurodegeneration through dysfunctional lysosomal storage and impairs long-term memory formation (Reolon et al., 2006), were among the differentially expressed genes. In the mouse cerebellum, I found overexpression of *INPP5D* in slow learners, which negatively regulates immune signalling and expression of which increases as Alzheimer's disease progresses (Tsai et al., 2021). Interestingly, an intronic SNP in *INPP5D* that was associated with a lowered risk of Alzheimer's disease, was also associated with lower protein expression of *IDUA* (Heath et al., 2022), providing a potential link between *IDUA* and *INPP5D*. The ribosome pathway was significantly activated in fast learners of both species. Local protein synthesis is crucial for memory formation and synaptic plasticity, suggesting that slow learners have altered protein translations compared to fast learners. Additionally, there were overlapping pathways related to metabolism, such as protein metabolic processes and oxidative phosphorylation. Considering the high energetic costs of information processing in the cerebellum, most neurons of which show extremely high intrinsic activity that is modulated during learning , and given the energetic costs that come with associated learning and memory performance (Laughlin, 2001), it seems intuitive that individual differences in energy metabolism or allocation may underlie individual differences in cognitive performance in both species.

Surprisingly, gene expression differences in between fast and slow reversing great tits were negatively correlated between the cerebellum and striatum, with opposite patterns of gene expression in pathways related to cilium functioning and cell projection assembly. Both striatal and cerebellar neurons play a role in the processing of rewards and encode prediction errors (Cools et al., 2002; Schultz, 2006; Klanker et al., 2015, 2017; Wagner et al., 2017; Pierce and Péron, 2022). Perhaps upregulation of these pathways in the striatum in slow learners causes stronger stimulus-reward memories to be formed which are more difficult to reverse (Aljadeff and Lotem, 2021), whereas upregulation of these pathways in the cerebellum of fast learners ascertain proper normal cerebellar error sensitivity. Whether this means an opposite requirement of these pathways in different brain regions in relation to the reversal learning process remains to be studied.

For the hippocampus, I only explored gene expression data originating from great tits. Here, among others the genes *FANCM*, part of a repair pathway involved in neurogenesis and important for survival and maintenance of neural progenitor cells (Sii-Felice et al., 2008), and *MLC1*, a gene that predicts dementia status (Simon et al., 2018), were differentially expressed. Differences in gene expression were generally small and perhaps consequently no GO or KEGG terms were significantly enriched in the hippocampus, perhaps suggesting that performance on our reversal learning task is not hippocampus-dependent. Indeed, in mammals the hippocampus was shown to be less crucial for shifting behavioural strategies than the striatum (Regier et al., 2015). Whereas the relative contribution of the hippocampus to reversal learning performance as measured in this thesis may be lower, the striatum and hippocampus likely work in concert to influence cognitive flexibility. The striatum receives projections from the hippocampus (Atoji et al., 2002; Husband and Shimizu, 2011), and I found that gene expression differences between the reversal phenotypes were correlated between the hippocampus and striatum. The hippocampus plays a crucial role in avian spatial learning and memory (Mayer et al., 2013; Pravosudov et al., 2013) and is frequently discussed as a candidate region for spatial reversal learning, specifically the role of hippocampal neurogenesis in proactive interference (Epp et al., 2016; Anacker and Hen, 2017; Tello-Ramos et al., 2019). Sharpe *et al.*, (2019) suggest that the hippocampus provides information about the structure of the environment, whereas the striatum supports appropriate action selection. Crucially, information from both structures is integrated in the mammalian cortical regions to contribute to flexible behaviour. Since the nidopallium caudolaterale is the functional avian equivalent to the mammalian cortex (Güntürkün and Bugnyar, 2016), this is likely where integration of these signals occurs in the avian brain. Lesions and dopamine glutamate receptor blockades have indicated the critical contribution of this brain region to reversal learning ability (Hartmann and Güntürkün, 1998; Diekamp et al., 2000; Lissek et al., 2002), which would therefore be a promising brain region to include in future research on neurogenetic mechanisms of cognitive flexibility.

Altogether, these result show that in each brain region and each species, unique genes are differentially expressed between fast and slow reversal learners, in accordance with the distinct functions of the striatum, hippocampus and cerebellum in reversal learning ability. Most enriched gene ontology terms overlapped within brain regions rather than within species, suggesting that brain region-specific involvement of molecular mechanisms underlying reversal learning performance. This could suggest that between-individual differences across species have evolved from different genes with shared functional pathways (Rittschof and Robinson, 2014). Differentially expressed genes were not shared between species, in contrast to cross-species gene expression patterns for other behavioural traits, such as affective disorders across zebrafish, rats and humans (Demin et al., 2022) and personality traits across different fish species (Rey et al., 2021). Perhaps the gene correlates of reversal learning performance are indeed species specific, or the lack of overlap could be due to power limitations, explaining why we find different genes to be differentially expressed, but similar enrichment

of gene sets. Currently, the species-specify of the contribution of identical genes to individual variation in cognitive flexibility remains unresolved. Whereas midbrain dopamine D2 receptor density was correlated with reversal learning in mice (Laughlin et al., 2011), neither dopamine D1 and D2 receptor expression correlated with reversal learning in red junglefowl (Boddington et al., 2020). However, expression of serotonin receptor genes (5HT2A and 5HT2B) was linked to reversal learning performance (Boddington et al., 2020), consistent with the role of cortical serotonin in reversal learning ability in mammals (Brigman et al., 2010). The extent to which the same genes underlie individual variation in similar phenotypes across species will remain an important question to understand the translatability of findings from one study system to another, but also to uncover mechanisms underlying behavioural adaptation (Jourjine and Hoekstra, 2021).

Cognitive flexibility is explained by chromatin accessibility and gene expression, but only to a small extent

In **Chapter 5**, I studied to what extent patterns of differential gene expression between fast and slow reversal learners are explained by differences in epigenetic mechanisms. I found a positive correlation between differential gene expression and differential chromatin accessibility between striatal neurons from fast and slow reversal learners, specifically when focusing on promoter and intronic regions. This means that genes associated with chromatin opening are more likely to be upregulated, and vice versa, in relation to reversal learning performance. Furthermore, all differentially accessible regions in striatal neurons of fast and slow reversers resided in intronic and intergenic genomic regions, rather than promoter regions. This is consistent with the functional significance of distal enhancers in gene expression (Corces et al., 2018; Sigalova et al., 2020) and consistent with the findings in **Chapter 3**. Cis-regulatory enhancers can regulate multiple genes, and can be located very distant from the TSS of the gene they control and including in the introns of other genes (Perenthaler et al., 2019), explaining why the association between chromatin accessibility in these regions is less predictive of the expression of its nearest gene. In hippocampal neurons, I found no differentially accessible regions between fast and slow reversal learners and no evidence for any correlation between chromatin accessibility and gene expression. This may suggest that, in contrast to in the striatum, differential hippocampal functioning is not regulated via chromatin accessibility. This also reflects the relatively small differences in gene expression in the hippocampus as discussed above and suggest that differential gene regulation in the hippocampus between fast and slow reversers may not be as relevant to reversal learning performance.

The genes with differentially accessible regions in the striatum have a link to reversal learning ability. Differential accessibility of intronic regions of the gene *KDM4C* and *SPP2* suggests that negative regulation of BDNF is linked to reversal learning ability in the striatum of great tits (Deogracias et al., 2012; O'Sullivan and Dev, 2013; Cascante et al., 2014; Motyl and Strosznajder, 2018). Increased accessibility in distant intergenic regions of *GALNT9* and *NT5E* in fast reversal learners hint at a role for neuronal plasticity (Cunha, 2001; Zimmermann et al.,

2012; Ena et al., 2013a; Sun et al., 2019), and increased accessibility in distant intergenic regions of *DUSP10* and *CHMP2B* in slow reversers suggest differential neurodevelopment underlying differences in reversal leaning ability (Ghazi-Noori et al., 2012; Kim et al., 2016; Clayton et al., 2022). Increased accessibility of a distant intergenic region of the gene *TMEM18* in slow reversers suggests that individual variation in reward sensitivity may underlie variation in reversal learning performance (Larder et al., 2017). Furthermore, genes that show concordant patterns of gene expression and open chromatin in promoter regions in striatal neurons were enriched for functions including postsynaptic membrane potential and neurotransmitter receptor activity. This suggests that genes in pathways relevant to the function of the striatum in a reversal learning task are potentially regulated by differential chromatin accessibility of the promoter.

However, the correlation patterns we observe in **Chapter 5** are strikingly less strong than the clear relationship we observed between chromatin accessibility and gene expression in relation to cell type differences in **Chapter 3**, and there was no differential expression of any of the genes that contained a differentially accessible region, or vice versa. We can hypothesize that, compared to cell type differences in gene expression, many more factors determine the gene expression differences related to a behavioural phenotype, which are generally less distinctive and more gradual. Whereas cell differentiation largely relies on epigenetic regulatory elements to modulate gene expression (Ong and Corces, 2011), differential gene expression underlying behavioural differences can be regulated by many additional factors including environmental influences and gene-behaviour feedback loops, acting via multiple regulatory pathways (Fischer et al., 2021). Altogether, our results suggest that although, at least in the striatum, differential chromatin accessibility partially explains the variation in gene expression patterns that correlate with reversal learning performance, chromatin accessibility alone does not explain the variation in gene expression and that likely other regulatory mechanisms are also at play.

For example, in addition to differences in chromatin accessibility, I also found multiple differentially methylated sites in the striatum in relation to reversal learning performance, and an expected correlation between an increase in CpG site methylation and a decrease in expression of the associated gene, specifically for CpG sites in the promoter and TSS regions. Genes carrying differentially methylated sites were related to functions such as regulation of synapse assembly and neurogenesis, meaning that differential expression of genes with these functions in relation to reversal learning performance is to some extent established by differences in DNA methylation. We found that 15 genes contained a differentially methylated site in the transcription start site, including the thyroid hormone receptor *THRB*, which is associated with learning and cognitive abilities and plays a modulatory role in striatal gene expression (Bernal, 2000) and *APBB2,* involved in the formation the senile plaques that are characteristic for Alzheimer's disease and linked to cognitive impairment (Golanska et al., 2013). Other genes were less strongly linked to cognition, but had a direct link to behaviour, such as solute

transporter *SLC35F2* which was among the top SNPs for anxious temperament in several brain areas including the striatum (Gonda et al., 2021). Yet other genes are associated with neural system development (*LRTM1, FLCN*) (Kenyon et al., 2016; Samata et al., 2016) and neuronal signalling (*SLC35A48*) (Richard et al., 2001). Together, these findings indicate a functional role for DNA methylation in regulating gene expression variation in relation to learning and behaviour, as well as neuronal structure and development.

Collectively, the results from **Chapter 4** and **Chapter 5** support the idea that transcriptomic and epigenomic signatures differ between individuals that vary in their reversal learning performance, that these differences are brain region-specific, and that these differences correlate across genomic and epigenetic functions, especially in the striatum. In the species comparison, most overlapping gene ontology terms occurred within brain regions, suggesting that even across-taxa, individual differences in reversal learning performance are brain region-specific. Furthermore, such common molecular correlates of reversal learning in great tits and mice support the idea that in fact the same phenotype is being assessed with this task across species.

Future research

Future ideas for epigenomics of cognitive flexibility

In this thesis, I performed pairwise analyses, but subtler relationships between gene expression and anatomically distinct regions as well as behaviourally distinct phenotypes can in the future be explored in more detail by performing gene co-expression network analysis. Such an approach can be used to identify networks of genes that are active simultaneously, which can be very informative, because genes with similar expression patterns are likely to share functions (van Dam et al., 2018). Whereas pairwise comparisons focus on distinct expression profiles, co-expression patterns might reveal condition-specific gene modules as well as shared expression networks across brain regions or reversal learning phenotypes. In addition, gene co-expression networks can aid in predicting the regulatory role of non-coding RNAs, which also play a role in epigenetic regulation (Aristizabal et al., 2020; Chen et al., 2022). This approach can be combined with, and applied to, other epigenetic marks such as DNA methylation or chromatin accessibility to identify regulatory elements and transcription factors that affect the expression of genes in top-ranked (e.g. brain region- or phenotype-specific) modules to obtain a complete view on the gene regulatory network (Yin et al., 2020). Such an approach was for example used to conclude that differentially methylated regions, via induction of differential chromatin accessibility, were causal to gene expression differences in Alzheimer's disease (Wang et al., 2023). Another important addition to the current epigenetics works will be the identification of the transcription factor binding sites in the putative enhancer regions we identified. Enhancer regions are likely to harbour motifs, specific sequences that transcription factors can bind to (Klemm et al., 2019). Assessing which motifs are enriched in differentially accessible regions can

provide a prediction about the transcription factors that are involved, which could be linked to the expression patterns of those genes (Yan et al., 2020).

The approach I used in **Chapter 4** and **Chapter 5** was to assess differential expression, accessibility and methylation and to test enrichment of biological processes between individuals differing in reversal learning performance. Although this approach has been useful to obtain potential regulators of natural variation in cognitive flexibility, it comes with two important downsides. Firstly, we here assess the gene expression of individuals of extreme 'fast' and 'slow' phenotypes, whereas the phenotype 'trials to criterion' is continuous. Such a reduction to binary phenotypes may lead to information loss. This might be resolved by applying linear regression analysis to associate the continuous reversal learning phenotype with the genomic data, although this approach would be most informative if many more individuals are included in the dataset, including individuals performing at intermediate levels (Fanter et al., 2022). With sequencing data from enough individuals, one could even include measures of personality traits in the model, to assess whether differences in brain gene expression between different reversal learning phenotypes are personality-specific. This would be interesting, because individual differences in reward processing is not only an important component of cognitive flexibility, but also of personality, and the two behaviours may partially be explained by the same neurobiological mechanisms (Coppens et al., 2010). Secondly, the results presented in this thesis are only correlational, and therefore do not allow us to identify cause and effect. Targeted gene knockouts to can provide a functional validation of the role of specific genes to reversal learning ability (Moore et al., 2021). However, naturally occurring variation in cognition is expected to be regulated by many genes of small effect (Rittschof and Robinson, 2014). Therefore, although the idea to manipulate gene function is intuitively attractive, though perhaps less feasible in non-model species, the question is to what extent this would be helpful in understanding the mechanisms underlying a complex trait like reversal learning ability.

The combined results of **Chapter 2, Chapter 4** and **Chapter 5** suggest that there is still a great deal of individual variation unaccounted for. An interesting approach for the field of behavioural ecology would be to focus on the question how cognitive flexibility is shaped by genetic and environmental (during developmental phases as well as later in life) influences, the role of epigenetics therein, and whether cognitive flexibility is favoured by selection (Boogert et al., 2018). One could for example assess whether (early) life experiences can lead to altered cognitive flexibility, and whether that coincides with epigenetic changes and fitness consequences (Dunlap and Stephens, 2012; Morand-Ferron et al., 2016). Several great examples exists of such studies, showing effects of early-life predator experience and cortisol treatment (Bannier et al., 2017; Reyes-Contreras and Taborsky, 2022), natal brood size and growth rate (Nettle et al., 2015) and varying effects of natural variation in developmental stress (Bebus et al., 2016; Sonnenberg et al., 2022) on reversal learning performance. Experimental work on early developmental effects is relatively easy to execute in wild great tits and has been

shown to affect DNA methylation of behaviourally relevant genes (Sepers et al., 2021). It would be very interesting to combine such work with measurements of reversal learning performance and fitness traits.

Estimating selection

The RFID-based feeder setup that I used in this thesis has been designed to not only assess reversal learning performance in captive, but also wild great tits. This collected data may in the future be used to quantify the heritability of reversal learning performance in a natural population, using animal models based on available pedigree data (Quinn et al., 2016). Furthermore, this data may be used to quantify fitness consequences. Current evidence for fitness consequences is mixed, showing a negative relationship (Madden et al., 2018) and no relationship between reversal learning ability and survival (Sonnenberg et al., 2019). If there would be selection, this is likely to be spatially as well as temporally heterogeneous, and thus ideally, such a study would be performed on data collected over several years and ideally over different populations (Mouchet et al., 2021). Inclusion of additional behavioural traits will be fruitful to also test for indirect and/or correlational selection using multivariate selection analysis (Lande and Arnold, 1983; Morrissey, 2014), because selection will likely not act on these behavioural traits in isolation. For example, reversal learning ability was negatively associated with novel feeder discovery, suggesting that individuals with worse cognitive performance use a different foraging strategy and rely more on their ability to actively search novel food sources (Heinen et al., 2021). It would also be interesting to assess whether there exist population-level differences in cognitive flexibility between urban and rural great tit populations (Salmón et al., 2021), the role of environmental variability in such a relationship (Vardi and Berger-Tal, 2022), and whether these differences would be inherited or acquired through experience.

Concluding remarks

In this thesis, I investigated the causal mechanisms underlying cognitive flexibility using the reversal learning paradigm. I showed that reversal learning performance is marginally repeatable, and not explained by additive genetic variation in great tits. This indicates that reversal learning performance has low evolutionary potential, but also suggests the influence of many unaccounted internal and external sources to explain individual variation in performance. Further studies will benefit from a careful exploration of why individuals make certain choices as they progress through the task, and how these choices are influenced by personality traits and previous experience. To explore the contribution of plastic aspects of the genome to reversal learning performance, I made use of innovative transcriptomic and epigenomic sequencing tools to reveal brain region-specific regulation of gene expression. I identified molecular (epi)genetic candidates for reversal learning performance, and showed how chromatin accessibility and DNA methylation relate to differential gene expression. Altogether, the results of this thesis have brought us closer to understanding individual variation in cognitive flexibility. This opens up opportunities for studying neurobiological aspects of

cognitive flexibility in an ecological model species, the great tit. In this thesis, the first steps have been made to comprehend how the genome dynamically interacts with the environment, and how the epigenome integrates past experiences to regulate individuality in cognitive flexibility. These findings provide a basis for future work integrating the causal mechanisms of cognitive flexibility into ultimate studies, thereby unravelling how those mechanisms shape, and are shaped by the evolutionary trajectory of individual variation in cognitive flexibility.


369

References

Adamaszek, M., D'Agata, F., Ferrucci, R., Habas, C., Keulen, S., Kirkby, K. C., et al. (2017). Consensus Paper: Cerebellum and Emotion. *Cerebellum* 16, 552–576. doi: 10.1007/s12311-016-0815-8.

Akalin, A., Kormaksson, M., Li, S., Garrett-Bakelman, F. E., Figueroa, M. E., Melnick, A., et al. (2012). methylKit: a comprehensive R package for the analysis of genome-wide DNA methylation profiles. *Genome Biol* 13, R87. doi: 10.1186/gb-2012-13-10-r87.

Ali, M. Z., and Dholaniya, P. S. (2022). Oxidative phosphorylation mediated pathogenesis of Parkinson's disease and its implication via Akt signaling. *Neurochemistry International* 157, 105344. doi: 10.1016/j.neuint.2022.105344.

Aljadeff, N., and Lotem, A. (2021). Task-dependent reversal learning dynamics challenge the reversal paradigm of measuring cognitive flexibility. *Animal Behaviour* 179, 183–197. doi: 10.1016/j.anbehav.2021.07.002.

Allen, P. B., Ouimet, C. C., and Greengard, P. (1997). Spinophilin, a novel protein phosphatase 1 binding protein localized to dendritic spines. *Proceedings of the National Academy of Sciences* 94, 9956–9961. doi: 10.1073/pnas.94.18.9956.

Almén, M. S., Jacobsson, J. A., Shaik, J. H., Olszewski, P. K., Cedernaes, J., Alsiö, J., et al. (2010). The obesity gene, TMEM18, is of ancient origin, found in majority of neuronal cells in all major brain regions and associated with obesity in severely obese children. *BMC Med Genet* 11, 1–13. doi: 10.1186/1471-2350-11-58.

Alsiö, J., Phillips, B. U., Sala-Bayo, J., Nilsson, S. R. O., Calafat-Pla, T. C., Rizwand, A., et al. (2019). Dopamine D2-like receptor stimulation blocks negative feedback in visual and spatial reversal learning in the rat: behavioural and computational evidence. *Psychopharmacology* 236, 2307–2323. doi: 10.1007/s00213-019-05296-y.

Amy, M., van Oers, K., and Naguib, M. (2012). Worms under cover: relationships between performance in learning tasks and personality in great tits (Parus major). *Anim Cogn* 15, 763–770. doi: 10.1007/s10071-012-0500-3.

Anacker, C., and Hen, R. (2017). Adult hippocampal neurogenesis and cognitive flexibility — linking memory and mood. *Nat Rev Neurosci* 18, 335–346. doi: 10.1038/nrn.2017.45.

Andersen, P. K., and Pohar Perme, M. (2010). Pseudo-observations in survival analysis. *Stat Methods Med Res* 19, 71–99. doi: 10.1177/0962280209105020.

Anderson, M. C., and Neely, J. H. (1996). "Chapter 8 - Interference and Inhibition in Memory Retrieval," in *Memory*, eds. E. L. Bjork and R. A. Bjork (San Diego: Academic Press), 237–313. doi: 10.1016/B978-012102570-0/50010-0.

Andrews, S. (2010). FastQC: A Quality Control tool for High Throughput Sequence Data. Available at: https://www.bioinformatics.babraham.ac.uk/projects/fastqc/ [Accessed December 14, 2022].

Arendt, J., and Reznick, D. (2008). Convergence and parallelism reconsidered: what have we learned about the genetics of adaptation? *Trends in Ecology & Evolution* 23, 26–32. doi: 10.1016/j.tree.2007.09.011.

Aristizabal, M. J., Anreiter, I., Halldorsdottir, T., Odgers, C. L., McDade, T. W., Goldenberg, A., et al. (2020). Biological embedding of experience: A primer on epigenetics. *Proc Natl Acad Sci USA* 117, 23261–23269. doi: 10.1073/pnas.1820838116.

Arvidsson, L. K., and Matthysen, E. (2016). Individual differences in foraging decisions: information-gathering strategies or flexibility? *BEHECO* 27, 1353–1361. doi: 10.1093/beheco/arw054.

Ashton, B. J., Ridley, A. R., Edwards, E. K., and Thornton, A. (2018). Cognitive performance is linked to group size and affects fitness in Australian magpies. *Nature* 554, 364–367. doi: 10.1038/nature25503.

Ashton, B. J., Thornton, A., Cauchoix, M., and Ridley, A. R. (2022). Long-term repeatability of cognitive performance. *R. Soc. open sci.* 9, 220069. doi: 10.1098/rsos.220069.

Atoji, Y., Wild, J. M., Yamamoto, Y., and Suzuki, Y. (2002). Intratelencephalic connections of the hippocampus in pigeons (Columba livia). *Journal of Comparative Neurology* 447, 177–199. doi: 10.1002/cne.10239.

Audet, J.-N., and Lefebvre, L. (2017). What's flexible in behavioral flexibility? *Behavioral Ecology* 28, 943–947. doi: 10.1093/beheco/arx007.

Avigan, P. D., Cammack, K., and Shapiro, M. L. (2020). Flexible spatial learning requires both the dorsal and ventral hippocampus and their functional interactions with the prefrontal cortex. *Hippocampus* 30, 733–744. doi: 10.1002/hipo.23198.

Badura, A., Verpeut, J. L., Metzger, J. W., Pereira, T. D., Pisano, T. J., Deverett, B., et al. (2018). Normal cognitive and social development require posterior cerebellar activity. *eLife* 7, e36401. doi: 10.7554/eLife.36401.

Bagley, J. R., Bailey, L. S., Gagnon, L. H., He, H., Philip, V. M., Reinholdt, L. G., et al. (2022). Behavioral phenotypes revealed during reversal learning are linked with novel genetic loci in diversity outbred mice. *Addiction Neuroscience* 4, 100045. doi: 10.1016/j.addicn.2022.100045.

Bailey, L. S., Bagley, J. R., Dodd, R., Olson, A., Bolduc, M., Philip, V. M., et al. (2021). Heritable variation in locomotion, reward sensitivity and impulsive behaviors in a genetically diverse inbred mouse panel. *Genes, Brain and Behavior* 20. doi: 10.1111/gbb.12773.

Banerjee, A., Parente, G., Teutsch, J., Lewis, C., Voigt, F. F., and Helmchen, F. (2020). Value-guided remapping of sensory cortex by lateral orbitofrontal cortex. *Nature* 585, 245–250. doi: 10.1038/s41586-020-2704-z.

Bannier, F., Tebbich, S., and Taborsky, B. (2017). Early experience affects learning performance and neophobia in a cooperatively breeding cichlid. *Ethology* 123, 712–723. doi: 10.1111/eth.12646.

Barlow, R. L., Alsiö, J., Jupp, B., Rabinovich, R., Shrestha, S., Roberts, A. C., et al. (2015). Markers of Serotonergic Function in the Orbitofrontal Cortex and Dorsal Raphé Nucleus Predict Individual Variation in Spatial-Discrimination Serial Reversal Learning. *Neuropsychopharmacol* 40, 1619–1630. doi: 10.1038/npp.2014.335.

Barnea, A., and Pravosudov, V. (2011). Birds as a model to study adult neurogenesis: bridging evolutionary, comparative and neuroethological

approaches: Adult neurogenesis in birds. *European Journal of Neuroscience* 34, 884–907. doi: 10.1111/j.1460-9568.2011.07851.x.
Barron, A. B., and Robinson, G. E. (2008). The utility of behavioral models and modules in molecular analyses of social behavior. *Genes, Brain and Behavior* 7, 257–265. doi: 10.1111/j.1601-183X.2007.00344.x.
Batabyal, A., and Thaker, M. (2019). Lizards from suburban areas learn faster to stay safe. *Biol. Lett.* 15, 20190009. doi: 10.1098/rsbl.2019.0009.
Bates, D., Mächler, M., Bolker, B., and Walker, S. (2015). Fitting Linear Mixed-Effects Models Using **lme4**. *J. Stat. Soft.* 67. doi: 10.18637/jss.v067.i01.
Bebus, S. E., Small, T. W., Jones, B. C., Elderbrock, E. K., and Schoech, S. J. (2016). Associative learning is inversely related to reversal learning and varies with nestling corticosterone exposure. *Animal Behaviour* 111, 251–260. doi: 10.1016/j.anbehav.2015.10.027.
Bedrosian, T. A., Quayle, C., Novaresi, N., and Gage, Fred. H. (2018). Early life experience drives structural variation of neural genomes in mice. *Science* 359, 1395–1399. doi: 10.1126/science.aah3378.
Belgard, T. G., Montiel, J. F., Wang, W. Z., García-Moreno, F., Margulies, E. H., Ponting, C. P., et al. (2013). Adult pallium transcriptomes surprise in not reflecting predicted homologies across diverse chicken and mouse pallial sectors. *Proceedings of the National Academy of Sciences* 110, 13150–13155. doi: 10.1073/pnas.1307444110.
Bell, A. M. (2020). Individual variation and the challenge hypothesis. *Horm Behav* 123, 104549. doi: 10.1016/j.yhbeh.2019.06.013.
Bell, A. M., Hankison, S. J., and Laskowski, K. L. (2009). The repeatability of behaviour: a meta-analysis. *Animal Behaviour* 77, 771–783. doi: 10.1016/j.anbehav.2008.12.022.
Bell, A. M., and Robinson, G. E. (2011). Behavior and the Dynamic Genome. *Science* 332, 1161–1162. doi: 10.1126/science.1203295.
Benedict, L. M., Heinen, V. K., Sonnenberg, B. R., Bridge, E. S., and Pravosudov, V. V. (2023). Learning predictably changing spatial patterns across days in a food-caching bird. *Animal Behaviour* 196, 55–81. doi: 10.1016/j.anbehav.2022.11.005.
Bengston, S. E., Dahan, R. A., Donaldson, Z., Phelps, S. M., van Oers, K., Sih, A., et al. (2018). Genomic tools for behavioural ecologists to understand repeatable individual differences in behaviour. *Nat Ecol Evol* 2, 944–955. doi: 10.1038/s41559-017-0411-4.
Benner, S., Endo, T., Endo, N., Kakeyama, M., and Tohyama, C. (2014). Early deprivation induces competitive subordinance in C57BL/6 male mice. *Physiology & Behavior* 137, 42–52. doi: 10.1016/j.physbeh.2014.06.018.
Benowitz, K. M., McKinney, E. C., Cunningham, C. B., and Moore, A. J. (2019). Predictable gene expression related to behavioral variation in parenting. *Behavioral Ecology* 30, 402–407. doi: 10.1093/beheco/ary179.
Bensky, M. K., and Bell, A. M. (2020). Predictors of individual variation in reversal learning performance in three-spined sticklebacks. *Anim Cogn* 23, 925–938. doi: 10.1007/s10071-020-01399-8.
Berberoglu, M. A., Dong, Z., Li, G., Zheng, J., Trejo Martinez, L. d. C. G., Peng, J., et al. (2014). Heterogeneously Expressed fezf2 Patterns Gradient Notch Activity in

Balancing the Quiescence, Proliferation, and Differentiation of Adult Neural Stem Cells. *Journal of Neuroscience* 34, 13911–13923. doi: 10.1523/JNEUROSCI.1976-14.2014.

Berland, C., Montalban, E., Perrin, E., Di Miceli, M., Nakamura, Y., Martinat, M., et al. (2020). Circulating Triglycerides Gate Dopamine-Associated Behaviors through DRD2-Expressing Neurons. *Cell Metabolism* 31, 773-790.e11. doi: 10.1016/j.cmet.2020.02.010.

Bernal, J. (2000). "Thyroid Hormones in Brain Development and Function," in *Endotext*, eds. K. R. Feingold, B. Anawalt, M. R. Blackman, A. Boyce, G. Chrousos, E. Corpas, et al. (South Dartmouth (MA): MDText.com, Inc.). Available at: http://www.ncbi.nlm.nih.gov/books/NBK285549/ [Accessed February 5, 2023].

Biergans, S. D., Claudianos, C., Reinhard, J., and Galizia, C. G. (2016). DNA Methylation Adjusts the Specificity of Memories Depending on the Learning Context and Promotes Relearning in Honeybees. *Front. Mol. Neurosci.* 9. doi: 10.3389/fnmol.2016.00082.

Bingman, V. P., Gasser, B., and Colombo, M. (2008). Responses of pigeon (Columba livia) Wulst neurons during acquisition and reversal of a visual discrimination task. *Behavioral Neuroscience* 122, 1139–1147. doi: 10.1037/a0012586.

Bitterman, M. E. (1965). The Evolution of Intelligence. *Scientific American* 212, 92–101.

Blighe, K. (2018). EnhancedVolcano. doi: 10.18129/B9.BIOC.ENHANCEDVOLCANO.

Boake, C. R. B., Arnold, S. J., Breden, F., Meffert, L. M., Ritchie, M. G., Taylor, B. J., et al. (2002). Genetic Tools for Studying Adaptation and the Evolution of Behavior. *The American Naturalist* 160, S143–S159. doi: 10.1086/342902.

Bobrowicz, K., and Greiff, S. (2022). Executive Functions in Birds. *Birds* 3, 184–220. doi: 10.3390/birds3020013.

Bocchi, V. D., Conforti, P., Vezzoli, E., Besusso, D., Cappadona, C., Lischetti, T., et al. (2021). The coding and long noncoding single-cell atlas of the developing human fetal striatum. *Science* 372, eabf5759. doi: 10.1126/science.abf5759.

Boddington, R., Gómez Dunlop, C. A., Garnham, L. C., Ryding, S., Abbey-Lee, R. N., Kreshchenko, A., et al. (2020). The relationship between monoaminergic gene expression, learning, and optimism in red junglefowl chicks. *Anim Cogn* 23, 901–911. doi: 10.1007/s10071-020-01394-z.

Bond, A. B., Kamil, A. C., and Balda, R. P. (2007). Serial reversal learning and the evolution of behavioral flexibility in three species of North American corvids (Gymnorhinus cyanocephalus, Nucifraga columbiana, Aphelocoma californica). *Journal of Comparative Psychology* 121, 372–379. doi: 10.1037/0735-7036.121.4.372.

Boogert, N. J., Anderson, R. C., Peters, S., Searcy, W. A., and Nowicki, S. (2011). Song repertoire size in male song sparrows correlates with detour reaching, but not with other cognitive measures. *Animal Behaviour* 81, 1209–1216. doi: 10.1016/j.anbehav.2011.03.004.

Boogert, N. J., Madden, J. R., Morand-Ferron, J., and Thornton, A. (2018). Measuring and understanding individual differences in cognition. *Phil. Trans. R. Soc. B* 373, 20170280. doi: 10.1098/rstb.2017.0280.

Boogert, N. J., Monceau, K., and Lefebvre, L. (2010). A field test of behavioural flexibility in Zenaida doves (Zenaida aurita). *Behavioural Processes* 85, 135–141. doi: 10.1016/j.beproc.2010.06.020.

Boussard, A., Buechel, S. D., Amcoff, M., Kotrschal, A., and Kolm, N. (2020). Brain size does not predict learning strategies in a serial reversal learning test. *Journal of Experimental Biology* 223, jeb224741. doi: 10.1242/jeb.224741.

Bowie, E., and Goetz, S. C. (2020). TTBK2 and primary cilia are essential for the connectivity and survival of cerebellar Purkinje neurons. *eLife* 9, e51166. doi: 10.7554/eLife.51166.

Boyce, W. T., and Kobor, M. S. (2015). Development and the epigenome: the 'synapse' of gene–environment interplay. *Developmental Science* 18, 1–23. doi: 10.1111/desc.12282.

Branch, C. L., Semenov, G. A., Wagner, D. N., Sonnenberg, B. R., Pitera, A. M., Bridge, E. S., et al. (2022). The genetic basis of spatial cognitive variation in a food-caching bird. *Current Biology* 32, 210-219.e4. doi: 10.1016/j.cub.2021.10.036.

Brigman, J. L., Mathur, P., Harvey-White, J., Izquierdo, A., Saksida, L. M., Bussey, T. J., et al. (2010). Pharmacological or Genetic Inactivation of the Serotonin Transporter Improves Reversal Learning in Mice. *Cerebral Cortex* 20, 1955–1963. doi: 10.1093/cercor/bhp266.

Brigman, J. L., and Rothblat, L. A. (2008). Stimulus specific deficit on visual reversal learning after lesions of medial prefrontal cortex in the mouse. *Behavioural Brain Research* 187, 405–410. doi: 10.1016/j.bbr.2007.10.004.

Brown, S. E., Weaver, I. C. G., Meaney, M. J., and Szyf, M. (2008). Regional-specific global cytosine methylation and DNA methyltransferase expression in the adult rat hippocampus. *Neuroscience Letters* 440, 49–53. doi: 10.1016/j.neulet.2008.05.028.

Brust, V., and Guenther, A. (2015). Domestication effects on behavioural traits and learning performance: comparing wild cavies to guinea pigs. *Anim Cogn* 18, 99–109. doi: 10.1007/s10071-014-0781-9.

Buechel, S. D., Boussard, A., Kotrschal, A., van der Bijl, W., and Kolm, N. (2018). Brain size affects performance in a reversal-learning test. *Proc. R. Soc. B.* 285, 20172031. doi: 10.1098/rspb.2017.2031.

Buenrostro, J., Wu, B., Chang, H., and Greenleaf, W. (2015). ATAC-seq: A Method for Assaying Chromatin Accessibility Genome-Wide. *Curr Protoc Mol Biol* 109, 21.29.1-21.29.9. doi: 10.1002/0471142727.mb2129s109.

Burton, A. C., Nakamura, K., and Roesch, M. R. (2015). From ventral-medial to dorsal-lateral striatum: Neural correlates of reward-guided decision-making. *Neurobiology of Learning and Memory* 117, 51–59. doi: 10.1016/j.nlm.2014.05.003.

Butler, D. G., Cullis, B. R., Gilmour, A. R., Gogel, B. J., and Thompson, R. (2017). ASReml-R Reference Manual Version 4. *VSN International Ltd, Hemel Hempstead, HP1 1ES, UK*.

Caligiore, D., Pezzulo, G., Baldassarre, G., Bostan, A. C., Strick, P. L., Doya, K., et al. (2017). Consensus Paper: Towards a Systems-Level View of Cerebellar Function: the Interplay Between Cerebellum, Basal Ganglia, and Cortex. *Cerebellum* 16, 203–229. doi: 10.1007/s12311-016-0763-3.

Campbell, R. R., and Wood, M. A. (2019). How the epigenome integrates information and reshapes the synapse. *Nat Rev Neurosci* 20, 133–147. doi: 10.1038/s41583-019-0121-9.

Cascante, A., Klum, S., Biswas, M., Antolin-Fontes, B., Barnabé-Heider, F., and Hermanson, O. (2014). Gene-specific methylation control of H3K9 and H3K36 on neurotrophic BDNF versus astroglial GFAP genes by KDM4A/C regulates neural stem cell differentiation. *J Mol Biol* 426, 3467–3477. doi: 10.1016/j.jmb.2014.04.008.

Cauchoix, M., Chow, P. K. Y., van Horik, J. O., Atance, C. M., Barbeau, E. J., Barragan-Jason, G., et al. (2018). The repeatability of cognitive performance: a meta-analysis. *Phil. Trans. R. Soc. B* 373, 20170281. doi: 10.1098/rstb.2017.0281.

Cauchoix, M., Hermer, E., Chaine, A. S., and Morand-Ferron, J. (2017). Cognition in the field: comparison of reversal learning performance in captive and wild passerines. *Sci Rep* 7, 12945. doi: 10.1038/s41598-017-13179-5.

Chandra, S. B. C., Hunt, G. J., Cobey, S., and Smith, B. H. (2001). Quantitative Trait Loci Associated with Reversal Learning and Latent Inhibition in Honeybees (Apis mellifera). *Behav Genet* 31, 275–285. doi: 10.1023/A:1012227308783.

Charles Darwin (1859). *On the origin of species by means of natural selection, or, The preservation of favoured races in the struggle for life*. London: Murray.

Chen, H., McCaffery, J. M., and Chan, D. C. (2007). Mitochondrial Fusion Protects against Neurodegeneration in the Cerebellum. *Cell* 130, 548–562. doi: 10.1016/j.cell.2007.06.026.

Chen, P. B., Kawaguchi, R., Blum, C., Achiro, J. M., Coppola, G., O'Dell, T. J., et al. (2017). Mapping Gene Expression in Excitatory Neurons during Hippocampal Late-Phase Long-Term Potentiation. *Frontiers in Molecular Neuroscience* 10. Available at: https://www.frontiersin.org/articles/10.3389/fnmol.2017.00039 [Accessed November 28, 2022].

Chen, W., Li, J., Huang, S., Li, X., Zhang, X., Hu, X., et al. (2022). GCEN: An Easy-to-Use Toolkit for Gene Co-Expression Network Analysis and lncRNAs Annotation. *Current Issues in Molecular Biology* 44, 1479–1487. doi: 10.3390/cimb44040100.

Chermon, D., and Birk, R. (2023). Drinking Habits and Physical Activity Interact and Attenuate Obesity Predisposition of TMEM18 Polymorphisms Carriers. *Nutrients* 15, 266. doi: 10.3390/nu15020266.

Chittka, L., Thomson, J. D., and Waser, N. M. (1999). Flower Constancy, Insect Psychology, and Plant Evolution. *Naturwissenschaften* 86, 361–377. doi: 10.1007/s001140050636.

Cholewa-Waclaw, J., Bird, A., Schimmelmann, M. von, Schaefer, A., Yu, H., Song, H., et al. (2016). The Role of Epigenetic Mechanisms in the Regulation of Gene Expression in the Nervous System. *J. Neurosci.* 36, 11427–11434. doi: 10.1523/JNEUROSCI.2492-16.2016.

Class, B., Brommer, J. E., and Oers, K. (2019). Exploratory behavior undergoes genotype–age interactions in a wild bird. *Ecol Evol* 9, 8987–8994. doi: 10.1002/ece3.5430.

Clayton, E. L., Bonnycastle, K., Isaacs, A. M., Cousin, M. A., and Schorge, S. (2022). A novel synaptopathy-defective synaptic vesicle protein trafficking in the mutant CHMP2B mouse model of frontotemporal dementia. *Journal of Neurochemistry* 160, 412–425. doi: 10.1111/jnc.15551.

Cole, E. F., Cram, D. L., and Quinn, J. L. (2011). Individual variation in spontaneous problem-solving performance among wild great tits. *Animal Behaviour* 81, 491–498. doi: 10.1016/j.anbehav.2010.11.025.

Cole, E. F., Morand-Ferron, J., Hinks, A. E., and Quinn, J. L. (2012). Cognitive Ability Influences Reproductive Life History Variation in the Wild. *Current Biology* 22, 1808–1812. doi: 10.1016/j.cub.2012.07.051.

Colombo, M., and Broadbent, N. (2000). Is the avian hippocampus a functional homologue of the mammalian hippocampus? *Neuroscience & Biobehavioral Reviews* 24, 465–484. doi: 10.1016/S0149-7634(00)00016-6.

Cooke, A. C., Davidson, G. L., van Oers, K., and Quinn, J. L. (2021). Motivation, accuracy and positive feedback through experience explain innovative problem solving and its repeatability. *Animal Behaviour* 174, 249–261. doi: 10.1016/j.anbehav.2021.01.024.

Cools, R., Clark, L., Owen, A. M., and Robbins, T. W. (2002). Defining the Neural Mechanisms of Probabilistic Reversal Learning Using Event-Related Functional Magnetic Resonance Imaging. *J. Neurosci.* 22, 4563–4567. doi: 10.1523/JNEUROSCI.22-11-04563.2002.

Coomes, J. R., Davidson, G. L., Reichert, M. S., Kulahci, I. G., Troisi, C. A., and Quinn, J. L. (2022). Inhibitory control, exploration behaviour and manipulated ecological context are associated with foraging flexibility in the great tit. *Journal of Animal Ecology* 91, 320–333. doi: 10.1111/1365-2656.13600.

Coppens, C. M., de Boer, S. F., and Koolhaas, J. M. (2010). Coping styles and behavioural flexibility: towards underlying mechanisms. *Philosophical Transactions of the Royal Society B: Biological Sciences* 365, 4021–4028. doi: 10.1098/rstb.2010.0217.

Corces, M. R., Granja, J. M., Shams, S., Louie, B. H., Seoane, J. A., Zhou, W., et al. (2018). The chromatin accessibility landscape of primary human cancers. *Science* 362, eaav1898. doi: 10.1126/science.aav1898.

Corces, M. R., Trevino, A. E., Hamilton, E. G., Greenside, P. G., Sinnott-Armstrong, N. A., Vesuna, S., et al. (2017). An improved ATAC-seq protocol reduces background and enables interrogation of frozen tissues. *Nat Methods* 14, 959–962. doi: 10.1038/nmeth.4396.

Cortés-Mendoza, J., Díaz de León-Guerrero, S., Pedraza-Alva, G., and Pérez-Martínez, L. (2013). Shaping synaptic plasticity: The role of activity-mediated epigenetic regulation on gene transcription. *International Journal of Developmental Neuroscience* 31, 359–369. doi: 10.1016/j.ijdevneu.2013.04.003.

Costa-Mattioli, M., Sossin, W. S., Klann, E., and Sonenberg, N. (2009). Translational Control of Long-Lasting Synaptic Plasticity and Memory. *Neuron* 61, 10–26. doi: 10.1016/j.neuron.2008.10.055.

Croston, R., Branch, C. L., Kozlovsky, D. Y., Dukas, R., and Pravosudov, V. V. (2015a). Heritability and the evolution of cognitive traits. *BEHECO* 26, 1447–1459. doi: 10.1093/beheco/arv088.

Croston, R., Branch, C. L., Kozlovsky, D. Y., Dukas, R., and Pravosudov, V. V. (2015b). The importance of heritability estimates for understanding the evolution of cognition: a response to comments on Croston et al. *BEHECO* 26, 1463–1464. doi: 10.1093/beheco/arv192.

Croston, R., Branch, C. L., Pitera, A. M., Kozlovsky, D. Y., Bridge, E. S., Parchman, T. L., et al. (2017). Predictably harsh environment is associated with reduced cognitive flexibility in wild food-caching mountain chickadees. *Animal Behaviour* 123, 139–149. doi: 10.1016/j.anbehav.2016.10.004.

Cunha, R. A. (2001). Adenosine as a neuromodulator and as a homeostatic regulator in the nervous system: different roles, different sources and different receptors. *Neurochemistry International* 38, 107–125. doi: 10.1016/S0197-0186(00)00034-6.

D'Agostino, G., Cristiano, C., Lyons, D. J., Citraro, R., Russo, E., Avagliano, C., et al. (2015). Peroxisome proliferator-activated receptor alpha plays a crucial role in behavioral repetition and cognitive flexibility in mice. *Molecular Metabolism* 4, 528–536. doi: 10.1016/j.molmet.2015.04.005.

Danecek, P., Bonfield, J. K., Liddle, J., Marshall, J., Ohan, V., Pollard, M. O., et al. (2021). Twelve years of SAMtools and BCFtools. *GigaScience* 10, giab008. doi: 10.1093/gigascience/giab008.

Sweatt, J.D. (2019). The epigenetic basis of individuality. *Current Opinion in Behavioral Sciences* 25, 51–56. doi: 10.1016/j.cobeha.2018.06.009.

Day, J. J., Childs, D., Guzman-Karlsson, M. C., Kibe, M., Moulden, J., Song, E., et al. (2013). DNA methylation regulates associative reward learning. *Nat Neurosci* 16, 1445–1452. doi: 10.1038/nn.3504.

Day, J. J., Roitman, M. F., Wightman, R. M., and Carelli, R. M. (2007). Associative learning mediates dynamic shifts in dopamine signaling in the nucleus accumbens. *Nature Neuroscience* 10, 1020–1028. doi: 10.1038/nn1923.

De Meester, G., Pafilis, P., and Van Damme, R. (2022a). Bold and bright: shy and supple? The effect of habitat type on personality–cognition covariance in the Aegean wall lizard (Podarcis erhardii). *Anim Cogn* 25, 745–767. doi: 10.1007/s10071-021-01587-0.

De Meester, G., Pafilis, P., Vasilakis, G., and Van Damme, R. (2022b). Exploration and spatial cognition show long-term repeatability but no heritability in the Aegean wall lizard. *Animal Behaviour* 190, 167–185. doi: 10.1016/j.anbehav.2022.06.007.

De Meester, G., Van Linden, L., Torfs, J., Pafilis, P., Šunje, E., Steenssens, D., et al. (2022c). Learning with lacertids: Studying the link between ecology and cognition within a comparative framework. *Evolution* 76, 2531–2552. doi: 10.1111/evo.14618.

De Zeeuw, C. I. (2021). Bidirectional learning in upbound and downbound microzones of the cerebellum. *Nature Reviews. Neuroscience* 22, 92–110. doi: 10.1038/s41583-020-00392-x.

De Zeeuw, C. I., Hoebeek, F. E., Bosman, L. W. J., Schonewille, M., Witter, L., and Koekkoek, S. K. (2011). Spatiotemporal firing patterns in the cerebellum. *Nat Rev Neurosci* 12, 327–344. doi: 10.1038/nrn3011.

Del Giudice, M., and Crespi, B. J. (2018). Basic functional trade-offs in cognition: An integrative framework. *Cognition* 179, 56–70. doi: 10.1016/j.cognition.2018.06.008.

Demin, K. A., Krotova, N. A., Ilyin, N. P., Galstyan, D. S., Kolesnikova, T. O., Strekalova, T., et al. (2022). Evolutionarily conserved gene expression patterns for affective disorders revealed using cross-species brain transcriptomic analyses in humans, rats and zebrafish. *Sci Rep* 12, 20836. doi: 10.1038/s41598-022-22688-x.

Deogracias, R., Yazdani, M., Dekkers, M. P. J., Guy, J., Ionescu, M. C. S., Vogt, K. E., et al. (2012). Fingolimod, a sphingosine-1 phosphate receptor modulator, increases BDNF levels and improves symptoms of a mouse model of Rett syndrome. *Proc Natl Acad Sci U S A* 109, 14230–14235. doi: 10.1073/pnas.1206093109.

Dhawan, S. S., Tait, D. S., and Brown, V. J. (2019). More rapid reversal learning following overtraining in the rat is evidence that behavioural and cognitive flexibility are dissociable. *Behavioural Brain Research* 363, 45–52. doi: 10.1016/j.bbr.2019.01.055.

Dickson, P. E., Cairns, J., Goldowitz, D., and Mittleman, G. (2017). Cerebellar contribution to higher and lower order rule learning and cognitive flexibility in mice. *Neuroscience* 345, 99–109. doi: 10.1016/j.neuroscience.2016.03.040.

Diddens, J., Coussement, L., Frankl-Vilches, C., Majumdar, G., Steyaert, S., Ter Haar, S. M., et al. (2021). DNA Methylation Regulates Transcription Factor-Specific Neurodevelopmental but Not Sexually Dimorphic Gene Expression Dynamics in Zebra Finch Telencephalon. *Front. Cell Dev. Biol.* 9, 583555. doi: 10.3389/fcell.2021.583555.

Diekamp, B., Kalt, T., Ruhm, A., Koch, M., and Güntürkün, O. (2000). Impairment in a discrimination reversal task after D1 receptor blockade in the pigeon "prefrontal cortex". *Behavioral Neuroscience* 114, 1145–1155. doi: 10.1037/0735-7044.114.6.1145.

Dingemanse, N. J., Both, C., Drent, P. J., van Oers, K., and van Noordwijk, A. J. (2002). Repeatability and heritability of exploratory behaviour in great tits from the wild. *Animal Behaviour* 64, 929–938. doi: 10.1006/anbe.2002.2006.

Dohm, M. R. (2002). Repeatability estimates do not always set an upper limit to heritability: *Interpreting repeatability estimates*. *Functional Ecology* 16, 273–280. doi: 10.1046/j.1365-2435.2002.00621.x.

Dougherty, L. R., and Guillette, L. M. (2018). Linking personality and cognition: a meta-analysis. *Phil. Trans. R. Soc. B* 373, 20170282. doi: 10.1098/rstb.2017.0282.

Drent, P. J., van Oers, K., and van Noordwijk, A. J. (2003). Realized heritability of personalities in the great tit (*Parus major*). *Proc. R. Soc. Lond. B* 270, 45–51. doi: 10.1098/rspb.2002.2168.

Duckworth, R. A. (2010). Evolution of Personality: Developmental Constraints on Behavioral Flexibility. *The Auk* 127, 752–758. doi: 10.1525/auk.2010.127.4.752.

Dudde, A., Phi Van, L., Schrader, L., Obert, A. J., and Krause, E. T. (2022). Brain gain-Is the cognitive performance of domestic hens affected by a functional polymorphism in the serotonin transporter gene? *Front Psychol* 13, 901022. doi: 10.3389/fpsyg.2022.901022.

Dukas, R. (2004). Evolutionary Biology of Animal Cognition. *Annu. Rev. Ecol. Evol. Syst.* 35, 347–374. doi: 10.1146/annurev.ecolsys.35.112202.130152.

Duke, C. G., Kennedy, A. J., Gavin, C. F., Day, J. J., and Sweatt, J. D. (2017). Experience-dependent epigenomic reorganization in the hippocampus. *Learn Mem* 24, 278–288. doi: 10.1101/lm.045112.117.

Dunlap, A. S., and Stephens, D. W. (2012). Tracking a changing environment: optimal sampling, adaptive memory and overnight effects. *Behavioural Processes* 89, 86–94. doi: 10.1016/j.beproc.2011.10.005.

Dunlap, A. S., and Stephens, D. W. (2014). Experimental evolution of prepared learning. *Proceedings of the National Academy of Sciences* 111, 11750–11755. doi: 10.1073/pnas.1404176111.

Durinck, S., Moreau, Y., Kasprzyk, A., Davis, S., De Moor, B., Brazma, A., et al. (2005). BioMart and Bioconductor: a powerful link between biological databases and microarray data analysis. *Bioinformatics* 21, 3439–3440. doi: 10.1093/bioinformatics/bti525.

Durinck, S., Spellman, P. T., Birney, E., and Huber, W. (2009). Mapping identifiers for the integration of genomic datasets with the R/Bioconductor package biomaRt. *Nat Protoc* 4, 1184–1191. doi: 10.1038/nprot.2009.97.

Durston, A. J., Timmermans, J. P. M., Hage, W. J., Hendriks, H. F. J., de Vries, N. J., Heideveld, M., et al. (1989). Retinoic acid causes an anteroposterior transformation in the developing central nervous system. *Nature* 340, 140–144. doi: 10.1038/340140a0.

Ebneter, C., Pick, J. L., and Tschirren, B. (2016). A trade-off between reproductive investment and maternal cerebellum size in a precocial bird. *Biology Letters* 12, 20160659. doi: 10.1098/rsbl.2016.0659.

Edwards, S. C., Hall, Z. J., Ihalainen, E., Bishop, V. R., Nicklas, E. T., Healy, S. D., et al. (2020). Neural Circuits Underlying Nest Building in Male Zebra Finches. *Integrative and Comparative Biology* 60, 943–954. doi: 10.1093/icb/icaa108.

eIanov, L., eRani, A., Beas, B. S., eKumar, A., and Foster, T. C. (2016). Transcription profile of aging and cognition-related genes in the medial prefrontal cortex. *Frontiers in Aging Neuroscience* 8. doi: 10.3389/fnagi.2016.00113.

Eling, N., Morgan, M. D., and Marioni, J. C. (2019). Challenges in measuring and understanding biological noise. *Nat Rev Genet* 20, 536–548. doi: 10.1038/s41576-019-0130-6.

Ena, S. L., Backer, J.-F. D., Schiffmann, S. N., and d'Exaerde, A. de K. (2013a). FACS Array Profiling Identifies Ecto-5′ Nucleotidase as a Striatopallidal Neuron-Specific Gene Involved in Striatal-Dependent Learning. *J. Neurosci.* 33, 8794–8809. doi: 10.1523/JNEUROSCI.2989-12.2013.

Ena, S. L., De Backer, J.-F., Schiffmann, S. N., and de Kerchove d'Exaerde, A. (2013b). FACS Array Profiling Identifies Ecto-5' Nucleotidase as a Striatopallidal Neuron-Specific Gene Involved in Striatal-Dependent Learning. *Journal of Neuroscience* 33, 8794–8809. doi: 10.1523/JNEUROSCI.2989-12.2013.

Epp, J. R., Mera, R. S., Köhler, S., Josselyn, S. A., and Frankland, P. W. (2016). Neurogenesis-mediated forgetting minimizes proactive interference. *Nature Communications* 7. doi: 10.1038/ncomms10838.

Ewels, P., Magnusson, M., Lundin, S., and Käller, M. (2016). MultiQC: summarize analysis results for multiple tools and samples in a single report. *Bioinformatics* 32, 3047–3048. doi: 10.1093/bioinformatics/btw354.

Falconer, D. S. (1989). *Introduction to quantitative genetics*. 3. ed. New York: Longman Scientific & Technical.

Fanter, C., Madelaire, C., Genereux, D. P., van Breukelen, F., Levesque, D., and Hindle, A. (2022). Epigenomics as a paradigm to understand the nuances of phenotypes. *Journal of Experimental Biology* 225, jeb243411. doi: 10.1242/jeb.243411.

Fawcett, T. W., Hamblin, S., and Giraldeau, L.-A. (2012). Exposing the behavioral gambit: the evolution of learning and decision rules. *Behavioral Ecology* 24, 2–11. doi: 10.1093/beheco/ars085.

Ferguson, H. J., Cobey, S., and Smith, B. H. (2001). Sensitivity to a change in reward is heritable in the honeybee, Apis mellifera. *Animal Behaviour* 61, 527–534. doi: 10.1006/anbe.2000.1635.

Fernandez-Albert, J., Lipinski, M., Lopez-Cascales, M. T., Rowley, M. J., Martin-Gonzalez, A. M., del Blanco, B., et al. (2019). Immediate and deferred epigenomic signatures of in vivo neuronal activation in mouse hippocampus. *Nat Neurosci* 22, 1718–1730. doi: 10.1038/s41593-019-0476-2.

Fischer, E. K., Hauber, M. E., and Bell, A. M. (2021). Back to the basics? Transcriptomics offers integrative insights into the role of space, time and the environment for gene expression and behaviour. *Biol. Lett.* 17, 20210293. doi: 10.1098/rsbl.2021.0293.

Fox, J., and Weisberg, S. (2019). *An R Companion to Applied Regression*. Thousand Oaks CA: Sage Available at: https://socialsciences.mcmaster.ca/jfox/Books/Companion/ [Accessed September 1, 2022].

Fraser, H. B., Hirsh, A. E., Giaever, G., Kumm, J., and Eisen, M. B. (2004). Noise Minimization in Eukaryotic Gene Expression. *PLOS Biology* 2, e137. doi: 10.1371/journal.pbio.0020137.

Friedman, N. P., Miyake, A., Young, S. E., DeFries, J. C., Corley, R. P., and Hewitt, J. K. (2008). Individual differences in executive functions are almost entirely genetic in origin. *Journal of Experimental Psychology: General* 137, 201–225. doi: 10.1037/0096-3445.137.2.201.

Fullard, J. F., Hauberg, M. E., Bendl, J., Egervari, G., Cirnaru, M.-D., Reach, S. M., et al. (2018). An atlas of chromatin accessibility in the adult human brain. *Genome Res.* 28, 1243–1252. doi: 10.1101/gr.232488.117.

Gao, M., Pusch, R., and Güntürkün, O. (2019). Blocking NMDA-Receptors in the Pigeon's Medial Striatum Impairs Extinction Acquisition and Induces a Motoric Disinhibition in an Appetitive Classical Conditioning Paradigm. *Front. Behav. Neurosci.* 13, 153. doi: 10.3389/fnbeh.2019.00153.

Gao, Z., Davis, C., Thomas, A. M., Economo, M. N., Abrego, A. M., Svoboda, K., et al. (2018). A cortico-cerebellar loop for motor planning. *Nature* 563, 113–116. doi: 10.1038/s41586-018-0633-x.

Gauthier, J. L., and Tank, D. W. (2018). A Dedicated Population for Reward Coding in the Hippocampus. *Neuron* 99, 179-193.e7. doi: 10.1016/j.neuron.2018.06.008.

Gedman, G., Haase, B., Durieux, G., Biegler, M. T., Fedrigo, O., and Jarvis, E. D. (2021). As above, so below: Whole transcriptome profiling demonstrates strong molecular similarities between avian dorsal and ventral pallial subdivisions. *Journal of Comparative Neurology* 529, 3222–3246. doi: 10.1002/cne.25159.

Ghazi-Noori, S., Froud, K. E., Mizielinska, S., Powell, C., Smidak, M., Fernandez de Marco, M., et al. (2012). Progressive neuronal inclusion formation and axonal degeneration in CHMP2B mutant transgenic mice. *Brain* 135, 819–832. doi: 10.1093/brain/aws006.

Gibney, E. R., and Nolan, C. M. (2010). Epigenetics and gene expression. *Heredity* 105, 4–13. doi: 10.1038/hdy.2010.54.

Golanska, E., Sieruta, M., Gresner, S. M., Hulas-Bigoszewska, K., Corder, E. H., Styczynska, M., et al. (2008). Analysis of APBB2 gene polymorphisms in sporadic Alzheimer's disease. *Neuroscience Letters* 447, 164–166. doi: 10.1016/j.neulet.2008.10.003.

Golanska, E., Sieruta, M., Gresner, S. M., Pfeffer, A., Chodakowska-Zebrowska, M., Sobow, T. M., et al. (2013). APBB2 genetic polymorphisms are associated with severe cognitive impairment in centenarians. *Experimental Gerontology* 48, 391–394. doi: 10.1016/j.exger.2013.01.013.

Gonda, X., Eszlari, N., Torok, D., Gal, Z., Bokor, J., Millinghoffer, A., et al. (2021). Genetic underpinnings of affective temperaments: a pilot GWAS investigation identifies a new genome-wide significant SNP for anxious temperament in ADGRB3 gene. *Transl Psychiatry* 11, 1–15. doi: 10.1038/s41398-021-01436-1.

Good, M. (1987). The effects of hippocampal-area parahippocampalis lesions on discrimination learning in the pigeon. *Behavioural Brain Research* 26, 171–184. doi: 10.1016/0166-4328(87)90165-3.

Gosler, A. (1993). *The great tit*. London: Hamlyn.

Grafen, A. (1984). Natural selection, kin selection and group selection. *Behavioural ecology : an evolutionary approach / edited by J.R. Krebs and N.B. Davies*. Available at: https://scholar.google.com/scholar_lookup?title=Natural+selection%2C+kin+selection+and+group+selection+%5BPolistes+fuscatus%2C+wasps%5D&author=Grafen%2C+A.&publication_year=1984 [Accessed March 2, 2023].

Grandi, F. C., Modi, H., Kampman, L., and Corces, M. R. (2022). Chromatin accessibility profiling by ATAC-seq. *Nat Protoc*. doi: 10.1038/s41596-022-00692-9.

Graybeal, C., Feyder, M., Schulman, E., Saksida, L. M., Bussey, T. J., Brigman, J. L., et al. (2011). Paradoxical reversal learning enhancement by stress or prefrontal cortical damage: rescue with BDNF. *Nat Neurosci* 14, 1507–1509. doi: 10.1038/nn.2954.

Greggor, A. L., Trimmer, P. C., Barrett, B. J., and Sih, A. (2019). Challenges of Learning to Escape Evolutionary Traps. *Front. Ecol. Evol.* 7, 408. doi: 10.3389/fevo.2019.00408.

Griebling, H. J., Sluka, C. M., Stanton, L. A., Barrett, L. P., Bastos, J. B., and Benson-Amram, S. (2022). How technology can advance the study of animal cognition in the wild. *Current Opinion in Behavioral Sciences* 45, 101120. doi: 10.1016/j.cobeha.2022.101120.

Griffin, A. S., Guez, D., Lermite, F., and Patience, M. (2013). Tracking changing environments: Innovators are fast, but not flexible learners. *PLoS ONE* 8. doi: 10.1371/journal.pone.0084907.

Griffin, A. S., Guillette, L. M., and Healy, S. D. (2015). Cognition and personality: an analysis of an emerging field. *Trends in Ecology & Evolution* 30, 207–214. doi: 10.1016/j.tree.2015.01.012.

Groman, S. M., James, A. S., Seu, E., Crawford, M. A., Harpster, S. N., and Jentsch, J. D. (2013). Monoamine Levels Within the Orbitofrontal Cortex and Putamen Interact to Predict Reversal Learning Performance. *Biological Psychiatry* 73, 756–762. doi: 10.1016/j.biopsych.2012.12.002.

Groman, S. M., James, A. S., Seu, E., Tran, S., Clark, T. A., Harpster, S. N., et al. (2014). In the Blink of an Eye: Relating Positive-Feedback Sensitivity to Striatal Dopamine D2-Like Receptors through Blink Rate. *J. Neurosci.* 34, 14443–14454. doi: 10.1523/JNEUROSCI.3037-14.2014.

Groman, S. M., Lee, B., London, E. D., Mandelkern, M. A., James, A. S., Feiler, K., et al. (2011). Dorsal Striatal D_2 -Like Receptor Availability Covaries with Sensitivity to Positive Reinforcement during Discrimination Learning. *J. Neurosci.* 31, 7291–7299. doi: 10.1523/JNEUROSCI.0363-11.2011.

Groman, S. M., Smith, N. J., Petrullli, J. R., Massi, B., Chen, L., Ropchan, J., et al. (2016). Dopamine D_3 Receptor Availability Is Associated with Inflexible Decision Making. *J. Neurosci.* 36, 6732–6741. doi: 10.1523/JNEUROSCI.3253-15.2016.

Guillette, L. M., Hahn, A. H., Hoeschele, M., Przyslupski, A.-M., and Sturdy, C. B. (2015). Individual differences in learning speed, performance accuracy and exploratory behaviour in black-capped chickadees. *Anim Cogn* 18, 165–178. doi: 10.1007/s10071-014-0787-3.

Guillette, L. M., Reddon, A. R., Hoeschele, M., and Sturdy, C. B. (2011). Sometimes slower is better: slow-exploring birds are more sensitive to changes in a vocal discrimination task. *Proc. R. Soc. B.* 278, 767–773. doi: 10.1098/rspb.2010.1669.

Guitar, N. A., and Sherry, D. F. (2018). Decreased Neurogenesis Increases Spatial Reversal Errors in Chickadees (Poecile atricapillus). *Developmental Neurobiology* 78, 1206–1217. doi: 10.1002/dneu.22641.

Güntürkün, O., and Bugnyar, T. (2016). Cognition without Cortex. *Trends in Cognitive Sciences* 20, 291–303. doi: 10.1016/j.tics.2016.02.001.

Güntürkün, O., von Eugen, K., Packheiser, J., and Pusch, R. (2021). Avian pallial circuits and cognition: A comparison to mammals. *Current Opinion in Neurobiology* 71, 29–36. doi: 10.1016/j.conb.2021.08.007.

Guo, J., Otis, J. M., Higginbotham, H., Monckton, C., Cheng, J., Asokan, A., et al. (2017). Primary Cilia Signaling Shapes the Development of Interneuronal

Connectivity. *Developmental Cell* 42, 286-300.e4. doi: 10.1016/j.devcel.2017.07.010.
Guzowski, J. F., Setlow, B., Wagner, E. K., and McGaugh, J. L. (2001). Experience-Dependent Gene Expression in the Rat Hippocampus after Spatial Learning: A Comparison of the Immediate-Early GenesArc, c-fos, and zif268. *J. Neurosci.* 21, 5089–5098. doi: 10.1523/JNEUROSCI.21-14-05089.2001.
Hall, Z. J., Street, S. E., and Healy, S. D. (2013). The evolution of cerebellum structure correlates with nest complexity. *Biology Letters* 9, 20130687. doi: 10.1098/rsbl.2013.0687.
Han, X., Wang, W., Xue, X., Shao, F., and Li, N. (2011). Brief social isolation in early adolescence affects reversal learning and forebrain BDNF expression in adult rats. *Brain Research Bulletin* 86, 173–178. doi: 10.1016/j.brainresbull.2011.07.008.
Hartmann, B., and Güntürkün, O. (1998). Selective deficits in reversal learning after neostriatum caudolaterale lesions in pigeons: Possible behavioral equivalencies to the mammalian prefrontal system. *Behavioural Brain Research* 96, 125–133. doi: 10.1016/S0166-4328(98)00006-0.
Hashimoto, H., Vertino, P. M., and Cheng, X. (2010). Molecular coupling of DNA methylation and histone methylation. *Epigenomics* 2, 657–669.
Hashimshony, T., Senderovich, N., Avital, G., Klochendler, A., de Leeuw, Y., Anavy, L., et al. (2016). CEL-Seq2: sensitive highly-multiplexed single-cell RNA-Seq. *Genome Biol* 17, 77. doi: 10.1186/s13059-016-0938-8.
Hassett, T. C., and Hampton, R. R. (2017). Change in the relative contributions of habit and working memory facilitates serial reversal learning expertise in rhesus monkeys. *Anim Cogn* 20, 485–497. doi: 10.1007/s10071-017-1076-8.
Heath, L., Earls, J. C., Magis, A. T., Kornilov, S. A., Lovejoy, J. C., Funk, C. C., et al. (2022). Manifestations of Alzheimer's disease genetic risk in the blood are evident in a multiomic analysis in healthy adults aged 18 to 90. *Sci Rep* 12, 6117. doi: 10.1038/s41598-022-09825-2.
Heffley, W., and Hull, C. (2019). Classical conditioning drives learned reward prediction signals in climbing fibers across the lateral cerebellum. *eLife* 8, e46764. doi: 10.7554/eLife.46764.
Heinen, V. K., Pitera, A. M., Sonnenberg, B. R., Benedict, L. M., Bridge, E. S., Farine, D. R., et al. (2021). Food discovery is associated with different reliance on social learning and lower cognitive flexibility across environments in a food-caching bird. *Proceedings of the Royal Society B: Biological Sciences* 288, 20202843. doi: 10.1098/rspb.2020.2843.
Heinz, S., Benner, C., Spann, N., Bertolino, E., Lin, Y. C., Laslo, P., et al. (2010). Simple combinations of lineage-determining transcription factors prime cis-regulatory elements required for macrophage and B cell identities. *Mol Cell* 38, 576–589. doi: 10.1016/j.molcel.2010.05.004.
Hermer, E., Cauchoix, M., Chaine, A. S., and Morand-Ferron, J. (2018). Elevation-related difference in serial reversal learning ability in a nonscatter hoarding passerine. *Behavioral Ecology* 29, 840–847. doi: 10.1093/beheco/ary067.
Hermer, E., Murphy, B., Chaine, A. S., and Morand-Ferron, J. (2021). Great tits who remember more accurately have difficulty forgetting, but variation is not driven

by environmental harshness. *Sci Rep* 11, 10083. doi: 10.1038/s41598-021-89125-3.
Herold, C. (2010). NMDA and D2-like receptors modulate cognitive flexibility in a color discrimination reversal task in pigeons. *Behavioral Neuroscience* 124, 381–390. doi: 10.1037/a0019504.
Herold, C., Ockermann, P. N., and Amunts, K. (2022). Behavioral Training Related Neurotransmitter Receptor Expression Dynamics in the Nidopallium Caudolaterale and the Hippocampal Formation of Pigeons. *Frontiers in Physiology* 13. Available at: https://www.frontiersin.org/articles/10.3389/fphys.2022.883029 [Accessed January 10, 2023].
Herold, C., Palomero-Gallagher, N., Güntürkün, O., and Zilles, K. (2012). Serotonin 5-HT1A receptor binding sites in the brain of the pigeon (Columba livia). *Neuroscience* 200, 1–12. doi: 10.1016/j.neuroscience.2011.10.050.
Herold, C., Schlömer, P., Mafoppa-Fomat, I., Mehlhorn, J., Amunts, K., and Axer, M. (2019). The hippocampus of birds in a view of evolutionary connectomics. *Cortex* 118, 165–187. doi: 10.1016/j.cortex.2018.09.025.
Herre, M., and Korb, E. (2019). The chromatin landscape of neuronal plasticity. *Current Opinion in Neurobiology* 59, 79–86. doi: 10.1016/j.conb.2019.04.006.
Highgate, Q., and Schenk, S. (2021). Cognitive flexibility in humans and other laboratory animals. *Journal of the Royal Society of New Zealand* 51, 97–127. doi: 10.1080/03036758.2020.1784240.
Hol, E. M., van Leeuwen, F. W., and Fischer, D. F. (2005). The proteasome in Alzheimer's disease and Parkinson's disease: lessons from ubiquitin B+1. *Trends in Molecular Medicine* 11, 488–495. doi: 10.1016/j.molmed.2005.09.001.
Horio, N., Yoshida, R., Yasumatsu, K., Yanagawa, Y., Ishimaru, Y., and Matsunami, H. (2010). PKD2L1 is associated with the sour taste transduction. *Neuroscience Research* Supplement 1, e385. doi: 10.1016/j.neures.2010.07.1703.
Houle, D. (1992). Comparing evolvability and variability of quantitative traits. *Genetics* 130, 195–204. doi: 10.1093/genetics/130.1.195.
Husband, S. A., and Shimizu, T. (2011). Calcium-binding protein distributions and fiber connections of the nucleus accumbens in the pigeon (columba livia). *Journal of Comparative Neurology* 519, 1371–1394. doi: 10.1002/cne.22575.
Izquierdo, A., Brigman, J. L., Radke, A. K., Rudebeck, P. H., and Holmes, A. (2017). The neural basis of reversal learning: An updated perspective. *Neuroscience* 345, 12–26. doi: 10.1016/j.neuroscience.2016.03.021.
Izquierdo, A., Darling, C., Manos, N., Pozos, H., Kim, C., Ostrander, S., et al. (2013). Basolateral Amygdala Lesions Facilitate Reward Choices after Negative Feedback in Rats. *J. Neurosci.* 33, 4105–4109. doi: 10.1523/JNEUROSCI.4942-12.2013.
Izquierdo, A., and Jentsch, J. D. (2012). Reversal learning as a measure of impulsive and compulsive behavior in addictions. *Psychopharmacology* 219, 607–620. doi: 10.1007/s00213-011-2579-7.
Izquierdo, A., Newman, T. K., Higley, J. D., and Murray, E. A. (2007). Genetic modulation of cognitive flexibility and socioemotional behavior in rhesus

monkeys. *Proceedings of the National Academy of Sciences* 104, 14128–14133. doi: 10.1073/pnas.0706583104.
Izquierdo, A., Wiedholz, L. M., Millstein, R. A., Yang, R. J., Bussey, T. J., Saksida, L. M., et al. (2006). Genetic and dopaminergic modulation of reversal learning in a touchscreen-based operant procedure for mice. *Behavioural Brain Research* 171, 181–188. doi: 10.1016/j.bbr.2006.03.029.
Jarvis, E. D., Güntürkün, O., Bruce, L., Csillag, A., Karten, H., Kuenzel, W., et al. (2005). Avian brains and a new understanding of vertebrate brain evolution. *Nat Rev Neurosci* 6, 151–159. doi: 10.1038/nrn1606.
Jarvis, E. D., Yu, J., Rivas, M. V., Horita, H., Feenders, G., Whitney, O., et al. (2013). Global view of the functional molecular organization of the avian cerebrum: Mirror images and functional columns. *J. Comp. Neurol.* 521, 3614–3665. doi: 10.1002/cne.23404.
Ji, S., Fakhry, A., and Deng, H. (2014). Integrative analysis of the connectivity and gene expression atlases in the mouse brain. *NeuroImage* 84, 245–253. doi: 10.1016/j.neuroimage.2013.08.049.
Jocham, G., Klein, T. A., Neumann, J., von Cramon, D. Y., Reuter, M., and Ullsperger, M. (2009). Dopamine DRD2 Polymorphism Alters Reversal Learning and Associated Neural Activity. *Journal of Neuroscience* 29, 3695–3704. doi: 10.1523/JNEUROSCI.5195-08.2009.
Jourjine, N., and Hoekstra, H. E. (2021). Expanding evolutionary neuroscience: insights from comparing variation in behavior. *Neuron* 109, 1084–1099. doi: 10.1016/j.neuron.2021.02.002.
Kabelik, D., Julien, A. R., Ramirez, D., and O'Connell, L. A. (2021). Social boldness correlates with brain gene expression in male green anoles. *Hormones and Behavior* 133, 105007. doi: 10.1016/j.yhbeh.2021.105007.
Kahnt, T., and Tobler, P. N. (2017). Dopamine Modulates the Functional Organization of the Orbitofrontal Cortex. *J Neurosci* 37, 1493–1504. doi: 10.1523/JNEUROSCI.2827-16.2016.
Karlsson, R. M., Wang, A. S., Sonti, A. N., and Cameron, H. A. (2018). Adult neurogenesis affects motivation to obtain weak, but not strong, reward in operant tasks. *Hippocampus* 28, 512–522. doi: 10.1002/hipo.22950.
Katajamaa, R., Wright, D., Henriksen, R., and Jensen, P. (2021). Cerebellum size is related to fear memory and domestication of chickens. *Biology Letters* 17, 20200790. doi: 10.1098/rsbl.2020.0790.
Kawarai, T., Tajima, A., Kuroda, Y., Saji, N., Orlacchio, A., Terasawa, H., et al. (2016). A homozygous mutation of VWA3B causes cerebellar ataxia with intellectual disability. *J Neurol Neurosurg Psychiatry* 87, 656–662. doi: 10.1136/jnnp-2014-309828.
Kebschull, J. M., Richman, E. B., Ringach, N., Friedmann, D., Albarran, E., Kolluru, S. S., et al. (2020). Cerebellar nuclei evolved by repeatedly duplicating a conserved cell-type set. *Science* 370, eabd5059. doi: 10.1126/science.abd5059.
Keefer, S. E., and Petrovich, G. D. (2020). The basolateral amygdala-medial prefrontal cortex circuitry regulates behavioral flexibility during appetitive reversal learning. *Behav Neurosci* 134, 34–44. doi: 10.1037/bne0000349.

Kelly, T. K., Ahmadiantehrani, S., Blattler, A., and London, S. E. (2018). Epigenetic regulation of transcriptional plasticity associated with developmental song learning. *Proc. R. Soc. B.* 285, 20180160. doi: 10.1098/rspb.2018.0160.

Kemp, J. M., and Powell, T. P. S. (1971). The structure of the caudate nucleus of the cat: light and electron microscopy. *Phil. Trans. R. Soc. Lond. B* 262, 383–401. doi: 10.1098/rstb.1971.0102.

Kempermann, G., Lopes, J. B., Zocher, S., Schilling, S., Ehret, F., Garthe, A., et al. (2022). The individuality paradigm: Automated longitudinal activity tracking of large cohorts of genetically identical mice in an enriched environment. *Neurobiology of Disease* 175, 105916. doi: 10.1016/j.nbd.2022.105916.

Kenyon, E. J., Luijten, M. N. H., Gill, H., Li, N., Rawlings, M., Bull, J. C., et al. (2016). Expression and knockdown of zebrafish folliculin suggests requirement for embryonic brain morphogenesis. *BMC Dev Biol* 16, 23. doi: 10.1186/s12861-016-0119-8.

Kerr, A. L., Steuer, E. L., Pochtarev, V., and Swain, R. A. (2010). Angiogenesis but not neurogenesis is critical for normal learning and memory acquisition. *Neuroscience* 171, 214–226. doi: 10.1016/j.neuroscience.2010.08.008.

Kilvitis, H. J., Ardia, D. R., Thiam, M., and Martin, L. B. (2018). Corticosterone is correlated to mediators of neural plasticity and epigenetic potential in the hippocampus of Senegalese house sparrows (Passer domesticus). *General and Comparative Endocrinology* 269, 177–183. doi: 10.1016/j.ygcen.2018.09.014.

Kim, D., Paggi, J. M., Park, C., Bennett, C., and Salzberg, S. L. (2019). Graph-based genome alignment and genotyping with HISAT2 and HISAT-genotype. *Nat Biotechnol* 37, 907–915. doi: 10.1038/s41587-019-0201-4.

Kim, S. Y., Oh, M., Lee, K.-S., Kim, W.-K., Oh, K.-J., Lee, S. C., et al. (2016). Profiling analysis of protein tyrosine phosphatases during neuronal differentiation. *Neuroscience Letters* 612, 219–224. doi: 10.1016/j.neulet.2015.12.027.

Klanker, M., Feenstra, M., and Denys, D. (2013). Dopaminergic control of cognitive flexibility in humans and animals. *Front. Neurosci.* 7. doi: 10.3389/fnins.2013.00201.

Klanker, M., Fellinger, L., Feenstra, M., Willuhn, I., and Denys, D. (2017). Regionally distinct phasic dopamine release patterns in the striatum during reversal learning. *Neuroscience* 345, 110–123. doi: 10.1016/j.neuroscience.2016.05.011.

Klanker, M., Sandberg, T., Joosten, R., Willuhn, I., Feenstra, M., and Denys, D. (2015). Phasic dopamine release induced by positive feedback predicts individual differences in reversal learning. *Neurobiology of Learning and Memory* 125, 135–145. doi: 10.1016/j.nlm.2015.08.011.

Kleene, R., and Schachner, M. (2004). Glycans and neural cell interactions. *Nat Rev Neurosci* 5, 195–208. doi: 10.1038/nrn1349.

Klemm, S. L., Shipony, Z., and Greenleaf, W. J. (2019). Chromatin accessibility and the regulatory epigenome. *Nat Rev Genet* 20, 207–220. doi: 10.1038/s41576-018-0089-8.

Kolde, R. (2019). pheatmap: Pretty Heatmaps. Available at: https://CRAN.R-project.org/package=pheatmap [Accessed February 14, 2023].

Konopka, G. ed. (2017). Cognitive genomics: Linking genes to behavior in the human brain. *Network Neuroscience* 1, 3–13. doi: 10.1162/NETN_a_00003.

Kosaki, Y., and Watanabe, S. (2012). Dissociable roles of the medial prefrontal cortex, the anterior cingulate cortex, and the hippocampus in behavioural flexibility revealed by serial reversal of three-choice discrimination in rats. *Behavioural Brain Research* 227, 81–90. doi: 10.1016/j.bbr.2011.10.039.

Kotrschal, A., Rogell, B., Bundsen, A., Svensson, B., Zajitschek, S., Brännström, I., et al. (2013). Artificial Selection on Relative Brain Size in the Guppy Reveals Costs and Benefits of Evolving a Larger Brain. *Current Biology* 23, 168–171. doi: 10.1016/j.cub.2012.11.058.

Krebs, J. R., Kacelnik, A., and Taylor, P. (1978). Test of optimal sampling by foraging great tits. *Nature* 275, 27–31. doi: 10.1038/275027a0.

Krueger, F. (2023). Trim Galore. Available at: https://github.com/FelixKrueger/TrimGalore [Accessed February 13, 2023].

Krueger, F., and Andrews, S. R. (2011). Bismark: a flexible aligner and methylation caller for Bisulfite-Seq applications. *Bioinformatics* 27, 1571–1572. doi: 10.1093/bioinformatics/btr167.

Kuenzel, W. J., Medina, L., Csillag, A., Perkel, D. J., and Reiner, A. (2011). The avian subpallium: New insights into structural and functional subdivisions occupying the lateral subpallial wall and their embryological origins. *Brain Research* 1424, 67–101. doi: 10.1016/j.brainres.2011.09.037.

Kumpan, L. T. (2020). Animal cognition in the field: performance of wild vervet monkeys (Chlorocebus pygerythrus) on a reversal learning task. *Animal Cognition*, 12.

Laine, V. N., Gossmann, T. I., Schachtschneider, K. M., Garroway, C. J., Madsen, O., Verhoeven, K. J. F., et al. (2016). Evolutionary signals of selection on cognition from the great tit genome and methylome. *Nat Commun* 7, 10474. doi: 10.1038/ncomms10474.

Laine, V. N., and van Oers, K. (2017). "The Quantitative and Molecular Genetics of Individual Differences in Animal Personality," in *Personality in Nonhuman Animals*, eds. J. Vonk, A. Weiss, and S. A. Kuczaj (Cham: Springer International Publishing), 55–72. doi: 10.1007/978-3-319-59300-5_4.

Laland, K. N., Odling-Smee, J., Hoppitt, W., and Uller, T. (2013). More on how and why: cause and effect in biology revisited. *Biol Philos* 28, 719–745. doi: 10.1007/s10539-012-9335-1.

Lambert, C. T., and Guillette, L. M. (2021). The impact of environmental and social factors on learning abilities: a meta-analysis. *Biological Reviews*, 2871–2889. doi: 10.1111/brv.12783.

Lambert, S. A., Jolma, A., Campitelli, L. F., Das, P. K., Yin, Y., Albu, M., et al. (2018). The Human Transcription Factors. *Cell* 172, 650–665. doi: 10.1016/j.cell.2018.01.029.

Lande, R., and Arnold, S. J. (1983). The Measurement of Selection on Correlated Characters. *Evolution* 37, 1210–1226. doi: 10.2307/2408842.

Lander, S. S., Linder-Shacham, D., and Gaisler-Salomon, I. (2017). Differential effects of social isolation in adolescent and adult mice on behavior and cortical gene expression. *Behavioural Brain Research* 316, 245–254. doi: 10.1016/j.bbr.2016.09.005.

Langmead, B., and Salzberg, S. L. (2012). Fast gapped-read alignment with Bowtie 2. *Nat Methods* 9, 357–359. doi: 10.1038/nmeth.1923.

Larder, R., Sim, M. F. M., Gulati, P., Antrobus, R., Tung, Y. C. L., Rimmington, D., et al. (2017). Obesity-associated gene TMEM18 has a role in the central control of appetite and body weight regulation. *Proceedings of the National Academy of Sciences* 114, 9421–9426. doi: 10.1073/pnas.1707310114.

Lattin, C. R., Kelly, T. R., Kelly, M. W., and Johnson, K. M. (2022). Constitutive gene expression differs in three brain regions important for cognition in neophobic and non-neophobic house sparrows (Passer domesticus). *PLOS ONE* 17, e0267180. doi: 10.1371/journal.pone.0267180.

Laughlin, R. E., Grant, T. L., Williams, R. W., and Jentsch, J. D. (2011). Genetic Dissection of Behavioral Flexibility: Reversal Learning in Mice. *Biological Psychiatry* 69, 1109–1116. doi: 10.1016/j.biopsych.2011.01.014.

Laughlin, S. B. (2001). Energy as a constraint on the coding and processing of sensory information. *Current Opinion in Neurobiology* 11, 475–480. doi: 10.1016/S0959-4388(00)00237-3.

Lauss, M., Kriegner, A., Vierlinger, K., and Noehammer, C. (2007). Characterization of the drugged human genome. *Pharmacogenomics* 8, 1063–1073. doi: 10.2217/14622416.8.8.1063.

Ledon-Rettig, C. C., Richards, C. L., and Martin, L. B. (2013). Epigenetics for behavioral ecologists. *Behavioral Ecology* 24, 311–324. doi: 10.1093/beheco/ars145.

Lenth, R. V., Buerkner, P., Herve, M., Jung, M., Love, J., Miguez, F., et al. (2022). emmeans: Estimated Marginal Means, aka Least-Squares Means. Available at: https://CRAN.R-project.org/package=emmeans [Accessed September 1, 2022].

Li, M., Du, W., Shao, F., and Wang, W. (2016). Cognitive dysfunction and epigenetic alterations of the BDNF gene are induced by social isolation during early adolescence. *Behavioural Brain Research* 313, 177–183. doi: 10.1016/j.bbr.2016.07.025.

Liang, D., Elwell, A. L., Aygün, N., Krupa, O., Wolter, J. M., Kyere, F. A., et al. (2021). Cell-type-specific effects of genetic variation on chromatin accessibility during human neuronal differentiation. *Nat Neurosci* 24, 941–953. doi: 10.1038/s41593-021-00858-w.

Liao, Y., Smyth, G. K., and Shi, W. (2014). featureCounts: an efficient general purpose program for assigning sequence reads to genomic features. *Bioinformatics* 30, 923–930. doi: 10.1093/bioinformatics/btt656.

Lin, M. T., and Beal, M. F. (2006). Mitochondrial dysfunction and oxidative stress in neurodegenerative diseases. *Nature* 443, 787–795. doi: 10.1038/nature05292.

Lin, W. C., Liu, C., Kosillo, P., Tai, L.-H., Galarce, E., Bateup, H. S., et al. (2022). Transient food insecurity during the juvenile-adolescent period affects adult weight, cognitive flexibility, and dopamine neurobiology. *Current Biology* 32, 3690-3703.e5. doi: 10.1016/j.cub.2022.06.089.

Linden, J., James, A. S., McDaniel, C., and Jentsch, J. D. (2018). Dopamine D2 Receptors in Dopaminergic Neurons Modulate Performance in a Reversal Learning Task in Mice. *eNeuro* 5, ENEURO.0229-17.2018. doi: 10.1523/ENEURO.0229-17.2018.

Lissek, S., Diekamp, B., and Güntürkün, O. (2002). Impaired learning of a color reversal task after NMDA receptor blockade in the pigeon (Columbia livia) associative forebrain (Neostriatum Caudolaterale). *Behavioral Neuroscience* 116, 523–529. doi: 10.1037/0735-7044.116.4.523.

Liu, J., Shelkar, G. P., Gandhi, P. J., Gawande, D. Y., Hoover, A., Villalba, R. M., et al. (2020). Striatal glutamate delta-1 receptor regulates behavioral flexibility and thalamostriatal connectivity. *Neurobiology of Disease* 137, 104746. doi: 10.1016/j.nbd.2020.104746.

Lobo, M. K., Karsten, S. L., Gray, M., Geschwind, D. H., and Yang, X. W. (2006). FACS-array profiling of striatal projection neuron subtypes in juvenile and adult mouse brains. *Nat Neurosci* 9, 443–452. doi: 10.1038/nn1654.

Lousada, E., Kliesmete, Z., Janjic, A., Burguière, E., Enard, W., and Schreiweis, C. (2023). Expression profiling of the learning striatum. 2023.01.03.522560. doi: 10.1101/2023.01.03.522560.

Love, M. I., Huber, W., and Anders, S. (2014). Moderated estimation of fold change and dispersion for RNA-seq data with DESeq2. *Genome Biology* 15, 550. doi: 10.1186/s13059-014-0550-8.

Lovell, P. V., Wirthlin, M., Kaser, T., Buckner, A. A., Carleton, J. B., Snider, B. R., et al. (2020). ZEBrA: Zebra finch Expression Brain Atlas—A resource for comparative molecular neuroanatomy and brain evolution studies. *J Comp Neurol* 528, 2099–2131. doi: 10.1002/cne.24879.

Lynch, M., and Walsh, B. (1998). *Genetics and analysis of quantitative traits*. Sunderland, Mass: Sinauer.

Mabb, A. M., and Ehlers, M. D. (2010). Ubiquitination in postsynaptic function and plasticity. *Annu Rev Cell Dev Biol* 26, 179–210. doi: 10.1146/annurev-cellbio-100109-104129.

Mackintosh, N. J., Mcgonigle, B., and Holgate, V. (1968). Factors underlying improvement in serial reversal learning. *Canadian Journal of Psychology / Revue canadienne de psychologie* 22, 85–95. doi: 10.1037/h0082753.

MACS: Model-based Analysis for ChIP-Seq (2023). Available at: https://github.com/macs3-project/MACS [Accessed February 13, 2023].

Madden, J. R., Langley, E. J. G., Whiteside, M. A., Beardsworth, C. E., and van Horik, J. O. (2018). The quick are the dead: pheasants that are slow to reverse a learned association survive for longer in the wild. *Phil. Trans. R. Soc. B* 373, 20170297. doi: 10.1098/rstb.2017.0297.

Malvaez, M., Greenfield, V. Y., Matheos, D. P., Angelillis, N. A., Murphy, M. D., Kennedy, P. J., et al. (2018). Habits Are Negatively Regulated by Histone Deacetylase 3 in the Dorsal Striatum. *Biological Psychiatry* 84, 383–392. doi: 10.1016/j.biopsych.2018.01.025.

Mancini, N., Hranova, S., Weber, J., Weiglein, A., Schleyer, M., Weber, D., et al. (2019). Reversal learning in *Drosophila* larvae. *Learn. Mem.* 26, 424–435. doi: 10.1101/lm.049510.119.

Manto, M., Bower, J. M., Conforto, A. B., Delgado-García, J. M., da Guarda, S. N. F., Gerwig, M., et al. (2012). Consensus Paper: Roles of the Cerebellum in Motor Control—The Diversity of Ideas on Cerebellar Involvement in Movement. *Cerebellum* 11, 457–487. doi: 10.1007/s12311-011-0331-9.

Marchetti, C., and Drent, P. J. (2000). Individual differences in the use of social information in foraging by captive great tits. *Animal Behaviour* 60, 131–140. doi: 10.1006/anbe.2000.1443.
Matsumoto, K., Ieda, T., Saito, N., Ono, T., and Shimada, K. (1998). Role of retinoic acid in regulation of mRNA expression of CaBP-D28k in the cerebellum of the chicken. *Comparative Biochemistry and Physiology Part A: Molecular & Integrative Physiology* 120, 237–242. doi: 10.1016/S1095-6433(98)00022-1.
Matzel, L. D., and Sauce, B. (2017). Individual differences: Case studies of rodent and primate intelligence. *J Exp Psychol Anim Learn Cogn* 43, 325–340. doi: 10.1037/xan0000152.
Mayer, U., Watanabe, S., and Bischof, H.-J. (2013). Spatial memory and the avian hippocampus: Research in zebra finches. *Journal of Physiology-Paris* 107, 2–12. doi: 10.1016/j.jphysparis.2012.05.002.
Mazza, V., Eccard, J. A., Zaccaroni, M., Jacob, J., and Dammhahn, M. (2018). The fast and the flexible: cognitive style drives individual variation in cognition in a small mammal. *Animal Behaviour* 137, 119–132. doi: 10.1016/j.anbehav.2018.01.011.
McCarthy, D. M., Bell, G. A., Cannon, E. N., Mueller, K. A., Huizenga, M. N., Sadri-Vakili, G., et al. (2016). Reversal Learning Deficits Associated with Increased Frontal Cortical Brain-Derived Neurotrophic Factor Tyrosine Kinase B Signaling in a Prenatal Cocaine Exposure Mouse Model. *DNE* 38, 354–364. doi: 10.1159/000452739.
McCurdy, L. Y., Sareen, P., Davoudian, P. A., and Nitabach, M. N. (2021). Dopaminergic mechanism underlying reward-encoding of punishment omission during reversal learning in Drosophila. *Nat Commun* 12, 1115. doi: 10.1038/s41467-021-21388-w.
McGinty, R. K., and Tan, S. (2015). Nucleosome Structure and Function. *Chem. Rev.* 115, 2255–2273. doi: 10.1021/cr500373h.
McNamara, J. M., and Dall, S. R. X. (2010). Information is a fitness enhancing resource. *Oikos* 119, 231–236. doi: 10.1111/j.1600-0706.2009.17509.x.
McQuown, S. C., and Wood, M. A. (2011). HDAC3 and the molecular brake pad hypothesis. *Neurobiology of Learning and Memory* 96, 27–34. doi: 10.1016/j.nlm.2011.04.005.
Medina, L., and Reiner, A. (1995). Neurotransmitter Organization and Connectivity of the Basal Ganglia in Vertebrates: Implications for the Evolution of Basal Ganglia (Part 1 of 2). *Brain Behav Evol* 46, 235–246. doi: 10.1159/000113277.
Meléndez-Ramírez, C., Cuevas-Diaz Duran, R., Barrios-García, T., Giacoman-Lozano, M., López-Ornelas, A., Herrera-Gamboa, J., et al. (2021). Dynamic landscape of chromatin accessibility and transcriptomic changes during differentiation of human embryonic stem cells into dopaminergic neurons. *Sci Rep* 11, 16977. doi: 10.1038/s41598-021-96263-1.
Mery, F., and Burns, J. G. (2010). Behavioural plasticity: an interaction between evolution and experience. *Evol Ecol* 24, 571–583. doi: 10.1007/s10682-009-9336-y.
Miller, C. A., Campbell, S. L., and Sweatt, J. D. (2008). DNA methylation and histone acetylation work in concert to regulate memory formation and synaptic

plasticity. *Neurobiology of Learning and Memory* 89, 599–603. doi: 10.1016/j.nlm.2007.07.016.
Miyoshi, K., Kasahara, K., Murakami, S., Takeshima, M., Kumamoto, N., Sato, A., et al. (2014). Lack of Dopaminergic Inputs Elongates the Primary Cilia of Striatal Neurons. *PLOS ONE* 9, e97918. doi: 10.1371/journal.pone.0097918.
Mo, A., Mukamel, E. A., Davis, F. P., Luo, C., Henry, G. L., Picard, S., et al. (2015). Epigenomic Signatures of Neuronal Diversity in the Mammalian Brain. *Neuron* 86, 1369–1384. doi: 10.1016/j.neuron.2015.05.018.
Modi, A., Vai, S., Caramelli, D., and Lari, M. (2021). "The Illumina Sequencing Protocol and the NovaSeq 6000 System," in *Bacterial Pangenomics: Methods and Protocols* Methods in Molecular Biology., eds. A. Mengoni, G. Bacci, and M. Fondi (New York, NY: Springer US), 15–42. doi: 10.1007/978-1-0716-1099-2_2.
Moncada, D., Ballarini, F., and Viola, H. (2015). Behavioral Tagging: A Translation of the Synaptic Tagging and Capture Hypothesis. *Neural Plast* 2015, 650780. doi: 10.1155/2015/650780.
Moody, L., Chen, H., and Pan, Y.-X. (2017). Early-Life Nutritional Programming of Cognition—The Fundamental Role of Epigenetic Mechanisms in Mediating the Relation between Early-Life Environment and Learning and Memory Process. *Adv Nutr* 8, 337–350. doi: 10.3945/an.116.014209.
Moore, A., Linden, J., and Jentsch, J. D. (2021). Syn3 Gene Knockout Negatively Impacts Aspects of Reversal Learning Performance. *eNeuro* 8, ENEURO.0251-21.2021. doi: 10.1523/ENEURO.0251-21.2021.
Morand-Ferron, J., Cole, E. F., and Quinn, J. L. (2016). Studying the evolutionary ecology of cognition in the wild: a review of practical and conceptual challenges: Evolutionary ecology of cognition in the wild. *Biol Rev* 91, 367–389. doi: 10.1111/brv.12174.
Morand-Ferron, J., Reichert, M. S., and Quinn, J. L. (2022). Cognitive flexibility in the wild: Individual differences in reversal learning are explained primarily by proactive interference, not by sampling strategies, in two passerine bird species. *Learn Behav* 50, 153–166. doi: 10.3758/s13420-021-00505-1.
Morello, F., Borshagovski, D., Survila, M., Tikker, L., Sadik-Ogli, S., Kirjavainen, A., et al. (2020). Molecular Fingerprint and Developmental Regulation of the Tegmental GABAergic and Glutamatergic Neurons Derived from the Anterior Hindbrain. *Cell Reports* 33, 108268. doi: 10.1016/j.celrep.2020.108268.
Moreno, J. A., and Mallucci, G. R. (2010). Dysfunction and recovery of synapses in prion disease: implications for neurodegeneration. *Biochemical Society Transactions* 38, 482–487. doi: 10.1042/BST0380482.
Morris, R. G. M., Garrud, P., Rawlins, J. N. P., and O'Keefe, J. (1982). Place navigation impaired in rats with hippocampal lesions. *Nature* 297, 681–683. doi: 10.1038/297681a0.
Morrissey, M. B. (2014). In search of the best methods for multivariate selection analysis. *Methods in Ecology and Evolution* 5, 1095–1109. doi: 10.1111/2041-210X.12259.
Mota, T., and Giurfa, M. (2010). Multiple Reversal Olfactory Learning in Honeybees. *Frontiers in Behavioral Neuroscience* 4. Available at:

https://www.frontiersin.org/articles/10.3389/fnbeh.2010.00048 [Accessed March 3, 2023].

Motyl, J., and Strosznajder, J. B. (2018). Sphingosine kinase 1/sphingosine-1-phosphate receptors dependent signalling in neurodegenerative diseases. The promising target for neuroprotection in Parkinson's disease. *Pharmacol. Rep* 70, 1010–1014. doi: 10.1016/j.pharep.2018.05.002.

Mouchet, A., Cole, E. F., Matthysen, E., Nicolaus, M., Quinn, J. L., Roth, A. M., et al. (2021). Heterogeneous selection on exploration behavior within and among West European populations of a passerine bird. *Proc Natl Acad Sci USA* 118, e2024994118. doi: 10.1073/pnas.2024994118.

Murmu, R. P., Li, W., Szepesi, Z., and Li, J.-Y. (2015). Altered sensory experience exacerbates stable dendritic spine and synapse loss in a mouse model of Huntington's disease. *J Neurosci* 35, 287–298. doi: 10.1523/JNEUROSCI.0244-14.2015.

Murphy, K. P. S. J., Carter, R. J., Lione, L. A., Mangiarini, L., Mahal, A., Bates, G. P., et al. (2000). Abnormal Synaptic Plasticity and Impaired Spatial Cognition in Mice Transgenic for Exon 1 of the Human Huntington's Disease Mutation. *J. Neurosci.* 20, 5115–5123. doi: 10.1523/JNEUROSCI.20-13-05115.2000.

Naef-Daenzer, B., and Keller, L. F. (1999). The foraging performance of great and blue tits (Parus major and P. caeruleus) in relation to caterpillar development, and its consequences for nestling growth and fledging weight. *Journal of Animal Ecology* 68, 708–718. doi: 10.1046/j.1365-2656.1999.00318.x.

Negi, S. K., and Guda, C. (2017). Global gene expression profiling of healthy human brain and its application in studying neurological disorders. *Sci Rep* 7, 897. doi: 10.1038/s41598-017-00952-9.

Nettle, D., Andrews, C. P., Monaghan, P., Brilot, B. O., Bedford, T., Gillespie, R., et al. (2015). Developmental and familial predictors of adult cognitive traits in the European starling. *Animal Behaviour* 107, 239–248. doi: 10.1016/j.anbehav.2015.07.002.

Nickchen, K., Boehme, R., del Mar Amador, M., Hälbig, T. D., Dehnicke, K., Panneck, P., et al. (2017). Reversal learning reveals cognitive deficits and altered prediction error encoding in the ventral striatum in Huntington's disease. *Brain Imaging and Behavior* 11, 1862–1872. doi: 10.1007/s11682-016-9660-0.

Niemelä, P. T., Vainikka, A., Forsman, J. T., Loukola, O. J., and Kortet, R. (2013). How does variation in the environment and individual cognition explain the existence of consistent behavioral differences? *Ecology and Evolution* 3, 457–464. doi: 10.1002/ece3.451.

Nilsson, S. R. O., Alsiö, J., Somerville, E. M., and Clifton, P. G. (2015). The rat's not for turning: Dissociating the psychological components of cognitive inflexibility. *Neuroscience & Biobehavioral Reviews* 56, 1–14. doi: 10.1016/j.neubiorev.2015.06.015.

Noschang, C., Krolow, R., Arcego, D. M., Toniazzo, A. P., Huffell, A. P., and Dalmaz, C. (2012). Neonatal handling affects learning, reversal learning and antioxidant enzymes activities in a sex-specific manner in rats. *International Journal of Developmental Neuroscience* 30, 285–291. doi: 10.1016/j.ijdevneu.2012.01.010.

Noworyta-Sokolowska, K., Kozub, A., Jablonska, J., Rodriguez Parkitna, J., Drozd, R., and Rygula, R. (2019). Sensitivity to negative and positive feedback as a stable and enduring behavioural trait in rats. *Psychopharmacology* 236, 2389–2403. doi: 10.1007/s00213-019-05333-w.

Olkowicz, S., Kocourek, M., Lučan, R. K., Porteš, M., Fitch, W. T., Herculano-Houzel, S., et al. (2016). Birds have primate-like numbers of neurons in the forebrain. *Proc Natl Acad Sci USA* 113, 7255–7260. doi: 10.1073/pnas.1517131113.

Ong, C.-T., and Corces, V. G. (2011). Enhancer function: new insights into the regulation of tissue-specific gene expression. *Nat Rev Genet* 12, 283–293. doi: 10.1038/nrg2957.

O'Sullivan, C., and Dev, K. K. (2013). The structure and function of the S1P1 receptor. *Trends in Pharmacological Sciences* 34, 401–412. doi: 10.1016/j.tips.2013.05.002.

Padron-Rivera, G., Romero-Molina, A. O., Diaz, R., Vaca-Palomares, I., Ochoa-Morales, A., Romero-Rebollar, C., et al. (2022). Frontostriatal Circuits Alterations Associated with Cognitive Flexibility Deterioration in Huntington's Disease. *NDD* 22, 24–28. doi: 10.1159/000526778.

Paraskevopoulou, F., Herman, M. A., and Rosenmund, C. (2019). Glutamatergic Innervation onto Striatal Neurons Potentiates GABAergic Synaptic Output. *J Neurosci* 39, 4448–4460. doi: 10.1523/JNEUROSCI.2630-18.2019.

Parenti, R., and Cicirata, F. (2004). Retinoids and binding proteins in the cerebellum during lifetime. *Cerebellum* 3, 16–20. doi: 10.1080/14734220310017186.

Pennartz, C. M. A., Berke, J. D., Graybiel, A. M., Ito, R., Lansink, C. S., Meer, M. van der, et al. (2009). Corticostriatal Interactions during Learning, Memory Processing, and Decision Making. *J. Neurosci.* 29, 12831–12838. doi: 10.1523/JNEUROSCI.3177-09.2009.

Perenthaler, E., Yousefi, S., Niggl, E., and Barakat, T. S. (2019). Beyond the Exome: The Non-coding Genome and Enhancers in Neurodevelopmental Disorders and Malformations of Cortical Development. *Frontiers in Cellular Neuroscience* 13. doi: 10.3389/fncel.2019.00352.

Person, A. L., Gale, S. D., Farries, M. A., and Perkel, D. J. (2008). Organization of the songbird basal ganglia, including area X. *Journal of Comparative Neurology* 508, 840–866. doi: 10.1002/cne.21699.

Peterburs, J., Hofmann, D., Becker, M. P. I., Nitsch, A. M., Miltner, W. H. R., and Straube, T. (2018). The role of the cerebellum for feedback processing and behavioral switching in a reversal-learning task. *Brain and Cognition* 125, 142–148. doi: 10.1016/j.bandc.2018.07.001.

Phelps, S. M., Okhovat, M., and Berrio, A. (2017). Individual differences in social behavior and cortical vasopressin receptor: Genetics, epigenetics, and evolution. *Frontiers in Neuroscience* 11, 1–12. doi: 10.3389/fnins.2017.00537.

Pidoux, L., Le Blanc, P., Levenes, C., and Leblois, A. (2018). A subcortical circuit linking the cerebellum to the basal ganglia engaged in vocal learning. *eLife* 7, e32167. doi: 10.7554/eLife.32167.

Pierce, J. E., and Péron, J. (2020). The basal ganglia and the cerebellum in human emotion. *Social Cognitive and Affective Neuroscience* 15, 599–613. doi: 10.1093/scan/nsaa076.

Pierce, J. E., and Péron, J. A. (2022). "Reward-Based Learning and Emotional Habit Formation in the Cerebellum," in *The Emotional Cerebellum* Advances in Experimental Medicine and Biology., eds. M. Adamaszek, M. Manto, and D. J. L. G. Schutter (Cham: Springer International Publishing), 125–140. doi: 10.1007/978-3-030-99550-8_9.

Poissant, J., Réale, D., Martin, J. g. a., Festa-Bianchet, M., and Coltman, D. w. (2013). A quantitative trait locus analysis of personality in wild bighorn sheep. *Ecology and Evolution* 3, 474–481. doi: 10.1002/ece3.468.

Pravosudov, V. V. (2022). Cognitive ecology in the wild — advances and challenges in avian cognition research. *Current Opinion in Behavioral Sciences* 45, 101138. doi: 10.1016/j.cobeha.2022.101138.

Pravosudov, V. V., Roth, T. C., Forister, M. L., LaDage, L. D., Kramer, R., Schilkey, F., et al. (2013). Differential hippocampal gene expression is associated with climate-related natural variation in memory and the hippocampus in food-caching chickadees. *Mol Ecol* 22, 397–408. doi: 10.1111/mec.12146.

Prentice, P. M., Thorton, A., and Wilson, A. J. (2021). A multivariate view of cognitive performance reveals positive correlation in the Trinidadian Guppy (*Poecilia reticulata*). Animal Behavior and Cognition doi: 10.1101/2021.11.04.467320.

Pribut, H. J., Vázquez, D., Wei, A. D., Tennyson, S. S., Davis, I. R., Roesch, M. R., et al. (2021). Overexpressing Histone Deacetylase 5 in Rat Dorsal Striatum Alters Reward-Guided Decision-Making and Associated Neural Encoding. *J. Neurosci.* 41, 10080–10090. doi: 10.1523/JNEUROSCI.0916-21.2021.

Puelles, L., Kuwana, E., Puelles, E., Bulfone, A., Shimamura, K., Keleher, J., et al. (2000). Pallial and subpallial derivatives in the embryonic chick and mouse telencephalon, traced by the expression of the genes Dlx-2, Emx-1, Nkx-2.1, Pax-6, and Tbr-1. *Journal of Comparative Neurology* 424, 409–438. doi: 10.1002/1096-9861(20000828)424:3<409::AID-CNE3>3.0.CO;2-7.

Quinlan, A. R., and Hall, I. M. (2010). BEDTools: a flexible suite of utilities for comparing genomic features. *Bioinformatics* 26, 841–842. doi: 10.1093/bioinformatics/btq033.

Quinn, J. L., Cole, E. F., Reed, T. E., and Morand-Ferron, J. (2016). Environmental and genetic determinants of innovativeness in a natural population of birds. *Phil. Trans. R. Soc. B* 371, 20150184. doi: 10.1098/rstb.2015.0184.

Quinn, J. L., Patrick, S. C., Bouwhuis, S., Wilkin, T. A., and Sheldon, B. C. (2009). Heterogeneous selection on a heritable temperament trait in a variable environment. *Journal of Animal Ecology* 78, 1203–1215. doi: 10.1111/j.1365-2656.2009.01585.x.

R Core Team (2022). R: A language and environment for statistical computing. Available at: https://www.R-project.org/.

Ragozzino, M. E. (2007). The Contribution of the Medial Prefrontal Cortex, Orbitofrontal Cortex, and Dorsomedial Striatum to Behavioral Flexibility. *Annals*

of the New York Academy of Sciences 1121, 355–375. doi: 10.1196/annals.1401.013.
Rahman, M. F., and McGowan, P. O. (2022). Cell-type-specific epigenetic effects of early life stress on the brain. *Transl Psychiatry* 12, 1–10. doi: 10.1038/s41398-022-02076-9.
Raine, N. E., and Chittka, L. (2012). No Trade-Off between Learning Speed and Associative Flexibility in Bumblebees: A Reversal Learning Test with Multiple Colonies. *PLoS ONE* 7, e45096. doi: 10.1371/journal.pone.0045096.
Raus, A. M., Fuller, T. D., Nelson, N. E., Valientes, D. A., Bayat, A., and Ivy, A. S. (2023). Early-life exercise primes the murine neural epigenome to facilitate gene expression and hippocampal memory consolidation. *Commun Biol* 6, 1–18. doi: 10.1038/s42003-022-04393-7.
Rayburn-Reeves, R. M., Stagner, J. P., Kirk, C. R., and Zentall, T. R. (2013). Reversal learning in rats (Rattus norvegicus) and pigeons (Columba livia): Qualitative differences in behavioral flexibility. *Journal of Comparative Psychology* 127, 202–211. doi: 10.1037/a0026311.
Regier, P. S., Amemiya, S., and Redish, A. D. (2015). Hippocampus and subregions of the dorsal striatum respond differently to a behavioral strategy change on a spatial navigation task. *Journal of Neurophysiology* 114, 1399–1416. doi: 10.1152/jn.00189.2015.
Reichert, M. S., Crofts, S. J., Davidson, G. L., Firth, J. A., Kulahci, I. G., and Quinn, J. L. (2020). Multiple factors affect discrimination learning performance, but not between-individual variation, in wild mixed-species flocks of birds. *R. Soc. open sci.* 7, 192107. doi: 10.1098/rsos.192107.
Reiner, A., Medina, L., and Veenman, C. L. (1998). Structural and functional evolution of the basal ganglia in vertebrates. *Brain Research Reviews* 28, 235–285. doi: 10.1016/S0165-0173(98)00016-2.
Remmelink, E., Smit, A. B., Verhage, M., and Loos, M. (2016). Measuring discrimination- and reversal learning in mouse models within 4 days and without prior food deprivation. *Learn. Mem.* 23, 660–667. doi: 10.1101/lm.042085.116.
Reolon, G. K., Braga, L. M., Camassola, M., Luft, T., Henriques, J. A. P., Nardi, N. B., et al. (2006). Long-term memory for aversive training is impaired in Idua−/− mice, a genetic model of mucopolysaccharidosis type I. *Brain Research* 1076, 225–230. doi: 10.1016/j.brainres.2006.01.008.
Rey, S., Jin, X., Damsgård, B., Bégout, M.-L., and Mackenzie, S. (2021). Analysis across diverse fish species highlights no conserved transcriptome signature for proactive behaviour. *BMC Genomics* 22. doi: 10.1186/s12864-020-07317-z.
Reyes-Contreras, M., and Taborsky, B. (2022). Stress axis programming generates long-term effects on cognitive abilities in a cooperative breeder. *Proceedings of the Royal Society B: Biological Sciences* 289, 20220117. doi: 10.1098/rspb.2022.0117.
Richard, D., Clavel, S., Huang, Q., Sanchis, D., and Ricquier, D. (2001). Uncoupling protein 2 in the brain: distribution and function. *Biochemical Society Transactions* 29, 812–817. doi: 10.1042/bst0290812.

Río-Álamos, C., Piludu, M. A., Gerbolés, C., Barroso, D., Oliveras, I., Sánchez-González, A., et al. (2019). Volumetric brain differences between the Roman rat strains: Neonatal handling effects, sensorimotor gating and working memory. *Behavioural Brain Research* 361, 74–85. doi: 10.1016/j.bbr.2018.12.033.

Rittschof, C. C., and Robinson, G. E. (2014). Genomics: moving behavioural ecology beyond the phenotypic gambit. *Animal Behaviour* 92, 263–270. doi: 10.1016/j.anbehav.2014.02.028.

Rizzardi, L. F., Hickey, P. F., Rodriguez DiBlasi, V., Tryggvadóttir, R., Callahan, C. M., Idrizi, A., et al. (2019). Neuronal brain-region-specific DNA methylation and chromatin accessibility are associated with neuropsychiatric trait heritability. *Nat Neurosci* 22, 307–316. doi: 10.1038/s41593-018-0297-8.

Rochais, C., Hotte, H., and Pillay, N. (2021). Seasonal variation in reversal learning reveals greater female cognitive flexibility in African striped mice. *Sci Rep* 11, 20061. doi: 10.1038/s41598-021-99619-9.

Rocks, D., Jaric, I., Tesfa, L., Greally, J. M., Suzuki, M., and Kundakovic, M. (2022). Cell type-specific chromatin accessibility analysis in the mouse and human brain. *Epigenetics* 17, 202–219. doi: 10.1080/15592294.2021.1896983.

Rojas-Ferrer, I., Thompson, M. J., and Morand-Ferron, J. (2020). Is exploration a metric for information gathering? Attraction to novelty and plasticity in black-capped chickadees. *Ethology* 126, 383–392. doi: 10.1111/eth.12982.

Rook, N., Letzner, S., Packheiser, J., Güntürkün, O., and Beste, C. (2020). Immediate early gene fingerprints of multi-component behaviour. *Sci Rep* 10, 384. doi: 10.1038/s41598-019-56998-4.

Rose, J., Schiffer, A. M., and Güntürkün, O. (2013a). Striatal dopamine D1 receptors are involved in the dissociation of learning based on reward-magnitude. *Neuroscience* 230, 132–138. doi: 10.1016/j.neuroscience.2012.10.064.

Rose, J., Schiffer, A.-M., and Güntürkün, O. (2013b). Striatal dopamine D1 receptors are involved in the dissociation of learning based on reward-magnitude. *Neuroscience* 230, 132–138. doi: 10.1016/j.neuroscience.2012.10.064.

Rowe, C., and Healy, S. D. (2014). Measuring variation in cognition. *Behavioral Ecology* 25, 1287–1292. doi: 10.1093/beheco/aru090.

Rudebeck, P. H., and Izquierdo, A. (2022). Foraging with the frontal cortex: A cross-species evaluation of reward-guided behavior. *Neuropsychopharmacol.* 47, 134–146. doi: 10.1038/s41386-021-01140-0.

Sabariego, M., Morón, I., Gómez, M. J., Donaire, R., Tobeña, A., Fernández-Teruel, A., et al. (2013). Incentive loss and hippocampal gene expression in inbred Roman high- (RHA-I) and Roman low- (RLA-I) avoidance rats. *Behavioural Brain Research* 257, 62–70. doi: 10.1016/j.bbr.2013.09.025.

Sahr, K. E., Taylor, W. M., Daniels, B. P., Rubin, H. L., and Jarolim, P. (1994). The Structure and Organization of the Human Erythroid Anion Exchanger (AE1) Gene. *Genomics* 24, 491–501. doi: 10.1006/geno.1994.1658.

Sala-Bayo, J., Fiddian, L., Nilsson, S. R. O., Hervig, M. E., McKenzie, C., Mareschi, A., et al. (2020). Dorsal and ventral striatal dopamine D1 and D2 receptors differentially modulate distinct phases of serial visual reversal learning. *Neuropsychopharmacol.* 45, 736–744. doi: 10.1038/s41386-020-0612-4.

Salmón, P., Jacobs, A., Ahrén, D., Biard, C., Dingemanse, N. J., Dominoni, D. M., et al. (2021). Continent-wide genomic signatures of adaptation to urbanisation in a songbird across Europe. *Nat Commun* 12, 2983. doi: 10.1038/s41467-021-23027-w.

Samata, B., Doi, D., Nishimura, K., Kikuchi, T., Watanabe, A., Sakamoto, Y., et al. (2016). Purification of functional human ES and iPSC-derived midbrain dopaminergic progenitors using LRTM1. *Nat Commun* 7, 13097. doi: 10.1038/ncomms13097.

Sauce, B., Wass, C., Smith, A., Kwan, S., and Matzel, L. D. (2014). The external–internal loop of interference: Two types of attention and their influence on the learning abilities of mice. *Neurobiology of Learning and Memory* 116, 181–192. doi: 10.1016/j.nlm.2014.10.005.

Schmauss, C. (2017). The roles of class I histone deacetylases (HDACs) in memory, learning, and executive cognitive functions: A review. *Neuroscience & Biobehavioral Reviews* 83, 63–71. doi: 10.1016/j.neubiorev.2017.10.004.

Schultz, W. (2006). Behavioral Theories and the Neurophysiology of Reward. *Annual Review of Psychology* 57, 87–115. doi: 10.1146/annurev.psych.56.091103.070229.

Seib, D. R., Espinueva, D. F., Floresco, S. B., and Snyder, J. S. (2020). A role for neurogenesis in probabilistic reward learning. *Behavioral Neuroscience* 134, 283–295. doi: 10.1037/bne0000370.

Seki, Y., Hessler, N. A., Xie, K., and Okanoya, K. (2014). Food rewards modulate the activity of song neurons in Bengalese finches. *European Journal of Neuroscience* 39, 975–983. doi: 10.1111/ejn.12457.

Sepers, B., Erven, J. A. M., Gawehns, F., Laine, V. N., and van Oers, K. (2021). Epigenetics and Early Life Stress: Experimental Brood Size Affects DNA Methylation in Great Tits (Parus major). *Frontiers in Ecology and Evolution* 9. Available at: https://www.frontiersin.org/articles/10.3389/fevo.2021.609061 [Accessed February 13, 2023].

Sepers, B., van den Heuvel, K., Lindner, M., Viitaniemi, H., Husby, A., and van Oers, K. (2019). Avian ecological epigenetics: pitfalls and promises. *J Ornithol* 160, 1183–1203. doi: 10.1007/s10336-019-01684-5.

Serrano, F., and Klann, E. (2004). Reactive oxygen species and synaptic plasticity in the aging hippocampus. *Ageing Research Reviews* 3, 431–443. doi: 10.1016/j.arr.2004.05.002.

Shang, A., and Bieszczad, K. M. (2022). Epigenetic mechanisms regulate cue memory underlying discriminative behavior. *Neuroscience & Biobehavioral Reviews* 141, 104811. doi: 10.1016/j.neubiorev.2022.104811.

Sharanek, A., and Jahani-Asl, A. (2022). "Monitoring Mitochondrial Respiration in Mouse Cerebellar Granule Neurons," in *Neuronal Cell Death: Methods and Protocols* Methods in Molecular Biology., ed. A. Jahani-Asl (New York, NY: Springer US), 1–15. doi: 10.1007/978-1-0716-2409-8_1.

Sharpe, M. J., Stalnaker, T., Schuck, N. W., Killcross, S., Schoenbaum, G., and Niv, Y. (2019). An Integrated Model of Action Selection: Distinct Modes of Cortical Control of Striatal Decision Making. *Annu. Rev. Psychol.* 70, 53–76. doi: 10.1146/annurev-psych-010418-102824.

Shaw, R. C., Boogert, N. J., Clayton, N. S., and Burns, K. C. (2015). Wild psychometrics: evidence for 'general' cognitive performance in wild New Zealand robins, Petroica longipes. *Animal Behaviour* 109, 101–111. doi: 10.1016/j.anbehav.2015.08.001.

Sheng, M., and Greenberg, M. E. (1990). The regulation and function of c-fos and other immediate early genes in the nervous system. *Neuron* 4, 477–485. doi: 10.1016/0896-6273(90)90106-P.

Shettleworth, S. J. (2010). *Cognition, Evolution, and Behavior*. (2nd ed.). New York, NY: Oxford University Press.

Shimizu, T., and Hibi, M. (2009). Formation and patterning of the forebrain and olfactory system by zinc-finger genes Fezf1 and Fezf2: Zinc-finger genes Fezf1 and Fezf2. *Development, Growth & Differentiation* 51, 221–231. doi: 10.1111/j.1440-169X.2009.01088.x.

Shipman, M. L., and Green, J. T. (2020). Cerebellum and cognition: Does the rodent cerebellum participate in cognitive functions? *Neurobiology of Learning and Memory* 170, 106996. doi: 10.1016/j.nlm.2019.02.006.

Shumake, J., Furgeson-Moreira, S., and Monfils, M. H. (2009). Predictability and heritability of individual differences in fear learning. *Animal Cognition*. doi: 10.1007/s10071-014-0752-1.

Siegfried, Z., Eden, S., Mendelsohn, M., Feng, X., Tsuberi, B.-Z., and Cedar, H. (1999). DNA methylation represses transcription in vivo. *Nat Genet* 22, 203–206. doi: 10.1038/9727.

Sigalova, O. M., Shaeiri, A., Forneris, M., Furlong, E. E., and Zaugg, J. B. (2020). Predictive features of gene expression variation reveal mechanistic link with differential expression. *Molecular Systems Biology* 16, e9539. doi: 10.15252/msb.20209539.

Sih, A., and Del Giudice, M. (2012). Linking behavioural syndromes and cognition: a behavioural ecology perspective. *Phil. Trans. R. Soc. B* 367, 2762–2772. doi: 10.1098/rstb.2012.0216.

Sii-Felice, K., Etienne, O., Hoffschir, F., Mathieu, C., Riou, L., Barroca, V., et al. (2008). Fanconi DNA repair pathway is required for survival and long-term maintenance of neural progenitors. *The EMBO Journal* 27, 770–781. doi: 10.1038/emboj.2008.14.

Simmini, S., Bialecka, M., Huch, M., Kester, L., van de Wetering, M., Sato, T., et al. (2014). Transformation of intestinal stem cells into gastric stem cells on loss of transcription factor Cdx2. *Nat Commun* 5, 5728. doi: 10.1038/ncomms6728.

Simon, M. J., Wang, M. X., Murchison, C. F., Roese, N. E., Boespflug, E. L., Woltjer, R. L., et al. (2018). Transcriptional network analysis of human astrocytic endfoot genes reveals region-specific associations with dementia status and tau pathology. *Sci Rep* 8, 12389. doi: 10.1038/s41598-018-30779-x.

Slate, J. (2005). INVITED REVIEW: Quantitative trait locus mapping in natural populations: progress, caveats and future directions. *Molecular Ecology* 14, 363–379. doi: 10.1111/j.1365-294X.2004.02378.x.

Smit, J. A. H., and van Oers, K. (2019). Personality types vary in their personal and social information use. *Animal Behaviour* 151, 185–193. doi: 10.1016/j.anbehav.2019.02.002.

Smulders, T. V. (2017). The Avian Hippocampal Formation and the Stress Response. *BBE* 90, 81–91. doi: 10.1159/000477654.
Soha, J. A., Peters, S., Anderson, R. C., Searcy, W. A., and Nowicki, S. (2019). Performance on tests of cognitive ability is not repeatable across years in a songbird. *Animal Behaviour* 158, 281–288. doi: 10.1016/j.anbehav.2019.09.020.
Sonnenberg, B. R., Branch, C. L., Pitera, A. M., Bridge, E., and Pravosudov, V. V. (2019). Natural Selection and Spatial Cognition in Wild Food-Caching Mountain Chickadees. *Current Biology* 29, 670-676.e3. doi: 10.1016/j.cub.2019.01.006.
Sonnenberg, B. R., Heinen, V. K., Pitera, A. M., Benedict, L. M., Branch, C. L., Bridge, E. S., et al. (2022). Natural variation in developmental condition has limited effect on spatial cognition in a wild food-caching bird. *Proceedings of the Royal Society B: Biological Sciences* 289, 20221169. doi: 10.1098/rspb.2022.1169.
Sorato, E., Zidar, J., Garnham, L., Wilson, A., and Løvlie, H. (2018). Heritabilities and co-variation among cognitive traits in red junglefowl. *Phil. Trans. R. Soc. B* 373, 20170285. doi: 10.1098/rstb.2017.0285.
Soravia, C., Ashton, B. J., Thornton, A., and Ridley, A. R. (2022). General cognitive performance declines with female age and is negatively related to fledging success in a wild bird. *Proceedings of the Royal Society B: Biological Sciences* 289, 20221748. doi: 10.1098/rspb.2022.1748.
Spitz, F., and Furlong, E. E. M. (2012). Transcription factors: from enhancer binding to developmental control. *Nat Rev Genet* 13, 613–626. doi: 10.1038/nrg3207.
Stanton, L. A., Bridge, E. S., Huizinga, J., and Benson-Amram, S. (2022). Environmental, individual and social traits of free-ranging raccoons influence performance in cognitive testing. *Journal of Experimental Biology* 225, jeb243726. doi: 10.1242/jeb.243726.
Stingo-Hirmas, D., Cunha, F., Cardoso, R. F., Carra, L. G., Rönnegård, L., Wright, D., et al. (2022). Proportional Cerebellum Size Predicts Fear Habituation in Chickens. *Frontiers in Physiology* 13. doi: 10.3389/fphys.2022.826178.
Stolyarova, A., O'Dell, S. J., Marshall, J. F., and Izquierdo, A. (2014). Positive and negative feedback learning and associated dopamine and serotonin transporter binding after methamphetamine. *Behavioural Brain Research* 271, 195–202. doi: 10.1016/j.bbr.2014.06.031.
Stolyarova, A., Rakhshan, M., Hart, E. E., O'Dell, T. J., Peters, M. A. K., Lau, H., et al. (2019). Contributions of anterior cingulate cortex and basolateral amygdala to decision confidence and learning under uncertainty. *Nat Commun* 10, 4704. doi: 10.1038/s41467-019-12725-1.
Strand, A. D., Aragaki, A. K., Baquet, Z. C., Hodges, A., Cunningham, P., Holmans, P., et al. (2007). Conservation of Regional Gene Expression in Mouse and Human Brain. *PLOS Genetics* 3, e59. doi: 10.1371/journal.pgen.0030059.
Strang, C. G., and Sherry, D. F. (2014). Serial reversal learning in bumblebees (Bombus impatiens). *Anim Cogn* 17, 723–734. doi: 10.1007/s10071-013-0704-1.
Strata, P. (2015). The Emotional Cerebellum. *Cerebellum* 14, 570–577. doi: 10.1007/s12311-015-0649-9.
Stuber, G. D., Klanker, M., De Ridder, B., Bowers, M. S., Joosten, R. N., Feenstra, M. G., et al. (2008). Reward-predictive cues enhance excitatory synaptic strength

onto midbrain dopamine neurons. *Science* 321, 1690–1692. doi: 10.1126/science.1160873.
Su, Y., Shin, J., Zhong, C., Wang, S., Roychowdhury, P., Lim, J., et al. (2017). Neuronal activity modifies the chromatin accessibility landscape in the adult brain. *Nat Neurosci* 20, 476–483. doi: 10.1038/nn.4494.
Sun, Z., Xu, X., He, J., Murray, A., Sun, M., Wei, X., et al. (2019). EGR1 recruits TET1 to shape the brain methylome during development and upon neuronal activity. *Nat Commun* 10, 3892. doi: 10.1038/s41467-019-11905-3.
Teijido, O., Casaroli-Marano, R., Kharkovets, T., Aguado, F., Zorzano, A., Palacín, M., et al. (2007). Expression patterns of MLC1 protein in the central and peripheral nervous systems. *Neurobiol Dis* 26, 532–545. doi: 10.1016/j.nbd.2007.01.016.
Tello-Ramos, M. C., Branch, C. L., Kozlovsky, D. Y., Pitera, A. M., and Pravosudov, V. V. (2019). Spatial memory and cognitive flexibility trade-offs: to be or not to be flexible, that is the question. *Animal Behaviour* 147, 129–136. doi: 10.1016/j.anbehav.2018.02.019.
Tello-Ramos, M. C., Branch, C. L., Pitera, A. M., Kozlovsky, D. Y., Bridge, E. S., and Pravosudov, V. V. (2018). Memory in wild mountain chickadees from different elevations: comparing first-year birds with older survivors. *Animal Behaviour* 137, 149–160. doi: 10.1016/j.anbehav.2017.12.019.
Therneau, T. M., Lumley, T., Elizabeth, A., and Cynthia, C. (2022). survival: Survival Analysis. Available at: https://CRAN.R-project.org/package=survival [Accessed September 1, 2022].
Thoma, P., Bellebaum, C., Koch, B., Schwarz, M., and Daum, I. (2008). The Cerebellum Is Involved in Reward-based Reversal Learning. *Cerebellum* 7, 433–443. doi: 10.1007/s12311-008-0046-8.
Thompson, S. M., Josey, M., Holmes, A., and Brigman, J. L. (2015). Conditional loss of GluN2B in cortex and hippocampus impairs attentional set formation. *Behav Neurosci* 129, 105–112. doi: 10.1037/bne0000045.
Thonnard, D., Callaerts-Vegh, Z., and D'Hooge, R. (2021). Effects of orbitofrontal cortex and ventral hippocampus disconnection on spatial reversal learning. *Neuroscience Letters* 750, 135711. doi: 10.1016/j.neulet.2021.135711.
Thonnard, D., Dreesen, E., Callaerts-Vegh, Z., and D'Hooge, R. (2019). NMDA receptor dependence of reversal learning and the flexible use of cognitively demanding search strategies in mice. *Progress in Neuro-Psychopharmacology and Biological Psychiatry* 90, 235–244. doi: 10.1016/j.pnpbp.2018.12.003.
Thornton, A., and Lukas, D. (2012). Individual variation in cognitive performance: developmental and evolutionary perspectives. *Phil. Trans. R. Soc. B* 367, 2773–2783. doi: 10.1098/rstb.2012.0214.
Thurman, R. E., Rynes, E., Humbert, R., Vierstra, J., Maurano, M. T., Haugen, E., et al. (2012). The accessible chromatin landscape of the human genome. *Nature* 489, 75–82. doi: 10.1038/nature11232.
Titulaer, M., van Oers, K., and Naguib, M. (2012). Personality affects learning performance in difficult tasks in a sex-dependent way. *Animal Behaviour* 83, 723–730. doi: 10.1016/j.anbehav.2011.12.020.
Toba, S., Tenno, M., Konishi, M., Mikami, T., Itoh, N., and Kurosaka, A. (2000). Brain-specific expression of a novel human UDP-GalNAc:polypeptide N-

acetylgalactosaminyltransferase (GalNAc-T9)1The nucleotide sequence presented in this paper will appear in the DDBJ, EMBL and GenBank Nucleotide Sequence databases under accession number AB040672.1. *Biochimica et Biophysica Acta (BBA) - Gene Structure and Expression* 1493, 264–268. doi: 10.1016/S0167-4781(00)00180-9.

Toda, T., and Gage, F. H. (2018). Review: adult neurogenesis contributes to hippocampal plasticity. *Cell and Tissue Research* 373, 693–709. doi: 10.1007/s00441-017-2735-4.

Tolosa, E., Wenning, G., and Poewe, W. (2006). The diagnosis of Parkinson's disease. *The Lancet Neurology* 5, 75–86. doi: 10.1016/S1474-4422(05)70285-4.

Tsai, A. P., Bor-Chian, L. P., Dong, C., Moutinho, M., Casali, B. T., Liu, Y., et al. (2021). INPP5D expression is associated with risk for Alzheimer's disease and induced by plaque-associated microglia. *Neurobiology of disease* 153, 105303. doi: 10.1016/j.nbd.2021.105303.

Tsakanikos, E., and Reed, P. (2022). Individual differences in proactive interference in rats (Rattus Norvegicus). *Psychon Bull Rev* 29, 203–211. doi: 10.3758/s13423-021-01998-7.

Uddin, L. Q. (2021). Cognitive and behavioural flexibility: neural mechanisms and clinical considerations. *Nature Reviews. Neuroscience* 22, 167–179. doi: 10.1038/s41583-021-00428-w.

Vaissière, T., Sawan, C., and Herceg, Z. (2008). Epigenetic interplay between histone modifications and DNA methylation in gene silencing. *Mutation Research/Reviews in Mutation Research* 659, 40–48. doi: 10.1016/j.mrrev.2008.02.004.

Vaisvila, R., Ponnaluri, V. K. C., Sun, Z., Langhorst, B. W., Saleh, L., Guan, S., et al. (2021). Enzymatic methyl sequencing detects DNA methylation at single-base resolution from picograms of DNA. *Genome Res.* 31, 1280–1289. doi: 10.1101/gr.266551.120.

Vallender, E. J., Lynch, L., Novak, M. A., and Miller, G. M. (2009). Polymorphisms in the 3′ UTR of the serotonin transporter are associated with cognitive flexibility in rhesus macaques. *American Journal of Medical Genetics Part B: Neuropsychiatric Genetics* 150B, 467–475. doi: 10.1002/ajmg.b.30835.

van Dam, S., Võsa, U., van der Graaf, A., Franke, L., and de Magalhães, J. P. (2018). Gene co-expression analysis for functional classification and gene–disease predictions. *Briefings in Bioinformatics* 19, 575–592. doi: 10.1093/bib/bbw139.

van Horik, J. O., and Emery, N. J. (2018). Serial reversal learning and cognitive flexibility in two species of Neotropical parrots (Diopsittaca nobilis and Pionites melanocephala). *Behavioural Processes* 157, 664–672. doi: 10.1016/j.beproc.2018.04.002.

van Horik, J. O., Langley, E. J. G., Whiteside, M. A., and Madden, J. R. (2019). A single factor explanation for associative learning performance on colour discrimination problems in common pheasants (Phasianus colchicus). *Intelligence* 74, 53–61. doi: 10.1016/j.intell.2018.07.001.

van Oers, K., Drent, P. J., de Goede, P., and van Noordwijk, A. J. (2004). Realized heritability and repeatability of risk-taking behaviour in relation to avian personalities. *Proc. R. Soc. Lond. B* 271, 65–73. doi: 10.1098/rspb.2003.2518.

van Oers, K., Klunder, M., and Drent, P. J. (2005). Context dependence of personalities: risk-taking behavior in a social and a nonsocial situation. *Behavioral Ecology*, 8. doi: doi:10.1093/beheco/ari045.

van Oers, K., and Mueller, J. C. (2010). Evolutionary genomics of animal personality. *Phil. Trans. R. Soc. B* 365, 3991–4000. doi: 10.1098/rstb.2010.0178.

Vardi, R., and Berger-Tal, O. (2022). Environmental variability as a predictor of behavioral flexibility in urban environments. *Behavioral Ecology*, arac002. doi: 10.1093/beheco/arac002.

Vardi, R., Goulet, C. T., Matthews, G., Berger-Tal, O., Wong, B. B. M., and Chapple, D. G. (2020). Spatial learning in captive and wild-born lizards: heritability and environmental effects. *Behav Ecol Sociobiol* 74, 23. doi: 10.1007/s00265-020-2805-6.

Verbeek, M. E. M., Drent, P. J., and Wiepkema, P. R. (1994). Consistent individual differences in early exploratory behaviour of male great tits. *Animal Behaviour* 48, 1113–1121. doi: 10.1006/anbe.1994.1344.

Verhagen, I., Gienapp, P., Laine, V. N., Grevenhof, E. M., Mateman, A. C., Oers, K., et al. (2019). Genetic and phenotypic responses to genomic selection for timing of breeding in a wild songbird. *Funct Ecol* 33, 1708–1721. doi: 10.1111/1365-2435.13360.

Viernes, D. R., Choi, L. B., Kerr, W. G., and Chisholm, J. D. (2014). Discovery and Development of Small Molecule SHIP Phosphatase Modulators. *Medicinal Research Reviews* 34, 795–824. doi: 10.1002/med.21305.

Vilà-Balló, A., Mas-Herrero, E., Ripollés, P., Simó, M., Miró, J., Cucurell, D., et al. (2017). Unraveling the Role of the Hippocampus in Reversal Learning. *J Neurosci* 37, 6686–6697. doi: 10.1523/JNEUROSCI.3212-16.2017.

Wagner, M. J., Kim, T. H., Savall, J., Schnitzer, M. J., and Luo, L. (2017). Cerebellar granule cells encode the expectation of reward. *Nature* 544, 96–100. doi: 10.1038/nature21726.

Wang, E., Wang, M., Guo, L., Fullard, J. F., Micallef, C., Bendl, J., et al. (2023). Genome-wide methylomic regulation of multiscale gene networks in Alzheimer's disease. *Alzheimer's & Dementia* n/a. doi: 10.1002/alz.12969.

Wang, Q., Li, M., Du, W., Shao, F., and Wang, W. (2015a). The different effects of maternal separation on spatial learning and reversal learning in rats. *Behavioural Brain Research* 280, 16–23. doi: 10.1016/j.bbr.2014.11.040.

Wang, Q., Li, M., Wu, T., Zhan, L., Li, L., Chen, M., et al. (2022). Exploring Epigenomic Datasets by ChIPseeker. *Current Protocols* 2. doi: 10.1002/cpz1.585.

Wang, Q., Shao, F., and Wang, W. (2015b). Maternal separation produces alterations of forebrain brain-derived neurotrophic factor expression in differently aged rats. *Frontiers in Molecular Neuroscience* 8. Available at: https://www.frontiersin.org/articles/10.3389/fnmol.2015.00049 [Accessed December 2, 2022].

Watanabe, S. (2005). Lesions in the basal ganglion and hippocampus on performance in a Wisconsin Card Sorting Test-like task in pigeons. *Physiology & Behavior* 85, 324–332. doi: 10.1016/j.physbeh.2005.04.020.

Wickham, H. (2016). *ggplot2: Elegant Graphics for Data Analysis*. 2nd ed. 2016. Cham: Springer International Publishing : Imprint: Springer doi: 10.1007/978-3-319-24277-4.
Wilson, A. J., Réale, D., Clements, M. N., Morrissey, M. M., Postma, E., Walling, C. A., et al. (2010). An ecologist's guide to the animal model. *Journal of Animal Ecology* 79, 13–26. doi: 10.1111/j.1365-2656.2009.01639.x.
Wingett, S. (2022). StevenWingett/FastQ-Screen: FastQ Screen v0.15.2. doi: 10.5281/ZENODO.1344583.
Wong, B. B. M., and Candolin, U. (2015). Behavioral responses to changing environments. *Behavioral Ecology* 26, 665–673. doi: 10.1093/beheco/aru183.
Wright, J., Haaland, T. R., Dingemanse, N. J., and Westneat, D. F. (2022). A reaction norm framework for the evolution of learning: how cumulative experience shapes phenotypic plasticity. *Biological Reviews*, brv.12879. doi: 10.1111/brv.12879.
Wu, T., and Hallett, M. (2013). The cerebellum in Parkinson's disease. *Brain* 136, 696–709. doi: 10.1093/brain/aws360.
Yan, F., Powell, D. R., Curtis, D. J., and Wong, N. C. (2020). From reads to insight: a hitchhiker's guide to ATAC-seq data analysis. *Genome Biol* 21, 22. doi: 10.1186/s13059-020-1929-3.
Yang, W., Zhou, X., and Ma, T. (2019). Memory Decline and Behavioral Inflexibility in Aged Mice Are Correlated With Dysregulation of Protein Synthesis Capacity. *Frontiers in Aging Neuroscience* 11. Available at: https://www.frontiersin.org/articles/10.3389/fnagi.2019.00246 [Accessed November 28, 2022].
Yin, S., Lu, K., Tan, T., Tang, J., Wei, J., Liu, X., et al. (2020). Transcriptomic and open chromatin atlas of high-resolution anatomical regions in the rhesus macaque brain. *Nat Commun* 11, 474. doi: 10.1038/s41467-020-14368-z.
Yopak, K. E., Pakan, J. M. P., and Wylie, D. (2017). "The Cerebellum of Nonmammalian Vertebrates," in *Evolution of Nervous Systems* (Elsevier), 373–385. doi: 10.1016/B978-0-12-804042-3.00015-4.
Yu, B., Zhang, Q., Lin, L., Zhou, X., Ma, W., Wen, S., et al. (2023). Molecular and cellular evolution of the amygdala across species analyzed by single-nucleus transcriptome profiling. *Cell Discov* 9, 1–22. doi: 10.1038/s41421-022-00506-y.
Yu, G., Wang, L.-G., Han, Y., and He, Q.-Y. (2012). clusterProfiler: an R Package for Comparing Biological Themes Among Gene Clusters. *OMICS: A Journal of Integrative Biology* 16, 284–287. doi: 10.1089/omi.2011.0118.
Zeleznikow-Johnston, A., Burrows, E. L., Renoir, T., and Hannan, A. J. (2017). Environmental enrichment enhances cognitive flexibility in C57BL/6 mice on a touchscreen reversal learning task. *Neuropharmacology* 117, 219–226. doi: 10.1016/j.neuropharm.2017.02.009.
Zhang, T.-Y., Keown, C. L., Wen, X., Li, J., Vousden, D. A., Anacker, C., et al. (2018). Environmental enrichment increases transcriptional and epigenetic differentiation between mouse dorsal and ventral dentate gyrus. *Nat Commun* 9, 298. doi: 10.1038/s41467-017-02748-x.
Zhang, Y., Iwasaki, H., Wang, H., Kudo, T., Kalka, T. B., Hennet, T., et al. (2003). Cloning and Characterization of a New Human UDP-N-Acetyl-α-d-

galactosamine:PolypeptideN-Acetylgalactosaminyltransferase, Designated pp-GalNAc-T13, That Is Specifically Expressed in Neurons and Synthesizes GalNAc α-Serine/Threonine Antigen *. *Journal of Biological Chemistry* 278, 573–584. doi: 10.1074/jbc.M203094200.

Zhang, Y., Liu, T., Meyer, C. A., Eeckhoute, J., Johnson, D. S., Bernstein, B. E., et al. (2008). Model-based Analysis of ChIP-Seq (MACS). *Genome Biology* 9, R137. doi: 10.1186/gb-2008-9-9-r137.

Zhong, L., Zhou, J., Chen, X., Liu, J., Liu, Z., Chen, Y., et al. (2017). Quantitative proteomics reveals EVA1A-related proteins involved in neuronal differentiation. *PROTEOMICS* 17, 1600294. doi: 10.1002/pmic.201600294.

Zimmermann, H., Zebisch, M., and Sträter, N. (2012). Cellular function and molecular structure of ecto-nucleotidases. *Purinergic Signalling* 8, 437–502. doi: 10.1007/s11302-012-9309-4.

Zocher, S., Overall, R. W., Berdugo-Vega, G., Rund, N., Karasinsky, A., Adusumilli, V. S., et al. (2021). De novo DNA methylation controls neuronal maturation during adult hippocampal neurogenesis. *The EMBO Journal* 40, e107100. doi: 10.15252/embj.2020107100.

Zuguang Gu (2017). ComplexHeatmap. doi: 10.18129/B9.BIOC.COMPLEXHEATMAP.

Zyla, J., Marczyk, M., Weiner, J., and Polanska, J. (2017). Ranking metrics in gene set enrichment analysis: do they matter? *BMC Bioinformatics* 18, 256. doi: 10.1186/s12859-017-1674-0.


LIVE YOUR ADVENTUR

Summary

The conditions in which an organism finds itself can change over different time intervals, both within a lifetime and across generations. Rapid and extensive environmental changes induced by human activities are found to occur more frequently, and behavioural changes are an important mechanism allowing species to adapt to changing environmental conditions. Cognitive flexibility, the ability to adaptively change a learned behaviour in response to changed contingencies in the environment has been postulated to be of high importance for individuals living in rapidly fluctuating environments. To predict whether and how selective pressures caused by environmental changes will drive the evolution of cognitive flexibility, we need a better understanding of the causes of individual differences within a population.

Causes of individual variation in cognitive flexibility may be shaped by genetic, developmental, and environmental factors leading to differences in functioning of the neurobiological systems that support cognitive flexibility. However, despite the ecological relevance of cognitive flexibility, the way individuals vary in this ability and which mechanisms shape the expression of cognitive flexibility, has seldom been investigated in an ecologically relevant system. The aim of this thesis was therefore to explore the causes of individual differences in cognitive flexibility using the great tit (*Parus major),* as a model system. Where possible, I directly linked these findings to already validated rodent models, to better understand how findings in rodent species could be used to make predictions in ecologically relevant species. I developed a high-throughput reversal learning task to assess cognitive flexibility repeatedly in a large number of individuals, in order to assess to what extent reversal learning is repeatable and heritable in the great tit (**Chapter 2**). To explore the molecular mechanisms underlying cognitive flexibility, I first investigated how chromatin accessibility contributes to cell type heterogeneity and tissue specificity of brain regions relevant to reversal learning performance (**Chapter 3**) and then assessed whether individual differences in reversal learning performance are explained by variation in chromatin accessibility and gene expression in these brain regions (**Chapter 4 and 5**).

In **Chapter 2**, I showed that the repeatability of reversal learning performance is relatively low, indicating that individuals vary in performance across repeated measures. Whereas I found that individual variation in boldness is linked to associative learning performance, I did not see a link between personality and reversal learning performance. I observed a negative link between associative and reversal learning performance, indicative of a trade-off between learning and flexibility. Lastly, I found no evidence for a heritable basis of reversal learning performance, suggesting limited potential for cognitive flexibility to evolve.

In **Chapter 3** I found that distinct patterns of gene expression between different brain regions, and cell types within those brain regions, are associated with

differences in chromatin accessibility. Most cell type- and brain region-specific accessible regions are located in intronic and distal intergenic regions, whereas promoter accessibility is most predictive of gene expression variation. This suggests the presence of cell type-specific enhancers, which regulate gene expression elsewhere.

In **Chapter 4** and **Chapter 5** I studied to what extent epigenomic and transcriptomic differences explain individual variation in cognitive flexibility. I found that individuals differing in reversal learning performance show subtle differences in gene expression, with different processes involved depending on the brain region. Different genes are involved in reversal learning ability between great tits and mice, although some have overlapping functions, such as energy metabolism in the cerebellum and synaptic functioning in the striatum. In the striatum, but not in the hippocampus, I found that differences in chromatin accessibility were positively linked to gene expression, especially in promoter and intronic regions. However, the majority of differentially accessible regions were located in distal intergenic regions. DNA methylation was negatively linked with gene expression and chromatin accessibility, and DNA methylation differences were observed in genes involved neural development.

Altogether, the results of my thesis have brought us closer to understanding what causes individual variation in cognitive flexibility in the great tit. The contribution of heritable genetic variation is too low to detect, suggesting that cognitive flexibility resembles a direct response to variation in the current and past environment. Especially the contribution of an individual's short-term and long-term cumulative experience is likely to be high, and I argue that these carry-over effects will be a fruitful avenue for further study. Epigenetic factors play a major role in explaining the molecular mechanisms underlying cognitive flexibility. Since epigenetic marks can be altered as a result of experiences and maintain over longer time spans, they are likely to underlie this information storage. Indeed, we find that two dynamic aspects of the genome, DNA methylation and chromatin accessibility, are both associated to gene expression variation in relation to cognitive flexibility. In the bird brain, I found that this is particularly true for the striatum, a brain region involved in reward learning. In the future, careful experimental work is needed to investigate how experience-driven epigenetic changes interact with the genome to affect individual variation in cognitive flexibility. This knowledge will be pivotal to understand the role for cognitive flexibility in adaptation in response to rapid climate change.

Samenvatting

De omstandigheden waarin een organisme zich bevindt, kunnen veranderen over verschillende tijdsintervallen, zowel binnen een leven als tussen generaties. Snelle en wijdverspreide milieuveranderingen veroorzaakt door menselijke activiteiten komen steeds vaker voor. Gedragsveranderingen zijn een belangrijk mechanisme waarmee soorten zich kunnen aanpassen aan zulke veranderende omgevingsomstandigheden. Cognitieve flexibiliteit, het vermogen om aangeleerd gedrag adaptief te veranderen, wordt verondersteld van groot belang te zijn voor individuen die leven in snel fluctuerende omgevingen. Om te voorspellen of en hoe selectiedrukken die worden veroorzaakt door milieuveranderingen de evolutie van cognitieve flexibiliteit teweeg kunnen brengen, hebben we een beter begrip nodig van de oorzaken van individuele verschillen binnen een populatie.

Zowel genetische, ontwikkelings- alsook omgevingsfactoren kunnen ten grondslag liggen aan individuele variatie in cognitieve flexibiliteit. Al deze factoren leiden tot verschillen in de werking van neurobiologische systemen die cognitieve flexibiliteit ondersteunen. Ondanks de ecologische relevantie van cognitieve flexibiliteit is er nog weinig onderzoek gedaan naar de manier waarop individuen verschillen in deze vaardigheid en welke mechanismen de expressie van cognitieve flexibiliteit bepalen in een ecologisch relevant onderzoekssysteem. Het doel van dit proefschrift was dan ook om de oorzaken van individuele verschillen in cognitieve flexibiliteit te onderzoeken met de koolmees (*Parus major*) als modelorganisme. Waar mogelijk heb ik deze bevindingen direct gekoppeld aan reeds gevalideerde knaagdieren, om beter te begrijpen hoe bevindingen bij modelsoorten kunnen worden gebruikt om voorspellingen te doen bij ecologisch relevante soorten. Ik heb een testapparaat ontwikkeld waarmee ik het omleervermogen van koolmezen kan meten om cognitieve flexibiliteit herhaaldelijk te testen bij een groot aantal individuen. Dit stelde mij in staat om te bepalen in hoeverre het omleervermogen consistent en erfelijk is in de koolmees (**Hoofdstuk 2**). Om de moleculaire mechanismen die ten grondslag liggen aan individuele verschillen in cognitieve flexibiliteit te onderzoeken, heb ik eerst bepaald hoe de compactheid van chromatine bijdraagt aan celtype- en weefsel-specifieke genexpressie in hersengebieden die relevant zijn voor het omleervermogen (**Hoofdstuk 3**). Vervolgens heb ik getest of individuele verschillen in het omleervermogen kunnen worden verklaard door variatie in chromatine-toegankelijkheid en genexpressie in deze hersengebieden (**Hoofdstuk 4 en 5**).

In **Hoofdstuk 2** heb ik aangetoond dat het omleervermogen beperkt consistent is, wat aangeeft dat individuen variërend presteren bij herhaalde metingen. Hoewel ik heb vastgesteld dat individuele variatie in brutaalheid is gekoppeld aan het associatief leervermogen, vond ik geen verband tussen persoonlijkheidskenmerken en omleervermogen. Ik vond een negatieve verband tussen associatief leervermogen en omleervermogen, wat duidt op een trade-off tussen leren en flexibiliteit. Ten slotte vond ik geen bewijs voor een erfelijke basis

van omleervermogen, wat wijst op beperkt potentieel voor de evolueerbaarheid van cognitieve flexibiliteit.

In **Hoofdstuk 3** heb ik aangetoond dat patronen van genexpressie verschillen tussen hersengebieden, en celtypes binnen die hersengebieden. Bovendien zijn deze verschillen geassocieerd met variatie in chromatine-compactheid. De meeste celtype- en hersengebied-specifieke toegankelijke chromatineregio's bevinden zich in intronische en distale intergene regio's, terwijl toegankelijkheid van promotors het meest voorspellend is voor variatie in genexpressie. Dit suggereert de aanwezigheid van celtype-specifieke 'enhancers', die elders op het genoom genexpressie reguleren.

In **Hoofdstuk 4** en **Hoofdstuk 5** heb ik onderzocht in hoeverre individuele variatie in cognitieve flexibiliteit kan worden verklaard door epigenomische en transcriptomische verschillen. Ik heb vastgesteld dat individuen die verschillen in omleervermogen, subtiele verschillen in genexpressie vertonen. De genen die verschillend tot expressie kwamen zijn betrokken bij een reeks aan processen die afhangen van het hersengebied waar ze tot expressie komen. Hoewel sommige genen overlappende functies hebben, zoals energiemetabolisme in het cerebellum en synaptische werking in het striatum, zijn uiteenlopende genen zijn betrokken bij het omleervermogen bij koolmezen en muizen. Ik heb vastgesteld dat in het striatum, maar niet in de hippocampus, verschillen in chromatine-compactheid en dus genoomtoegankelijkheid positief geassocieerd zijn met genexpressie, vooral in promotor- en intronische regio's. Het merendeel van de regio's die verschil toonden in genoom toegankelijkheid tussen de snelle en langzame omleerders bevond zich echter in distale intergene regionen. DNA-methylatie was negatief geassocieerd met genexpressie en chromatine-compactheid, en verschillen in DNA-methylatie tussen snelle en langzame omleerders bevonden zich in genen die betrokken zijn bij neuronale ontwikkeling.

Al met al hebben de resultaten van mijn proefschrift ons beter inzicht gegeven in de oorzaken van individuele variatie in cognitieve flexibiliteit bij de koolmees. De bijdrage van erfelijke genetische variatie is te laag om te detecteren, wat suggereert dat cognitieve flexibiliteit het resultaat is van een directe respons op variatie in de huidige en voorgaande omgeving. Vooral de bijdrage van een individuele korte- en lange-termijn-ervaring is waarschijnlijk groot, en ik beargumenteer dat onderzoek naar deze carry-over effecten een waardevolle toevoeging zouden zijn aan het huidige onderzoek. Epigenetische factoren spelen een belangrijke rol bij het verklaren van de moleculaire mechanismen die ten grondslag liggen aan cognitieve flexibiliteit. Aangezien epigenetische markeringen kunnen veranderen als gevolg van ervaringen en langere tijd behouden kunnen blijven, is het waarschijnlijk dat ze ten grondslag liggen aan de opslag en verwerking van opgedane informatie. Sterker nog, we vinden dat twee dynamische aspecten van het genoom, DNA-methylatie en chromatine-toegankelijkheid, beide geassocieerd zijn met variatie in genexpressie gerelateerd aan cognitieve flexibiliteit. In het koolmeesbrein heb ik vastgesteld dat dit met name geldt voor het striatum, een hersengebied dat al

bekend stond betrokken te zijn bij het leren van beloningen. In de toekomst is zorgvuldig experimenteel werk nodig om te onderzoeken hoe ervaringsgerelateerde epigenetische veranderingen interageren met het genoom om individuele variatie in cognitieve flexibiliteit te beïnvloeden. Deze kennis zal essentieel zijn om de rol van cognitieve flexibiliteit als adaptatie via de reactie op snelle klimaatverandering te begrijpen.

Curriculum vitae

Krista van den Heuvel was born on the 24th of July 1993 in Gouda, the Netherlands. Following secondary school, she studied Biology at Wageningen University, specializing in organismal and developmental biology. As part of her bachelor's degree, she went on Erasmus Exchange to Uppsala University. Her bachelor thesis at the Behavioural Ecology group concerned neighbourhood effects on singing activity in the great tit (WUR). After obtaining her bachelor's degree in July 2014, she continued her studies with a master programme at Wageningen University, specializing in animal adaptation and behavioural biology. For her master thesis at the Entomology group she studied the neural circuitry of learning and memory formation in *Nasonia* wasps (WUR). She performed an internship at the Max Planck Institute for Chemical Ecology, studying the anatomy of the olfactory lobe in the fruit fly (Jena, Germany). After her studies, she briefly worked as a high school student tutor and hiking shoe saleswomen. She then became trainee at the Danish Institute of Translational Neuroscience, focusing on the neural circuitry of courtship behaviour and reward in the fruit fly (Aarhus, Denmark).

She started her PhD in March 2018 with Prof. Dr Kees van Oers and Dr Alexander Kotrschal at the NIOO-KNAW and WUR, as part of the collaborative EpiBRAIN project. This PhD project focused on the causes and consequences of individual variation in cognitive flexibility, collaborating with researchers from Erasmus MC and UMC Utrecht to study molecular and epigenetic mechanisms. The main focus species was the great tit, but by collaborating with researchers from the Netherlands Institute for Neuroscience, data from mice and rats was also included in this study. The results of this project are presented in this thesis.

List of scientific publications

Peer-reviewed

Sepers, B., **van den Heuvel, K.**, Lindner, M., Viitaniemi, H., Husby, A., & van Oers, K. (2019). Avian ecological epigenetics: pitfalls and promises. *Journal of Ornithology*, *160*, 1183-1203.

Groothuis, J., **van den Heuvel, K**., & Smid, H. M. (2020). Species-and size-related differences in dopamine-like immunoreactive clusters in the brain of Nasonia vitripennis and N. giraulti. *Cell and tissue research*, *379*, 261-273.

van Oers, K., **van den Heuvel, K**., & Sepers, B. (2023). The Epigenetics of Animal Personality. *Neuroscience & Biobehavioral Reviews*, 105194.

Submitted/under review

van den Heuvel, K., Quinn, J.L., Kotrschal, A., van Oers, K. (*Submitted*). Artificial selection for reversal learning reveals limited repeatability and no heritability of cognitive flexibility in great tits (Parus major). *Proceedings of the Royal Society B*.

To be submitted/in preparation

van den Heuvel, K., Yildiz, B., Timpanaro, I., Badura, A., de Zeeuw, C., Willuhn, I., Kotrschal, A., Creyghton, M., van Oers, K. (*In prep*). Cell type- and brain region-specific patterns of differential gene expression and chromatin accessibility in great tits (*Parus major*)

van den Heuvel, K., Yildiz, B., Timpanaro, I., van den Boom, B.J.G., Badura, A., de Zeeuw, C., Willuhn, I., Kotrschal, A., Creyghton, M., van Oers, K. (*In prep*). Transcriptomic correlates of cognitive flexibility in two homologue brain regions of songbirds and rodents

van den Heuvel, K., Yildiz, B., Timpanaro, I., Mateman, A.C., Kotrschal, A., Creyghton, M., van Oers, K. (*In prep*). Molecular and epigenetic mechanisms underlying individual differences in cognitive flexibility in a songbird

Acknowledgements

I feel so lucky to have been supported by the most amazing colleagues, friends and family, and this support has been paramount to my wellbeing and the completion of this thesis. I am forever grateful for the time that I have spent with each one of you and all that I have learned about your personalities, life choices, ideas and cultures and I will take these lessons with me for the rest of my life.

First of all, I want to express my gratitude for my promoter and co-promoter. **Kees**, thank you for embarking on this journey with me and for becoming my mentor. You taught me how to be a researcher in the fields of behavioural and molecular ecology, and you always made sure to let me choose my own path. I have learned so much from our discussions, and I liked how talking about cognition often ended up being almost philosophical. Thank you for putting up with my difficulty in meeting deadlines and for going at lengths to give me feedback on time. On top of that, I look back fondly on all our long talks about ethics, politics, photography and nature. **Alex**, thank you for always offering your honest view and critical questions. Kees and I have the tendency to leave a lot of room for vagueness, you always managed to pierce right through that. On top of that, I have learned a lot from your writing tips and techniques.

I want to thank everyone in the 'EpiBRAIN' consortium for the trans-disciplinary discussions, thank you **Menno**, **Chris**, **Ingo**, **Aleksandra**, **Nicole** and **Cynthia**, for your flexibility and confidence in me as our project plans evolved, and for helping with collection and interpretation of the data. **Ilia**, especially your contribution has been indispensable, thank you so much for helping us out with all that lab work.

Beril, you joined us as a bioinformatician in the final years of the project, and helped us work through an incredible amount of data – the good and the bad. Thank you for creating all those overview tables and PowerPoints, and your patience while trying to explain the data to Kees and me. I am really happy to have had you as a co-worker on my project, and we had a lot of good times together.

I have experienced the **Animal Ecology Department** as an incredibly inclusive and friendly working environment, and **Marcel**, I think that is partially thanks to your open-minded and amicable attitude that has shaped the group into a cohesive whole. I want to thank all the PI's, postdocs and PhD students for the insightful, stimulating and fun conversations and discussions during science lunches, journal clubs, coffee breaks, and of course Friday beer o'clocks. I also want to thank all current and former members of the **Kees Group** for the fun and fruitful discussions.

From within the department, I have been lucky to receive help from many laboratory assistants, animal caretakers, field assistants, database managers and bioinformaticians, without whom my PhD project would have been entirely unfeasible. Thank you **Louis, Manon, Peter, Bart, Maartje, Martijn, Judith,**

Christa, Agaat, Ruben, Anne, Franca, Coretta, Nina and **Marylou**. I also want to give a shout-out to all of those that helped with hand-rearing, for keeping the great tit chicks safe and well-fed.

Piet, in only a few weeks you showed me how to perform efficient fieldwork in way that is respectful to the birds, while also enjoying the wonders of the forest. What you taught me has opened up the world of birds to me. I will never walk in a forest the same way as before, thank you for that.

Ruben and **Michiel V.**, thank you for helping me with the dissections, a mentally very challenging part of my PhD, worsened by covid. Masks and microscopes are definitely a terrible combination.

A big thank you to all the Animal Ecology PhD students for all the fun we've had together. **Tjomme,** thanks for the often sarcastic, but also supportive, comments that came from behind the computer screen on the other side of the desk. **Aurelia, Claire, Eva, Lisenka, Melanie, Morgane, Natalie** and **Nelleke,** we had so much fun at the clothing swaps (confusing our supervisors by wearing each other's clothes the day after), pizza, sushi and cookie nights!

To all my colleagues on the WUR side of the road from the **Behavioural Ecology Group**: although we did not spend much time together, it was great to have you as a second research family, and I greatly enjoyed meeting you at courses and conferences to hear about all your amazing projects.

With great pleasure I have supervised many students. **Sara**, thank you for the brilliant idea of using freeze-dried mealworms as rewards, **Corne**, **Nina, Ioanna** and **Youri**, without your help I would still be assembling feeders in building 3, thank you for bearing with me. **Robin**, you achieved the unachievable by making sense of the feeder data. I also want to thank **Myrthe, Anne, Kyle, Madelon, Daan, Femke, Guido** and **Jari** for their help with fieldwork, behavioural tests and epigenetic analyses.

Eva, thank you for being my partner in crime with our struggles with the feeders and behavioural statistics, but mostly for being such a good friend and for teaching me how to channel my inner Spaniard. **Utku**, **Joey** and **Stefan** thank you for providing the very welcome comical distractions while I was struggling with the difficult final months of my PhD.

Bernice, **Morgane** and **Melanie**, I still can't believe how fortunate we were to all start our projects together, that we found each other and became such close colleagues and friends. It was a lot of fun to explore Wageningen again through your eyes, to travel around the Netherlands from the Efteling to the Sallandse Heuvelrug, and to go to conferences together. My PhD life has been so much more fun and exciting because of you three.

Arjan, Denise, Duco, Femke, Joren, Julian, Luc and **Lisa**, thank you for all the small and big adventures and for reminding me what life is about. **Laurien, Lieke** and **Romy**, I love that you have always been there and I know you'll always be.

Also, a word of thanks to all great tits, those that still are, and those that aren't anymore, for your unending curiosity for go pro's, feeder parts, my shoes and my hair, for your love for crispy mealworms and sunflower seeds, for your rightfully angry bites and calls. Getting to know your wits and your behaviours has been the most valuable life lesson of all.

Pap, **Mam**, **Ingrid** en **Dagmar**, we zijn met zijn allen heerlijk nieuwsgierige aagjes. Ik vind het bijzonder om zo veel van mezelf in jullie terug te zien, de goede en de minder goede eigenschappen, en we zijn nooit uitgeleerd over elkaar en elkaars wereldbeeld. Jullie hebben me eindeloos uitgehoord over mijn werk, zowel over de inhoud als over het leven als onderzoeker. Dankjulliewel voor jullie interesse, steun en zelfs hulp bij de handopfok.

Lieve **Ties**, mijn maatje en zo veel meer dan dat, geen van beiden hadden we durven dromen dat we na alle onzekerheden en verhuizingen samen op zo'n fijn plekje in Wageningen terecht zouden komen. Dankjewel voor je onvoorwaardelijke steun in de afgelopen jaren, ik denk niet dat ik zonder jou nog rechtop had gestaan aan het einde van mijn thesis. We hebben in de afgelopen vijf jaar ontelbaar keer met onze backpacks bij bushalte Arboretumlaan gestaan om vanaf daar naar de mooiste uithoeken van Europa te trekken, van de Finse merenvlakte tot hoog in de Franse alpen, en het was steeds weer zó fijn om samen weer helemaal tot rust te komen in de natuur. Ik ben ontzettend blij dat ik met jou de wereld en het leven mag verkennen, en ik kan niet wachten op wat ons nog te wachten staat.

Training and Supervision Plan (TSP)

	Year	Credits*
A. The Basic Package (mandatory)		3
WIAS - Introduction Day	2018	
WGS - Scientific Integrity and Ethics in Animal Sciences	2019	
WIAS - Introduction course on personal effectiveness for your PhD	2021	
B. Disciplinary Competences		**13**
PhD proposal	2018	
Species Specific Birds Course, *NIOO-KNAW*	2018	
The Fundamentals of Animal Emotion, *WIAS*	2019	
Advanced Statistics course Design of Experiments, *WIAS/PE&RC*	2019	
How mother can influence offspring, *WUR*	2021	
Workshop The evolution of personality in animals and humans	2021	
Life History Theory, *RUG*	2021	
C. Professional Competences		**3**
Career Orientation, *WGS*	2021	
Presenting with impact, *Wageningen into Languages*	2021	
The Final Touch, *WIAS*	2021	
D. Societal Relevance		**4**
Societal impact of your research, *WIAS*	2022	
Familielezing Teylers museum, *Haarlem*	2021	
Kinderlezing Museum Jeugd Universiteit Natuurhistorisch Museum, *Rotterdam*	2022	
Inleiding leesclub Avonden met Vleugels, *Nijmegen*	2022	
E. Presentation Skills		**4**
<u>Poster presentations</u>		
Netherlands Society for Evolutionary Biology, Ede	2019	
Poster presentation - European Society for Evolutionary Biology, Turku	2019	
<u>Oral presentations</u>		
STRANGE Meeting, Online	2021	
Netherlands Society for Behavioural Biology, Egmond aan Zee	2021	
International Society for Behavioural Ecology, Stockholm	2022	
European Society for Evolutionary Biology, Prague	2022	
F. Teaching competences		**6**
Supervision of eight MSc students	2018-22	
Supervision of three HBO students	2020-22	
Supervision of one MBO student	2021	
Education and Training Total (minimum 30 credits)*		**34**
One ECTS credit equals a study load of approximately 28 hours		

The research presented in this thesis was conducted at the Department of Animal Ecology of the Netherlands Institute of Ecology (NIOO-KNAW), Wageningen.

The research described in this thesis was financially supported by the Royal Netherlands Academy of Arts and Sciences (KNAW), Academy Research Grant 'EpiBRAIN', awarded to Kees van Oers, one grant from the Lucie Burgers Foundation for Comparative Behaviour Research to Krista van den Heuvel and one grant from the Dr. J.L. Dobberke Foundation to Krista van den Heuvel.

Financial support from Wageningen University and the Netherlands Institute of Ecology (NIOO-KNAW) for printing this thesis is gratefully acknowledged.

This thesis is NIOO Thesis 203
Image credits by Perro de Jong/NIOO-KNAW, Ties Blaauw and Krista van den Heuvel
Cover art by Rebeca Arredondo
Printed by proefschriftmaken.nl